Flow-Injection Analysis of the Platinum-Group Metals

A Thesis Presented for the Degree of

DOCTOR OF PHILOSOPHY

in the Department of CHEMISTRY

UNIVERSITY OF CAPE TOWN

February 1995

by

DEREK AUER

Flow-Injection Analysis of the Platinum-Group Metals

Derek Auer

Flow-Injection Analysis of the Platinum-Group Metals

by

Derek Auer

Supervisor : Associate Professor Klaus R. Koch,
Department of Chemistry, University of Cape Town,
South Africa.

Flow-Injection Analysis of the Platinum-Group Metals

by

Derek Auer

Process Analytical Science Group, Analytical Science Division,

Council for Mineral Technology, Randburg, Republic of South Africa

February 1995

ABSTRACT

To date the principle methods for the determination of the platinum-group metals (PGMs) use an "off-line" assay with flame-atomic absorption spectrometry and visible spectrometry. Both suffer numerous interferences and involve time-consuming and arduous laboratory separation methods prior to analysis. An "on-line" method for the rapid assay of the PGMs is indeed a lacking component in the analysts' repertoire of methods.

This study describes the development of spectrophotometric methods for the determination of the PGMs using flow-injection analysis (FIA). The principle of exploiting the remarkably specific and selective reaction of stannous halides with the PGMs to yield a series of intensely coloured complexes in acidic solutions forms the basis of these methods. The reaction is subject to relatively few interferences from other transition metals.

A high speed scanning spectrophotometer is employed to obtain second order data. The successful manipulation of the data enables the determination of PGMs as single components and also simultaneously in mixtures. Attention is focused on the establishment of principles for successful multi-component analysis of PGMs. The development of a software program for multi-wavelength data manipulation was mandatory and is described. Criteria for successful selection of analytical wavelengths are discussed.

The usefulness of multi-dimensional graphical data representation is demonstrated in a stop-flow study of the palladium reaction with tin(II) chloride. Qualitative information is provided regarding the nature of complexes and their interactions. Correlation of spectrophotometric data with complex solution colour changes is made. The requirements for future progress in multi-component FIA determinations as well as the direction for future research conclude the study.

Table of Contents

List of Figures

List of Tables

Acknowledgements

First and foremost, this work was made possible by the permission and generous financial assistance of the Council for Mineral Technology. The author further wishes to express his appreciation to the management of the Analytical Science Division, specifically Mr Ron Mallett, Dr Graham Marshall, and Mrs Tina Pohlandt-Watson, for supporting this work and making those difficult decisions that were ultimately in my best interests.

Special thanks must go to Dr Graham D. Marshall for his valued comments on this thesis, even when other responsibilities required his attention. His resourceful approaches contributed significantly to the success of this work.

I would also like to extend my sincerest appreciation to my supervisor, Associate Professor Klaus R. Koch, for sharing his passion for Analytical Chemistry with me, and for introducing me to the world of flow-injection analysis.

To all my friends in the Chemistry Department at the University of Cape Town - particularly Tarron Meyer - thank you for your support and listening ear when the "going got tough." To my colleagues and friends at Mintek - Deon, Dick, Malcolm, and Vincente - thank you for your encouragement during the latter stages of this project.

To my family - Mom, Dad, Gary, and Emma-Jayne - many thanks for your love and support throughout my studies and research at University. Every minute was worth it !

Finally, I wish to express my most profound gratitude to my precious wife, Bronwyn Leigh, for all her love and support during the pleasant and trying times of this doctoral work. I will never be able to compute the contribution and difference she made to this work and to my life. Thank you ever so much, my sweetheart !!!

In loving memory of my grandparents who were unable to view this completed work -

Leonard Charles Mason (1920 - 1993)

Rosy Auer (1914 - 1994)

"Their strength is to sit still. Now go, write it before them in a table, and note it in a book, that it may be for time to come for ever and ever."

Isaiah 30:7b,8.

Chapter 1.

Introduction

The platinum-group metals, gold and silver, collectively referred to as the noble metals, have throughout history occupied a position of considerable social and economic importance. The demand for specifically the platinum-group metals (PGMs) over recent years has increased significantly whilst their wide range of technological applications from catalysts to cancer chemotherapy clearly shows their importance in the world market.[1]

The automotive industry is currently using the largest share of the world production of the PGMs.[2,3] This is a direct consequence of the incorporation of platinum and palladium, as oxidative catalysts, and rhodium, as a reduction catalyst for nitrous oxides, in automobile catalytic converters. Use in these applications will grow substantially in the next decade as ever more stringent exhaust-gas emission standards are introduced by legislation in the developed world.[4] The "clean air" legislation introduced by the European Economic Community (EEC) made the incorporation of autocatalysts in all new European gasoline-powered vehicles compulsory with effect from the beginning of 1993.[3] Similar steps are being initiated in the United States of America.[5] Platinum oxidation catalysts are used outside the automobile industry in numerous air-pollution abatement processes to remove carbon monoxide and harmful organic vapours.

The chemical and petrochemical industries exploit the efficient catalytic properties of the PGMs. An example of this is the use of platinum, or a platinum-rhodium alloy, as a gauze, to catalyse the partial combustion (oxidation) of ammonia to yield nitric oxide. Nitric oxide is used as a raw material for the production of nitric acid, fertilisers and explosives. PGMs are also used as catalysts for organic syntheses. Hydrogenation, dehydrogenation, isomerisation and oligmerisation are typical examples of this. Platinum catalysts in the petrochemical industry assist in the production of high octane gasoline and aromatic compounds.

Frequent use is made of platinum vessels when melting special types of glasses. Traces of platinum are introduced into the molten silicate mass. This incorporation of platinum into the glass matrix changes its expected properties. The market for glass and glass fibres is healthy in world terms, with applications in the housing, marine and optical industries. Glass fibres are used in the production of printed circuit boards. These printed circuit boards are important in our modern computer age.

The precious metals also fill a traditional role in the jewellery industry. Apart from the conventional solid solution gold-jewellery alloys, the production of coloured platinum intermetallic compounds and ordered intermetallic compounds of gold, called "Spangold",[6] are a recent local development in the jewellery industry. Platinum jewellery has made inroads into the gold-dominated market for items such as marriage rings, earrings, pendants and bracelets.

The electrical and electronic industries use alloys of the PGMs in low voltage, low energy and other electrical contacts, thick- and thin-film circuits, high temperature thermocouples, spark plug electrodes, wires, and oxygen sensors. The booming world-wide demand for mobile telephones has helped the price of palladium to double in the past year.[7] This precious metal is needed for the multi-layer ceramic capacitors used in cellular telephones. The new wide-screen television sets and computers also use palladium in their electronic components.

Fuel cells[3] in which catalytic platinum electrodes convert fuel directly into electricity will become an increasing consumer of platinum in the future. The 1990s should see the establishment of a firm market for the fuel cell. Some are already commercially available and operational. A growing awareness for clean, efficient, and versatile sources of power for the future, has spurred the growth of this market.

The significance of the PGMs in the medical and dental industry, particularly with respect to platinum in cancer chemotherapy, is growing.[8] The discovery of the antitumor activity of certain platinum amine compounds,[9] a commonly known one being *cis*-diamminedichloro platinum(II) (cisplatin), led to the launch of intensive research efforts in attempts to successfully treat human malignancies. Applications of the PGMs extend to the manufacture of some pharmaceuticals, antibiotics (Paracetamol is a common analgesic manufactured with

the aid of platinum), and as dental restorative materials (palladium based alloys). They find application in the construction of medical equipment such as heart pacemakers, catheters and hypodermic-needle tubing.

Miscellaneous applications of the PGMs and their alloys extend to decorative work on china, glass and ceramics, and use in laboratory apparatus such as crucibles used for high-temperature fusion. There are considerable investment opportunities, particularly in platinum, as coins and bars (500g and 1000g). Speculative investment often results from the regular fluctuation of the price of platinum.

These growing demands for the PGMs present a formidable challenge to the precious-metal industry to improve the efficiency of methods of recovery, separation, preconcentration, and analysis across the full range of concentration levels.

There are two principle sources of the PGMs. The smaller of the two is the reprocessing industry that recovers and refines precious metal scrap and spent catalysts. PGMs obtained in this manner are known as "secondary platinum-group metals".

The other supply of the PGMs, and the more important one, is from mining of ore deposits containing the precious metals. There are two major types of ore deposits found in countries of the world's largest producers - Russia, the Republic of South Africa, Canada, Colombia, and the United States of America. The first type, which is the more significant contributor, are large igneous ore bodies. The second are placer ore bodies.

Large igneous ore bodies, that are often layered intrusions, contain mafic and ultramafic rocks that are the largest source of PGMs. The major PGM minerals in these bodies are sulphides, arsenides, sperrylite ($PtAs_2$), cooperite (PtS) and braggite ((Pt, Pd, Ni)S). These minerals are often associated with other sulphides, such as copper, nickel, iron, and with chromite. In placer ore deposits, the precious metals generally occur in their native form.

The rarity and demand for the PGMs has resulted in their commanding high prices. The financial value attached to the PGMs makes it imperative that the metallurgical recovery of the metals from these geological deposits and from industrial waste products be efficient and economical. The flow chart in Figure 1.1 shows the essential steps in the recovery procedure

of the PGMs prior to refining and individual element analysis used at Rustenburg Platinum Mines.[1]

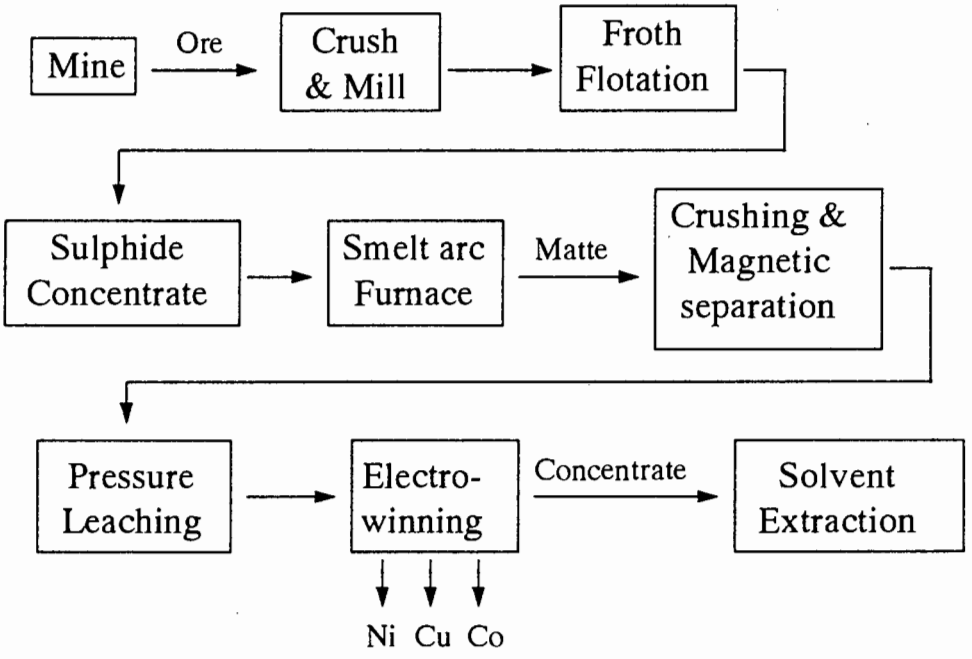

Figure 1.1 *Flow production chart for treatment of ores to the concentrate stage. Adapted from Kirk-Othmer Encyclopaedia of Chemical Technology.*[1]

The mined ore is crushed, milled to a suitable size, and mixed with water. Hydrophobic organic reagents added to this mixture coat the precious metal particles and sulphides. These ore particles and sulphides float to the surface on bubbles introduced into this slurry as a froth. The froth containing a sulphide concentrate is smelted in an arc furnace to give a matte. This matte contains both the precious metals and the sulphides of Cu, Ni, Fe and possibly minor quantities of other base metals such as cobalt.

Subsequent treatment of the matte by magnetic separation serves to remove the iron sulphide. Pressure leaching and electrowinning remove the bulk of the Cu, Ni and Co to yield a concentrate with an approximate 60% PGM content. Subsequent treatment of concentrates and secondary metals varies depending upon the impurities, the ratios of the PGMs present, and the final use. In many processing plants today the actual separation of the PGMs from each other is performed by precipitation and solvent extraction.

The refining of the concentrate to separate the precious metals from one another takes advantage of the ready solubility of gold, platinum, and palladium in *aqua regia*. Rhodium, iridium, ruthenium, osmium, and silver are insoluble in *aqua regia*. Gold is separated from the soluble elements by reduction to the metallic form from the chloride solution by addition of ferrous salts or sulphur dioxide. The solution is then treated with ammonium chloride to precipitate the platinum as ammonium chloroplatinate, leaving palladium in solution.

A solution of palladium(II) tetrammine dichloride is obtained on heating the solution with ammonia and hydrochloric acid. Addition of hydrochloric acid precipitates palladium dichloride diammine, which is soluble in cold dilute ammonia. This series of reactions gives a high purity salt which is readily converted to the metal on heating.

The undissolved material after *aqua regia* treatment, plus minor amounts of platinum-group metals recovered from solutions after removal of platinum and palladium, is mixed with any available concentrates high in rhodium, iridium, and ruthenium. Fluxing materials, including lead carbonate and carbon, are added. The mixture is elevated to a high temperature in a crucible. The molten charge is poured into a conical mould. After solidification, the slag is removed and the lead, containing rhodium, iridium, silver and ruthenium, is melted, granulated and treated with nitric acid. Lead and silver are dissolved, removed, and recovered by this treatment. The insoluble residue contains the platinum by-metals. Sodium bisulphate fusion and a complex series of steps including precipitation, acid treatment, reduction, heat treatment and purification, yield rhodium sponge, ruthenium and iridium powder and potassium osmate. There is notable dependence of the treatment procedure on the precious metals contained in the sample.

1.1 Determination of the Platinum-Group Metals

In recent years, considerable interest has been shown in the development of techniques for the determination of the PGMs. This interest has been stimulated by the development of sophisticated and expensive instrumentation of high sensitivity (particularly inductively coupled plasma-mass spectrometry, ICP-MS) capable of extending applications to samples containing

$\mu g.dm^{-3}$ * levels of these elements. Despite these advances in instrumentation, most analytical techniques require a preconcentration and separation step so that these $\mu g.dm^{-3}$ detection limits can be achieved. Separation is usually required in order to overcome interferences during the measurement process.

Many current procedures use fire assay. This technique originated in biblical times and, with certain modifications, is practised widely today. The reason for the requirement of fire assay is that the PGMs occur in nature at very low concentration levels and are frequently inhomogeneously distributed in the rock as discrete metal particles. In order to obtain reasonably representative samples and to be able to determine to $\mu g.dm^{-3}$ levels, or lower, it is necessary to take larger samples, typically 50 to 100g. Enormous improvements in detection limits have been achieved,[10] particularly when fire assay is used as a collection technique prior to detection using an ultra-sensitive instrumental technique.

The traditional lead fire assay collection[11,12] provides a means of preconcentrating gold, platinum, palladium and rhodium. Their efficient collection on a silver cupellation button is critically dependant on the "flux" composition (the mixture of reagents added to the sample prior to fusion) and assay conditions. Low recoveries for rhodium are not uncommon.

The neo-classical fire assay procedure with nickel sulphide collection[13] is gaining popularity because it provides efficient collection for the complete range of PGMs. Special techniques are required to avoid the loss of volatile osmium compounds at the button dissolution stage. The procedure is somewhat more time consuming as the removal of the nickel sulphide matrix requires acid dissolution. Unfortunately, the recovery of gold is not as efficient as with lead collection.

Subsequent to the preconcentration step is the final measurement of the individual elements. Such a measurement technique must show specific sensitivity to the element of interest and provide the required accuracy and precision. The analysis is complicated since very rarely does only one PGM occur in a sample and interference from the other PGMs is

---

* $\mu g.dm^{-3}$ ≡ parts per billion

widespread. An overview of the prevalent measurement techniques for the PGMs demonstrates the complexity of the procedures and instrumentation.

Prior to 1960, spectrophotometric methods were the techniques of choice for trace analysis. There are an abundance of colour forming reagents for the PGMs[14] and a surplus of methods for the quantitative determination of the PGMs. The most frequently used concentration ranges used are nearer the lower $\mu g.cm^{-3}$† regions. A selection of colour-forming reagents for platinum, palladium, and rhodium is outlined. Some are used directly whereas others are used in conjunction with an extraction step.

Platinum can be determined over a broad concentration range, extending from a lower level of 0.07 $\mu g.cm^{-3}$ using 1-phenylthiosemicarbazide[15], to 1170 $\mu g.cm^{-3}$ using the compound of platinum ammoniate with eosine.[16] The most sensitive reagents for the determination of platinum[29] are 1-phenylthiosemicarbazide (with a lower limit of detection of approximately 0.07 $\mu g.cm^{-3}$), dithizone (0.2 $\mu g.cm^{-3}$), tin(II) chloride (0.4 $\mu g.cm^{-3}$), and *p*-nitrosodimethylaniline (0.7 $\mu g.cm^{-3}$).

The reagents are typically organic compounds with functional groups containing nitrogen or sulphur, or both these electron donors. Typical reagents include nitrosoamines and nitrosonaphthols, amino acids, thiosemicarbazide and its derivatives, thiourea, and heterocyclic compounds with nitrogen and sulphur atoms (thiozolethiones and azolethiones), or inorganic reagents such as the widely used, tin(II) chloride. Use of other inorganic reagents such as tin(II) bromide[17] and the complex thiocyanates of platinum[18] are modest.

For general applicability, the preferred reagents for the determination of platinum are tin(II) chloride and *p*-nitrosodimethylaniline.[19] These two reagents are superior from the viewpoints of sensitivity, freedom from interference, application range, and accessibility to descriptive chemistry in the literature.

---

† $\mu g.cm^{-3} \equiv$ parts per million

Palladium may be determined by numerous spectrophotometric methods - more so than any other PGM. The majority of reagents for palladium are organic.[20] The widest concentration range for palladium by a single reagent include 2-mercaptobenzimidazole[21] (0.01-100 $\mu g.cm^{-3}$), 8-mercaptoquinoline[22] (5-270 $\mu g.cm^{-3}$), 2-mercapto-4,5-dimethylthiazole[23] (7-172 $\mu g.cm^{-3}$), and tin(II) bromide[24] (37-369 $\mu g.cm^{-3}$).

Useful reagents for the determination of palladium include nitrosoamines, for example the highly sensitive *p*-nitrosodimethylaniline,[25] oximes, particularly α-furildioxime,[26] nitrosonaphthols and their derivative,[27] and azo reagents, particularly monoazo compounds such as 1-(2-pyridylazo)-2-naphthol (PAN) and 1-(2-pyridylazo) resorcinol (PAR).[28] Furthermore, mercapto reagents, such as 2-mercaptobenzimidazole,[29] and thio reagents, such as thionalide[30] and thiourea,[31] are also useful reagents for the determination of palladium. Other reagents used for the determination of palladium are ethylenediaminetetraacetic acid (EDTA),[32] the stannous halides (chlorides and bromides)[24, 33], and complex palladium halides.[34]

Rhodium, in turn, has far fewer spectrophotometric methods than platinum and palladium. However, the determination of rhodium is possible over a wide range of concentrations (0.04-160 $\mu g.cm^{-3}$) using organic and inorganic reagents.[29] The most sensitive reagents for the determination of rhodium are 2-mercaptobenzimidazole[21] (0.04 $\mu g.cm^{-3}$), 2-mercaptobenzoxazole[35] (0.1 $\mu g.cm^{-3}$), *p*-nitrosodimethylaniline[36] (0.15 $\mu g.cm^{-3}$), 1,5-diphenylcarbazone[37] (0.3 $\mu g.cm^{-3}$), tin(II) bromide[38] (0.4 $\mu g.cm^{-3}$), and 1-(2-pyridylazo)-2-naphthol[39] (0.4 $\mu g.cm^{-3}$).

Most organic reagents for rhodium[29] are nitrosoamines of the benzene series - nitrosonaphthols, aliphatic amines, heterocyclic azo compounds, thio acids, heterocyclic compounds with sulphur and nitrogen atoms, and dyes (for example, xylenol orange[40]).

The stannous halides, which include tin(II) chloride,[41] tin(II) bromide,[38] and tin(II) iodide,[42] are the most notable inorganic reagents for rhodium. They have all been used successfully for the sensitive determination of rhodium. Finally, oxidising agents that convert rhodium to compounds of higher oxidation states with bright blue and violet colours should be noted. Rhodium is, for example, oxidised by sodium hypochlorite,[43] and by sodium

hypobromite[44] in alkaline solutions. The latter is the preferred method[29] for determinations of this type.

The lack of knowledge regarding the solution chemistry of the PGMs has contributed to the difficulty of developing methods for their efficient separation and determination. Practically all the methods mentioned deal with the problem of interfering constituents, particularly from other PGMs present in the solution.[45]

Spectrophotometric methods are still important for the determination of microgram amounts of iridium, osmium and ruthenium, the common methods being leuco-crystal violet,[46] thiourea,[47] and sodium thiocyanate[48], respectively. Nevertheless, their general use for the remainder of the PGMs has declined sharply with the advent of other spectroscopic methods.[49]

The most common final measurement techniques include flame-atomic absorption spectrometry (FAAS), instrumental neutron activation analysis (INAA) and inductively coupled plasma-atomic emission spectrometry (ICP-AES). As FAAS is relatively inexpensive and relatively easy to operate, it has come within reach of most industries, and become a widely used technique. FAAS is basically a single element technique with $\mu g.cm^{-3}$ sensitivity. However, it suffers from serious matrix and mutual element interferences[50,51] and only when used in conjunction with graphite furnace-atomic absorption spectrometry (GFAAS), does it compete with the $\mu g.dm^{-3}$ sensitivity of INAA.

The multi-element capability of INAA and ICP-AES is offset by the need for sophisticated hardware (a reactor) and time for the former, and the lack of heavy-element sensitivity for the latter. The current technique of choice at low concentrations would therefore be GFAAS, although the need for careful control of the solution chemistry is of paramount importance.

New and powerful tools, such as ICP-MS, are capable of sensitivity comparable to GFAAS and spark-analysis-for-traces (SAFT).[52] SAFT is based on sparking a sample collected into a lead button which has been flattened to give a disk. Measurement of the intensity of the elemental lines is made relative to lead. This approach was initially investigated

at MINTEK.[‡] Although new instrumental techniques are often extremely sensitive, there is still a great need for separation and preconcentration of the analyte of interest.

It is evident from the consideration of the spectrophotometric methods and instrumental techniques used for the determination of the PGMs that as the complexity of the determinations increase, so too does the cost of the instrumentation.

1.2 The Platinum-Tin(II) Chloride Complex

The reaction of tin(II) chloride with platinum-group metals has been known for over a century.[53,54,55,56] The reaction, first reported by Wöhler,[55] between tin(II) chloride and $PtCl_4^{2-}$ or $PtCl_6^{2-}$ in dilute hydrochloric acid (HCl) solutions (greater than 0.5 mol.dm^{-3} [§] (M) HCl), rapidly leads to the development of an intense red-orange colour. This colour has been exploited analytically for the spectrophotometric determination of trace amounts of platinum.[57,58,34] The nature of this interaction of tin(II) chloride has been the subject of a number of studies utilising absorptiometric,[59,60] preparative,[61,62] Mössbauer,[63] and heteronuclear nuclear magnetic resonance (NMR) spectroscopic techniques.[64,65]

Many authors have tried to isolate the complexes formed on platinum reaction with tin(II) chloride and to study their properties. The lack of agreement regarding the nature and composition of these complexes, and the formal oxidation state of the platinum in these complexes, has afforded numerous publications.[55,66,67] Notable disagreement as to the origin of the red-orange colour is evident.

Wöhler[55] suggested the red colour was due to colloidal platinum produced on reaction of tin(II) chloride with Pt(IV) but reported no definite stoichiometry. This reaction is analogous to the "purple of Cassius" when gold chloride is similarly treated.[56] This postulate was disproved by Ayres and Meyer[66] who showed that the coloured material readily passes through a semi-permeable membrane, such as colliodion. Further evidence against the postulate of a

---

[‡] Council for Mineral Technology, Randburg, Republic of South Africa.

[§] Molarity, mol.dm^{-3}, denoted as M.

colloidal material was outlined by Elizarova and Matvienko[67]. They argued that an increase in optical density (absorbance) of solutions at tin(II) chloride concentrations greater than that required for the reduction of platinum, was indicative of complex formation. Furthermore, the extractability of the red colour into organic solvents supports evidence for the presence of a complex. Ahmed and Koch[68] showed this in a study of platinum extraction into methyl isobutyl ketone (MIBK).

The red colour has also been attributed to chloroplatinous acid,[69] and Pt(II).[70] Both have been disproved by ingenious experiments on the part of Ayres and Meyer.[66] The former, chloroplatinous acid, may be discounted on the basis of colour comparisons between the reaction of tin(II) chloride and 10 $\mu g.cm^{-3}$ Pt(IV) , and the inherent colour of a concentrated, 1000 $\mu g.cm^{-3}$, chloroplatinous acid solution. Both final colours are approximately the same and the measured absorption spectra show vast differences. The latter, Pt(II), was discounted when Pt(IV) was evaporated to fumes with sulphuric acid to expel hydrochloric acid, and the solution treated with tin(II) sulphate. No colour developed. Therefore, simple reduction to Pt(II) cannot account for the colour reaction.

The origin of the red-orange colour on platinum reaction with tin(II) chloride is now known to result from the rapid reduction of any Pt(IV) species[71] to Pt(II), followed by, or concomitant with, complex formation of $PtCl_4^{2-}$ with the $SnCl_3^-$ moiety to yield a series of anionic $[Pt(SnCl_3)_nCl_{4-n}]^{2-}$ (n = 1 to 4) complexes, as well as the relatively stable $[Pt(SnCl_3)_5]^{3-}$ complex anion.[72,73] Characteristic absorption spectra show two absorbance maxima (λ = 310, 400 nm) and a shoulder at 475 nm.[72] The latter complex, $[Pt(SnCl_3)_5]^{3-}$, has been characterised by X-ray crystallography in the solid state,[74] and NMR studies prove its existence in hydrochloric acid solution.[64]

The configuration of the unusual quinqueco-ordinate ion, $[Pt(SnCl_3)_5]^{3-}$, diagrammed in Figure 1.2, has been shown to have a trigonal bipyramidal structure.[74] This structure comprises an equatorial platinum atom surrounded by five $SnCl_3^-$ ligands at the apices. These ligands are attached through platinum-tin bonds.[75] The trichlorostannato ion, with its lone pair of electrons, behaves as a weak σ-donor and, in accepting the electrons *via* back-bonding with the platinum, behaves as a strong π-acceptor.[76]

As a result of this, the five $SnCl_3^-$ ligands may be co-ordinated about platinum without excessive build-up of electron density on the central metal atom.

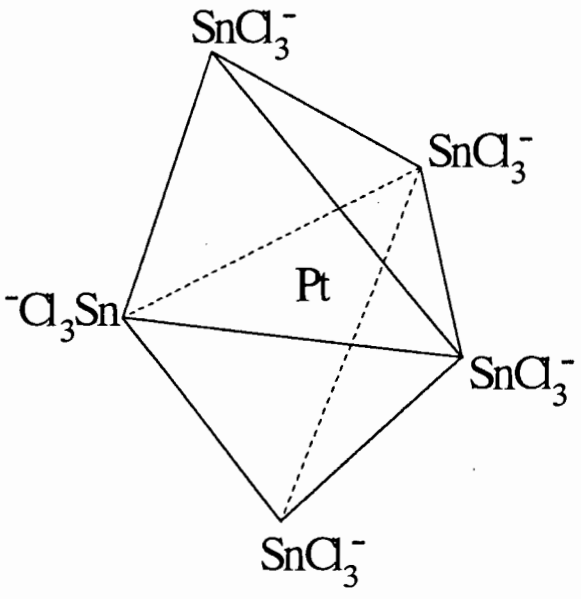

Figure 1.2 *The structural configuration of the unusual quinqueco-ordinate pentakis(trichlorostannato)platinum(II) anion.*

Most authors have assigned an oxidation state of two to platinum, and co-ordination numbers of 2 to 5 with respect to the $SnCl_3^-$ ligand. However, Ayres and Meyer[59] and Lindsey *et al.*[77] had previously detected Sn(IV) in solutions and suggested that the platinum had a zero-valent state. The nature of the complex was identified as a tetrapositive cation, $PtSn_4Cl_4^{4+}$, with the platinum in the zero-valent state, analogous to the zero-valent metal in tetracyanonickelate and tetracyanopalladate.[78] This formulation is largely discounted today.

Potentiometric and polarographic studies by Elizarova and Matvienko[67] on the same chemical system, established that complex formation with tin(II) chloride involves zero-valent platinum, not bivalent platinum. Shukla[79] demonstrated the presence of an anionic and not a cationic species by electrophoretic studies. Khattak and Magee[80] investigated the extractability of the complex by high molecular weight amines (HMWA) into organic solvents. They found that the coloured species was extracted and the same species was found in the aqueous and

amine phases by comparison of absorption spectra. This confirmed the findings of Shukla[79] but was in disagreement with the structure proposed by Ayres and Meyer.[59]

Extensive spectrophotometric studies on the reaction of tin(II) chloride and Pt(II), in hydrochloric acid solution, by Ayres and Meyer,[59] showed that the $SnCl_3^-$ moiety can bond to the platinum in several mole ratios - Pt(II):Sn(II) ratios of 1:4, 1:2, 1:1, 3:2, 2:1, 3:1, and 5:1 - with the principle complex having a Pt(II):Sn(II) mole ratio of 5:1.

Young *et al.*[72] determined the structure of a number of platinum-metal tin(II) complexes showing that they were anionic with formulated structures: *cis*- and *trans*- $[PtCl_2(SnCl_3)_2]^{2-}$, $[RuCl_2(SnCl_3)_2]^{2-}$, $[Rh_2Cl_2(SnCl_3)_4]^{4-}$, and $[Ir_2Cl_2(SnCl_3)_4]^{4-}$. The trichlorostannate(II) ion is considered to be acting as a donor anionic ligand of strength comparable to the chloride ion. Young and his co-workers were able to isolate the proposed square-planar *cis*- and *trans*-isomers of $[PtCl_2(SnCl_3)_2]^{2-}$ as the tetramethlyammonium salts - one yellow and the other red.

Although it was not possible for these workers to determine unequivocally the configurations of the two isomers, the yellow form was considered to be the *cis*-isomer. Some d_π-d_π bonding between platinum and tin would cause the *cis*-isomer to be more stable than the *trans*-isomer. This is because in the latter configuration there would be competition between the two $SnCl_3^-$ groups for the same *d*-orbitals of platinum. The result is a less stable complex and weaker bonding. Their results show that, while the red form is favoured kinetically, the yellow is more stable thermodynamically.

It is probable that several interdependent equilibria[72] exist simultaneously in solution and are of the type:

$$SnCl_2 + Cl^- \rightleftharpoons SnCl_3^-$$

$$[PtCl_4]^{2-} + SnCl_3^- \rightleftharpoons [PtCl_3(SnCl_3)]^{2-} + Cl^-$$

$$[PtCl_3(SnCl_3)]^{2-} + SnCl_3^- \rightleftharpoons \textit{trans}\text{-}[PtCl_2(SnCl_3)_2]^{2-} + Cl^-$$

$$\textit{trans}\text{-}[PtCl_2(SnCl_3)_2]^{2-} \rightleftharpoons \textit{cis}\text{-}[PtCl_2(SnCl_3)_2]^{2-}$$

$$\textit{cis}\text{- or }\textit{trans}\text{-}[PtCl_2(SnCl_3)_2]^{2-} + 3\,SnCl_3^- \rightleftharpoons [Pt(SnCl_3)_5]^{3-} + 2\,Cl^-$$

If substitution of $PtCl_4^{2-}$ by $SnCl_3^-$ takes place in two steps one would expect a *trans*-effect from $SnCl_3^-$ stronger than Cl^-, favouring initial formation of the *trans*-isomer. This was observed by Young and his co-workers.[72]

The ^{119}Sn-Mössbauer spectroscopic study of trichlorostannyl platinum complexes undertaken by Parish and Rowbotham[63] has questioned the existence of the *trans*-isomer, $[PtCl_2(SnCl_3)_2]^{2-}$. This is because this complex has identical Mössbauer and infra-red parameters as the red anion, $[Pt(SnCl_3)_5]^{3-}$. A more recent NMR study[64] has indicated that the predominant species present in 3 M HCl appears to be from a mixture of the yellow $[PtCl_2(SnCl_3)_2]^{2-}$ and red $[Pt(SnCl_3)_5]^{3-}$ complexes.

It may be concluded that the coloured species resultant from reaction of platinum with tin(II) chloride appears to be due to either,

(1) $[Pt(SnCl_3)_nCl_{4-n}]^{2-}$ (n = 1 to 4), or $[Pt(SnCl_3)_5]^{3-}$, or a mixture, and

(2) anionic in nature with both platinum and tin in the divalent oxidation state.

1.3 The Palladium-Tin(II) Chloride Complex

The most widely used method for the spectrophotometric determination of palladium is based on the compounds formed on reacting palladium with the stannous halides, particularly tin(II) chloride.[29] A slight variation of this reaction is the orange-red colour produced when a solution containing palladium is treated with tin(II) chloride together with mercury(II) chloride in hydrochloric acid. This was reported by Pollard[81] as a specific qualitative spot test for palladium.

As in the case of platinum, the existence of stable d_π-d_π bonds between the metal and stannous halides have been found.[75] Evidence of mixed polynuclear compounds that contain metal-halogen bridging bonds were also found. This bridging effect is more prevalent in complexes with rhodium and palladium than other PGMs.[82] In most instances, formation of these compounds, bridging and non-bridging, is accompanied by a change in the oxidation state of the PGM metal ion. The complexes are typical charge-transfer complexes so the study of

their electronic absorption spectra is of particular interest. A typical example of this approach is found in the study of the reaction between tin(II) chloride and palladium.

The reaction of Pd(II) with tin(II) chloride in hydrochloric acid solution is more rapid and apparently more complicated than that with Pt(II/IV), resulting in a series of rapid colour changes, from yellow-orange (λ = 420 nm) to red (λ = 355, 420 nm), through blue, and finally to dark green (λ = 380, 465, 636 nm). The origin of these colour changes is not well understood. It has been established that several complex species are involved. The nature of these complexes depends on *inter alia* the Pd(II):Sn(II) mole ratio and the hydrochloric acid concentration.[83,84] This accounts for variations in the reporting of the observed colours by some authors. Ayres and Meyer,[66] for example, report a black colour where blue has been reported elsewhere.[84]

The complexes of palladium with tin(II) chloride have been least studied. Young and his co-workers[72] studied the structures of the tin(II) chloride complexes of the other PGMs, but omitted palladium because an unstable complex was formed. Ayres and Meyer[66] found that the green complex was only extractable to a slight extent, and proposed it to be colloidal in nature; dialysis tests showed no evidence of it passing through a colloidion material.

Khattak and Magee[85] managed to precipitate the Pd-Sn anionic chloro-complex using tetraphenylarsonium chloride and, on the basis of their analytical data, suggested the following formula for the precipitated compound, $[(C_6H_5)_4As]_2[PdCl(SnCl_3)_2]$. Accordingly, it was proposed then that the structural formula for the Pd-Sn anionic chloro-complex be denoted as shown in Figure 1.3.

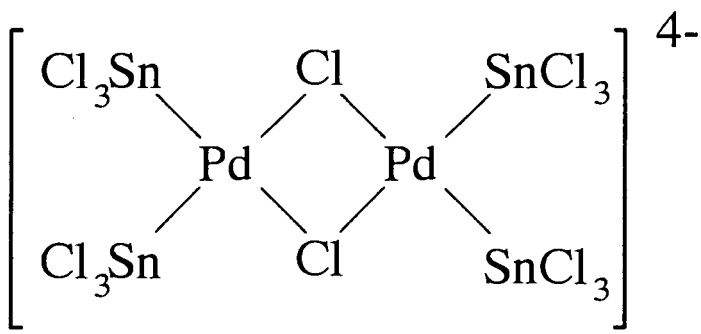

Figure 1.3 *The proposed structural formula for the Pd-Sn anionic chloro-complex.*

Further investigations by these authors involved the determination of the extractability of the complexes formed into tri-*n*-octylamine.[86] Two different complexes were found, the first red-brown, and the second yellow. Both are readily extracted into tri-*n*-octylamine in benzene. The yellow species possessed a definite absorption maximum (λ = 410 nm) in the amine phase, indicating stabilisation on extraction. This work, akin to work on platinum extraction by high molecular weight amines,[80] supported the conclusion that the species were anionic in nature.

The yellow and red complexes could be extracted into polar solvents, indicating their charged states. Absorption spectra taken of the red form in 3-methylbutanol revealed two absorption bands, at 355 nm and 420 nm (the latter being characteristic of the yellow form). The red complex appeared to be a short-lived species, sensitive to atmospheric oxygen, and converted to the yellow species rapidly. Addition of fresh tin(II) chloride leads to the production of the red form. This indicated that the red and yellow forms exist in solution in a state of dynamic equilibrium.[83]

Complexes of palladium with tin(II) chloride in hydrochloric acid solution showed the existence of at least three complex species, depending on the reaction conditions.[83] In addition to the postulated red and yellow species by Khattak and Magee,[86] a third and more stable complex resulting in a green colour exists. This complex is the final product at any concentrations of HCl, tin(II) chloride and Pd(II). Sufficiently high concentrations of tin(II) chloride leads to the rapid formation of the yellow and red colours, which are then converted to the green colour. Further increase in tin(II) chloride concentration was found to define the maximum characteristic of the green form (hyperchromic effect at 636 nm) more clearly. Further increase in tin(II) chloride concentration results in the decomposition of this species to give a brown solution from which metallic palladium separates. The remaining solution was almost colourless.

Zayats *et al.*[84] found that the nature of interaction in the tin(II) chloride, Pd(II), and HCl system depends on the mole ratio of palladium and tin(II) chloride in solution as well as the hydrochloric acid concentration. In solutions with a Pd(II):Sn(II) mole ratio of 1:2, or less, an unstable green palladium hydrosol is formed which coagulates on standing.

These authors[84] have proposed that this occurs according to the reaction:

$$Pd(II) + Sn(II) \rightleftharpoons Pd(0) + Sn(IV)$$

Metallic palladium may be recovered from the coagulated hydrosol. The characteristic absorption spectral bands are absent here. This is indicative of the absence of complex formation at these mole ratios.

At constant ratios of palladium and tin(II) chloride concentrations, the composition and stability of complexes formed was dependant on the hydrochloric acid concentration. The complexes formed with a Pd(II):Sn(II) mole ratio of 1:8, in 0.5 M HCl, gave a green colour to the solution. In 2 M HCl, yellow, and in 8 M HCl, red-brown colours are formed. The complex formation was found to be dependant on the total concentration of metal salts. At fixed Pd(II):Sn(II) ratios, a considerable decrease in the concentration of the metal salts in solution, irrespective of the acidity, resulted in the formation of the yellow colour. Proof was given that in 2 M HCl the interaction of components led to the formation of primarily the green colour in concentrated metal salt solutions. In 8 M HCl an unstable violet colour, which converts to red-brown, is formed in concentrated solutions. The yellow colour appears in less concentrated metal salt solutions.

In summary, as in the case of platinum, it appears that the palladium-tin(II) chloride complex is anionic. In contrast to platinum, several species exist depending on the conditions. The green colour appears to predominate over all the colours generated by other complex forms, and is a result of the most stable complex over the widest range of conditions.

1.4 The Rhodium-Tin(II) Chloride Complex

The existence of three complexes in solution has been established for the reaction of tin(II) chloride with rhodium in hydrochloric acid. Sandell[58] stated that either the red complex (λ = 300, 475 nm), developed in 2 M HCl, or the yellow complex (λ = 310, 425 nm), occurring in less acidic media, could be used for spectrophotometric determination of rhodium. The third complex is an intermediate complex with an absorption maximum at 372 nm.

Although use of the red form is a less sensitive way to determine rhodium than the yellow form, it is preferred because of its colour stability and reproducibility within the time interval of colour development. Difficulties were experienced[87] in applying the yellow colour to quantitative spectrophotometric work. These colours originally were the basis for detection of the presence of rhodium,[88] and later, after investigation of these colour reactions, formed the basis of routine quantitative determinations of rhodium.[41,58,89,90] The tin(II) chloride reaction has been applied to the determination of rhodium in alloys and materials, in plutonium,[91] in uranium and in uranium alloys,[92] and fission products.[93]

Formation of the red or yellow complexes is reported to be principally dependant on the $SnCl_3^-$:Cl^- ratio.[94] The red and yellow colours are reversibly developed - the latter is converted to the red complex by addition of hydrochloric acid. This is believed to be due to the dependence on the $SnCl_3^-$:Cl^- ratio rather than the Rh(III):Sn(II) ratio. The yellow form appears on addition of water. There are differences in opinions concerning the quantitative aspects of this change, and to optimum conditions for the formation of these complexes. Ayres *et al.*[95] stated that the full colour intensity was attained in 3 to 5 minutes near the boiling point, with variations of acid concentration from 0.1 to 4 M HCl. Stein[96] found that heating for at least 15 minutes was required, and even then constant absorbance was not obtained after standing for 60 minutes. Maynes and McBryde[97] found that after heating for 40 minutes the absorbance showed a slow drift on cooling. Heating for 60 minutes yielded a stable absorbance, after 30 minutes, for at least 24 hours. Beamish and Van Loon[98] also found heating for 60 minutes to be sufficient for a stable absorbance. The acidity, time and temperature of heating, are additional factors that affect the formation of reaction products.

The equilibria being studied by the aforementioned authors is considered to be of the form shown below. Of particular interest is the effect of the ratio of $SnCl_3^-$ to Cl^- [94] in the equilibria. The possibility of Rh(I) complexes is ignored.

$$[RhCl_{6-n}(H_2O)_n]^{3-} + mSnCl_3^- \rightleftharpoons [RhCl_{6-n-m}(SnCl_3)_m]^{3-} + mCl^- + nH_2O$$

Young *et al.*[72] determined the structure of a number of tin(II) complexes with PGMs showing that they were anionic with a formulated structure given in Figure 1.4. For the

rhodium complex the formula is given as $[Rh_2Cl_2(SnCl_3)_4]^{4-}$ with metal-halogen bridging bonds. Electrophoretic studies by Shukla also demonstrated the presence of anionic species[79] in the Rh(III)-Sn(II) system in hydrochloric acid. Extraction of the yellow species with high molecular weight amines by Khattak and Magee[99] confirmed its anionic nature. As the red species could not be extracted, they proposed that the bridging bonds were cleaved by ligands such as amines to give planar rhodium complexes. This is somewhat similar to the bridging bonds of an olefin complex, such as norbornadiene, being cleaved by high molecular weight amines.

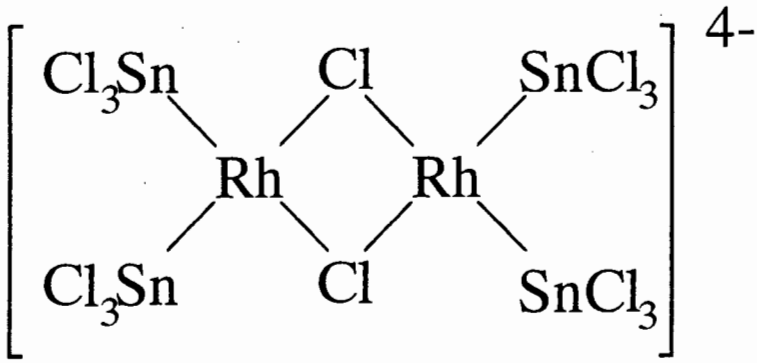

Figure 1.4 *A formulated structure for an anionic rhodium complex.*

The complexes formed when Rh(III) reacts with tin(II) chloride can be extracted with oxygen-containing solvents such as ethylacetate, *iso*-amylacetate, dibutyl ether, methyl hexylketone, and tributylphosphate.[58,100,101] More recently, extraction into MIBK was investigated by Wyrley-Birch and Koch[102] using NMR. They found, on the basis of ^{119}Sn and ^{1}H NMR data, that the predominant species in the MIBK phase was the *tetrakis*(trichlorostannato)rhodium(III) hydrido anion, $[RhH(SnCl_3)_4Cl]^{3-}$.

Furlani *et al.*[94] reported that a Rh(I) complex, $[AsPh_4]_3[Rh(SnCl_3)_4]SnCl_2$, was isolated from solutions with a mole ratio of Sn(II):Rh(III) as high as 100-500:1. This supported the view that the Rh(III) species are reduced by tin(II) under preparative conditions for spectrophotometric analysis. Young *et al.*[72,103] and Klinskaya *et al.*[104] suggested that the Rh(I) complexes were formed even for solutions in which the concentration of tin(II) chloride is of the same order as that of Rh(III).

In addition to the reported rhodium(I) complexes, rhodium(III) complexes, such as $[N(CH_3)_4]_3[Rh(SnCl_3)_nCl_{6-n}]$ (n = 1 to 4), have been isolated by Kimura *et al.*[105] from solutions with Sn(II):Rh(III) ratios of 1-4:1. The oxidation state of rhodium was determined by elemental analysis and the values of the reducing equivalents of the compounds in the reaction with iron(III). The existence of several rhodium(III)-tin(II) complexes, such as $[N(CH_3)_4]_3[Rh(SnCl_3)_nCl_{6-n}]$ (n = 2 to 5), in solutions having Rh(III):Sn(II) ratios of 1:2-8, was confirmed by ^{119}Sn Mössbauer spectroscopy.[106] Saito *et al.*[107] characterised a series of $[Rh(SnCl_3)_nCl_{6-n}]^{3-}$ (n = 1 to 5) complexes having Rh(III):Sn(II) ratios of 1:0.5-5, by Fourier-transform NMR in solutions of 3 M HCl. At a higher Rh(III):Sn(II) mole ratio of 1:6, the redox process between Rh(III) and tin(II) chloride to form the rhodium(I) complex anion, $[Rh(SnCl_3)_5]^{4-}$, was demonstrated. A kinetic investigation[108] also found evidence for a "purple species", assumed to be the $[Rh(SnCl_3)_5]^{4-}$ complex.

The complexity of the rhodium(III)-tin(II) chloride-hydrochloric acid system is evident and notably poorly understood, although advances in analytical instrumentation are permitting investigation into the true nature of the species present.

1.5 Tin(II) Bromide Complexes

Substitution of tin(II) bromide for tin(II) chloride gives greater sensitivity in the determination of the PGMs.[109] The reaction products and reaction schemes are presumed to be similar to those discussed for the tin(II) chloride system.[58] For example, it is known that the reaction of platinum with $SnCl_3^-$ and $SnBr_3^-$ produces platinum-tin(II) complexes of the type $[Pt(SnX_3)_nX_{4-n}]^{2-}$ (n = 1 to 4) and $[Pt(SnX_3)_5]^{3-}$ where X = Cl, Br.[110,111] Accordingly, attention is devoted in this section to absorption spectrum characteristics.

The absorption spectrum of the platinum-tin(II) complexes in 2 M hydrochloric acid have absorption maxima at λ = 310 nm and 400 nm, whereas in 2 M hydrobromic acid (HBr) the absorption maxima have shifted to longer wavelengths (λ = 358 nm and 460 nm).[112] This characteristic shift of the maximum absorbance to longer wavelengths is called a

"bathochromic shift" (also a red shift).** The shift arises from a difference in the ionisation potential of the halogens, chlorine and bromine. Bromine has a lower ionisation potential than chlorine. Hence, if all the chlorine atoms in the $Pt(SnCl_3)_5^{3-}$ anion were replaced with bromine atoms, its absorption spectra would show an absorption maximum shift to longer wavelengths.

The reactions of the PGMs with tin(II) bromide have not been investigated to the same extent as the tin(II) chloride reactions. Emphasis has been placed on the chloride system with minimal mention of the bromide system.[100,107] Nevertheless, the reactions of the PGMs with tin(II) bromide have been used analytically.[58] The reactions of four PGMs with tin(II) bromide are summarised below.

A red colour (λ = 463 nm) develops immediately at room temperature and is stable for several days on reaction of platinum with tin(II) bromide in HBr. The acidity should be 1 M HBr or greater. In the case of rhodium, a red-orange colour (λ = 475 nm) develops at room temperature but this changes to yellow (λ = 427 nm) after several hours. Perchloric acid stabilises the yellow colour. Reagent and acid concentrations require control. Palladium forms a yellow-brown colour (λ = 385 nm, plateau 440 to 460 nm) on reaction with tin(II) bromide, the intensity of which depends on the tin(II) bromide and HBr concentrations. The complex is stable for an hour under conditions of 3 M HBr and 0.1 M tin(II) bromide. In the case of iridium, no significant colour development is observed at room temperature, even after several days. A yellow colour develops on heating (λ = 403 nm), which is stable for several hours (~ 2-3 M HBr and 0.1-0.2 M tin(II) bromide). Tin(II) bromide itself absorbs below 400 nm, as does tin(II) chloride, and any minor absorbance from the reagent is readily corrected by the use of a blank solution.

It is evident from the text that both the tin(II) chloride and tin(II) bromide systems require critical control of the experimental conditions prior to spectrophotometric measurements. Should accurate control not be maintained, the experimental results would no doubt be in question. An analysis using a common manual spectrophotometric method (that is sample preparation, dilution, reagent addition, dilution, incubation for a fixed time period, and

---

** The opposite effect, to shorter wavelengths, is referred to as a hypsochromic (blue) shift.

finally measurement against known standard solutions taken through the same procedure) is lengthy and requires considerable analytical experience and capability. An improved experimental approach that would reduce the complexity of the steps, and thereby better the reproducibility prior to measurement, would be invaluable.

Having considered the complex chemistries taking place on reaction of the PGMs with tin(II) chloride and tin(II) bromide, one may be quite wary of attempting to study such a system with new flow-based technology. Nevertheless, these complex chemistries and associated problems with analysis posed a considerable challenge and opportunity to the author. The following section will detail the finer aspects of the flow-based technology used in this research.

1.6 Flow-Injection Analysis

Any measurement in a chemical laboratory involving liquids comprises the following operations: solution handling, analyte detection, data collection, and computation of the results. Computers and sophisticated detectors aid scientists in the latter two tasks, but solution handling requires an arsenal of skills essential to the successful completion of the task. Mixing, decanting, pipetting, and other volumetric operations are still performed manually, even in the most advanced laboratories, using apparatus that was designed more than 200 years ago. Moreover, volumetric glassware was designed for the manual handling of large volumes (5-500 cm^3) as one cannot readily manipulate smaller volumes with the required reproducibility using conventional glassware. The handling of large volumes translates into large volumes of hazardous laboratory waste, large quantities of expensive reagents, and a high probability of glass cuts and chemical burns as a result of chemical contact.

Some industrial laboratories have turned to robotics to enhance the efficiency of laboratory tasks and to remove humans from potential danger. However, robots are limited mechanically and conceptually by their inability to simulate human manipulations. Manual handling of robots requires extensive programming and active feedback control, and they are generally too expensive. Their use is justified in the case of repetitive operations (such as

weighing, handling radioactive materials, sample preparation, and chromatographic column sample injection) to be executed over prolonged periods.

A peek into a modern industrial research laboratory will reveal rapidly expanding use of flow-based methods where batch operations were previously used. Flow operations are much easier to automate since they involve motion of liquids in small bore tubing where the microvolumes are conveniently manipulated by pumping devices. Repeatable paths through which the solutions move are maintained, providing an environment where highly reproducible mixing of components and formation of reaction products takes place. The versatility of the flow operations is seen in the ability of flowing streams to be mixed, stopped, restarted, reversed, split, recombined, and sampled.

In addition, flow operations allow most detectors and sensors to be used in a more reproducible manner than when used in manual batch operations. This is evident to anyone who has used both conventional and flow-through cuvettes in spectrophotometry. The requirement of homogenous mixing and a "steady-state" signal, previously thought to be the only manner in which a reproducible measurement may be made, is obviated by repeatable flow operations where highly reproducible transient signals are attained.

Flow-injection analysis (FIA)[113] belongs to a family of methods, based on sample injection into a flowing stream, which transports the analyte under consideration through a chemical modulator into a detector.

This broad family of methods embraces chromatography, electrophoresis, field flow fractionation, and flow-injection analysis. The individual members differ in one fundamental respect, *viz.*, the function of the chemical modulator, which alters the original square-wave input, provided by the sample injection, into a chromatogram, electrophogram, fractogram, or fiagram, respectively, as depicted in Figure 1.5. The chemical modulator, or force that occurs within it, is a column for chromatography, an electric field for electrophoresis, an external force for field flow fractionation, and an open-tubular reactor (reaction coil) for flow-injection analysis.

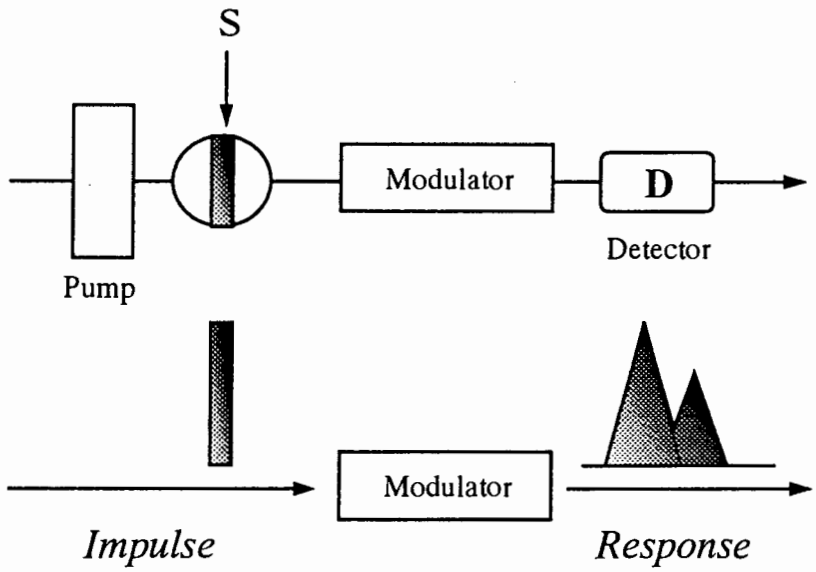

Figure 1.5 *Flow scheme (top) and concept (below) of analytical techniques based on the injection of the sample analyte into a flowing carrier stream.*[114]

Originally designed to automate serial assays,[113] FIA emerged during its first decade of use as a most powerful and versatile solution-handling and data-gathering technique,[115] *albeit* the youngest of the flow-based techniques. Irrefutable proof of its versatility lies in the large number of alternatives derived from the basic mode and the range of applications. FIA has encompassed a full range of reagent assays from inorganic to enzymatic, from ions to proteins, and from traces to highly concentrated analytes in aqueous or non-aqueous media. Industrial, clinical, research, environmental, and biotechnological applications of FIA have been described in over 4000 publications and several monographs[116,117,118,119] and discussed at numerous meetings, of which "Flow Analysis" is the most recognised international venue.

Flow-injection analysis, in its simplest and most commonly used form, is based on the injection of a liquid sample into a moving, non-segmented continuous carrier stream of a suitable liquid. The injected sample forms a zone that, during its transport towards a detector, disperses in the carrier stream and may be conditioned (for example, chemical reaction, ion-exchange, heating) *en route* to the detector. The detector continuously monitors the absorbance, electrode potential, fluorescence, chemiluminescence, or other physical parameter

of the solution as it continuously changes due to the passage of the sample through a flow cell.[116] The shape and magnitude of the resulting transient signal reflect the concentration of the injected analyte, along with thermodynamic and kinetic information of the processes occurring in the flowing stream.

The simplest, single-line, flow-injection analyser, Figure 1.6, consists essentially of four components. Together, the complete FIA system is termed a *manifold.* The main components of the manifold are a pump, valve, reactor, and a detector - the data acquisition device.

The pump is the first component and it is used to propel the carrier stream through a narrow tube. The pump is most often a multi-roller peristaltic pump, accommodating one or more pump channels, whereby, according to individual pump tube diameters, equal or different volumetric pumping rates may be obtained. Gas-pressurised reservoirs, piston or reciprocating pumps, and even gravity feeds have been used for FIA solution propulsion.[116] Each propulsion method has its own inherent advantages and disadvantages. FIA is not limited to laminar flow (convective flow) as one would expect. Other flow configurations that have been used successfully for specific applications include intermittent pumping (stopped-flow),[120] oscillating (reversed flow),[121] and sinusoidal flow (variable flow).[122]

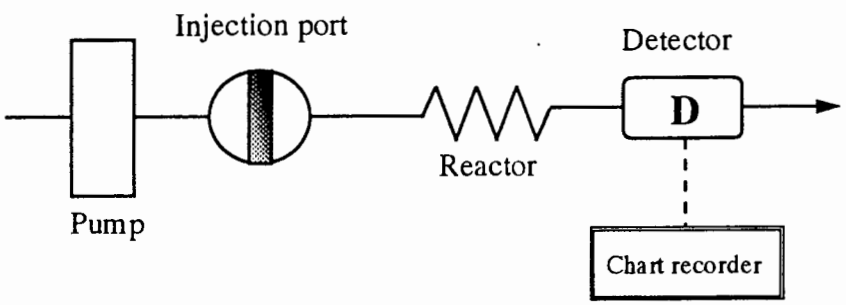

Figure 1.6 *Schematic of a single-line flow-injection analysis manifold with a chart recorder to record the transient detector response.*

The second component is an injection valve. This is the means by which a well-defined volume of the sample solution is introduced into the carrier stream in a highly reproducible manner. Four modes of injection have been used in FIA systems - syringe injection, valve injection, hydrodynamic injection, and time-based injection. The most primitive method is syringe injection[113] that uses a syringe furnished with a hypodermic needle that allowed introduction of the sample by piercing the tubing wall. This method relied heavily on operator skill in reproducibly dispensing an accurate volume of sample and is seldom still used. An improvement is the valve injection approach. This method of sample introduction is most commonly used today. Valves are either of the rotary type or commutation type.[123]

The rotary valve has two stages of operation - "injection" and "loading". A typical 6-port valve is shown in Figure 1.7. In the "load" position, a volumetric cavity (sample loop) is filled with the sample whilst the carrier is shunted directly through the valve to prevent any pressure increase. The valve is then switched to the "inject" position (manually, mechanically, or pneumatically) and the carrier sweeps the fixed sample volume (called a zone) toward the detector. During the inject stage the sample loop may be filled in preparation for the next injection.

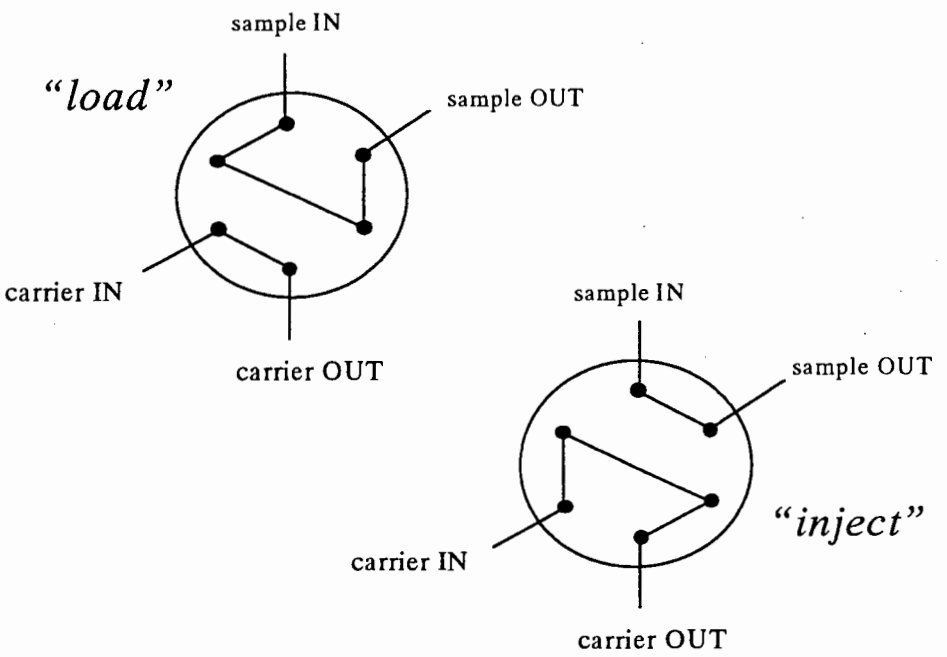

Figure 1.7 *Schematic of a six-port rotary injection valve showing the "load" and "inject" positions.*

Multi-port valves[124] enable the use of innumerable configurations for sample introduction, manipulation, and even on-line solvent extraction,[125] prior to detection.

Hydrodynamic injection[126] eliminates the moving parts of the sample introduction mechanism, where a peristaltic pump is used to "load" a sample zone into a stationary carrier stream. Once the sample zone is "injected" in this manner, the carrier recommences motion toward the detector.

Finally, the common approach for time-based injections[127] is that the sample volume is metered as a function of time. The sample loop, using the time-based injection method, is only partially emptied - the volume dispensed having been calibrated previously. Stepper motors are often used to "switch" rotary valves between the "inject" and "load" positions. These stepper motors are operated using microcomputer control.

The third component of a FIA system is the reactor (the modulator). The most commonly used reactors are made of plastic tubing (usually 0.5 to 1.0 mm I.D.[††]), which can be coiled, knotted, or knitted.[116,128] This geometric deformation has an effect on the sample zone dispersion, promotes radial mixing between the sample and reagent contained in the carrier stream, and thereby affects the resulting transient FIA response. Other reactors include miniaturised packed reactors containing solid reagents,[129] immobilised enzymes,[130] ion exchangers,[131] reductants,[116] or silica- or polymer-based C_{18} materials.[132] Solvent extraction, gas diffusion and titrations have also been performed by FIA with specialised reactors.[116] Selection of a reactor naturally depends on the required chemistries. In addition to these components, various other components have also been incorporated in the manifold. These include dialysis units, supported liquid membranes, phase separators, and various mixing points.

The fourth and final component of a manifold is the detector, and closely associated with this, the detector response recording device. Amongst the first procedures adapted for FIA were classical colorimetric methods (ammonia, phosphate, glucose and ethanol), where spectrophotometers were readily available. Installation of a flow-through cuvette immediately

---

[††] I.D. ≡ Inner diameter

enabled the detector to be used in a FIA system with no further capital outlay for sophisticated apparatus.

Besides the detectors we know for classical instrumental analyses[‡‡], a new breed of sensors, such as field-effect transistors, piezoelectric and optical-fiber-based devices, are being incorporated into FIA systems. Advances in instrument and microcomputer technology resulted in the development of scanning array detectors that now add a new dimension to FIA as multi-channel data, previously inaccessible, is now available. Miniature robust detectors are also available, or possible to construct, for work in areas where a laboratory instrument is too vulnerable. Large spectrophotometers are readily exchanged for "home-made" matchbox-sized light-emitting diodes (LEDs), phototransitors, and associated electronics.[133]

The recording device is indispensable in a FIA system. It not only records the response of the detector, from which the analytical result may be obtained, but it records the transient FIA profile that enables diagnosis of the operational status. The form of the recording device varies from the customary chart recorder to microcomputer-based software packages written with FIA profile capture in mind. When the detector is an array-type instrument, a microcomputer is essential to process and manipulate the vast quantities of data generated.[134] Software is usually available for such commercial instrumentation.

Having demonstrated the manual operation of FIA in the laboratory, the progression is to the partial or complete automation of FIA systems using microcomputers. In recent literature, most of the FIA systems implemented have a common denominator in the automation of the injection valve by some means with microcomputer control of sample introduction[135,136] and electronic data acquisition. Some systems have been automated to such an extent that they are able to operate for prolonged periods without operator assistance - aside from replenishing reagent solutions.[137] The pumps, injection valves, and possibly selection valves (for selecting either samples or standard solutions) can be readily automated. Some components of the manifold, pumps for example, are supplied with built-in remote control of pump flow direction

---

‡‡ *Viz.* spectrophotometers, flame-atomic absorption spectrometers, pH and ion-selective electrodes (ISE)

and flow rate (based on TTL control logic and voltage changes to give variable pump rotation speeds, respectively).

The detector output may be interfaced to the microcomputer via an analog-to-digital converter, enabling sophisticated signal processing and manipulation with the aid of the appropriate software. FIA has also been applied outside the pristine environs of a laboratory in process analysers. These process analysers are already widely used, particularly in the U.S.A. and Europe.

A closer look at a FIA manifold, particularly the detector output, reveals the uniqueness of this approach to sample analysis. The manifold depicted in Figure 1.8 is a merging-stream manifold where the two streams converge and mix at a point downstream.

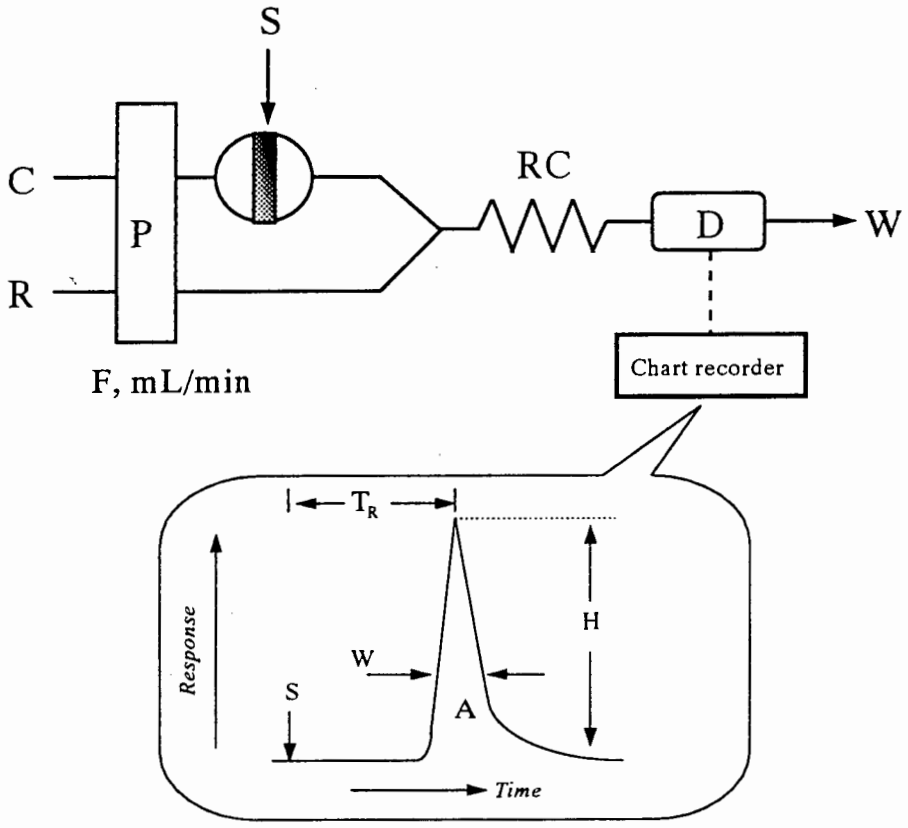

Figure 1.8 *Scheme of a two-line manifold (merging stream) with the characteristic transient signal response obtained. See text for details.*

The pump, P, propels the carrier stream, C, and the reagent stream, R, to a confluence point. The sample, S, is injected *via* an injection valve into the moving carrier stream, and the sample zone then merges with the reagent stream. Mixing occurs along the whole length of the sample zone and a reaction takes place (for example, a colour-forming reaction). The duration that the sample zone reacts with the reagent is controlled by the length of the reactor coil, RC, and the flow rate, F. The time from sample injection until the appearance of the maximum signal response is termed the residence time, T_R.

The detector monitors a response (for example, a photometer monitors the absorbance at a selected wavelength) generated by the products of the reaction. After passage through the detector, the waste, W, is discarded. A typical recorder response (enlarged) has the form of a peak. By using standard calibrant solutions, the height, H, width at a specific peak height, W, and area, A, may be related to the concentration of the injected sample.

In a well-designed FIA system the response is rapid and usually of the order of a few seconds (5-30 seconds). This low sample residence time enables high sampling rates (often in excess of 60 $hour^{-1}$). These figures of merit are an outstanding feature of FIA. Even when longer periods of time are necessary to enable adequate reaction product to form prior to detection, the residence times per sample need not extend to more than a few minutes.

Sample, reagent and carrier consumption may be of the order of micro- or millilitres per injection. However, in spite of the relatively low flow rates (~ 1 to 2 $cm^3.min^{-1}$) used, a FIA system in continuous operation consumes large volumes of these solutions (approximately 10 dm^3 per week). Nevertheless this disadvantage is offset by the overall economic advantage of using a FIA system to replace existing manual methodology. Certainly the volumes used in FIA are far more economical than manual batch processes.

Another notable feature of FIA is its inherent simplicity based on its components and easy operation. FIA is, as a rule, less sensitive than manual methods as a result of the shorter reaction times and non-equilibrium conditions, and the additional dispersion (or dilution) of the sample in the manifold streams. This does not detract from its performance. The increased tolerance for interferences is an additional feature when using FIA methods. This may be attributed to the kinetic character of the FIA technique in that undesirable reactions do not

have the opportunity to take place in the short residence period. Their effect on the final signal is thereby significantly reduced. These features have no doubt contributed to the world-wide use and recognition of FIA.

Future application of flow-injection analysis in the analytical laboratory and in industrial fields will no doubt be of notable proportion considering the advances made to date. Elo Hansen,[138] one of the two "inventors" of FIA, comments critically that FIA is far from being exploited because "*the ultimate test for an analytical technique is not that it can do better than what can be done by other means, but that it permits us to do something that cannot be done in any other manner.*" It is with this statement in mind that this work to study and determine the platinum-group metals by flow-injection analysis was undertaken.

1.7 Objectives of Research

In view of the wealth of information regarding the spectrophotometric determination of the PGMs, and considering the potential of FIA in the research and process environments, a combination of these two would no doubt be powerfully synergistic. Such a solution, or substantial improvements to the problems encountered in the batch-mode method of analysis, would be unique; particularly if multi-element capability could be added. A method for the simultaneous determination of the PGMs would require a suitable multi-channel data acquisition system and sophisticated software for processing this multi-channel data.

As analytes in multi-component systems are not physically separated in FIA, such data processing is required to enable accurate deconvolution of overlapping absorption spectra. The field of chemometrics involves the employment of mathematical methods to extract chemical information from data collected from multi-dimensional detectors. The current trends show a definite propensity toward the use of multi-channel detectors to enable resolution of multi-component systems.

Chapter 2 of this thesis is devoted to the theory and application of quantitative analytical visible spectrophotometry. Single and multi-component methods will be presented, along with criteria for the selection of analytical wavelengths to facilitate multi-component mixture

resolution. The principles of FIA as a powerful analytical tool based on controlled solution manipulation is introduced.

The requirements of a data acquisition system and sophisticated software for processing multi-channel data are addressed in Chapter 3. Computer-aided Flow Analysis methodology enables facile automation and control of the data acquisition. The development of a new and versatile software package, based on the Microsoft® Windows™ operating environment, is outlined and serves as the mathematical tool for single and multi-component analysis.

In Chapter 4, the design and optimisation of the FIA manifold is described. An emphasis is placed on the development of FIA methods where careful consideration of several experimental parameters is undertaken. The concept of "Flow Chemography",[139] where the data from flow-based techniques is presented graphically or pictorially, is illustrated by the use of the developed software, in conjunction with third-party graphical software, to represent three-dimensional surfaces that are used to facilitate manifold optimisation.

The development of single component methods for the determination of the PGMs in an "on-line" fashion using FIA is the topic of Chapter 5. Exploration of the finer details of the chemistry occurring in solution is undertaken by means of multi-dimensional plots. A critical investigation of the complexes formed on reaction of Pd(II) with tin(II) chloride will be undertaken. In addition, the effect of various interferences is determined.

Chapter 6 is devoted to the development of methodology for the multi-component determination of the PGMs by FIA. Binary component mixtures of some PGMs in tin(II) chloride are considered with the view to illustrate the complexity, yet in some ways simple task, of multi-component mixture resolution. Preliminary steps toward a mathematical method of wavelength selection for MCA will be outlined. The results of investigations into the use of tin(II) bromide as a reagent for the simultaneous determination of PGMs are reported.

A comprehensive summary of this work and its significant findings is presented in Chapter 7. The direction for future research involving multi-component FIA, and FIA in general, is given. Finally, details pertaining to the experimental work such as the analytical instrumentation used, chemicals and their suppliers, and FIA apparatus are noted in Chapter 8.

1.8 References

1. "*Kirk-Othmer Encyclopaedia of Chemical Technology*", 3rd edn., John Wiley & Sons, New York, 1982, Vol 18, 228.
2. Nathan, B., "*The Platinum Yearbook 1991*", Woodhead, London, 1991.
3. Coombes, J.S., "*Platinum 1993 : Interim Review*", Johnson Matthey, London.
4. Walsh, M.P., *Platinum Metals Rev.*, 1992, **36**, 126; *ibid*, 1993, **36**, 7.
5. Coombes, J.S., "*Platinum 1991*", Johnson Matthey, London.
6. "*Mintek Annual Report 1993*", Council for Mineral Technology, Randburg, Rep. S. Afr., 1993, 25.
7. Gooding, K., *Financial Times*, November 1994, 26.
8. Kelland, L.K., Clarke, S.J., and McKeage, M.J., *Platinum Metals Rev.*, 1992, **36**, 178.
9. Rosenberg, B., VanCamp, L., Trosko, J.E., and Mansour, V.H., *Nature* (London), 1969, **222**, 385.
10. Date, A.R., Davis, A.E., and Cheung, Y.Y., *Analyst*, 1987, **112**, 1217.
11. Smith, E.A., "*The Sampling and Assay of the Precious Metals*", Revised 2nd edn., Met-Chem. Research, Colorado, 1987.
12. Van Loon, J.C., *Pure Appl. Chem.*, 1977, **49**, 1495.
13. Robert, R.V.D., Van Wyk, E., and Palmer, R., *Nat. Inst. Metall., Rep. S. Afr.*, 1971, No.1371.
14. Marckzenko, Z., "*Separation and Spectrophotometric determination of the elements.*", 2nd edn., Ellis Horwood Ltd., England, 1986, 453.
15. Komatsu, S., and Onishi, K., *J. Chem. Soc. Japan*, 1955, **76**, 661.
16. El Ghaniry, M., and Frei, R., *Talanta*, 1969, **16**, 235.
17. Danilova, V.N., and Lisichenok, S.L., *Zh. Anal. Khim.*, 1969, **24**(7),1061.
18. Fortsythe, J.H.M., Magee, R.J., and Wilson, C.U., *Talanta*, 1960, **3**, 324.
19. Kirkland, J., and Yoe, J., *Analyt. Chem.*, 1954, **26**, 1335.
20. Beamish, F.E., and McBryde, W.A.E., *Anal. Chim. Acta*, 1958, **18**, 551.
21. Bera, B., and Chakrabartty, M., *Mikrochim. Acta*, 1966, **6**, 1094.
22. Bankovskii, Y.A., and Ievinysh, A.F., *Zh. Anal. Khim.*, 1960, **13**, 507.

23. Rodford, A.J., *Analyst*, 1960, **85**, 445.
24. Pantani, F., and Piccardi, G., *Anal. Chim. Acta*, 1960, **22**, 231.
25. Faye, G.H., and Inman, N.R., *Analyt. Chem.*, 1961, **33**, 278.
26. Menis, O., and Rains, T.C., *Anal. Chem.*, 1955, **27**, 532.
27. Cheng, K.L., *Anal. Chem.*, 1954, **26**, 1894.
28. Stanley, R.W., and Cheney, G.E., *Talanta*, 1966, **13**, 1619.
29. Ginzburg, S.I., *et al.*, "*Analytical Chemistry of the Platinum Metals*", John Wiley and Sons, New York, 1975.
30. Busev, A.I., and Shishkova, A.N., *Zh. Anal. Khim.*, 1968, **23**, 1675.
31. Nilsch, W., *Mikrochim. Acta*, 1954, 530.
32. MacNevin, W.M., and Kriege, O.H., *Anal. Chem.*, 1954, **26**, 1768.
33. Khattak, M.A., and Magee, R.J., *Anal. Chim. Acta*, 1966, **35**(1),17.
34. Payne, S.T., *Analyst*, 1960, **85**, 698.
35. Ryan, D., *Analyt. Chem.*, 1950, **22**, 599.
36. Wilson, R., and Jacobs, W., *Analyt.Chem.*, 1961, **33**, 1650.
37. Ayres, G., and Johnson, F., *Anal. Chim. Acta*, 1960, **23**, 448.
38. Berman, S., and Ironside, R., *Can. J. Chem.*, 1958, **36**, 1151.
39. Busev, A.I., Groessl, V.G., and Ivanov, V.M., *Anal. Lett.*, 1968, **1**(4), 267.
40. Otomo, M., *Japan Analyst*, 1968, **17**, 125.
41. Ayres, G.H., Tuffly, B.L., and Forrester, J.S., *Anal. Chem.*, 1955, **27**, 1742.
42. Berg, E.W., and Youmans, H.L., *Anal. Chim. Acta*, 1961, **25**, 366.
43. Ayres, G.H., and Young, F., *Analyt. Chem.*, 1952, **24**, 165.
44. Pantini, F., *Talanta*, 1962, **9**, 15.
45. Beamish, F.E., and Van Loon, J.C., "*Recent Advances in the Analytical Chemistry of the Noble Metals*", Vol. 48, Permagon Press, New York, 1972.
46. Ayres, G.H., and Bolleter, W.T., *Anal. Chem.*, 1957, **29**, 72.
47. Tschugaeff, L., *C. R. Acad. Sci. Paris*, 1918, **167**, 235.
48. Belew, W.L., Wilson, G.R., and Corbin, L.T., *Analyt. Chem.*, 1961, **33**, 886.
49. Van Loon, J.C., *Trends in Anal. Chem.*, 1985, **4**(4), 24.
50. Strasheim, A., and Wessels, G.J., *Appl. Spectrosc.*, 1963, **17**, 65.

51. Mallett, R.C., Pearton, D.C.G., Ring, E.J., and Steele, T.W., *Talanta*, 1972, **19**, 181.
52. *"Council for Mineral Technology Bulletin"*, Rep. S. Afr., No. 40, Aug., 1991.
53. Schneider, R., *Poggendorff's Ann.*, 1869, **136**, 105.
54. Ditte, M.A., *Ann. Chim. Phys.*, 1882, **27**, 145.
55. Wohler, L., *Chem. -Ztg.*, 1907, **31**, 938.
56. Spengel, A., and Wohler, L., *Z. Chem. Ind. Kolloide*, 1909, **7**, 243.
57. Thompson, S.O., Beamish, F.E., and Scott, M., *Ind. Eng. Chem.*, 1937, **9**, 420.
58. Sandell, E.B., *"Colorimetric Determination of Traces of Metals"*, 3rd edn., Interscience, New York, 1959.
59. Meyer, A.S., and Ayres, G.H., *J. Am. Chem. Soc.*, 1955, **77**, 2671.
60. Elizarova, G.L., and Matrienko, L.G., *Russ. J. Inorg. Chem.*, 1973, **18**, 254.
61. Young, J.F., Gillard, R.D., and Wilkinson, G., *J. Chem. Soc.*, 1964, 5176.
62. Baird, M.C., *J. Inorg. Nucl. Chem.*, 1967, **29**, 367.
63. Parish, R.V., and Rowbotham, P.J., *J. Chem. Soc. Dalton Trans.*, 1973, 37.
64. Nelson, J.H., Cooper, V., and Rudolph, R.W., *Inorg. Nucl. Chem. Lett.*, 1980, **16**, 263.
65. Koch, K.R., Fazakerley, G.V., and Dijkstra, E., *Inorg. Chim. Acta*, 1980, **45**(2), 51.
66. Ayres, G.H., and Meyer, A.S., *Anal. Chem.*, 1951, **23**(2), 299.
67. Elizarova, G.L., and Matrienko, L.G., *Russ. J. Inorg. Chem.*, 1970, **15**(6), 823.
68. Ahmed, N., and Koch, K.R., *Anal. Chim. Acta*, 1984, **162**, 347.
69. Treadwell, F.P., and Hall, W.T., *"Analytical Chemistry"*, 6th edn., Vol. 1, John Wiley and Sons, New York, 1921.
70. Hunter, D., Milton, R., and Perry, K.M.A., *Brit. J. Ind. Med.*, 1945, **2**, 95.
71. Moodley, K.G., and Nicol, M.J., *J. Chem. Soc. Dalton*, 1977, 239.
72. Young, J.F., Gillard, R.D., and Wilkinson, G., *J. Chem. Soc.*, 1964, 5176.
73. Wilson, W.L., Holt, M.S., and Nelson, J.H., *Chem. Rev.*, 1989, **89**, 11.
74. Alcock, N.W., and Nelson, J.H., *Inorg. Chem.*, 1982, **21**, 1196.
75. Cramer, R.D., Lindsey Jr, R.V., Prewitt, C.T., and Stolberg, U.G., *J. Amer. Chem. Soc.*, 1965, **87**(3), 658.
76. Lindsey Jr, R.V., Parshall, G.W., and Stolberg, U.G., *J. Amer. Chem. Soc.*, 1965, **87**(3), 659.

77. Lindsey Jr, R.V., Parshall, G.W., and Stolberg, U.G., *Inorg. Chem.*, 1966, **5**, 109.

78. Estes, J.W., and Burger, W.M., *J. Amer. Chem. Soc.*, 1942, **64**, 2715; 1943, **65**, 1484.

79. Shukla, S.K., *Ann. Chim.*(Paris), 1961, **13**, 1432.

80. Khattak, M.A., and Magee, R.J., *Talanta*, 1965, **12**, 733.

81. Pollard, W.B., *Analyst*, 1942, **67**, 184.

82. Adams, D.M., and Chandler, R.J., *Chem. Ind.*, 1965, No. 6, 269.

83. Shlenskaya, V.I., Biryukov, A.A., and Moryakova, L.N., *Russ. J. Inorg. Chem.*, 1969, **14**, 255.

84. Zayats, A.I., Psareva, T.S., and Shabanov, V.F., *Russ. J. Inorg. Chem.*, 1976, **21**, 393.

85. Khattak, M.A., and Magee, R.J., *Chem. Commun.*, 1959, **17**, 400.

86. Khattak, M.A., and Magee, R.J., *Anal. Chim. Acta*, 1966, **35**, 17.

87. McBryde, W.A.E., and Yoe, J.H., *Anal. Chem.*, 1948, **20**(11), 1094.

88. Wolbling, H., *Ber.*, 1934, **67**, 773.

89. Kalinin, S.K., and Yakovleva, G.A., *Zh. Anal. Khim.*, 1970, **25**(2), 312.

90. Beamish, F.E., *Talanta*, 1965, **12**, 789.

91. Smith, M.E., *Analyt. Chem.*, 1958, **30**, 912.

92. Karttunen, J.O., and Evans, H.B., *Analyt. Chem.*, 1963, **35**, 1043.

93. Cheneley, R.B., and Osmond, R.G., *U.S. Atomic Energy Res. Establ.*, 1956, No. 10, 1870.

94. Furlani, C., Zinato, E., and Furlan, F., *Atti. Accad. Naz. Lincei, Rend. Cl. Sci. Fis. Mat., natur.*, 1965, **38**, 517.

95. Ayres, G.H., Tuffly, B.L., and Forrester, J.S., *Anal. Chem.*, 1955, **27**, 230.

96. Stein, H.H., *M.Sc Thesis*, Univ. of Minnesota (cited in ref. 58).

97. Maynes, A.D., and McBryde, W.A.E., *Analyst*, 1954, **79**, 230.

98. Beamish, F.E., and Van Loon, J.C., "*Analysis of the Noble Metals*", Academic Press, New York, 1977.

99. Khattak, M.A., and Magee, R.J., *Anal. Chim. Acta*, 1969, **45**, 297.

100. Kalinin, S.K., Stolyarov, K.P., and Yakovleva, G.A., *Zh. Anal. Khim.*, 1970, **25**(1), 107.

101. Kalinin, S.K., and Yakovleva, G.A., *Zh. Anal. Khim.*, 1978, **33**(10), 1995.

102. Koch, K.R., and Wyrley-Birch, J.M., *Inorg. Chim. Acta*, 1985, **102**, L5.

103. Davies, A.G., Wilkinson, G., and Young, J.F., *J. Am. Chem. Soc.*, 1963, **85**, 1692.

104. Klinskaya, I. Yu., Rosenkevich, M.B., Sakharovski, Yu. I., *Kinet. Katal.*, 1978, **19**, 329.

105. Kimura, T., Miki, E., Mizumachi, K., and Ishimori, T., *Chem. Lett.*, 1976, 1325.

106. Antonov, P.G., Kukushkin, Yu. N., Anufriev, V.I., Vasil'ev, I.N., and Konovalov, L.V., *Russ. J. Inorg. Chem.*, 1979, **24**(2), 231.

107. Saito, Y., Moriyama, H., Aoki, T., and Shinoda, S., *J. Chem. Soc., Dalton. Trans.*, 1981, 639.

108. Iwasaki, S., Nagai, T., Miki, E., Mizumacji, K., and Ishimori, T., *Bull. Chem. Soc. Jpn.*, 1984, **57**, 386.

109. Pantani, F., and Piccardi, G., *Anal. Chim. Acta*, 1960, **22**, 231.

110. Pietropaolo, R., Grazini, M., and Beiluco, V., *Inorg. Chem.*, 1969, **8**, 7.

111. *Idem; ibid.*, 1969, **8**, 1506.

112. Beamish, F.E., "*The Analytical Chemistry of the Noble Metals*", Permagon Press, Oxford, 1966.

113. Ruzicka, J., and Hansen, E.H., *Anal. Chim. Acta*, 1975, **78**, 145.

114. Ruzicka, J., *Anal. Chim. Acta*, 1992, **261**, 3.

115. Ruzicka, J., and Hansen, E.H., *Anal. Chim. Acta*, 1986, **179**, 1.

116. Ruzicka, J., and Hansen, E.H., *"Flow Injection Analysis"*, 2nd edn., Wiley, New York, 1988; 1st edn., 1981.

117. Ueno, K., and Kina, K., *"Introduction to Flow Injection Analysis"*, Kodansha Scientific, Toyko, 1983.

118. Valcarcel, M., and Luque de Castro, M.D., *"Flow Injection Analysis. Principles and Applications."*, Horwood, Chichester, 1987.

119. Karlberg, B., and Pacey, G.E., *"Flow Injection Analysis - a Practical Guide"*, Elsevier, Amsterdam, 1989.

120. Ruzicka, J., and Hansen, E.H., *Anal. Chim. Acta*, 1978, **99**, 37.

121. Olsen, S., Ruzicka, J., and Hansen, E.H., *Anal. Chim. Acta*, 1982, **136**, 101.

122. Marshall, G.D., Ruzicka, J., and Christian, G.D., *Anal. Chem.*, 1990, **62**, 1891.

123. Bergamin, H., Krug, F.J., and Zagatto, E.A.G., *Anal. Chim. Acta*, 1986, **179**, 103.

124. Erickson, B.C., Ruzicka, J., and Kowalski, B., *Anal. Chem.*, 1987, **59**, 1246.

125. Karlberg, B., *Fres. Z. Anal. Chem.*, 1988, **329**, 660.

126. Ruzicka, J., and Hansen, E.H., *Anal. Chim. Acta*, 1983, **45**, 1.

127. Tyson, J.F., and Stone, D.C., *Analyst*, 1987, **112**, 515.

128. Selavka, C.M., Jiao, K-S., and Krull, I.S., *Anal. Chem.*, 1987, **55**, 2221.

129. Almuaibed, A.M., and Townshend, A., *Anal. Chim. Acta*, 1991, **245**, 115.

130. Gorton, L., and Ogren, L., *Anal. Chim. Acta*, 1981, **130**, 45.

131. Ruzicka, J., Hansen, E.H., Olsen, S., and Pessenda, L.C.R., *Analyst*, 1983, **108**, 905.

132. Ruzicka, J., and Arnhdahl, A., *Anal. Chim. Acta*, 1988, **216**, 243.

133. Marshall, G.D., Taylor, M.J.C., Barnes, D.E., and Williams, S.J.S., *Process Control and Quality*, 1992, **2**, 249.

134. Owen, A.J., "*The Diode-Array Advantage in UV/Visible Spectroscopy*", Hewlett Packard, Germany, 1988.

135. Rios, A., Valcercel, M., and Agudo, M., *Anal. Chim. Acta*, 1992, **264**, 265.

136. Romero-Saldana, M., Rios, A., Luque de Castro, M.D., and Valcarcel, M., *Talanta*, 1991, **38**(3), 291.

137. Toei, K., *et al.*, *Anal. Chim. Acta*, 1992, **261**, 345.

138. Hansen, E.H., *Quim. Analitica*, 1989, **8**(2), 139.

139. Kowalski, B.R., Ruzicka, J., and Christian, G.D., *Trends in Anal. Chem.*, 1990, **9**(1), 8.

Chapter 2.

Theory

2.1 Analytical Visible Spectrophotometry

Optical spectrospcopy encompasses methods developed for the investigation of matter with the aid of electromagnetic radiation, which may interact with the system. Spectrometry deals with the measurements of the physical phenomena that provide informative data on the system. One variant of spectroscopy is that of absorption methods.

Analytical visible spectrometric methods for the determination of elements are based on the absorption of visible radiation by sample solutions and are of particular significance for chemical analysis. Spectrometry involves the use of a spectrometer. A spectrometer is used to investigate absorption and emission spectra over almost the whole range of the electromagnetic spectrum. When a spectrometer is fitted with a phototransducer it is known as a spectrophotometer.

The basis of spectrophotometric methods is the relationship established between the emitted or absorbed radiation intensity and the concentration of atoms or molecules in a particular system.[1] In order to determine a species spectrophotometrically, the species is usually converted into a coloured complex by some form of reaction (for example, heat, reagent addition, pH change). The inherent colour of the original species is used less often.

Spectrophotometric methods are remarkable for their versatility, sensitivity, and precision. All the elements, except the noble gases, may be determined in this manner. A very extensive range of concentrations may be covered, from macroquantities to traces (less than 0.01% of a solid sample). These methods are among the most precise instrumental methods at the disposal of the analytical scientist.

Furthermore, the basic apparatus required, a spectrophotometer, is relatively inexpensive. Current trends in spectrophotometric instrumental development, particularly in

the fields of rapid scanning and diode-array technology, no doubt have also contributed to the wide-spread use of analytical visible spectrophotometry.

2.1.1 Absorption of Radiation

Absorption methods used in this work involve the irradiation of the sample with electromagnetic radiation from an external source. The incident rays may interact with the system components (chemical compounds, groups of atoms, etc.). As a result of these interactions one may observe absorption, reflection, refraction, polarisation, luminescence, phosphorescence, and so forth.

Colorimetric and spectrophotometric methods are widely used in quantitative analysis. There are however distinct differences between the two. The colorimetric methods are based on the ability of a coloured substance to absorb visible light. Visible light is that small part of the electromagnetic spectrum which is detectable by the human eye. It is for this reason that it was the first part of the spectrum to be used for chemical analysis. The electromagnetic spectrum extends from high energy cosmic rays ($\lambda \sim 10^{-8}$ nm) through X-rays ($\lambda \sim 10^{-4}$ nm), the ultraviolet (UV) (λ = 190 to 380 nm) and visible regions (λ = 380 to 800 nm), to infrared (IR) and low energy radiowaves. Spectrophotometric methods, in turn, are not limited to the visible regions and include the UV and IR regions of the electromagnetic spectrum. The relationship between energy and wavelength is shown in Equation 2.1.

$$E = h\nu$$

where E = energy
h = Plank's constant
ν = frequency

And, $\nu = c / \lambda$

where c = speed of light
λ = wavelength

Equation 2.1 *The relationship between energy, E, and wavelength, λ.*

Light is absorbed by a substance only when the energy of the light corresponds to the energy required to cause change in the chemical molecule. Thus, light of certain energies, or wavelengths, is absorbed whereas light of other wavelengths is not. The changes in the molecule caused by the absorption of radiation may be electronic (change in the electron distribution), vibrational (change in the average nuclei separation), or rotational (rotation of chemical dipole). Higher energy radiation is necessary to effect electronic transitions whereas rotational and vibrational transitions are a result of lower energy radiation. Hence, shorter wavelengths (*viz.* UV and visible), having higher energy, will cause electronic transitions, whereas longer wavelengths (*viz.* IR) will cause rotational and vibrational transitions.

Now consider an electron in the ground state. This electron will absorb radiation of a suitable energy (wavelength) to raise it to a higher energy level. A return to the lower energy level will occur through loss of energy as heat or occasionally by re-emission of radiation (fluorescence or phosphorescence). If only one type of transition takes place, then the UV/visible absorption spectrum would look like that shown in Figure 2.1, with a single absorption line at the wavelength corresponding to the energy required for the transition. This is the ideal case, and spectrophotometry here would be an excellent qualitative analytical tool with the exact wavelength of the absorption being characteristic of the molecule.

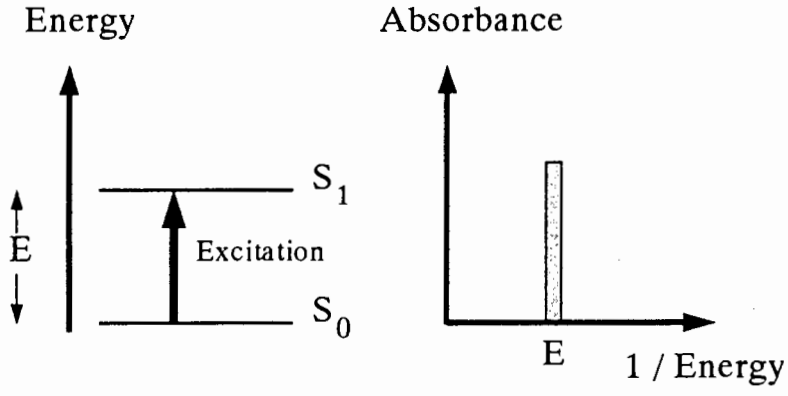

Figure 2.1 *Simplified model for light absorption.*

However, many other energy levels (due to molecular vibrations, rotations and translations) are superimposed on the electronic energy levels and there are many possible transitions as shown in Figure 2.2 (left). A system of vibrational levels corresponds to every electronic state, and every vibrational level comprises a rotational state system. The resulting absorption spectrum, depicted in Figure 2.2 (right), is a broad and relatively featureless continuous band.

The chemical environment of the sample molecules (for example, the solvent) can also affect the position and shape of the band. The result is that UV/visible spectroscopy provides relatively little qualitative information when compared to IR spectroscopy, because the vast information contained in these broad bands is not accessible.

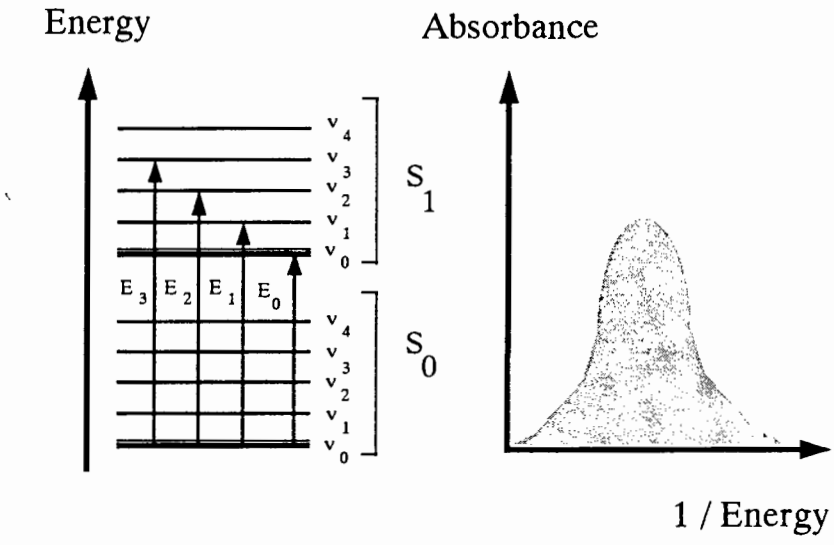

Figure 2.2 *Theoretical model for light absorption. E_X represent different electronic transitions, S_0 represents the ground electronic state and S_1 the excited electronic state. Vibration energy levels (v_x) are shown - rotational and translational levels being omitted for clarity.*

An important point to note for electronic transitions is that the energy difference is relatively large between the ground and excited states (Figure 2.2, left). Therefore, at room temperature, it is highly likely that all molecules are in the electronic ground state. Absorption and return to the ground state (known as relaxation) are fast processes and equilibrium is reached very quickly. Thus, absorption of visible radiation is quantitatively very accurate.

2.1.2 Absorption Laws

When a beam of parallel radiation (light) is passed through a layer of solution, as shown in Figure 2.3, the intensity of the emergent radiation (I) will always be less than the intensity of the incident radiation (I_o). This attenuation of the beam is a consequence of interactions between the photons and absorbing particles. Some radiant energy is absorbed, some transmitted, and some may be scattered and reflected. Scattering and reflection, overcome by the use of a reference solution and matching cuvettes, is usually regarded as a constant and neglected.

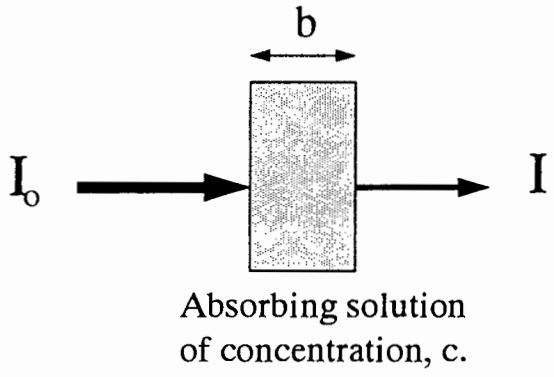

Figure 2.3 *Attenuation of a beam of radiation by an absorbing solution. The fraction of the incident radiation, I_o, that is absorbed is a function of the thickness, b (path length), of the solution layer, and the concentration, c, of the absorbing species in the light path.*

The relationship between transmittance and concentration is non-linear but the relationship between absorbance and concentration is linear and passes through the origin, and forms the basis of quantitative analysis. This relationship, shown in Equation 2.2, is most commonly known as Beer's Law. These mathematical formulations were however established together by Bouger (in 1729), Lambert (in 1760) and Beer (in 1852).

$$T = I / I_o$$

$$A = -\log_{10} T = \log (I_o / I) = a\ b\ c$$

Equation 2.2 *The functional relationship between the absorbance, A, and the concentration, c - known as Beer's Law. The letters represent transmittance, T, intensity of incident and transmitted radiation, I_o and I, absorptivity, a, and the path length, b.*

If the concentration, c, of the absorbing species in the solution is doubled, and the thickness of the layer, path length b, reduced by a factor of two, then the absorbance, A, will remain the same. This assumes that the total number of absorbing species remains constant.

When the concentration of the absorbing component is expressed in $mol.dm^{-3}$ then the absorptivity, a, is expressed as the molar absorptivity, ε, having the units, $dm^3.mol^{-1}.cm^{-1}$. The path length, b, is expressed in centimeters. The reasons for these units is based on the fact that absorbance is a dimensionless quantity, and the absorptivity, path length and concentration must have units that render the right side of Equation 2.2 dimensionless.

Beer's Law may also be applied to mixtures of two or more absorbing components. The law arising here is known as the "Law of Additivity of Absorption". It expresses the total absorbance of a medium, A_t, as a sum of the independent absorbances of the individual components (A_1, A_2, A_3, ..., A_n). The condition that no interaction occurs among the various components must be fulfilled. This law may be expressed as shown in Equation 2.3.

$$A_t = A_1 + A_2 + A_3 + \ldots + A_n = \sum_{i=1}^{n} A_i$$

$$A_t = a_1 b c_1 + a_2 b c_2 + a_3 b c_3 + \ldots + a_n b c_n = b \sum_{i=1}^{n} a_i c_i$$

Equation 2.3 *The Law of Additivity of Absorbance. A_t is the total absorbance of all the components; A_i is the absorbance of component i; b is the path length (a constant); a_i is the absorptivity of the component, i; and c_i is the concentration of the component i.*

Unfortunately, these equations are not always followed in practise as a result of various deviations from Beer's Law. Verification of whether or not the system under investigation obeys these laws is vital for reliable results to be obtained in quantitative spectrophotometric analysis.

Verification is performed by determining the absorptivity values for three or more substantially different concentrations of a given component. The extreme lowest, highest, and a middle, concentration are taken (naturally with absorbances still measurable), and at least five reference solutions of each are prepared. The absorbance is subsequently measured under the specified conditions (reagent concentration, temperature etc.). The computed absorptivity should, within the limits of experimental error, be constant. This means that the system satisfies Beer's Law within the highest and lowest concentration range. A similar approach should be taken with mixtures of components.

In practise, however, when a plot of absorbance *versus* concentration is linear, and passes through the origin, this is indicative of the absorbing component of a system fulfilling Beer's Law. The concentration range over which the law is obeyed is obtained by noting the linear portion of the plot. Verification is also required in the case of more than one absorbing component in solution (such as in multi-component systems).

Binary mixtures of the components, at varying concentrations, are prepared and the absorbance values of the solutions are made at the same previously selected wavelengths. Absorbance values are calculated for the same binary mixtures from their concentrations and individual absorptivities at each wavelength by means of Equation 2.3. A comparison of the experimental and calculated absorbances at each wavelength should, within experimental error, coincide. If so, then the system obeys the additivity law. As the number of components increase, so does the experimental error. A reasonable limit to the number of components that could be resolved by multi-component analysis is five or six.

The verification of additivity is performed far more rapidly by making use of advanced spectrophotometers linked to microcomputers. The absorption spectra of the pure components are stored in the microcomputer. Thereafter, the test mixture spectra are recorded. The measured spectra are compared electronically to the calculated mixture spectra that are derived from the stored pure component spectra. If no deviations from the additivity law occur, the calculated and actual pure component spectra should coincide.

2.1.3 Deviations from Beer's Law

Based on theoretical considerations, the relationship between absorbance, A, and concentration, c, is linear. In practise, however, some deviations from linearity do occur. Some of these deviations, shown graphically in Figure 2.4, are fundamental and represent real limitations to Beer's Law. Others occur as a consequence of the manner in which the absorbance measurements are made (instrumental deviations), or as a result of chemical changes associated with concentration changes (chemical deviations).

Beer's Law is successful in describing the absorption behaviour of dilute solutions only. At high concentrations, the average distances between particles of the absorbing species are diminished to the point where each particle affects the charge distribution of its neighbours. This interaction may alter their ability to absorb a given wavelength of radiation. A similar effect is sometimes encountered in dilute solutions of the absorbing species that contain high and varying concentrations of other species, for example electrolytes. The proximity of the

ions to the absorbing particles alters the molar absorptivity of the latter by means of electrostatic interactions, that result in departures from Beer's Law.

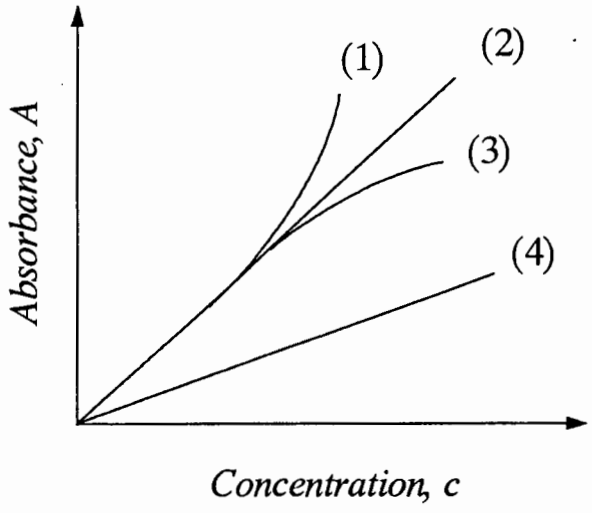

Figure 2.4. *Typical deviations from Beer's Law. The curves refer to: (1) a positive deviation, (2) a system that obeys the law, (3) negative deviation, and (4) deviation independent of concentration.*

The absorptivity is dependant on the refractive index[2] of the solution. As a result, concentration changes that significantly alter the refractive index result in departures from Beer's Law. In general, the refractive index effect is small and is rarely significant at low concentrations.

Chemical deviations are frequently encountered as a consequence of association, dissociation, or reaction of the absorbing species with the solvent. These deviations result from shifts in chemical equilibria and not from changes in molecular absorptivity.

One of the most critical instrumental deviations occurs due to a lack of strict monochromaticity. Beer's Law only applies when absorbance is measured with monochromatic radiation (such as lasers). True monochromatic sources are not practical for routine analysis; instead a polychromatic continuous source is employed in conjunction with a

grating or filter that isolates a more or less symmetric band of wavelengths around the desired wavelength. Experimental deviations from Beer's Law are not appreciable with this approach, provided the radiation used does not encompass a spectral region in which the absorbing species exhibits large changes in absorbance as a function of wavelength. An example of such a spectral region could be the steep side of an absorption peak.

Stray radiation is another source of instrumental deviations from Beer's Law. Stray radiation is primarily due to instrumental imperfections and arises from scattering phenomena off the surfaces of optical components such as prisms, lenses, filters, and optical windows. When the intensity of this stray radiation is of the order of the total radiation, a marked diminution of absorbance takes place. This is only likely to occur when considering high absorbances. Sometimes this stray radiation differs greatly in wavelength from the principle radiation, and may also not actually go through the sample or solvent. It can be shown that these instrumental deviations always lead to negative absorption errors (i.e. absorbances that are smaller than that dictated by theory.)[3]

Deviations from the absorption laws are undesirable in spectrophotometric work as they restrict the concentration ranges, make the requirement of correction factors necessary, and occasionally render the investigation difficult, or even impossible. Conversely, in research, they may be of importance in understanding the phenomenon and processes responsible for these deviations.

2.1.4 Spectrophotometric Detectors

The fundamental apparatus for measuring the absorbance of solutions comprises colorimeters equipped with interference filters and spectrophotometers, the latter being either single wavelength instruments or advanced multi-channel devices. The basis of operation for spectrophometers is provided by the photoelectric effect - an optical signal comprising photons (input) that is converted into an electrical signal (output) by the detecting device. A basic component block diagram of a photoelectric effect detector is shown in Figure 2.5. Although the configuration and layout vary from instrument to instrument, these components are present in all photoelectric-based detecting devices.

The components of a conventional single beam spectrophotometer are briefly detailed. First, a polychromatic light source is focused on the entrance slit of a monochromator which selectively transmits a narrow band of light at a pre-selected wavelength. This single wavelength light passes through another slit and travels through the sample solution in a cuvette, or flowcell in FIA, to the detecting device. The absorbance of the sample is subsequently obtained from the signal handling electronic circuitry.

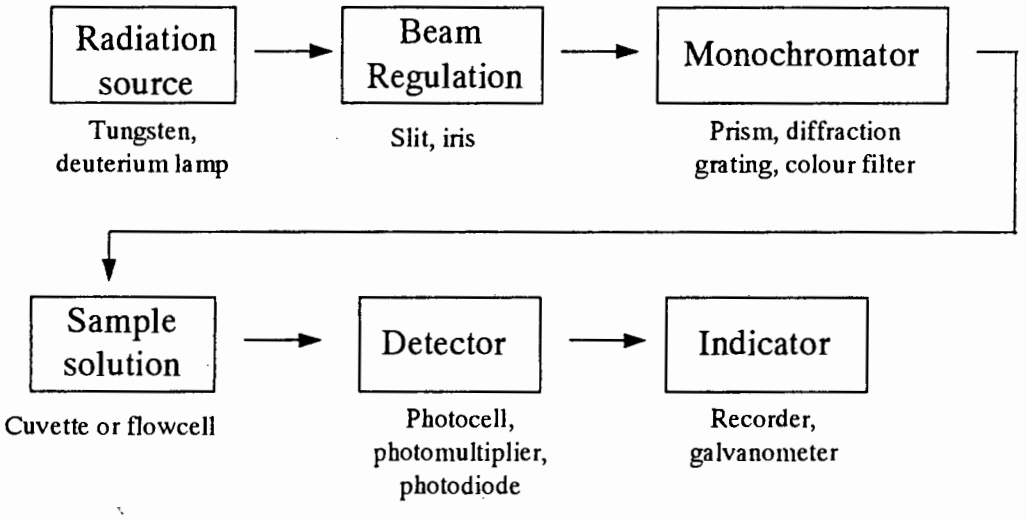

Figure 2.5 *Block diagram of a photoelectric effect-based detector.*

This approach for measuring the absorbance at a single wavelength is ideal. However, in practise, it is frequently necessary to measure the absorbance at different wavelengths for different species, or to obtain the complete visible spectra of a sample. To do this, parts of the monochromator must be moved to allow the wavelength changes. This introduces mechanical complexity and inherent problems of mechanical irreproducibility and associated wavelength resettability problems. In addition, data acquisition *via* scanning methods is relatively slow on these conventional spectrophotometers. Most of these limitations have been overcome by modern instruments.

A solution to these problems is the use of a diode-array instrument with no moving parts, aside from a shutter, that has perfect wavelength resettability. Operation is similar to that of a conventional instrument except in the order of components and the detection approach. The

polychromatic light source is passed through the sample solution, after being focused by a lens, and then passes through a slit. The light is dispersed by a polychromator into its component wavelengths (at 2 nm intervals). A photosensitive area, less than 2 cm^2, containing several hundred photodiode detector elements, measures the narrow band of the spectrum. The polychromator comprises an entrance slit and a holographic grating. The optics are said to be "reversed-optics" as the position of the sample and dispersive element are reversed in comparison with a conventional spectrophotometer.

Diode-array detectors also have limitations other than their extravagant costs. Background noise levels at very low absorbances (less than 0.05 A.U.*) are higher. The requirement for reasonably lengthy integration times (of the order of a few seconds) at low absorbances complicates measurement systems based on a constantly changing sample stream, particularly in FIA. Unfortunately, the designers of certain diode-array instruments did not consider the mounting of the cuvette holder to be significantly important. This could be improved by using optical fiber technology to reduce the stray light, noise levels, and slight flowcell movement considerably. The diode-array is far faster than conventional spectrophotometric detectors when considering relative sensitivity against spectral scanning time, but this is offset by the limitations of diode-arrays at lower absorbance levels. The relative sensitivity as a function of scanning time simply means that to attain equivalent sensitivity, a conventional instrument is required to scan for a considerably longer period than a diode-array instrument.

New high-speed drive technology for holographic diffraction gratings, permitting fast and reliable wavelength changes, low-noise operation, and on-the-fly spectral scanning, has revolutionised rapid scanning spectrophotometric detectors. These advances have placed rapid scanning detectors in a class of their own. The optical design in these instruments incorporates a concave holographic grating with an advanced servomechanism positioning system to achieve similar wavelength resettability as in diode-array instruments.

---

* A.U. ≡ Absorbance units

In particular, the Spectra FOCUS™ † forward optical scanning detector employed in this research, with unique dual-beam optical design offered virtually noise-free baselines at extremely low absorbances - even with solution flowing through the inert, pre-aligned flowcell. True double beam operation, not as is the case with single beam diode-array instruments, is provided by a fiber optics beam splitter, as shown in Figure 2.6.

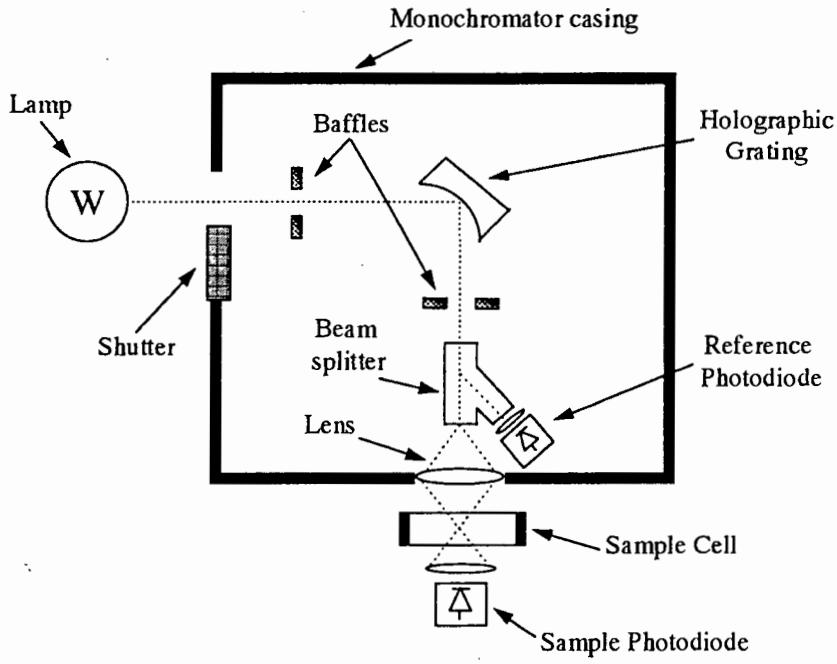

Figure 2.6 *Rapid forward optical scanning detector. Adapted from Spectra FOCUS™ Operators Manual, Spectra Physics, 1989, California, U.S.A.*

The spectral scanning rate extends to 96 data points per second which translates to a 610 nm wavelength range being scanned in 0.7 seconds. Although a diode-array instrument can scan the same range in just under 0.2 second, the aforementioned scanning device has far more sensitivity and much lower signal-to-noise ratios at the important low absorbance levels. Spectral scanning over reduced wavelength ranges, or monitoring at only a few preselected

† Spectra SYSTEM™ Detector, Spectra Physics, California, U.S.A.

wavelengths (to a maximum of 32) simultaneously, reduces the time per scan and instrument absorbance up-date time.

The large quantities of analytically useful data generated by such detectors is accessible to the user *via* the standard instrument rear-panel accessories (millivolt recorder outputs, auto-zero and remote start triggering, and an RS-232 serial interface port for remote digital control *via* microcomputer software).

2.2 Quantitation in Spectrophotometry

Absorption spectroscopy based on visible and ultraviolet radiation is indispensable to the analyst for quantitative analysis. The important characteristics related to quantitation are outlined.

- *Wide applicability.* A vast range of inorganic, organic and biochemical species absorb radiation and are thus amenable to quantitative determination. Several non-absorbing species may be determined after chemical conversion to absorbing derivatives.
- *High sensitivity.* Detection limits typically range from 10^{-2} to 10^{-6}%. The approximate absolute lower limit for solution absorption methods, in terms of constituent weight, is based on reactions with highly sensitive colour reagents. Extremely low levels (0.001 to 0.003 μg) of the element have been detected.
- *Moderate to high selectivity.* Wavelengths can be found where the analyte alone absorbs, making separations unnecessary. Corrections for overlapping bands may be made if additional wavelengths are used. More often than not, specific reagents which react with the one element of interest are not available, and partial separations may be required.
- *Good accuracy.* Relative errors in concentration with typical spectrophotometric methods are of the order of 1 to 5%. Special precautions can further reduce these.

- *Special techniques.* Techniques such as differential, derivative, and dual-wavelength spectrophotometry, not to mention multi-component analysis methods, have enabled analysis of highly complicated and otherwise unsolvable systems.

Quantitative spectrophotometric analysis techniques may be classified on the basis of certain criteria, *viz.* the number of components to be determined (i.e. single or multi-component) and whether direct or indirect methods are employed.

The underlying principle in direct methods is selective absorption of the component being determined. These components include organic compounds with a chromophoric group, and species which may react with a chromophoric reagent. A typical example is the reaction of iron(III) with thiocyanate to give a series of intensely red-coloured complexes. This enables the trace determination of iron(III) at a wavelength of 480 nm.

Indirect methods involve some operation giving rise to an absorption proportional to the component concentration. Operations may include complex formation, oxidation, reduction, and derivative formation. Indirect methods are used less frequently than the popular direct methods.

The most common and simplest spectrophotometric methods used today involve single component quantitation using a single analytical wavelength. In principle, mixtures containing two or more components may be analysed provided another measurement at a different wavelength per additional component is made. However, as the number of components increase, so does experimental error and any possible deviations from the absorptivity laws.

Components that have visible spectra similar to one another require an alternate approach for their accurate determination. This involves "overdetermining" the system by using more wavelengths than theoretically required in an effort to minimise errors. By using many wavelength data points, synthetic spectra are derived for various concentrations of the components known to be present. These component spectra are electronically fitted to the mixture spectrum until a close match is found. Of course, spectra for standard solutions of each component are required.

2.2.1 Single Component Analysis (SCA)

In spectrophotometric analysis the following are considered to be single component determinations:

- one absorbing component in a solution, or in a mixture of components, that do not absorb within the given spectral range,
- one absorbing component against a background of a sum of other absorbing components where the absorption can be eliminated, and
- selective absorption of the component to be determined by means of a suitable chemical reaction.

These single component methods usually entail the use of a single analytical wavelength. However, when background absorption of other components is to be eliminated, further measurements at additional wavelengths may be required. The wavelength associated with the strongest absorption band is commonly used as the analytical wavelength (the wavelength at which absorption measurements are taken) but medium-strength peaks and shoulders may also be used.

Preparation of a calibration curve from pure standards is essential in quantitative work. This calibration enables the verification of Beer's Law and the slope of the calibration curve yields the absorptivity of the component under investigation. The absorptivity is then used, along with the measured sample absorbance signal, to give a numerical evaluation of the sample concentration as outlined in Equation 2.4.

$$(1) \quad A_{std,\lambda} = a_\lambda \, b \, c_{std} \qquad \therefore \quad a_\lambda = A_{std,\lambda} / b \, c_{std}$$

$$(2) \quad A_{sample,\lambda} = a_\lambda \, b \, c_{sample} \quad \therefore \quad c_{sample} = A_{sample,\lambda} / a_\lambda \, b$$

Equation 2.4 *The calculation of a sample concentration at a single analytical wavelength, λ. $A_{std,\lambda}$ and $A_{sample,\lambda}$ represent the absorbances of the standard and sample at wavelength, λ; a_λ represents the absorptivity of the component; b is the path length; and c_{std} and c_{sample} are the concentrations of the standards and samples respectively.*

Furthermore, with the use of rapid scanning spectrophotometers, the quality of results obtained from single component analysis may be improved by a variety of means that are not normally investigated. Conventional spectrophotometers have wavelength resettability errors, and hence the wavelength of the absorption maximum is used. This is often not the best wavelength for linearity and/or reproducibility.

Access to a range of wavelengths through a scanning spectrophotometer enhances the selection of an analytical wavelength. This may be accomplished by software tools that, after measurements over a wavelength range, can display the calibration and the uncertainty in linearity and reproducibility of absorbance measurement at each wavelength.

Other analytical tools, shown in Figure 2.7, such as wavelength averaging over a wavelength range or the absorption peak maximum, may be used for quantitative work instead of the single absorbance values at a wavelength maximum.

Confirmation wavelengths, usually located on either side of the selected analytical wavelength, allow detection of impurities and/or other absorbing species by simple ratio methods. If there are no other absorbing species, then the ratio of the absorbance at two wavelengths would be constant. Any deviation from this indicates the presence of another species. This would be evident in Figure 2.7 with "b" interfering in the determination of "a".

Internal referencing methods allow for compensation of all effects that cause erroneous absorbance readings but which are mainly independent of wavelength (for example, lamp intensity changes and refractive index effects). The reference wavelength is selected at a position removed from the absorbing region of the analyte. These methods enhance the reliability of the single component results in terms of accuracy, precision, and dynamic ranges. Internal referencing may also be adapted in a manner that facilitates the subtraction of an interferent provided that (1) the absorption spectra of such an interferent is known, and (2) the absorbance of the interferent is constant at the wavelengths used over the concentration range expected in the sample. This approach is used in Chapter 6 for the subtraction of interfering absorbing components.

Figure 2.7 *The use of confirmation analysis, reference wavelengths, and wavelength averaging across the absorption maximum to enhance the reliability of single component analysis.*

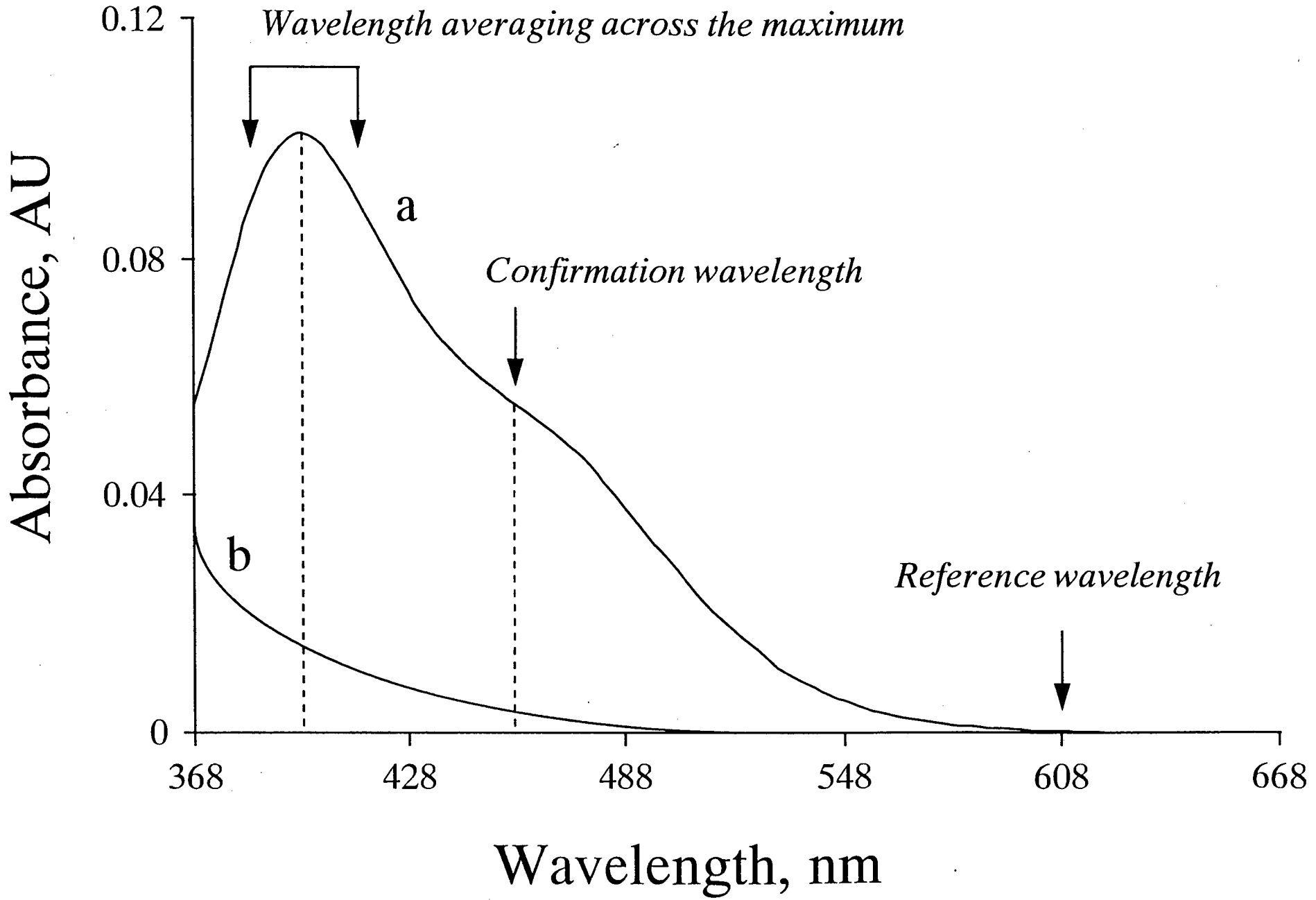
0.12
0.08
0.04
0
Absorbance, AU
Wavelength averaging across the maximum
a
b
Confirmation wavelength
Reference wavelength
368
428
488
548
608
668
Wavelength, nm

2.2.2 Multi-Component Analysis (MCA)

Multi-component analysis is the simultaneous determination of analyte concentrations in a mixture of components from their absorption spectra by making use of a least-square fit and assuming that Beer's Law is valid. The analysis of more than one absorbing component in a solution is becoming an attractive tool for the analyst as microprocessor based spectrophotometers are readily linked to powerful microcomputers.

Commercially available software packages[4] for spectrophotometric multi-component analysis and advanced chemometric applications are based on ordinary multiple regression methods. Either one wavelength-per-component or wide spectral ranges are employed. These are known as exactly "determined" systems and "over-determined" systems respectively.

Complex mathematical algorithms are required to resolve the mixtures when the spectra of the components of interest overlap extensively. The application of quantitative chemometrics, particularly principle component regression (PCR) and partial least-squares regression (PLSR), to multivariate chemical data from multi-channel FIA detector systems is becoming more widespread within research laboratories as more complex systems are required to be resolved and analysed.

These chemometric methods are examples of indirect calibration methods (i.e. not requiring individual component spectra to be known in advance). They do, however, require a comprehensive set of calibration samples which span the expected range of components and chemical interactions. These multivariate techniques are discussed in detail by Martens and Naes,[5,6] and Kowalski and Beebe.[7]

The conventional multi-component approach to a mixture is outlined in Figure 2.8. The absorbance of the two components is measured at two wavelengths (usually close to or at λ_{max} for each) to obtain the absorptivity, $a_{i,j}$, for each component, j, at wavelength, i.

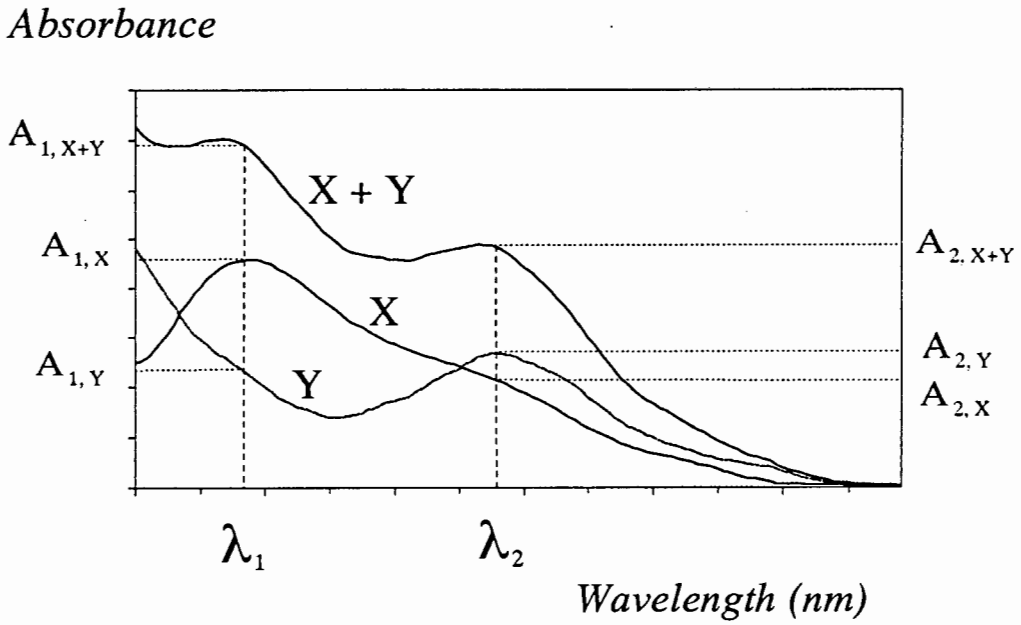

Figure 2.8 *Conventional multi-component analysis for a two component (X and Y) absorbing system using two wavelengths, λ_1 and λ_2.*

The absorbance at either wavelength will be the sum of the absorbances of both components for this mixture. The absorbance of the mixture is measured at the two wavelengths and the resulting equations, shown in Equation 2.5, are solved using simple matrix determinants to find the concentration of each component.

$$A_{1,\,X+Y} = A_{1,\,X} + A_{1,\,Y} = a_{1,\,X}\, b\, c_X + a_{1,\,Y}\, b\, c_Y$$

$$A_{2,\,X+Y} = A_{2,\,X} + A_{2,\,Y} = a_{2,\,X}\, b\, c_X + a_{2,\,Y}\, b\, c_Y$$

where $A_{i,\,X+Y}$ = absorbance of the mixture at λ_i

$A_{i,\,j}$ = absorbance of component j at λ_i

$a_{i,\,j}$ = absorptivity of component j at λ_i

b = path length

c_j = concentration of component j

Equation 2.5 *Equations used in the calculation of the concentrations for a two component system adhering to Beer's Law and the Law of Additivity of Absorbance.*

The analysis of mixtures using spectrophotometry is not new but, with conventional scanning spectrophotometers and the use of simultaneous equations, this approach has been limited to simple two component (binary systems) or, at the most, three components (ternary systems). At wavelengths where higher absorption of a component occurs, minimal spectral overlap and negligible absorbance from the other components is preferable though not a prerequisite.

In the case of considerable spectral overlap and similarity, relatively small measurement errors in absorbance at the selected wavelengths adversely affect the results for mixtures. The effect of random measurement errors on the multi-component quantitation for two component mixtures with different (Figure 2.9) and similar (Figure 2.10) spectra is illustrated for two components, X and Y, with a mixture of the two denoted as the sum, X + Y.

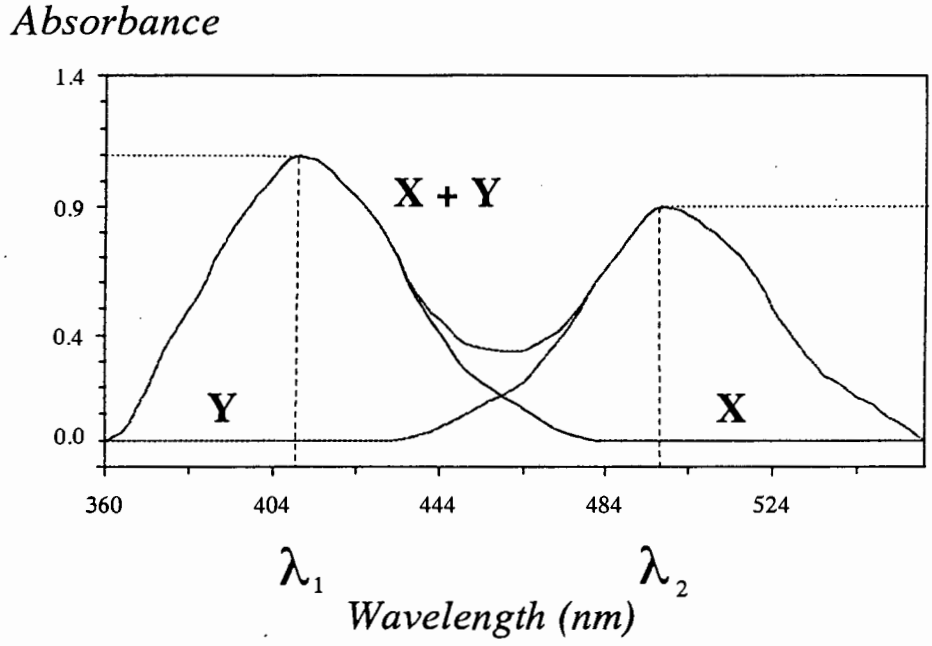

Figure 2.9 *The effect of random measurement errors on quantitative results using the simple classical multi-component calculation. Components X and Y have distinctly different spectra.*

Consider a mixture of X and Y with the concentrations of X and Y, $c_X = c_Y = 1$, where distinctly different spectra are present (Figure 2.9). The measured absorbances, using the same cell of path length 1.0 cm, at λ_1 and λ_2 should be:

$$A_{1,X+Y} = A_{1,X} + A_{1,Y} = 1.1 + 0.0 = 1.1$$

$$A_{2,X+Y} = A_{2,X} + A_{2,Y} = 0.0 + 0.9 = 0.9$$

If there is a 10% error in the measurement of $A_{1,X+Y}$ [i.e. $A_{1,X+Y} = 0.99$ (-10%)] and $A_{2,X+Y}$ [i.e. $A_{2,X+Y} = 0.99$ (+10%)], then the following solution for the above equations is obtained:

$$c_X = 0.90 \text{ (+ 10\% error)} \quad \text{and} \quad c_Y = 1.10 \text{ (- 10\% error)}$$

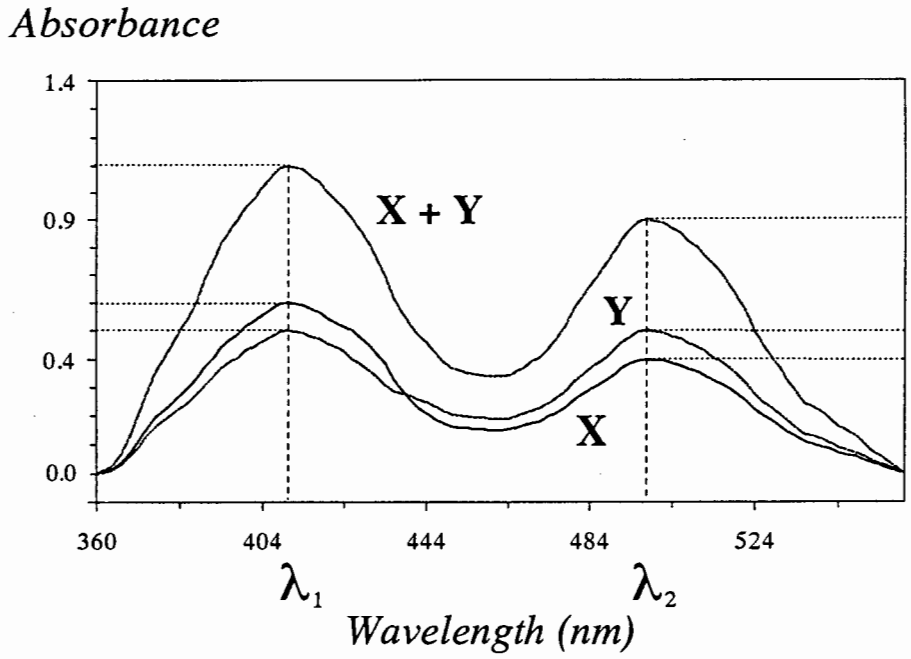

Figure 2.10 *The effect of random measurement errors on quantitative results using the simple classical multi-component calculation. Components X and Y have very similar, overlapping spectra.*

Now consider the case where similar spectra in a mixture of X and Y exist (Figure 2.10), with the concentrations of X and Y, $c_X = c_Y = 1$. The measured absorbances at λ_1 and λ_2, using the same cell of path length 1.0 cm, should be:

$$A_{1,X+Y} = A_{1,X} + A_{1,Y} = 0.6 + 0.5 = 1.1$$
$$A_{2,X+Y} = A_{2,X} + A_{2,Y} = 0.4 + 0.5 = 0.9$$

Again, if there is a 10% measurement error for $A_{1,X+Y}$ [i.e. $A_{1,X+Y} = 0.99$ (-10%)] and $A_{2,X+Y}$ [i.e. $A_{2,X+Y} = 0.99$ (+10%)], then the solution to the simultaneous equation yields the following:

$$c_X = 0.0 \text{ (-100\% error)} \quad \text{and} \quad c_Y = 1.98 \text{ (+ 98\% error)}$$

It may immediately be seen that with classical multi-component calculations relatively small errors have a considerable effect on the final concentrations when determining two component systems with extensive spectral overlap.

The effect of random noise and other associated errors can be reduced by using more spectral information that can be obtained using diode-arrays and high-speed scanning spectrophotometers. When more spectral data is used, an overdetermined system of linear equations results, which may be solved by least-square regression.

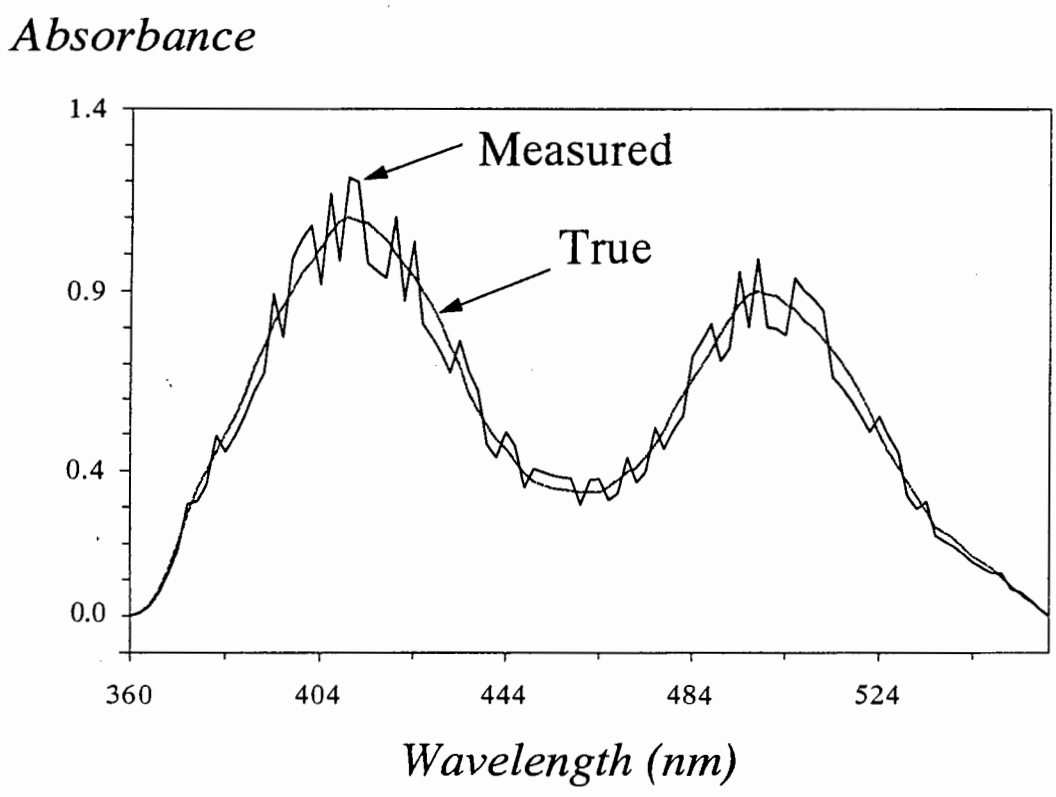

Figure 2.11 *The effect of random measurement errors on quantitative results using multi-component analysis by a least-square fit over a spectral range.*

A spectrum with a random error of 8 to 10% at each measurement point, for the two component mixture that was considered previously in Figure 2.10, is shown in Figure 2.11.

Using 100 data points (2 nm intervals from 360 nm to 558 nm), the quantitative results from the least-squares fit, shown below, have errors considerably lower than the *ca.* 100% errors from the same mixture being analysed at only two wavelengths.

$$c_X = 1.06 \ (+6\ \%\ \text{error}) \quad \text{and} \quad c_Y = 0.96 \ (-4\ \%\ \text{error})$$

Effectively, standards spectra are added together, at varying concentrations, to create a synthetic mixture spectrum which is matched as closely as possible to the measured mixture spectrum. Although this approach is significantly less sensitive to measurement error of a random nature, it is sensitive to the choice of wavelengths used because poor and high quality data are given equal weighting. It is important to select wavelengths, or wavelength ranges, that give high quality data.

According to the Law of Additivity of Absorbances, Equation 2.3, and provided ideal conditions prevail (for example, negligible noise and deviations), a system of linear equations, Equation 2.6, may be established for *n* absorbing components ($i = 1, \ldots, n$).

$$A_j = a_{1,j} b\, c_1 + a_{2,j} b\, c_2 + \ldots + a_{n,m} b\, c_n = b \sum_{i=1}^{n} a_{i,j} c_i$$

Equation 2.6 *Linear equations for a system of n components ($i = 1, \ldots, n$), at m wavelengths ($j = 1, \ldots, m$).*

The least-squares method uses these linear equations at *m* wavelengths ($m \geq n$) and minimises the sum of the squared deviations ($A_{exp} - A_{calc}$) in each of the m linear equations ($j = 1, \ldots, m$) (Equation 2.7). Terms may be included to compensate for matrix effects and chemical interactions which may cause significant deviations from the assumed zero intercept.

$$\sum_{j=1}^{m} \left[A_j - b \sum_{i=1}^{n} a_{i,j} c_i \right]^2 \rightarrow \text{Minimum}$$

Equation 2.7 *The generalised least-squares method.*

The least-squares technique may be refined if the quality (for example, the standard deviation) of each data point is known. This information may be used to weight the data points in the calculation, thus making the technique less sensitive to the choice of wavelengths. Appropriate weighting factors, $w_j > 0$, lead to the optimisation problem in Equation 2.8. The weights are usually chosen according to the estimated size of the errors. Partial differentiation of the left-hand side of the equation, and setting these partial derivatives equal to zero, yields a system of linear equations which may be solved.

$$\sum_{j=1}^{m} w_j \left[A_j - b \sum_{i=1}^{n} a_{i,j} c_i \right]^2 \rightarrow \text{Minimum}$$

Equation 2.8 *The generalised least-squares method incorporating corrective weighting factors.*

Finally, the evaluation of the multi-component analysis process, *via* verification against standard mixtures and by statistics, provides a strong indication of the quality of the results. Validation against standards is the most direct way. This should not be the sole criteria as decomposition of the standards with time may occur. Periodic preparation of fresh standard mixtures for verification of "aged" standards solutions is crucial.

Statistical verification of results may take various forms. Its simplest form involves access to the standard deviation of the computed concentration values to give an estimate of the precision of the measurements. This is calculated from the standard deviation of the standard and sample spectra.

The relative fit error (RFE), or match factor (MF),[8] provides an indication of how good the theoretical model fits the real sample. Least-squares analysis of the calculated and experimental absorbance values gives the MF correlation value according to Equation 2.9. A match factor of 0 indicates no match and 1000 indicates identical spectra. Generally, values above 950 indicate good spectral similarity, values between 850 and 950 indicate some similarity, but the result should be interpreted with care. All values below 850 mean, in effect, that two different spectra exist.

$$MF = \frac{10^3 \cdot \{ \sum x \cdot y - (\sum x \cdot \sum y) \}^2}{\{ \sum x^2 - (\sum x \cdot \sum x)/n \} \cdot \{ \sum y^2 - (\sum y \cdot \sum y)/n \}}$$

Equation 2.9 *Equation to compute the match factor correlation of two spectra; where x and y represent the absorbances in the first and second spectrum respectively at the same wavelength, and n is the number of data points.*

2.2.3 Multi-Wavelength Linear Regression Analysis (MLRA)

Multi-wavelength linear regression analysis[9] is a graphical approach to the least-squares method. Although MLRA is truly a sub-set of multi-component analysis, it is considered separately here. Instead of the least-squares being performed out-of-sight, this approach is transparent to the user and enables alteration of the input parameters (for example, wavelength selection and dynamic range of the calibration) as required. The derivation of the graphical MLRA equations is outlined.

Consider a binary mixture that obeys Beer's Law and the Law of Additivity of Absorbance. These conditions are summed up in the equation below, where $A_{mixture,j}$ denotes the absorbance of the mixture at wavelength j.

$$A_{mixture,j} = a_{1,j} b\, c_1 + a_{2,j} b\, c_2 = b \sum_{i=1}^{2} a_{i,j} c_i$$

The absorptivities, $a_{k,j}$, at each wavelength may be calculated from the absorbance of a pure standard solution of each component from the equation below, where k is the standard (k = 1 or 2), c_k is the corresponding concentration of standard k, and $A_{k,j}$ is the absorbance of the standard at wavelength j.

$$A_{k,j} = a_{k,j} b\, c_k$$

If the same cell (and hence the same path length) and normalised standard spectra of unit concentration are used, then appropriate substitution and rearrangement will give the following equation in the form of a straight line.

$$A_{1,j} / A_{mixture,j} = (1/c_1) - (c_2/c_1)(A_{2,j} / A_{mixture,j})$$

Plotting the values obtained at the different wavelengths, j, as $A_{1,j} / A_{mixture,j}$ *versus* $A_{2,j} / A_{mixture,j}$ gives a straight line of slope $-c_2 / c_1$ and a y-axis intercept of $1/c_1$. This allows calculation of the concentrations c_1 and c_2. This method is illustrated in Figure 2.12 for a mixture of 40 $\mu g.cm^{-3}$ Pt(IV) and 60 $\mu g.cm^{-3}$ Pd(II). The experimental absorption spectrum and the theoretical spectrum for this mixture is shown in Figure 2.13. Good agreement across the spectral range is evident.

Ranges of wavelengths, a complete spectrum, or specifically selected wavelengths over the full spectrum, are readily handled using MLRA. The system may be extended to ternary mixtures where a plane fitted to the data using a least-squares method - the intercepts and slopes in two dimensions are used to evaluate the three concentrations.

Figure 2.12 *A MLRA plot for a binary mixture of 40 μg.cm^{-3} Pt(IV) and 60 μg.cm^{-3} Pd(II). Each data point corresponds to a measurement at a wavelength in the range 368 to 484 nm at 4 nm intervals. Pt(IV) found, 39.5 μg.cm^{-3}, and Pd(II) found 59.9 μg.cm^{-3}. The MLRA correlation is -0.991 and Match Factor 999.8.*

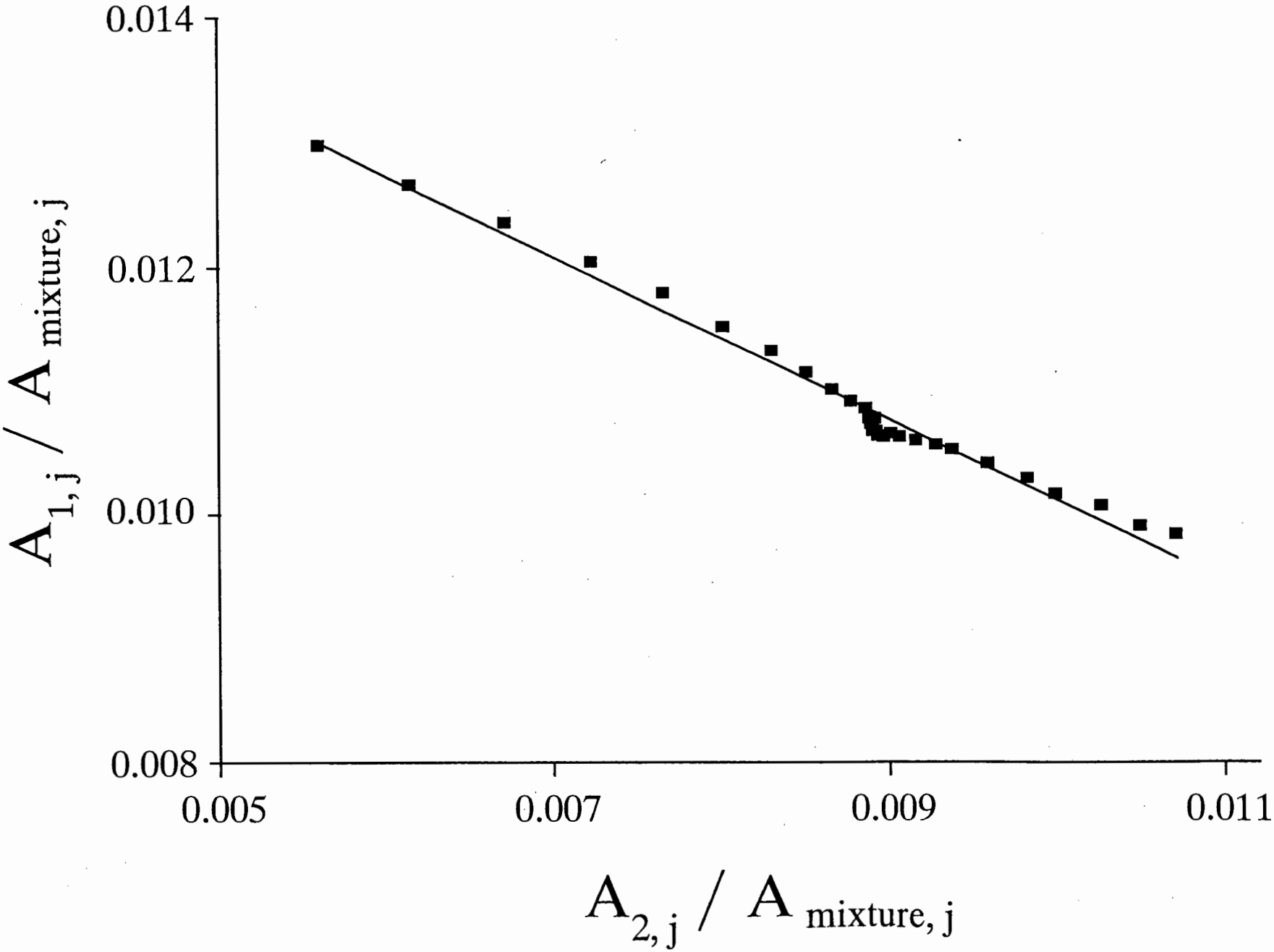
0.014
0.012
0.010
0.008
0.005
0.007
0.009
0.011
$A_{1,j} / A_{mixture,j}$
$A_{2,j} / A_{mixture,j}$

Figure 2.13 *The absorption spectrum (■) and theoretical spectrum (—) for a binary mixture of 40 μg.cm^{-3} Pt(IV) and 60 μg.cm^{-3} Pd(II). Each data point in the absorption spectrum corresponds to a measurement at a wavelength, λ_j.*

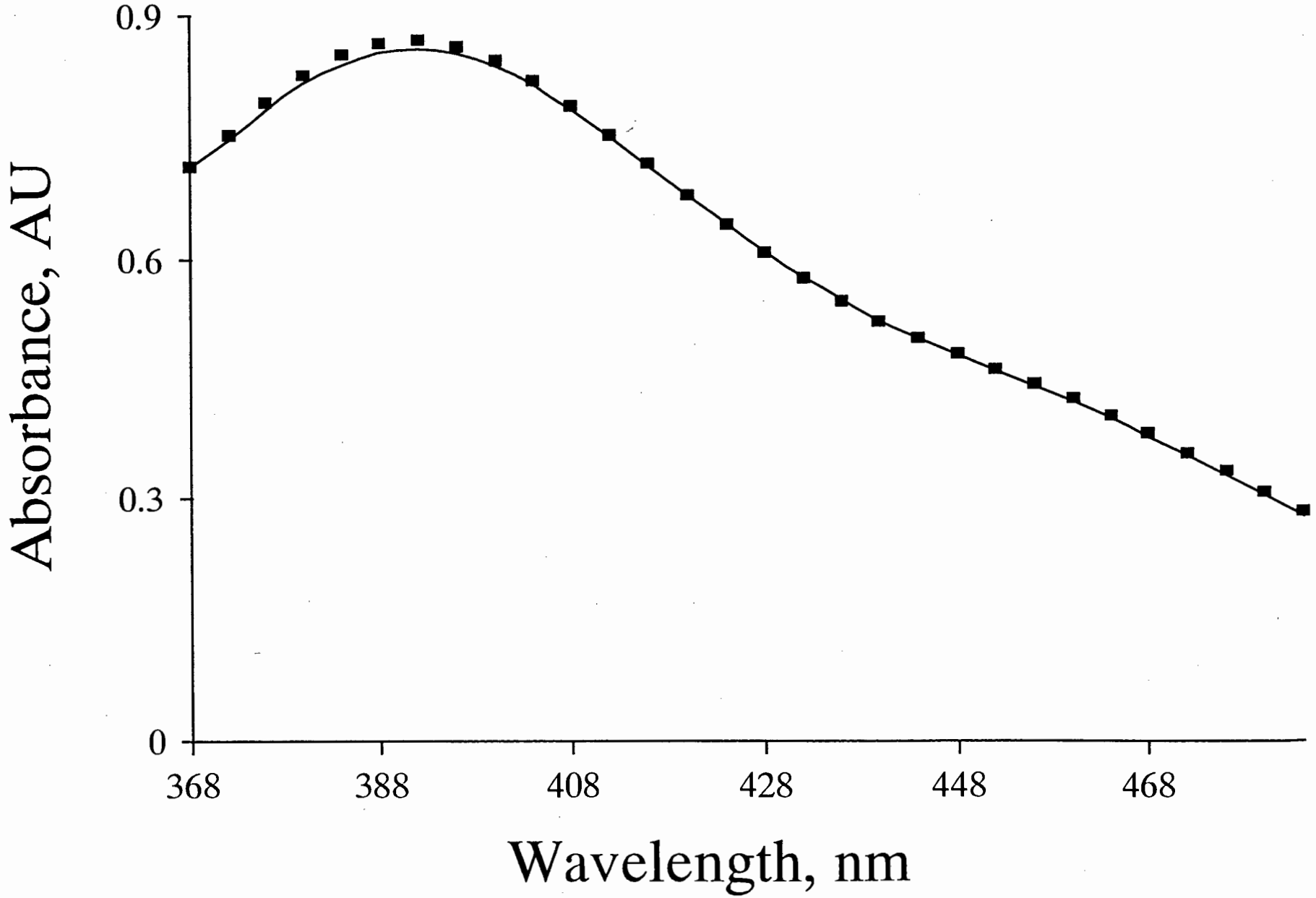
0.9
0.6
0.3
0
Absorbance, AU
368
388
408
428
448
468
Wavelength, nm

The least-squares fit is performed using the standard approach assuming that the y-axis contains all the error, and that the x-axis is "error-free". This was not so in this case. Nevertheless, this approach was employed throughout as the difference in final concentration when the axes were reversed was found to be minimal. It has been shown[10] that the artifice of averaging the results of a regression of y on x, and then, x on y, leads to similar errors.

2.2.4 Wavelength Selection

The selection of wavelengths at which measurements are made is crucial to the least-squares analysis of spectrophotometric data. The literature emphasises fairly complicated approaches to successfully select analytical wavelengths and wavelength ranges.[11,12,13,14] It is anticipated that considerably more attention will be placed on this wavelength selection problem as MCA becomes a routine task in analysis.

Usually the absorbance maximum, or regions of the greatest difference, in the spectra of the individual components are used as the fundamental criterion for wavelength selection. Consider the binary system (Equation 2.5) where the greatest difference between the spectra is desirable. The best way to find two wavelengths, or a range of wavelengths, that satisfy the criterion of curve divergence is to plot the ratio of absorptivities, $a_{1,j} / a_{2,j}$, over a range of wavelengths, j. The two wavelengths of maximum divergence will be the maximum and minimum in the plot. Such plots are used in Chapter 6 for wavelength selection.

The same approach of selecting wavelengths may be followed in overdetermined systems. The error caused by poor selection of wavelengths in the case where only a few (less than 5) wavelengths are used, may be reduced by the use of additional wavelengths.

There are several criteria that should be considered when using MCA. These criteria, though not comprehensive, give an indication of the factors to consider.

- The system must obey Beer's Law and the Law of Additivity of Absorbances.
- The number and identity of the components in the mixture must be known.
- The number of selected wavelengths must be larger than the number of components.
- There must be some degree of spectral difference between the components.
- The selected wavelengths should be distributed over the spectral range of larger absorptivities for each of the components to enable higher sensitivities (especially where overlap is prevalent).
- The wavelength axis is fixed and the calculation is done in the absorbance domain.
- The ratios between the absorptivities of each component should be as large as possible.

If any of these criteria do not hold, or are not met, the multi-component calculations may be severely affected. Finally, a practical consideration is the availability of standards in the pure form for the components of interest.

2.3 Principles of Flow-Injection Analysis

Flow-injection analysis (FIA) is based on four major factors: (1) reproducible and direct injection, (2) reproducible operational timing, (3) controlled dispersion processes, and (4) unsegmented flow characteristics. These factors combine to make FIA not only a new analytical tool, but a new analytical concept.[15] Although significant developments in FIA have been made, the quantity of dynamic (or physical) and kinetic (or chemical) information contained within the transient peak profile is far from being fully exploited.

Before the full capabilities of FIA are realised, a reasonable understanding of the basic fluid dynamics mechanisms occurring in a manifold are required. Manipulation of these basic transport principles can yield highly innovative FIA applications. The first, and probably the most important consideration, is that of dispersion and mixing processes within a manifold.

2.3.1 Dispersion and Mixing Processes

The purpose of transporting a sample through a flow-injection analysis manifold is to treat the sample (chemically and physically) in such a way that it will yield an analytical response that is highly reproducible. The sensitivity (response per unit concentration) of the FIA response is influenced by the physical processes occurring as a result of the manifold configuration such as solution flow rate, tube inner diameter, sample volume, and reactor length, as well as the chemical processes of formation of a species under conditions prevalent in the manifold.

The sample treatment occurs by a combination of physical phenomenon such as convection (laminar or Newtonian flow), secondary flow, molecular diffusion effects, and chemical effects due to a reaction occurring. In addition, turbulent (chaotic) flow can also be used to supplement the mixing process. In this case, reactors packed with small diameter beads[17] intensify mixing in all directions. Regions of turbulent flow may be created by using merging streams to enhance mixing across the whole length of the sample zone. These physical phenomenon are outlined below in greater detail.

2.3.1.1 Convection (Laminar flow)

The movement of a fluid in a flowing stream through cylindrical tubing under laminar flow conditions is controlled by convective forces and is a well understood and documented phenomenon.[16] In a straight tube a parabolic velocity profile is formed, where the elements of fluid have zero linear velocity at the tube walls whereas those at the centre of the tube have twice the average velocity.

The resultant velocity profile in a longitudinal cross-section of a straight tube is shown in Figure 2.14. The parallel lines depict isovelocity streamlines. A streamline is simply the path a liquid particle takes in a steady flow environment.

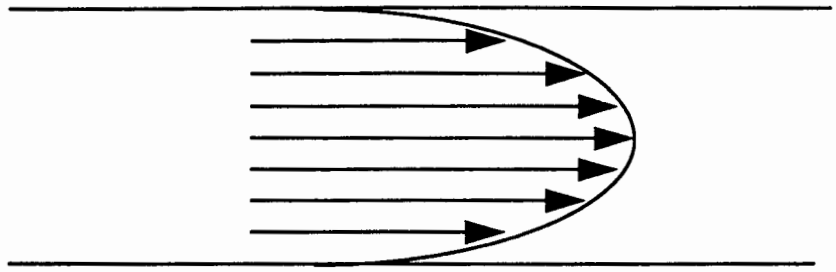

Figure 2.14 *Isovelocity streamlines under laminar flow (convective transport) conditions forming a parabolic flow velocity profile within a FIA manifold tube.*

It is widely accepted that laminar flow conditions do occur in FIA. It is also known that through secondary flow (induced by tubing curvature) the isovelocity streamlines may cross, thereby the enhancing mixing processes.

2.3.1.2 Secondary Flow

If there is any curvature of the manifold tubing (such as helical coiling) then secondary flow will be induced. Increased mixing and decreased dispersion are known to result.[17]

Consider laminar flow conditions in a straight tube. The central fluid elements will have twice the average velocity of the fluid. When encountering a curve in the manifold tubing the central element will tend to travel a greater distance under inertia than the outermost streamlines that have a lower velocity. Differences in the centrifugal forces of the streamlines generate a secondary flow pattern (Figure 2.15) within the manifold tubing.

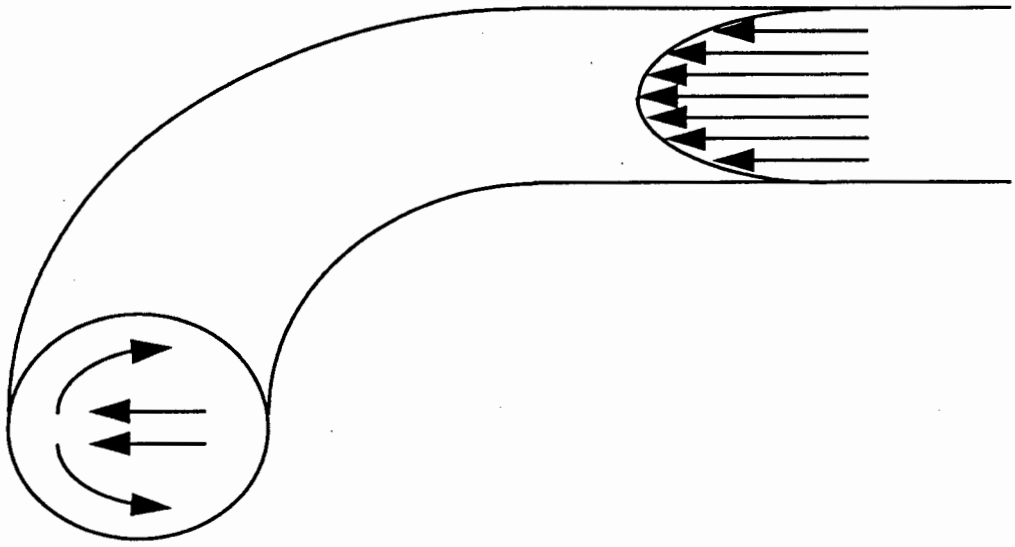

Figure 2.15 *Secondary flow characteristics on laminar flow conditions caused by the effect of a curved flow path.*

2.3.1.3 Molecular Diffusion

Molecular diffusion (diffusional transport) occurs as a result of concentration gradients being established whilst the fluid undergoes laminar and secondary flow in a tube. Substantial molecular diffusion occurs, even in the absence of secondary flow.

If the assumption that only laminar flow occurs in a straight tube applies then one may envisage, as a result of the molecules at the tube walls having zero velocity, that some sample would be still found in the injection valve (initial position) even after the central element of fluid (flowing at twice the average velocity) has passed through the detector. This does not occur due to molecular diffusion. Molecules can diffuse into faster moving stream lines. In a similar manner, the molecules from the faster moving regions will diffuse into regions with slower streamlines.

Diffusion is a result of the spontaneous motion of molecules from a region of higher concentration to a region of lower concentrations. Each molecule will tend to diffuse across streamlines, along the concentration gradients, in an attempt to uniformly distribute all molecules. The clearest example of this is the well-known Brownian motion experiment where

some smoke particles are introduced into a sealed chamber. These particles spread out so as to uniformly fill the chamber.

Axial diffusion (Figure 2.16, top) occurs in the axis parallel to the tube walls, though not necessarily in the direction of the flowing liquid. Radial diffusion (Figure 2.16, bottom) occurs orthogonal to the direction of the flowing liquid. Both types of diffusion aid the mixing of the sample zone and reagent stream within the manifold.

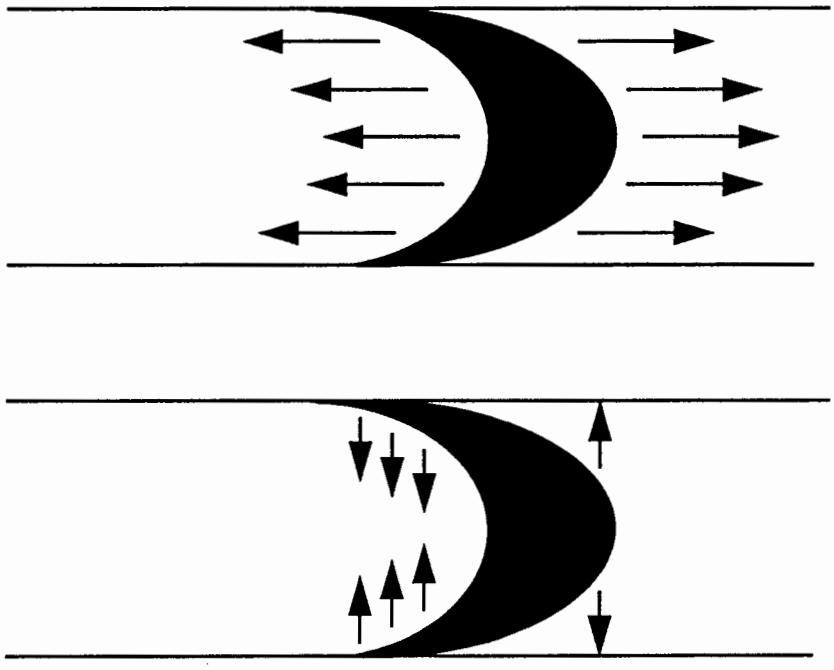

Figure 2.16 *The effect of molecular diffusion within a FIA manifold tube on the injected sample zone in the axial (top) and radial (bottom) directions.*

2.3.1.4 Turbulent (chaotic) flow

Turbulent flow may be induced by causing the streamlines within the manifold tubing to cross. Turbulent flow differs from secondary flow in that the flow channel is altered in a manner other than any form of tubing curvature, whereas the latter entails only curvature of the

manifold tubing. Such flow channel alterations may be in the form of single-bead string reactors, a stirred mixing chamber, or a tee-piece (enabling two streams to merge).[17]

The result of turbulent flow is a rapid averaging of the velocity profiles due to chaotic movement of the fluid elements with mixing taking place in all directions of similar intensity and rapidity. For example, when a tee-piece is used the sample zone is mixed along its whole length in a rapid and reproducible manner when the two streams merge.

2.3.2 The Dispersion Coefficient

An FIA peak may be characterised by (1) its position as a function of time, (2) its peak width generally measured at a convenient distance from the baseline, (3) the maximum peak height, and (4) the overall peak area. These values change as a function of the FIA manifold operating conditions (*viz.* flow rate, reaction coil length, merging streams, etc.) Another parameter which is very useful is the "Dispersion Coefficient."

Consider a sample solution, contained within the valve sample loop prior to injection as depicted in Figure 2.17. The sample is homogenous and has an original concentration C^0. The height of this original square wave signal would be proportional to the concentration. When the sample is injected into the moving carrier stream (Figure 2.17, Inj.), it follows the movement of this stream, forming a dispersed zone with a form dependant on the manifold geometry and flow velocity.

As a result of dispersion, the peak height of the transient signal will never exceed that of the theoretical square wave response unless of course an enrichment technique is used. The extent of dispersion[‡] is termed the "Dispersion Coefficient." This dispersion coefficient, D, has been defined as the ratio of concentrations of the sample material before (C^0) and after the dispersion process has taken place[17] as denoted in Equation 2.10.

[‡] The term *dispersion* is not only due to "pure" dispersion but also due to dilution when, for instance, other streams merge with the carrier stream.

Figure 2.17 *An originally homogenous sample zone (top right) disperses during its motion through a reaction coil (top center). This changes the original square profile (lower right) of concentration C^0, to a profile (center) comprising a continuum of concentrations with a maximum, C_{max}.*

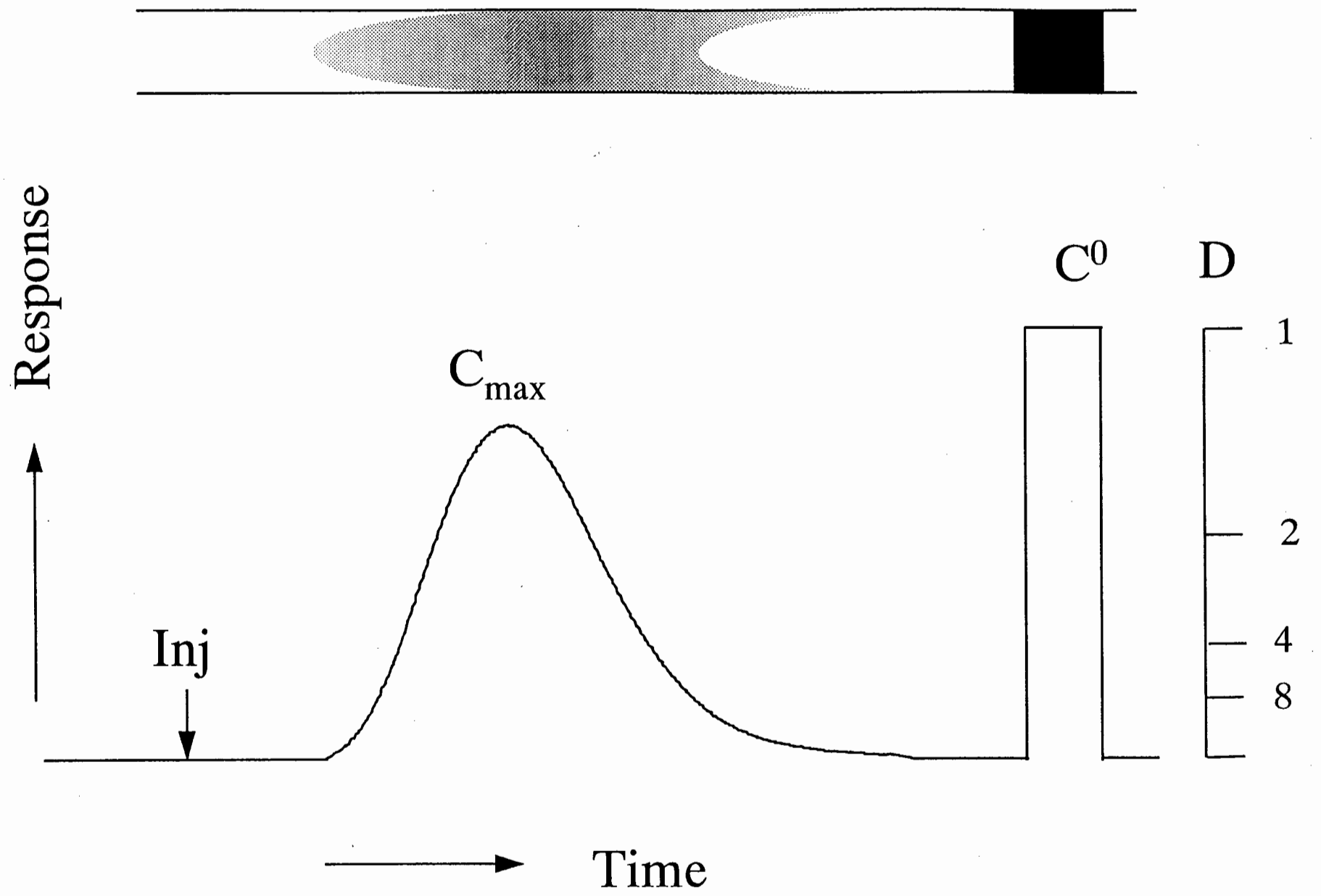
Response
C_{max}
Inj
Time
C^0
D
1
2
4
8

$$D = C^0 / C$$

Equation 2.10 *The Dispersion Coefficient, D, as a function of the ratio of concentrations of sample material before, C^0, and after, C, the dispersion process has occurred.*

The apparent concentration, C, may be measured at any point along the transient signal, and the dispersion would be calculated at that specific point. If the analytical readout is based on the peak height, H, the concentration within that element of fluid corresponds to the maximum of the recorded curve, C_{max}, and the dispersion equation may be denoted as in Equation 2.11.

$$D = C^0 / C_{max} = H^0 / H_{max}$$

Equation 2.11 *The Dispersion Coefficient, D, as determined at the transient signal peak maximum, having concentration C_{max}, and height, H_{max}. The height of the original sample zone prior to dispersion is H^0.*

The dispersion coefficient is a useful parameter in FIA and is an indication of the degree of dilution that the sample undergoes. For convenience, dispersion has been classified as limited (D = 1 to 3), medium (D = 3 to 10), and large (D > 10).[17]

In absorption spectrophotometry the corrected absorptivities may be calculated from the product of the apparent absorptivity and the dispersion coefficient. The apparent absorptivity in this FIA work is that which is found by regression of the response (peak height) *versus* the concentration. If the dispersion coefficient is two then the sample has been diluted twice with the carrier stream and therefore the true absorptivity is twice the apparent absorptivity.

The simplest way to measure the dispersion is to inject a well-defined volume of dye solution, such as bromothymol blue, into a colourless stream and continuously monitor the absorbance. The height of the transient flow-injection peak (H_{max}) is measured and compared

to the signal recorded when the flowcell is filled with undiluted dye (H^0). Provided that Beer's Law is followed, the dispersion coefficient may be calculated from Equation 2.11.

2.3.3 A Novel Non-equilibrium Environment

The pursuit of homogenous mixing and ensuring complete chemical reaction is a concept that has been engrained in analysts as a requirement for reproducible measurement, particularly in spectrophotometric techniques. This misconception clouded even the remote possibility of monitoring a reaction at any time other than at the reaction completion.

This concept of a "steady-state signal" can be abandoned in FIA. Although the reagent and sample mixing is incomplete, and chemical equilibrium is not attained, the use of the well-defined environment of the FIA manifold ensures highly reproducible results. This is a result of the manifolds' constant configuration, flow rate, and timing.

The immediate implications of this novel non-equilibrium environment are that the sampling frequency increases due to shorter reaction times, and solution consumption is decreased. Further ramifications of non-equilibrium conditions are that complete colour development is no longer a prerequisite and the possibility of studying transient species becomes a reality.

2.3.4 Manifold Design Criteria

In designing an effective FIA manifold, cognisance should be taken of several guidelines that have been summarised by Ruzicka and Hansen[17] in a series of rules. These rules relate, mathematically, the effect of sample volume, reactor length, flow rate, reactor geometry, and give an indication of the way to increase the sampling rate of a manifold. These rules aid in the optimisation of a manifold under construction. A combination of the application of the rules and an experimental optimisation approach is frequently used.

The common aims in optimisation include attempts to obtain high sample throughput, minimal dispersion, adequate sensitivity for the analyte, low peak widths, and reduce solution consumption. Some of these are mutually exclusive. The emphasis on any one factor varies between applications.

Marshall[18] summarised the typical approach used by FIA practitioners in method development with the remarkably accurate statement -

> "... many FIA practitioners prefer to rely on an empirical approach. FIA is quite forgiving in that a system which has not been optimised can yield satisfactory results. "

2.4 References

1. Nowicka-Jankowska, T., Gorczynska, K., Michalik, A., and Wieteska, E., *"Comprehensive Analytical Chemistry : Analytical Visible and Ultraviolet Spectrometry"*, Vol. XIX, Elsevier, New York, 1986.
2. Kortum, G., and Seiler, M., *Angew. Chem.*, 1939, **52**, 687.
3. Meehan, E.J., *"Treatise on Analytical Chemistry"*, 2nd edn., Interscience, New York, 1981.
4. *"The Unscrambler" Software Package*, Ver. 5.0, Camo AS, Norway, 1993.
5. Martens, H., and Naes, T., *Trends Anal. Chem.*, 1984, **3**, 204.
6. Martens, H., and Naes, T., *Trends Anal. Chem.*, 1984, **3**, 266.
7. Kowalski, B.R., and Beebe, K.R., *Anal. Chem.*, 1987, **59**(17), 1007A.
8. Huber, L., *"Applications of diode-array detection in HPLC"*, Hewlett Packard, West Germany, 1989.
9. Blanco, M., Gene, J., Iturriaga, H., Maspoch, S., and Riba, J., *Talanta*, 1987, **34**(12), 987.
10. York, D., *Can. J. Phys.*, 1966, **44**, 1079.
11. Frans, S.D., and Harris, J.M., *Anal. Chem.*, 1985, **57**, 2680.
12. Brown, C.W., *et al.*, *Anal. Chem.*, 1982, **54**, 1472.
13. Conners, K.A., and Chukwuenweniwe, J.E., *Anal. Chem.*, 1979, **51**(8), 1262.
14. Rossi, D.T., and Pardue, H.L., *Anal. Chim. Acta*, 1985, **175**, 153.
15. Hansen, E.H., *Quim. Anal.*, 1989, **8**(2), 139.
16. Knudsen, J.G., and Katz, D.L., *"Fluid Dynamics and Heat Transfer"*, McGraw-Hill, New York, 1958.
17. Ruzicka, J., and Hansen, E.H., *"Flow Injection Analysis"*, 2nd edn., Wiley Interscience, New York, 1988.
18. Marshall, G.D., *PhD Thesis*, University of Pretoria, Rep. S. Afr, 1994.

Chapter 3.

Data Acquisition and Analysis

Data acquisition and analysis are important aspects of chemical analysis. Data acquisition methods may vary from a simple steady-state measurement being noted, to a FIA transient profile being recorded on a chart recorder. Fortunately, the use of microcomputer data acquisition has become routine and it is possible to record the vast quantities of data required for multi-component analysis in a convenient fashion. This data acquisition includes any form of apparatus control antecedent to, and required by, the data acquisition procedure. Data analysis incorporates the handling and manipulation of the collected data in order to obtain results.

Automation and control of FIA apparatus has become an integral part of the data acquisition and analysis process. The ability of microcomputers to process vast quantities of data, and to facilitate the interface to analytical instrumentation enables complete automation of the control process from sample injection to result delivery.

Automation and control of the experimental apparatus are detailed in this chapter. Computer-aided Flow Analysis is introduced by means of a dedicated data acquisition and device control software package called FlowTEK™.[1,2] This software provides the necessary FIA manifold automation and control.

With the increased use of microcomputers to acquire data, it is essential that the researcher have a working knowledge of basic programming techniques and be *au fait* with statistical packages and spreadsheets. This will enable suitable manipulation, analysis, and presentation of FIA data. Many FIA methods generate data peculiar to the specific manifold used. Such data often require manipulations that commercial software programs do not provide.

The mathematical routines for quantitation in spectrophotometry were outlined in the previous chapter. Such computations clearly require the use of specific software. The development of a multi-purpose and versatile software program to manipulate and process multi-wavelength data is described. It is intended that this software development will lay the foundation for future work to exploit all the data available from a FIA profile, and when a multi-channel detector is used. The programming language to develop this software is introduced as a very powerful tool in analytical data processing.

3.1 Automation and Control

Microcomputer control requires some form of interface linking FIA devices to a microcomputer, and software to control the devices. A means to acquire data from the detector is also necessary. Microcomputer control allows similar samples to be analysed in a FIA-based analyser in an unattended and automated fashion for several days or longer.

Each FIA experiment produces large quantities of data in comparison to a single value result obtained from manual batch-type operations. This collected data requires storage, manipulation to a usable form, and finally computation and interpretation to yield the analytical results. Automation of these steps is highly desirable for several reasons.

3.1.1 Objectives of Automation

The objectives of automation in the laboratory or in a chemical process vary but both are a result of a consideration of at least a few, if not all, of the following points:

- Processing large numbers of samples
- Increased sample throughput
- Reduction of human participation to reduce errors and lower costs
- Process control
- Lowering reagent and sample consumption
- Facilitating an analysis
- Handling vast quantities of data

Most of these aforementioned points were considered in this work. Particular emphasis is placed on the latter points of facilitating analysis and processing vast data sets.

3.1.2 Computer-Aided Flow Analysis

A specialised microcomputer controlled software package, FlowTEK™, that uses a commercial interface card and a distribution board, was developed for FIA device control and data acquisition at MINTEK. This package provides the user simple and flexible device control, up to four channel data acquisition, and suitable data handling and manipulation facilities. Extensive use was made of the FlowTEK™ package in this work for device control.

The commercial interface card is a general-purpose analogue and digital input/output (I/O) board (PC-30B from Eagle Electric, Cape Town, South Africa). It uses a fully bussed, full length 8-bit slot of a computer. Digital I/O ports are programmable as input or output ports and are transistor-transistor logic (TTL) compatible. These ports enable the connection and control of user-definable devices (for example, peristaltic pumps, valves, on and off switches). Analogue ports (four are used by FlowTEK™) acquire data at a maximum rate of 30 KHz. These ports have an input range of 0 to 10 V.

Devices used in this work were not all TTL compatible and external relays were used to enable computer control. The relays and associated electronic switches were housed within the peristaltic pump casing, or in small plastic boxes as in the case of the injection and selection valves. Over-ride switches and LED position indicators were also included in the configuration. A schematic of the external relay for devices without built-in TTL control logic is shown in Figure 3.1.

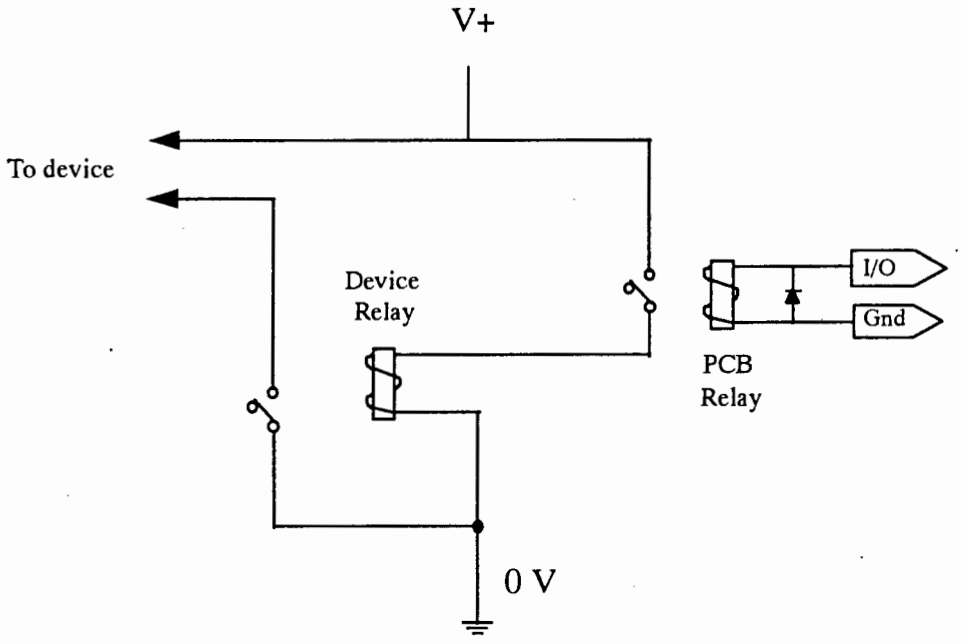

Figure 3.1 *External relay for devices without built-in TTL control logic.* PCB-relay *represents printed circuit board relay with a coil of 5V and 500Ω;* Device relay *represents a relay with coil matching the voltage requirements of the device;* V+ *represents the positive voltage requirement of the device;* Gnd *represents ground connection, and* I/O *represents the input/output ports of the distribution board.*

The FIA manifold configuration, used in conjunction with FlowTEK™ device control, is depicted in Figure 3.2. It comprised a two-line (merging stream) FIA manifold. The carrier and reagent streams were propelled by a peristaltic pump at a constant flow rate. Samples were introduced into the manifold *via* an injection valve. The injection valve was connected to a 6-port selection valve to enable selection of up to six different solutions for measurement. Both valves were pneumatically switched under computer control. The detector "autozero" and "remote start" controls were controlled by the computer *via* the FlowTEK™ distribution board.

Figure 3.2 *Schematic representation of the FIA manifold comprising a peristaltic pump, P; injection valve, IV; selection valve, SV; spectrophotometric detector, D; carrier stream, C; reagent stream, R; and waste, W. The general-purpose I/O interface card is housed within the computer and is linked to the detector and devices via the distribution board, DB. Digital (.....) and analog signals (----) are shown.*

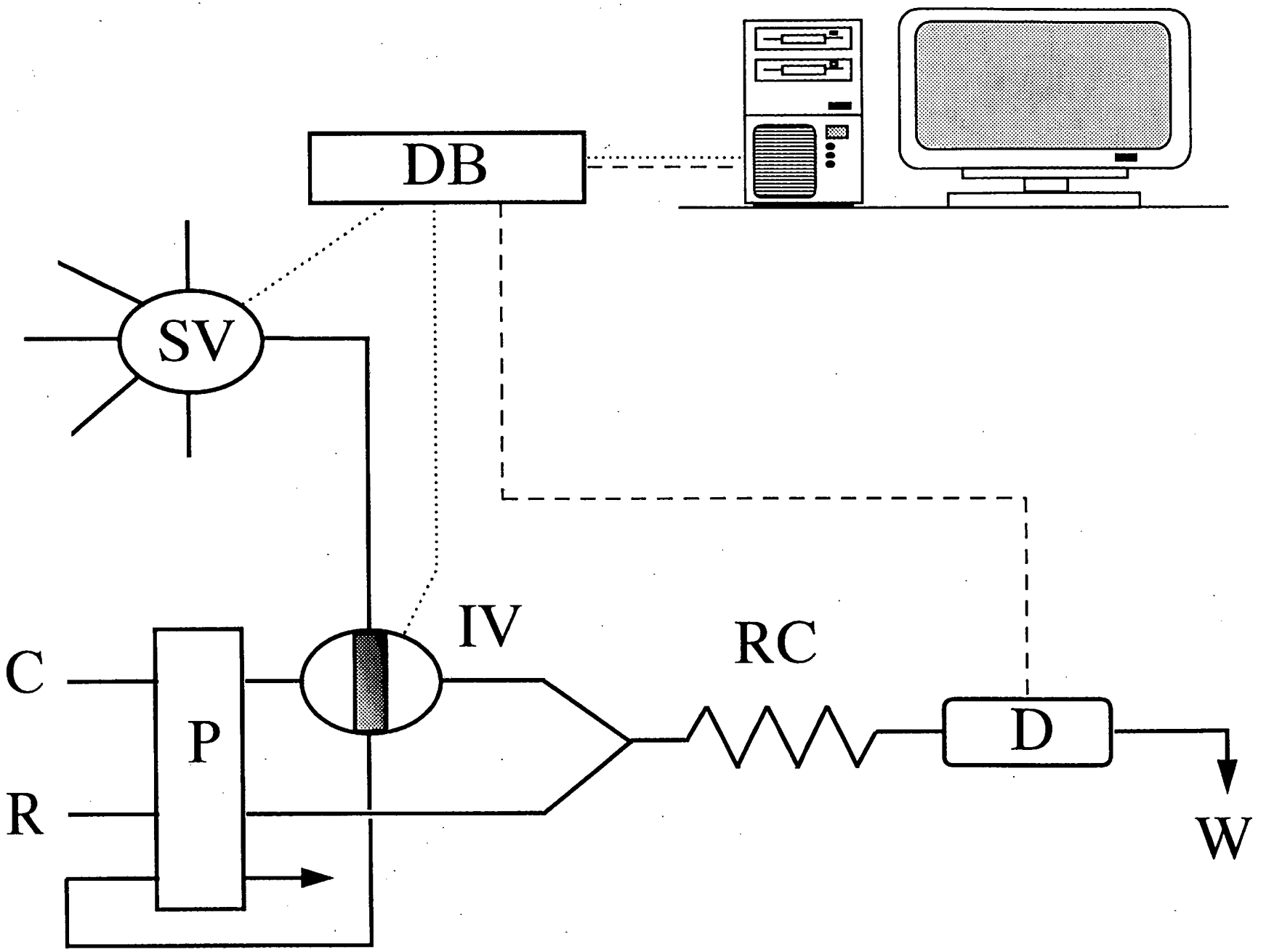
DB
SV
IV
RC
C
P
R
D
W

3.2 Microcomputer Software Development

The development of MCA methods for the determination of the PGMs necessitated the use of several analytical wavelengths. The high-speed scanning spectrophotometer used, the Spectra FOCUS™, was shipped with OS/2 and Microsoft® Windows™ version 2 based software programs that allow serial transfer of the recorded spectral scans to a remote computer. Neither of these software programs attained suitable operational status.

The cause of these problems seems to have been due to unknown conflicts between the software and the detector and computer hardware. It was also found from an operational system elsewhere that the spectral data were inaccessible due to the complex storage format. Furthermore, no comprehensive data manipulation or multi-component-based software exists for this instrument.

As the detector has only four analogue output ports, an alternative approach, although tedious, was used. The detector stored the recorded spectral scans and these scans were subsequently "played-back" through a single analogue output port. The FlowTEK™ software was used to collect this data. The detector "download" rate settings were adjusted to allow the *absorbance-time* data acquired by FlowTEK™ to be readily converted into *absorbance-wavelength* data.

Additional software was therefore required. to enable adequate data handling and analysis. As the author is most familiar with the Basic programming language, the selection of Visual Basic™ as the development tool was natural. The software developed can operate under the Microsoft® Windows and OS/2 platforms. The latter enabled true multi-tasking and allowed concurrent data collection *via* FlowTEK™ and data analysis by the user.

The software developed during the course of this study was tentatively called "ReduceTEK". The current version is 3.2. This version contains most of the features of previous versions.

3.2.1 Microcomputers and Accessories

Two computers were used - a 386 DX 33 MHz computer with 8 Megabytes (Mb) of RAM, an 80 Mb hard disk drive, an Intel® math co-processor, and a super visual graphics array (SVGA) screen, as well as a 286 12 MHz computer with 640 K memory, a 20 Mb hard disk drive, and a visual graphics array (VGA) screen. They were fitted with standard "floppy" (1.2 Mb) and "stiffy" (1.44 Mb) disk drives.

The FlowTEK™ package was run on either the 286 or 386 DX computer under a DOS® (Disk Operating System®) shell. Operation of FlowTEK™, in the DOS® shell, using the multi-tasking 32-bit OS/2 2.0 Presentation Manager™ platform was possible for the 386 DX computer. The Spectra FOCUS™ detector was coupled to the computer running the FlowTEK™ software. Most experimental data was acquired over the full absorption spectra (368 to 668 nm). In addition, data acquisition at only four wavelengths was performed in some cases.

An Epson LX-400 dot matrix printer was used for hard copies of the data files and results. A Microsoft® mouse was used throughout the work.

3.2.2 Meeting the Challenge of the Graphical User Interface

Visual Basic™ is a visual development environment (VDE) that offers a simple approach to Windows™ or OS/2 based program and interface design. The essential difference between Visual Basic™ code and a DOS® program is that the Visual Basic™ code does not operate in a procedural fashion (i.e. starting at the first command and moving through a sequence of commands). Instead, it is event-driven programming, where the code that is used remains idle until called upon to respond to a specific user- or system-initiated event.

In addition to this difference, Windows™-based programs share screen space and computing time. This allows multiple windows to be displayed simultaneously.

The event-driven application design makes the programmer more productive by providing the appropriate tools for the different aspects of graphical user interface (GUI)

development. The essential components of Visual Basic™ program development are shown with reference to a portion of sample code taken directly from ReduceTEK. The code in Figure 3.3 is from the file management part of the ReduceTEK software.

Some steps in graphic user interface (GUI) design and programming are outlined. First, the GUI for the application is created by drawing *objects* in a graphical way. An object can refer to a *form* or *control* (such as a command button, text box, file control lists, drop-down menu, etc.). The "Toolbox" has a selection of common *tools* needed in Visual Basic™ applications. In Figure 3.3 such objects are seen in the form "Select Data File ...". The current selection points to a command button ("OK") and a list of files is displayed in a file control list. The objects drawn are then refined by setting their *properties*. The "properties bar" shows the caption text for the current selection command button. The text entered, "OK", is displayed on the command button. Many other properties relating to the screen display and functioning of the objects may be set.

The interface is then made to react to the user by writing code that responds to *events* that occur in the GUI. In the "source code window" typical code for such an event is shown. The object here is the command button "OK" and the event (see the "event menu") is "Click" - a mouse button click. In other words, when a mouse-click is identified on the OK-button then the code shown is executed. Many other events, such as drag-and-drop options, double clicks, and mouse movement, can also be handled. A *form* and *module* in the minimised state are shown. The module, "Spectrum.BAS" here, is a collection of code that is not linked to a form. An event on a form accesses this code by means of sub-routine calls.

Meeting the challenge of the GUI is therefore essentially the development of software that makes full use of the provided features and capabilities of the programming language without forgetting the necessity for easy interaction with the user.

Figure 3.3 *The Visual Basic™ graphical user interface showing the various parts of the interface and their relationship with one another.*

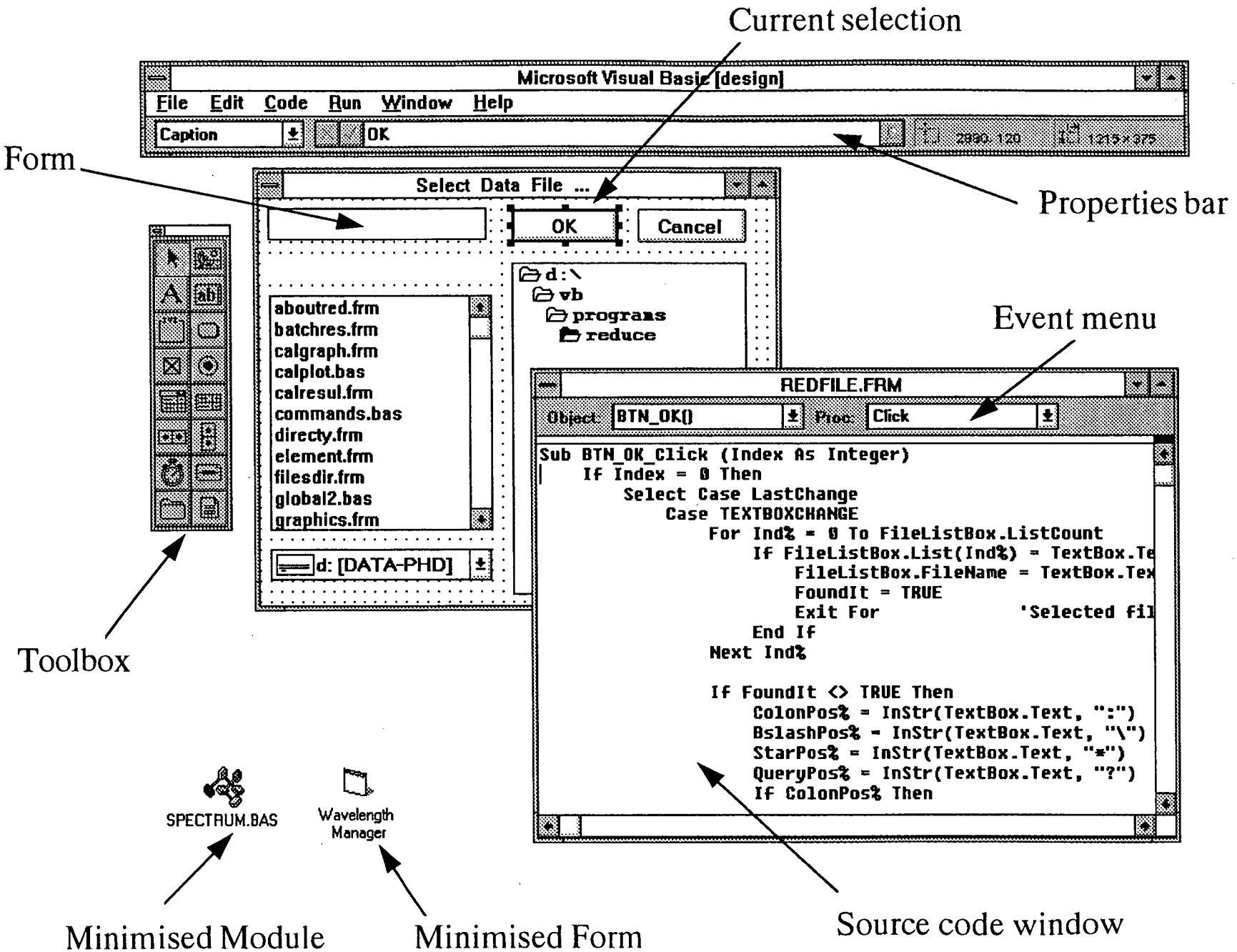
Current selection
Microsoft Visual Basic [design]
File Edit Code Run Window Help
Caption
OK
Properties bar
Form
Select Data File ...
OK
Cancel
aboutred.frm
batchres.frm
calgraph.frm
calplot.bas
calresul.frm
commands.bas
directy.frm
element.frm
filesdir.frm
global2.bas
graphics.frm
d:\
vb
programs
reduce
d: [DATA-PHD]
Event menu
REDFILE.FRM
Object: BTN_OK()
Proc: Click
Sub BTN_OK_Click (Index As Integer)
If Index = 0 Then
Select Case LastChange
Case TEXTBOXCHANGE
For Ind% = 0 To FileListBox.ListCount
If FileListBox.List(Ind%) = TextBox.Te
FileListBox.FileName = TextBox.Tex
FoundIt = TRUE
Exit For 'Selected fil
End If
Next Ind%
If FoundIt <> TRUE Then
ColonPos% = InStr(TextBox.Text, ":")
BslashPos% = InStr(TextBox.Text, "\")
StarPos% = InStr(TextBox.Text, "*")
QueryPos% = InStr(TextBox.Text, "?")
If ColonPos% Then
Toolbox
SPECTRUM.BAS
Wavelength Manager
Minimised Module
Minimised Form
Source code window

3.2.3 Program Structure and Design

ReduceTEK is a menu-driven program developed using Microsoft® Visual Basic™. The size of the executable file is 304 K. A 270 K Visual Basic™ DLL (dynamic link library)[3] and default ReduceTEK configuration files are required for program operation.

The modularity and flexibility of the program were achieved by the use of independent sub-routines and function calls within separate source code modules. The standard Windows™ GUI elements, such as pull-down menus and dialog boxes, were included as required. A dendrogram of the program is shown in Figure 3.4.

Each level in the program is activated through menu choices. These are selected by means of a pointing device, arrow keys, or "short-cut" keys (*viz.* Alt-F to access the "File" drop-down menu). The button bar performs the same function as the relevant main menu selection. These buttons have been included, along with "short-cut" keys, to enable more rapid selection of the most frequently used main menu options. Details of the main menu options are shown in Table 3.1.

Figure 3.4 *Dendrogram of the ReduceTEK program showing the various menu options and program functions.*

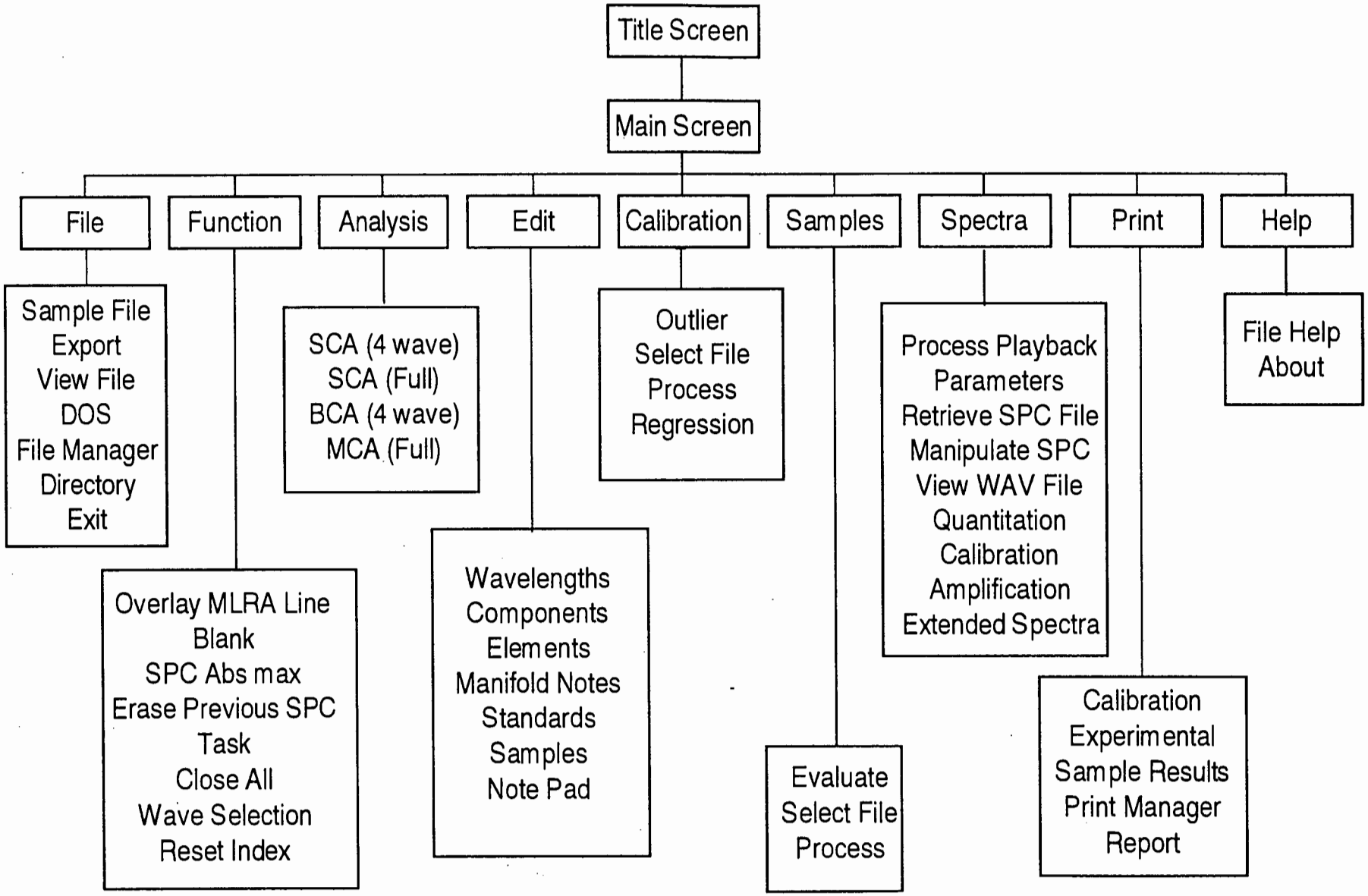
Title Screen
Main Screen
File
Function
Analysis
Edit
Calibration
Samples
Spectra
Print
Help
Sample File
Export
View File
DOS
File Manager
Directory
Exit
Overlay MLRA Line
Blank
SPC Abs max
Erase Previous SPC
Task
Close All
Wave Selection
Reset Index
SCA (4 wave)
SCA (Full)
BCA (4 wave)
MCA (Full)
Wavelengths
Components
Elements
Manifold Notes
Standards
Samples
Note Pad
Outlier
Select File
Process
Regression
Evaluate
Select File
Process
Process Playback
Parameters
Retrieve SPC File
Manipulate SPC
View WAV File
Quantitation
Calibration
Amplification
Extended Spectra
Calibration
Experimental
Sample Results
Print Manager
Report
File Help
About

Table 3.1 *ReduceTEK main menu options and descriptions.*

Menu option	Description
File	Allows file manipulations such as viewing files, directories, and exporting files. A shell to the disk operating system, DOS®, and Windows™ File Manager is provided.
Function	Provides the user with routine function operations for the analysis and viewing of processed data files.
Analysis	Options for single component (SCA), binary component, and multi-component (MCA) analysis at 4, or up to 100, wavelengths.
Edit	Editor for user-input of wavelengths, component names, concentrations, and a note pad for the current experimental details.
Calibration	Options for processing FlowTEK™ four channel data using SCA.
Samples	Evaluation of sample data at four wavelengths (SCA).
Spectra	Multi-component spectral analysis option. Processing raw data, quantitation, calibration and other manipulation functions.
Print	Option for printing experimental details and results to a printer.
Help	Help option primarily for file formats and information about the system memory and performance.

ReduceTEK is divided into several interlinked "modules", each accounting for an aspect of the data handling. These modules are separate units comprising a "pop-up" window and its requisite code. The module first prompts for the file to be viewed, retrieves that file, and displays it using appropriate scales and axes. For example, a view of the standard absorption spectra after averaging is shown in Figure 3.5 in the "Spectra window".

Multiple window views give the user the analysis parameters used, results in tabular and graphical format, and statistical analyses simultaneously. Each window is interlinked to the others so that a change in one automatically updates the others. A multiple window view for a multi-wavelength sample analysis is shown in Figure 3.6 illustrating the transparency of the analysis methodology to the user. Similar multiple-window views are used for manipulation of the data when using only a few wavelengths.

Figure 3.5 *Processed standard spectra view in ReduceTEK, operating under Windows™, showing spectral data acquired and processed between 368 and 668 nm for Pd(II) standards (10 to 100 μg.cm^{-3}). The various components of the display screen have been annotated (viz. menu, button bar, program icons).*

Main screen menu

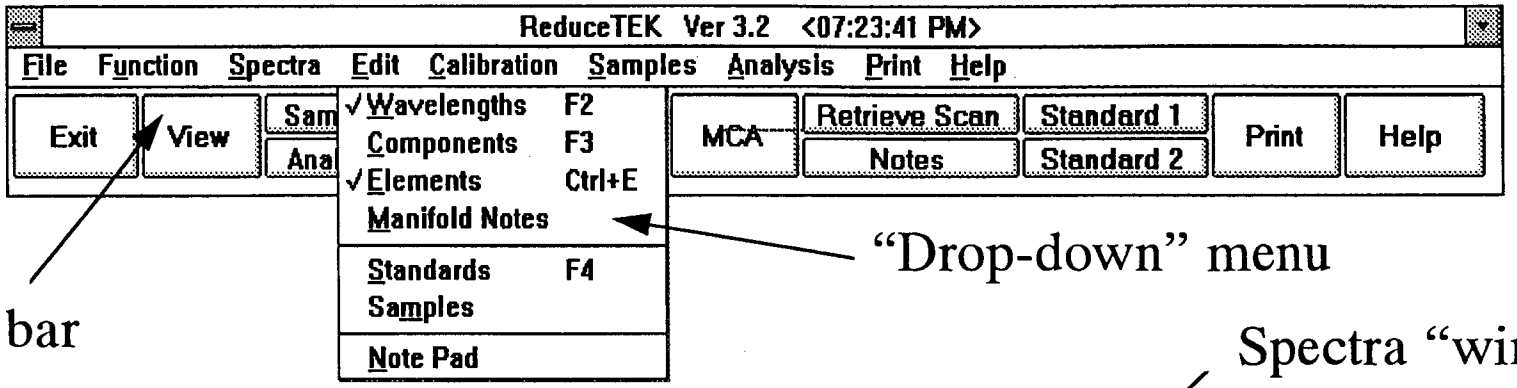

Button bar

"Drop-down" menu

Spectra "window"

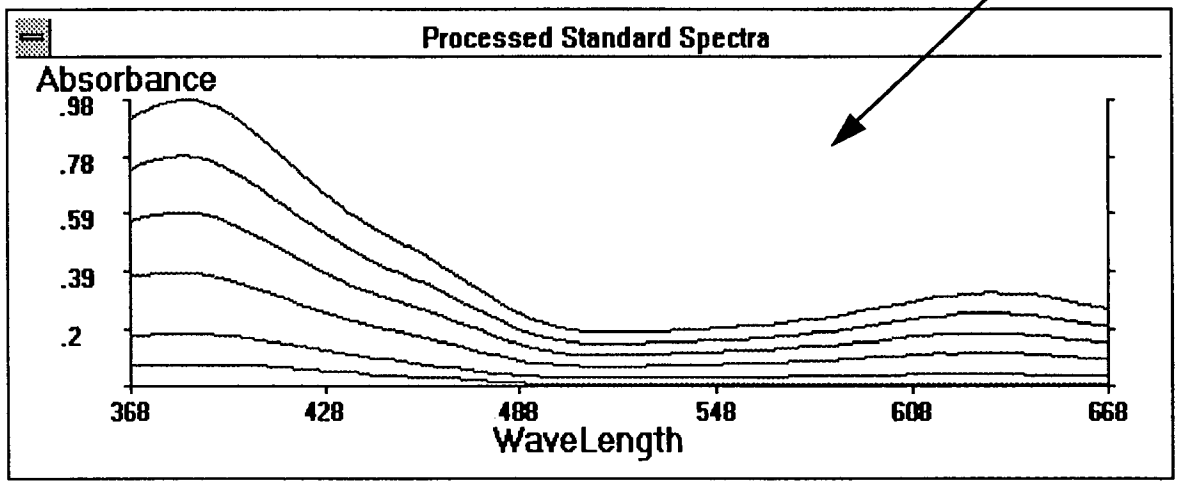

Windows' program icons

Figure 3.6 *Typical multi-linear regression analysis (MLRA) screen view as depicted during data processing of platinum-palladium mixtures in ReduceTEK 3.2. Each window is interlinked and any change in one automatically updates the others.*

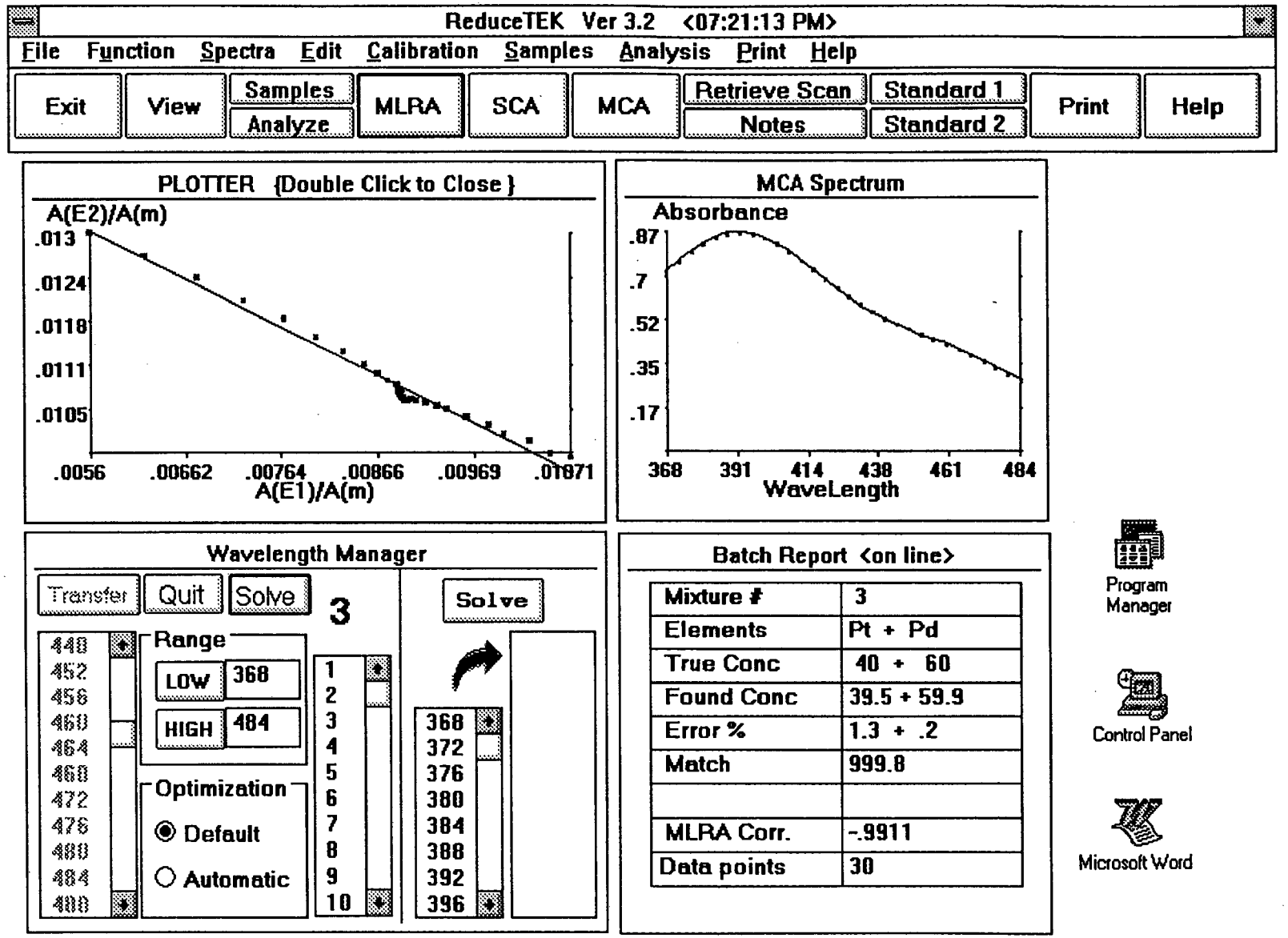
ReduceTEK Ver 3.2 <07:21:13 PM>
File Function Spectra Edit Calibration Samples Analysis Print Help
Exit
View
Samples
Analyze
MLRA
SCA
MCA
Retrieve Scan
Notes
Standard 1
Standard 2
Print
Help
PLOTTER {Double Click to Close }
A(E2)/A(m)
.013
.0124
.0118
.0111
.0105
.0056
.00662
.00764
.00866
.00969
.01071
A(E1)/A(m)
MCA Spectrum
Absorbance
.87
.7
.52
.35
.17
368
391
414
438
461
484
WaveLength
Wavelength Manager
Transfer
Quit
Solve
3
Range
LOW 368
HIGH 484
Optimization
Default
Automatic
Solve
Batch Report <on line>
Mixture # 3
Elements Pt + Pd
True Conc 40 + 60
Found Conc 39.5 + 59.9
Error % 1.3 + .2
Match 999.8
MLRA Corr. -.9911
Data points 30
Program Manager
Control Panel
Microsoft Word

3.2.4 Data Storage

All data files generated by FlowTEK™ and ReduceTEK are stored in the ASCII * format. Although the ASCII data files use more hard disk space than other methods of encoded or compressed storage, the requirement of facilitating data transfer to statistical packages, spreadsheets, and editors was important. Typical file extensions and file contents for ReduceTEK are tabulated in Table 3.2.

In FlowTEK™, the peak parameters (height, area, width, time, and concentration) together with the date and time of the measurement, and the profile names are stored in one data file called the "Reduced Data" file. The profile file contains the actual data points that describe the FIA response profile. The data is stored as the original raw data from the analog-to-digital converter.

In this work, data was either collected at four wavelengths using the four output channels of the Spectra FOCUS™ detector and the reduced data files were imported by ReduceTEK for data processing, or data was collected over the full absorption spectra (368 nm to 668 nm) and then "played-back" from the detector memory to FlowTEK™. The profile files were then accessed by ReduceTEK for analysis.

---

* ASCII ≡ American Standard Code for Information Interchange

Table 3.2 *File Extensions (*.Extension) and File Contents for ReduceTEK 3.2 (unless noted otherwise) files.*

File Extension	File Contents
RED	FlowTEK™ Reduced data file. Condensed FIA results.
1,2,3,...,99	FlowTEK™ Profile file ("fiagram") of experiment, or group of spectral scans, denoted by the numeral.
RST	Four wavelength concentration results file containing experimental statistical information.
CAL	Four wavelength calibration data file with regression results.
SPC	Spectral absorbance data file; processed from the FlowTEK™ profile file containing a group of scans.
WAV	Wavelength and final spectra file. Averaged spectral scans from SPC files and contains concentrations.
ASM	Spectral regression file containing calibration results for multi-component analysis of samples.
SEQ	Single sample quantitation file for multi-component analysis. Contains concentrations, absorbances and MLRA function values.
MCQ	Multi-component quantitation results files.
GP	GraphPad™ 2.0 file for regression verification purposes.
TXT	Text file containing notes and experimental details.

3.2.5 Software Performance and Validation

The OS/2 2.0 operating system enables the ReduceTEK software program to operate in a Win-OS/2 shell. The program is also fully compatible with the more familiar and popular Windows™ environment.

The program was specifically written for the Spectra FOCUS™ detector and FlowTEK™ package, but the Windows™-based manipulation of the data may be applied to any multi-channel detector where the data is acquired with FlowTEK™. Data may also be manually entered *via* an editor, in the FlowTEK™ data format, and processed as before by ReduceTEK.

All mathematical algorithms and program modules were tested with simulated data. Manual computations were also performed where applicable. No deviation in either validation approach was found. Statistical programs, such as GraphPAD™ 2.0, were also employed to verify the statistical functions. After any code alterations or additions, the mathematical tests were again performed to ensure reliability and confidence in the results.

The program print options are compatible with printers like the dot matrix Epson LX-400 and the Hewlett Packard LaserJet IIIP. Ideally, a mouse or pointing device should be used, although complete keyboard operation was built into the program.

3.3 Experimental Procedure

The experimental procedure followed involves a reasonably complex series of steps. Extensive investigation to find alternative options that could be followed for the particular detector used in this work proved fruitless. The semi-automatic procedure followed here allowed adequate investigation into the simultaneous determination of the PGMs by FIA with spectrophotometric detection.

The sequence of steps, from the initial FIA experiments, to the final results obtained from ReduceTEK using multi-component analysis over a range of wavelengths, are listed.

1. Perform FIA experiments, under FlowTEK™ control, and store the absorption spectral scans of each sample and standard in the detector memory.
2. "Play-back" the spectra *via* a FlowTEK™ input channel (up to 25 spectra can be "played-back" to FlowTEK™)
3. Store the spectra in a compressed format in FlowTEK™ profile files.
4. Correct spurious data points which result from the imperfect means of acquiring the data.
5. Enter various parameters required by ReduceTEK, such as the number of spectra, concentrations, absorbance full scale settings, element names, and number of components.
6. Store final blank corrected and averaged spectra for a particular standard or sample, with associated mixture information in a *.WAV file.
7. Quantitation performed by ReduceTEK using one of the quantitation options on retrieval of the stored standard and sample files.
8. The analytical results are viewed on screen, stored to file, and, if required, printed.

As would be expected, the time per analysis (including data processing) was longer as a result of the semi-automatic procedure of data handling. The FIA experiments were carried out in an unattended mode of operation. The detector also collected the spectral scans automatically. After a maximum of 25 scans had been collected, the data "play-back" to FlowTEK™ was started. This was fairly rapid as spectra may be "played-back" at an accelerated rate.

The task of checking and correcting each spectral scan for spurious peaks was by far the most tedious. A typical check of 20 spectral scans could take over an hour depending on the number of corrections necessary. In cases where several corrections were required, FIA experiments and data capture were repeated. The full quantitation and output of results by ReduceTEK is swift.

No doubt the procedure used has limitations, but these are not of a nature that render it invalid, or mathematically incorrect. The correction of spurious points is undesirable, however, the "intelligent" software required to handle the variability of spurious peaks is beyond the scope of this work. The preferred solution to overcome these limitations would be to use the international standard RS-232 serial-based communication with the spectrophotometer. This would obviate the analogue recording of the "played-back" data. Without access to the communication protocol (from the detector suppliers) this route cannot be utilised. Such possibilities are being investigated.

3.4 Programming Language Remarks

The usefulness of Visual Basic™ as a program development tool was clearly demonstrated. It facilitates convenient and powerful Windows™-based programming capabilities in the research environment. It is an ideal starting point for individuals launching into Windows™-based programming - especially from a DOS® programming background (such as MS-Quick Basic or GW-BASIC). Although minor variations in the code do occur, there is no need to learn a completely new programming language, such as Visual C++™.

The amount of time spent on designing a complex graphical user-interface is significantly reduced using Visual Basic™. At last the burden of creating the visual and highly interactive environmental framework within which the user writes the necessary source code has been placed on the applications developers. No longer does an application require half of its code to be devoted to the user-interface. The programmer's skills, efforts, and time may now be directed into "building that better mousetrap" within the developing software. Comprehensive on-line help and a tutorial within the programming language assist the user in the switch from a typical procedural, or "top-down", program structure, to the event-driven Visual Basic™ programming style.

3.5 Conclusions

The simplicity inherent in FIA was exploited significantly by automation of the manifold components and data acquisition process. The procedure employed in "down-loading" absorption spectra from the detector could be improved significantly by serial communications. Nevertheless, the rudimentary foundation to incorporating multi-channel manipulations of FIA data as a standard feature in future Computer-aided Flow Analysis software has been placed in position.

The powerful features of Visual Basic™ as a Windows™-based programming environment for software development was illustrated in the development of the software program, ReduceTEK. This software provided an efficient and versatile means of handling multi-channel data, and facilitated rapid processing of results.

The software user has a convenient tool whereby absorption spectra may be manipulated so as to extract significant amounts of otherwise inaccessible information. The framework of ReduceTEK, and expertise developed in Visual Basic™ coding, will no doubt facilitate further development of the software to include other complex chemometric functions.

3.6 References

1. Marshall, G.D., and Van Staden, J.F., *Anal. Instrum.*, 1992, **20**(1), 79.
2. FlowTEK™ Software Package, Council for Mineral Technology, Randburg, Rep. S. Afr.
3. Microsoft® Visual Basic™ Programmer's Guide, ver. 1.0, 1991.

Chapter 4.

Flow-Injection Analysis Manifold Design and Optimisation

The performance of an analytical instrument depends strongly on the optimisation of several parameters. Chemical variables (reagent and carrier solution concentration) and physical variables (flow rates, reaction coil lengths, sample injection volume) of the FIA manifold must all be optimised, as must the method of detection (wavelength range, number of replicate scans). Rarely are these parameters independent[1] and the purpose of optimisation is to find the best set of conditions to solve the particular analytical problem within a reasonable number of experiments.

A more complete characterisation of chemical systems may be obtained by using three-dimensional response surface plots. These highly informative plots assist in the optimisation and understanding of FIA systems and are a convenient means of visualising multivariate interactions. "Flow Chemography"[2] is the term used to describe such use of graphical representations of data from flow systems. Widespread use of this representation of data is anticipated as more information is required from experiments. Visual interpretation of the data allows the user to obtain insights into the complex chemical reactions occurring within the manifold, and facilitates selection of optimum experimental conditions.

This chapter details the initial FIA manifold design and configuration made prior to a thorough optimisation of the FIA manifold for tin(II) chloride methods. The optimisation of the manifold took into consideration that adequate sensitivity and high precision would be essential in the simultaneous determination of platinum and palladium. It must be noted that the optimum conditions for individual components are not necessarily optimum for an analysis of mixtures.

4.1 Preliminary Manifold Design Investigations

Initially, a single-line FIA manifold was configured to investigate the possibility of using the reaction of tin(II) chloride with platinum and palladium analytically.[3] The absorbance was initially monitored at a single wavelength. The development of sophisticated software to process multi-channel data made the use of a rapid scanning detector possible during the latter portion of this work.

Consider the reaction of platinum with tin(II) chloride in hydrochloric acid solution, and the FIA manifold depicted in Figure 4.1. Tin(II) chloride, in HCl, makes up the reagent stream. The sample is injected into a carrier stream of HCl. The two streams merge and mix on-line, with the reaction taking place on passage to the flowcell.

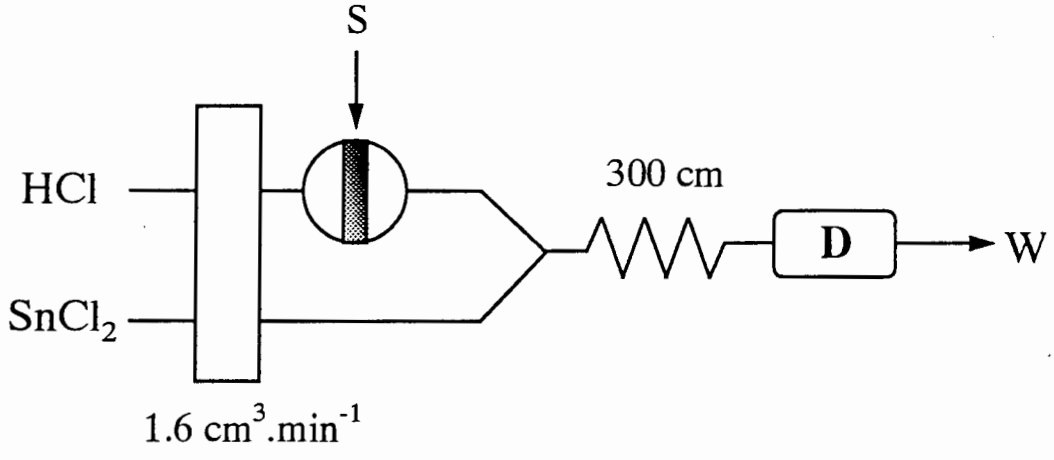

Figure 4.1 *Schematic diagram of the merging stream flow-injection manifold.*

On passing through the flowcell, the absorption spectra is captured by a rapid scanning spectrophotometer. A typical three-dimensional *time-absorbance-wavelength* response surface map is shown in Figure 4.2 to demonstrate the quantity of data that could be produced using a multi-channel detector. As a consequence of the limitations of the detector, only the absorption spectra at the FIA profile maxima, were used quantitatively in this work.

Figure 4.2 *Absorbance response surface map for a 125 μL sample of 100 μg.cm^{-3} Pt(IV) (FIA manifold as in Figure 4.1). Absorbance spectra of the reacted sample zone are captured at 2 second intervals here by the Spectra FOCUS™ scanning spectrophotometer.*

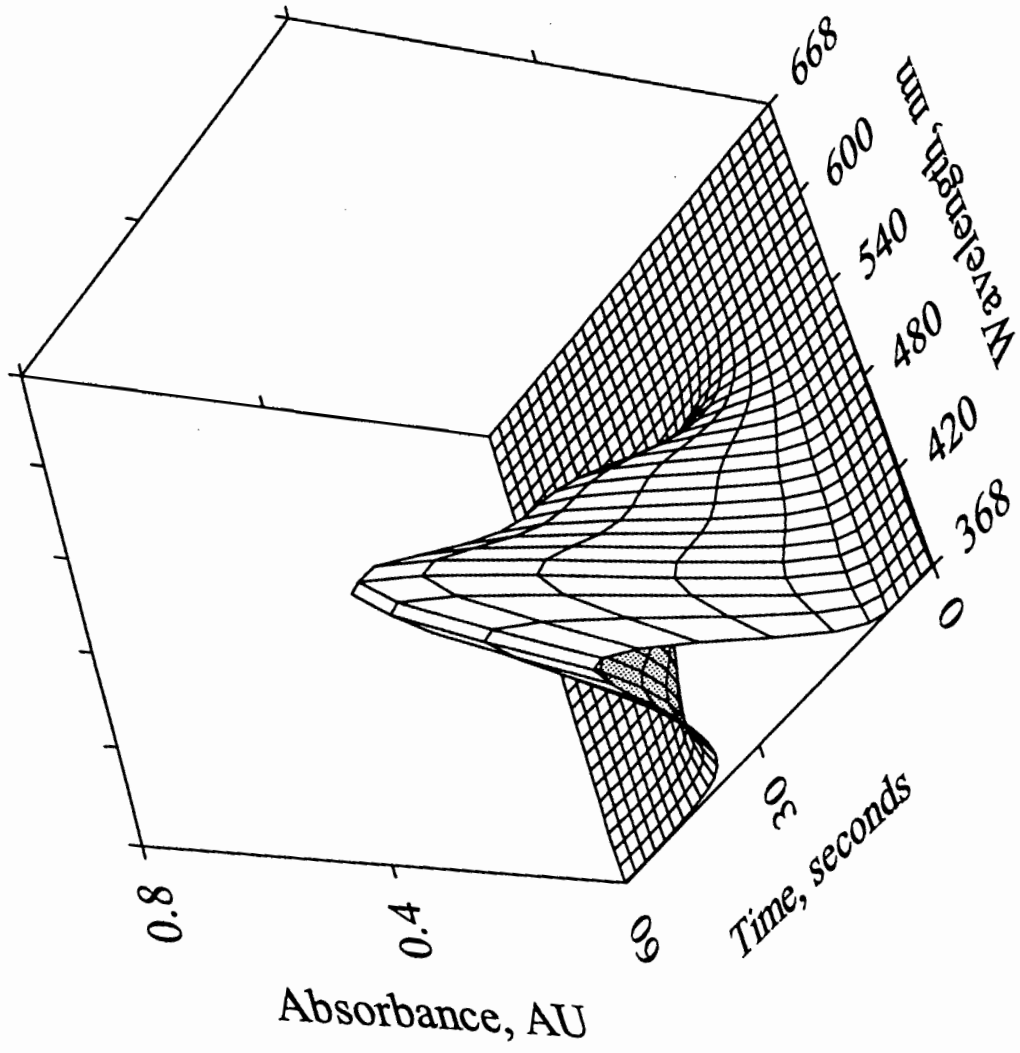
668
600
540
480
420
368
Wavelength, nm
0
30
Time, seconds
0.8
0.4
0
Absorbance, AU

Note that intersections on the grids of the response surface maps shown in this, and subsequent chapters, do not correspond to single data points. In each case, more data points than grid intersection points were used in the three-dimensional plotting. The grid intersections were limited for visual purposes and do not affect the overall trends observed.

4.1.1 Spectrophotometer Flowcell

The spectrophotometer flowcell is an important component of a FIA system. The flowcell produces significant effects that are caused by the finite volume sampled by the light beam, as well as the disruption of laminar flow conditions in the manifold tubing.[4] Selection of a flowcell should be made after careful consideration of its geometry, optical volume, and the composition of "wettable" components.

Three flowcells were considered. The first two were standard 10 mm path length Hellma quartz flowcells with illuminated volumes of 30 μL and 70 μL respectively. They were mounted in a flowcell housing accessory. Excessive dispersion of the sample zone was found on passage through these relatively large diameter flowcells. Stray light could not be excluded from the flowcell housing and these flowcells also tended to shift slightly in their housing with time. Any bubbles that were accidentally introduced into the system lodged in corners of these cells. All of the above-mentioned effects contributed to an increased baseline noise. These cells were not used in this work.

The third flowcell was a biocompatible flowcell shipped with the Spectra FOCUS™ detector. All "wettable" parts were made of Kel-F™ and the flowcell had sapphire windows. Although the path length was only 6 mm (illuminated volume of 9 μL), the added flowcell stability, lack of any stray light entering due to of its well-sealed housing, and limited additional dispersion, more than compensated for this shorter path length. The nature of the highly acidic solutions being used restricted the selection of a flowcell to one which had inert "wettable" components.

4.1.2 Manifold Configuration

A further consideration with regard to the FIA system was the actual manifold configuration. Two configurations were considered - a single stream manifold, and a two stream manifold where the streams merge prior to the detector. Two factors were considered in the configuration selection, *viz.* the magnitude of the analytical signal and the magnitude of the baseline noise. Both significantly affect the detection limit and are normally maximised and minimised respectively.

The immediate apparent advantage of using a single stream system over a merging stream system is the lack of further dilution at the confluence point. This consideration would appear to indicate a higher expected sensitivity* for the single stream system. However, sensitivity is not the only design criterion. A good signal-to-noise ratio is also important.

The blank and sample response could not be distinguished in the single-line manifold when injecting samples of low concentrations of platinum (< 0.1 $\mu g.cm^{-3}$). Both showed similar, although small, responses. This problem arises due to the Schlieren effect caused by mixing of solutions with different refractive indices.[5] Mixing occurs along the full length of the sample zone in the case of a merging stream manifold, and the refractive index effect is virtually eliminated. The blank response is not distinguishable from the baseline in the merging stream manifold. Considerable improvement in the lower limit of determination was obtained for platinum.

4.1.3 Ultra-Violet Spectrophotometric Detection

The sensitivity of the platinum-tin(II) chloride reaction can, in principle, be improved 2 to 4 times by monitoring the absorbance at a wavelength of 310 nm[6]. However, background interference precludes the use of this wavelength. Furthermore, the detector used could not simultaneously scan the visible and ultra-violet range of the absorption spectra. Consequently, attention was focused only on the visible regions of the absorption spectra.

---

* Sensitivity refers to the response of the analytical signal per unit concentration.

4.1.4 Peak Height or Peak Area Measurement ?

Another factor considered in the preliminary investigations for this work was the use of peak height and peak area measurements. In a FIA system, both the peak height and peak area are proportional to the analyte concentration,[7] hence either can be used for quantitative analysis. Ideally, a linear regression of the peak height *versus* peak area for the calibration standard set should have a unit correlation coefficient and zero intercept. This would indicate conformity of the transient peak profile across the calibration concentration range and that unexplained chemistries, causing deviations of the profile, were not the cause of any spurious peak height deviations. This was verified at several wavelengths across the absorption spectra for each analyte in a mixture. Linearity within the range of the calibration standards solutions was found in each case.

Besides the profile conformity verification, peak height measurements were employed throughout. The Spectra FOCUS™ detector, having limited memory and storage facilities, was unable to collect absorbance spectra satisfactorily across the entire flow-injection peak profile to enable peak area integration.

4.1.5 Spectra FOCUS™ Data Acquisition

The Spectra FOCUS™ detector has a mechanism to recognise the peak maximum (by the change in absorbance with time), and initiates spectral scanning itself. The desired wavelength range is scanned at a user-selectable rate which is determined by the number of wavelengths, wavelength intervals, and number of repetitive scans to be averaged. Despite the lower wavelength ability of the instrument being 360 nm, a lower wavelength of 368 nm was used. The upper limit of the instrument extends to 800 nm. The palladium-tin(II) chloride system has an absorbance maximum at 636 nm (Figure 4.3). An upper wavelength limit of 668 nm was selected to ensure incorporation of this maximum. This enabled a wavelength range of 300 nm to be used in all quantitative work. Some qualitative spectral scans were performed using a wavelength range extending to 768 nm.

Figure 4.3 *Absorbance response surface map for a 125 μL sample of 100 μg.cm^{-3} Pd(II) on passage through the detector flowcell (FIA manifold as in Figure 4.1). Note the distinct spectral character of the absorbance spectra shown.*

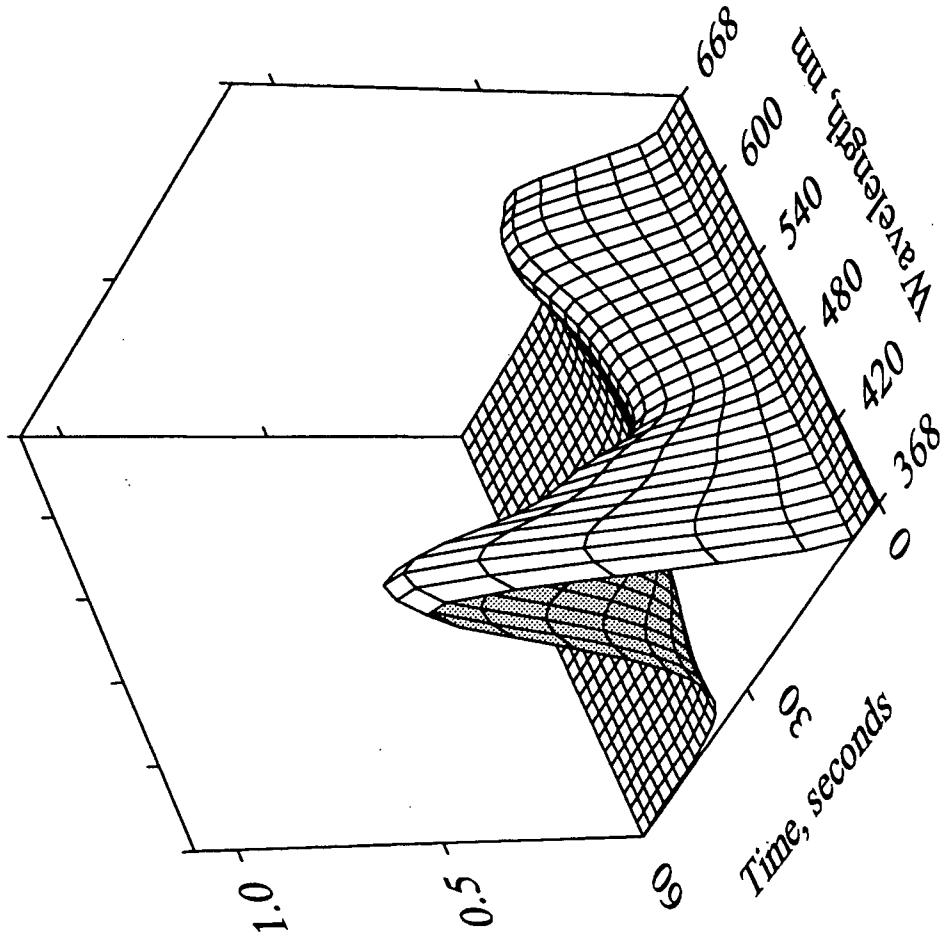
668
600
540
480
420
368
Wavelength, nm
0
30
60
Time, seconds
1.0
0.5
0
Absorbance, AU

Absorbance spectra were collected at wavelength intervals between 2 and 10 nm using single, duplicate, and quadruplicate scans. A spectral scan time for the peak height of more than a few seconds is not desired as the FIA signal is transient and rapid. The spectral scan should, ideally, be symmetrically distributed over the FIA profile maximum. Cognisance was taken of the detector's memory availability in the choice of the number of wavelengths to include.

A compromise between response, spectral scan time, and the memory limitations resulted in the use of a duplicate scan (average spectra were stored) at 4 nm intervals (affording 76 points to define the absorbance spectrum). A maximum of 25 spectra could be stored prior to the required down-loading from the detector. The duration of a typical single spectral scan was 0.95 seconds.

4.2 Optimisation of the FIA Manifold

The univariate method[7] of optimisation requires parameters to be independent. This method can produce sub-optimum settings if variables are dependant on one another. Furthermore, a large number of experiments are required because each parameter is optimised in a univariant fashion. However, if these interactions are not significant, the univariant approach functions well.[1]

A more efficient optimisation strategy is the simplex optimisation method. This method was first proposed by Spendley,[8] later modified by Nelder and Mead,[9] and has numerous variations.[10] Simplex optimisation involves an experimental re-adjustment of all the variable parameters toward an optimal configuration. Subsequent experimental conditions are suggested by the optimisation algorithm based on the previous experiment results.[11] The simplex method is widely used and the number of experiments required for optimisation is considerably less for complicated multi-variable systems. The chance of attaining sub-optimum settings is greatly reduced because this approach operates on a response surface, and therefore accommodates dependant variables.

An iterative univariate method of optimisation was used in this work. Once an optimum was found, or more often, a setting that enabled solution of the analytical problem, the

variables were adjusted around the optimum until no significant improvement was found. No sub-optimum settings were found. This result was further verified by viewing three-dimensional surfaces of the optimisation data.

A range of variables were examined (Table 4.1), each having set boundaries, chosen on the grounds of experimental experience, which were not traversed for practical reasons. Details on the apparatus used may be found in Chapter 8. Parameters such as the manifold tubing inner diameter (0.5 mm I.D. was used throughout) and temperature of the reaction coil (room temperature) were fixed. The carrier to reagent flow rate ratio, another potential variable, was kept constant at 1:1. No significant improvements where observed when changing this ratio.

Table 4.1

Range of variables examined for the FIA manifold optimisation for the simultaneous determination of platinum and palladium.

Variable	Range	Units
Tin(II) chloride concentration	0.01 - 0.4	$mol.dm^{-3}$
HCl concentration	0.5 - 4.0	$mol.dm^{-3}$
Sample HCl concentration	0.5 - 4.0	$mol.dm^{-3}$
Sample size	10 - 250	μL
Reaction coil length	60 - 380	cm
Flow rate	1.0 - 4.0	$cm^3.min^{-1}$

Optimisation of variables for distinctly differing systems, as in the case of platinum and palladium reactions, was done relative to one component and then the defined conditions were applied to the other component. The approach was found to be acceptable since the loss of sensitivity, relative to the optimum manifold for one component, was small in these compromise situations.

It is necessary to select a response which will indicate the best conditions in order to optimise the FIA manifold. It is important that the response chosen is reproducible to complete a successful optimisation.

The criteria used were based on compromises between several factors, namely,

- maximising the peak height for both the platinum- and palladium-tin(II) chloride systems,
- minimising the relative standard deviations (r.s.d.) of replicate experiments,
- maintaining a low peak width to yield higher sample throughput, and,
- maximising the signal-to-noise ratio (S/N) to maintain high levels of accuracy at the lower concentrations investigated.

4.2.1 Sample Injection Volume

The sample volume has a considerable effect on the response. The desired sample volume should enable high sample throughput (sampling rate), a negligible carry-over, and provide high reproducibility and sensitivity.

Absorbance changes recorded at increasing volumes of a fixed concentration of Pt(IV) are shown in Figure 4.4. The FIA profiles shown were recorded using a reaction coil length of 180 cm, tin(II) chloride concentration of 0.1 M, and flow rate of 1.8 $cm^3.min^{-1}$. The sample volume was controlled by the duration that the valve was in the "inject" position. The exact volume dispensed was titrimetrically calibrated at the chosen flow rate (Chapter 8). Aside from the effect on absorbance, very similar response trends were found for palladium, as well as when different tin(II) chloride concentrations, reaction coil lengths, and flow rates were used.

Peak height and peak width both increased with increasing sample size until a plateau formed at volumes greater than 200 μL. The r.s.d. of quadruplicate injections at each volume was better than 0.7% except at the lower volume extremes (< 50 μL) where the r.s.d. increased to over 1%.

Figure 4.4 *The effect of changing the injected sample volume. The profiles shown were recorded for a 10 μg.cm^{-3} Pt(IV) solution at the absorbance maximum, 400 nm. Larger sample volumes (not shown for clarity) did not increase the peak height absorbance significantly.*

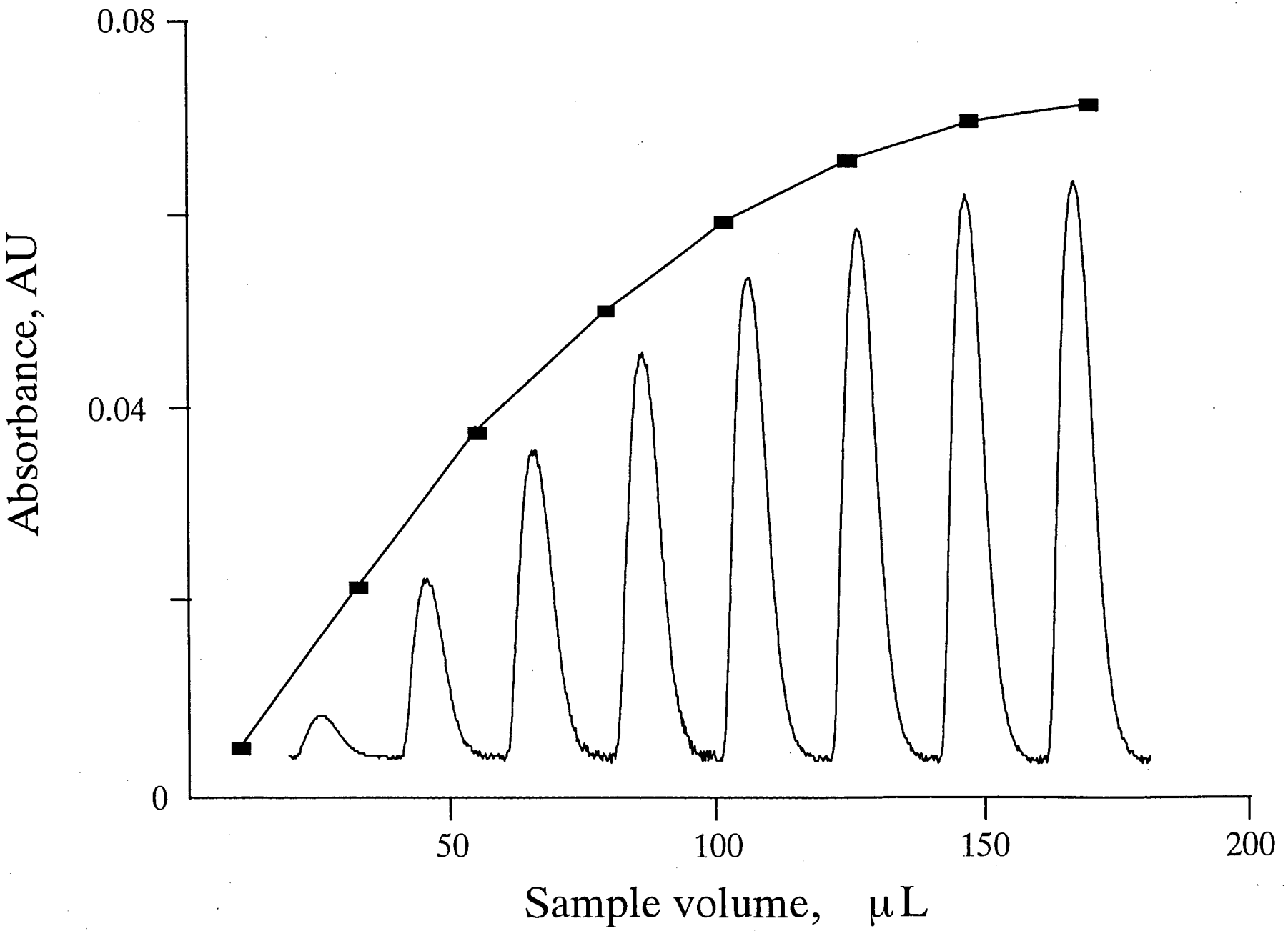
0.08
0.04
0
Absorbance, AU
50
100
150
200
Sample volume, μL

Peak widths broaden with increased sample volume and decreased the sample throughput as a result of increased tailing of the FIA peaks. Adequate sensitivity was found with a sample volume of 125 μL and tailing of the peak was kept to a minimum. The sample throughput of a FIA system is generally described by the number of samples per hour.[12] The sample throughput in this work was of the order of 54 $hour^{-1}$.

Two phenomena that affect the response take place *en route* to the detector - a chemical reaction and physical dispersion. The latter will decrease the signal with increasing coil length whereas the effect of the former depends on the nature of reaction and complexes forming or disappearing.[7] A combination of the two effects gives the final response recorded. In order to verify this, the effect of physical dispersion can be removed by stopping the sample within the flowcell. The chemical reaction is then monitored over time. The response over the whole spectra remained constant on reaction of platinum with tin(II) chloride, but several complex reactions take place on the reaction of palladium with tin(II) chloride. These effects will be elaborated upon later.

4.2.2 Reaction Coil Length

The effect of the reaction coil length is seen in Figure 4.5. An increase in reaction coil length resulted in a decrease in peak height absorbance in the case of palladium at 400 nm. In contrast, the response for platinum showed a slight increase in the peak height absorbance at this wavelength before decreasing as the effect of dispersion became a more dominant factor than the reaction kinetics.

A residence time which was long enough for the palladium reaction to pass through a series of colour changes to the relatively stable dark green colour (λ = 636 nm) is required. This residence time can be conveniently controlled by variation of the reaction coil length. The complexes giving rise to this colour provide the best compromise between spectral character and sensitivity.

Figure 4.5 *The effect of the reaction coil length, using a reagent concentration of 0.05 M tin(II) chloride, on the response of : A, 20 μg.cm^{-3} Pd(II) at λ = 400 nm,*

B, 10 μg.cm^{-3} Pt(IV) at λ = 400nm, and

C, 20 μg.cm^{-3} Pd(II) at λ = 635 nm.

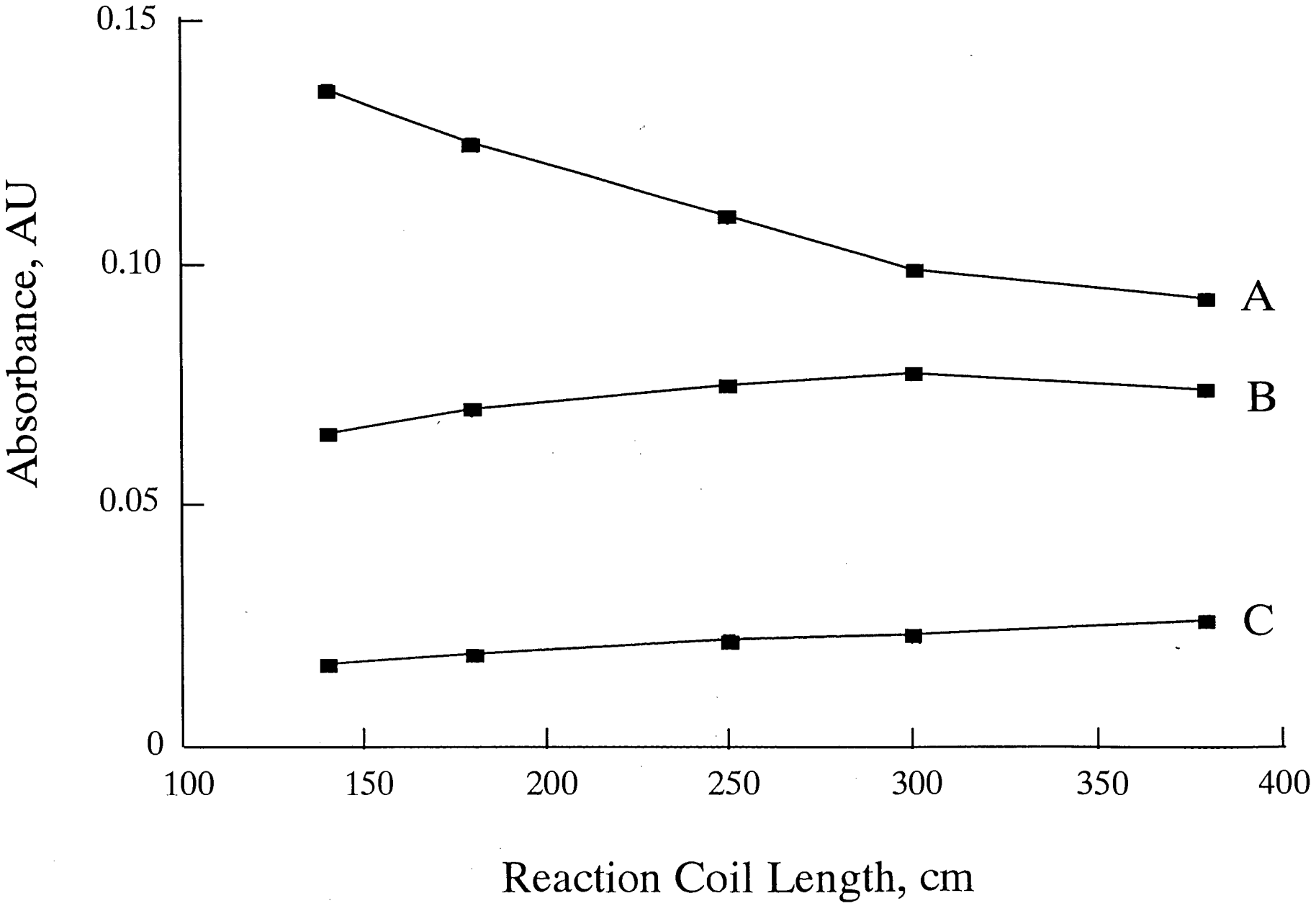
0.15
0.10
0.05
0
Absorbance, AU
100
150
200
250
300
350
400
Reaction Coil Length, cm
A
B
C

The length of the reaction coil was varied between 60 and 400 cm during the optimisation. Longer coil lengths only had the effect of decreasing the response as a result of physical dispersion effects. The shortest coil length used was limited to 60 cm as spikes generated when the valve was switched pneumatically resulted in a small spurious signal being generated. A reaction coil length of 60 cm was sufficient to separate the true FIA response from the spurious signal. Data acquisition was only commenced a few seconds later to ensure that the effect of the valve switching had subsided. It was found that reaction coils shorter than 100 cm gave irreproducible results. This was particularly true in the case of palladium. This is accounted for in that the complexes forming were unstable and still undergoing significant change. This would result in considerable variation in the absorption spectrum.

A reaction coil length of 300 cm was chosen for the platinum-palladium system. This length provided a measurable response for both elements, low r.s.d. of replicate injections, and sufficient time for the palladium reaction to proceed satisfactorily.

4.2.3 Reagent and Carrier Flow Rate

The effect of the flow rate, shown in Figure 4.6 and Figure 4.7, was two-fold. In the absence of a chemical reaction, an increased flow rate will tend to decrease the signal[13] due to dispersion. In the presence of a chemical reaction, the flow rate will affect the time that the reaction has to take place prior to detection. High flow rates will result in low sample residence times and, if a colour is still developing as detection takes place, will reduce the effective response.

A flow rate of 1.6 $cm^3.min^{-1}$ was selected as an optimum for subsequent analytical use. This resulted in low pulsing effects, a low r.s.d. for replicate injections, and provided sufficient time for the palladium reaction to proceed satisfactorily. The response for platinum was comparable to that found when lower flow rates were used. However, lower flow rates showed poor repeatability and were therefore unsuitable.

Figure 4.6 *Absorbance response surface map showing the effect of flow rate on peaks for a 10 μg.cm^{-3} Pt(IV) sample. The plot is composed of 8 peaks, observed at 400 nm, using different flow rates. There are 400 data points across each peak.*

Absorbance, AU
0.00
0.04
0.08
Flow rate, mL/min
1.0
1.7
2.4
3.1
3.8
Time, seconds
5
28
50
73
96

Figure 4.7 *Contour plot of Figure 4.6 showing the effect of flow rate on peaks for a 10 μg.cm^{-3} Pt(IV) sample. The change of the peak width with changing flow rate is clearly seen in the contour plot.*

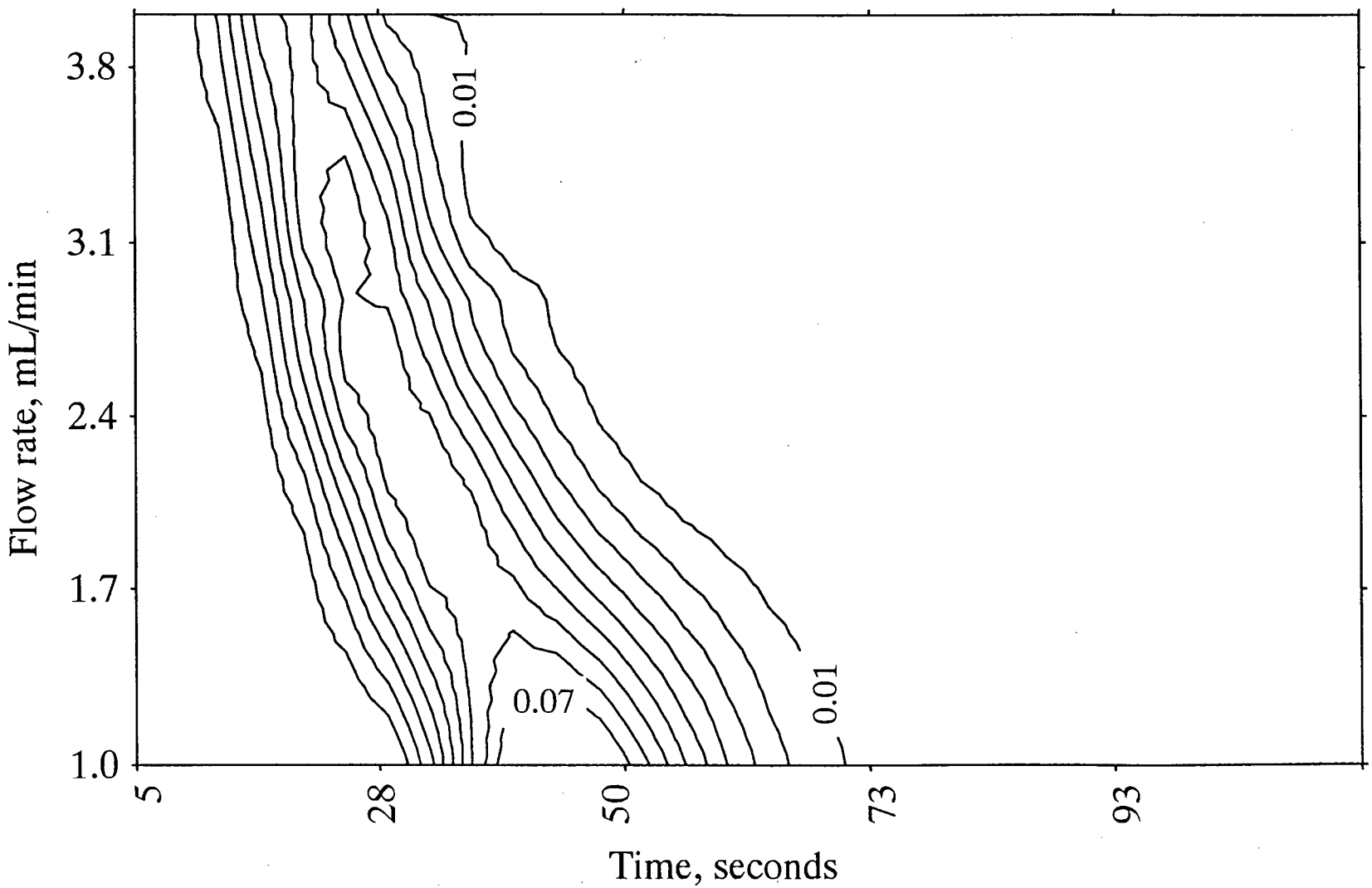
Flow rate, mL/min
3.8
3.1
2.4
1.7
1.0
0.01
0.07
0.01
5
28
50
73
93
Time, seconds

4.2.4 Reagent and Carrier Concentrations

The optimisation of the reagent and carrier solution concentrations, tin(II) chloride and hydrochloric acid, was of paramount importance. Although sensitivity was an important consideration, the requirement of additivity of the mixtures was naturally the limiting factor. Experiments were performed to determine the validity of the additivity principle over a range of mixtures and ratios.

In the absence of tin(II) chloride the only detectable colour is due to the inherent colour of the platinum chloride salt dissolved in hydrochloric acid. Addition of tin(II) chloride results in an immediate colour change to yellow. It is apparent from Figure 4.8 that the greatest response for platinum is attained at high tin(II) chloride and hydrochloric acid concentrations.

The greatest hydrochloric acid concentration used was 4 M HCl. This limit was set for practical reasons. It is undesirable to have such highly concentrated acid solutions passing through the peristaltic pump tubing. It is has also been shown[14] that oxidation of tin(II) chloride by dissolved oxygen is proportional to the concentration of $[HSnCl_3]^{1/2}$. The colour of the platinum-tin(II) chloride complexes formed also fades rapidly at higher acidities.[15] This is caused by oxidation of tin(II) to tin(IV). Tin(IV) is not known to complex with platinum in solution.[16]

The distribution of the tin(II) chloride complexes[17] as a function of hydrochloric acid concentration is shown in Figure 4.9. The only known tin(II) chloride species to complex with platinum and palladium species in solution is the $SnCl_3^-$ moiety. The variation of the concentration of the $SnCl_3^-$ species as a function of HCl concentration is clear.

Complete absorption spectra were recorded over the range of tin(II) chloride and hydrochloric acid concentrations. This was done to ensure that the absorbance maximum had not shifted as a result of reaction conditions. This could erroneously indicate a decreased absorbance at the absorbance measured. The interactions between system variables that cause shifts in the absorbance maxima are not explained readily in simple terms. No absorption spectra shifts were found in this regard.

Figure 4.8 *Absorbance response surface map on FIA profile peaks for 10 μg.cm^{-3} Pt(IV) at 400 nm. The tin(II) chloride concentration was varied in 0.05 M increments and the hydrochloric acid concentration in 0.5 M increments to create the surface.*

Absorbance, AU
0.12
0.06
0.0
Tin(II) Chloride, M
0.01
0.20
0.40
Hydrochloric acid, M
4.0
3.0
2.0
1.0

Figure 4.9 The distribution of tin(II) chloro species as a function of hydrochloric acid concentration.[17]

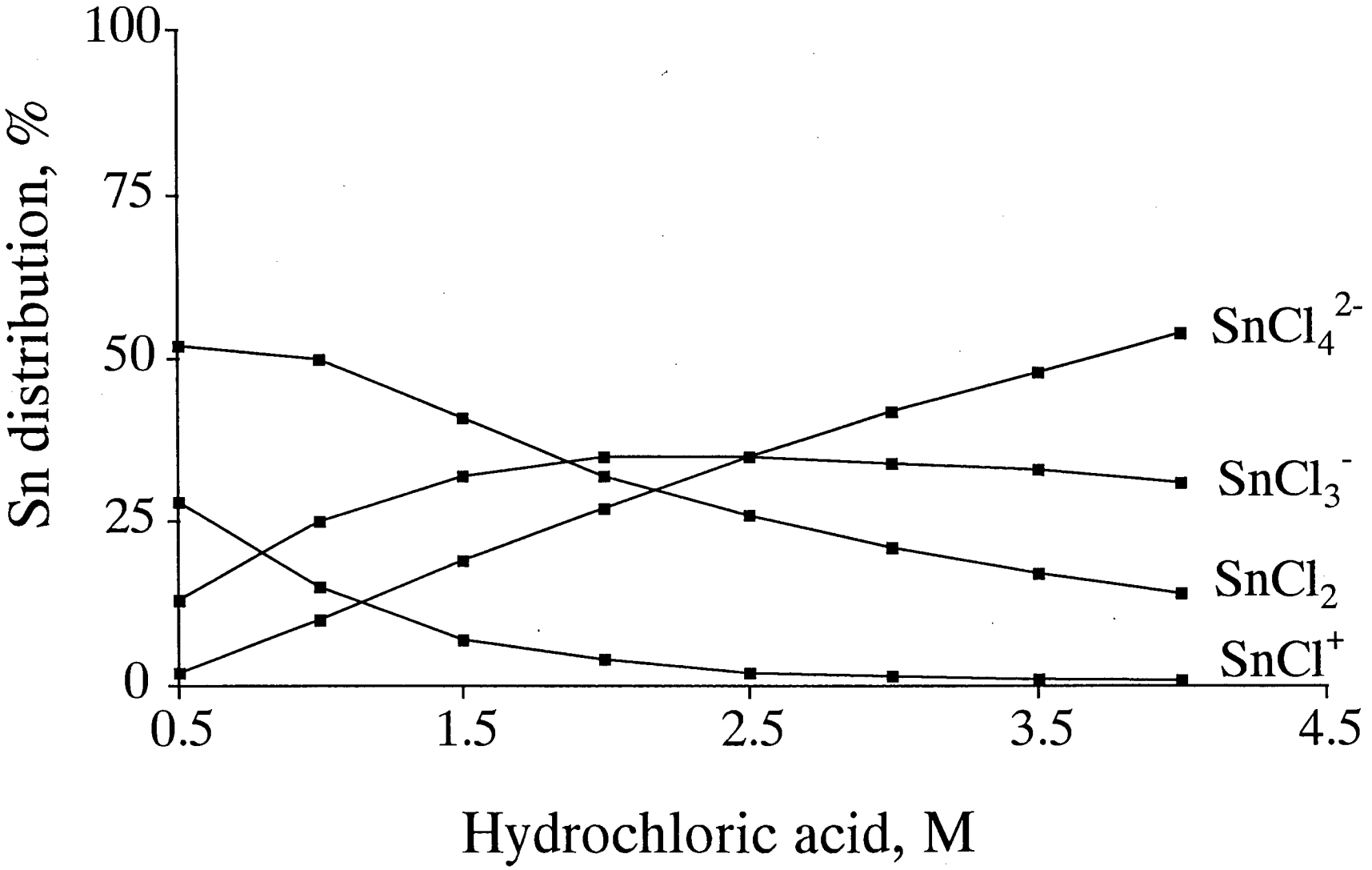
100
75
50
25
0
Sn distribution, %
0.5
1.5
2.5
3.5
4.5
Hydrochloric acid, M
$SnCl_4^{2-}$
$SnCl_3^-$
$SnCl_2$
$SnCl^+$

The criterion most commonly used in FIA optimisation is sensitivity, usually as the peak height. However, a failure to take repeatability into account can have dire consequences.[10] Repeatability is quantified here by the percentage relative standard deviation of replicate peak responses (at least triplicate experiments) across the search space. The areas of intersection between the lowest r.s.d. and highest sensitivity serve to confirm the best experimental conditions for the system. The r.s.d. is expected to be higher at lower absorbances due to the increased signal-to-noise ratio.

It was found that during acquisition of data that monitoring at four wavelengths, by linking the four analogue outputs of the detector directly to FlowTEK™, yielded lower r.s.d. values in comparison to scanning the spectrum over several wavelengths and then down-loading these spectral scans to FlowTEK™. The r.s.d. for single wavelength monitoring (used in this optimisation) were usually below 0.7%, even at wavelengths other than the absorbance maximum. The scanning approach yielded, at best, 0.6% r.s.d., commonly, 1.5% r.s.d., and in the worst cases, a maximum r.s.d. of 4% was found. This scatter was acceptable considering the process of data manipulation used.

In the case of platinum at a wavelength of 400 nm, an increase in tin(II) chloride and hydrochloric acid concentrations is accompanied by an increase in absorbance. This is shown in Figure 4.8. A plateau is reached at higher concentrations, *viz.* greater than 0.25 M tin(II) chloride and 2.5 M HCl. However, at these higher concentrations the r.s.d. is notably higher (Figure 4.10), of the order of 2 to 3 times greater, than at lower tin(II) chloride and HCl concentrations. The r.s.d. is adequately low at an acid concentration of 1 M HCl.

This increased r.s.d. is probably a result of a combination of physical effects, such as increased viscosity of the solutions and the resulting effect on the mixing process, and chemical effects, such as the effect of the experimental conditions on reaction rates and complex formation.

Figure 4.10 *Three-dimensional response surface plots to show the effect of tin(II) chloride and hydrochloric acid on the relative standard deviation for replicate experiments of 10 μg.cm^{-3} Pt(IV) measured at 400 nm. Each experiment was performed at least four times.*

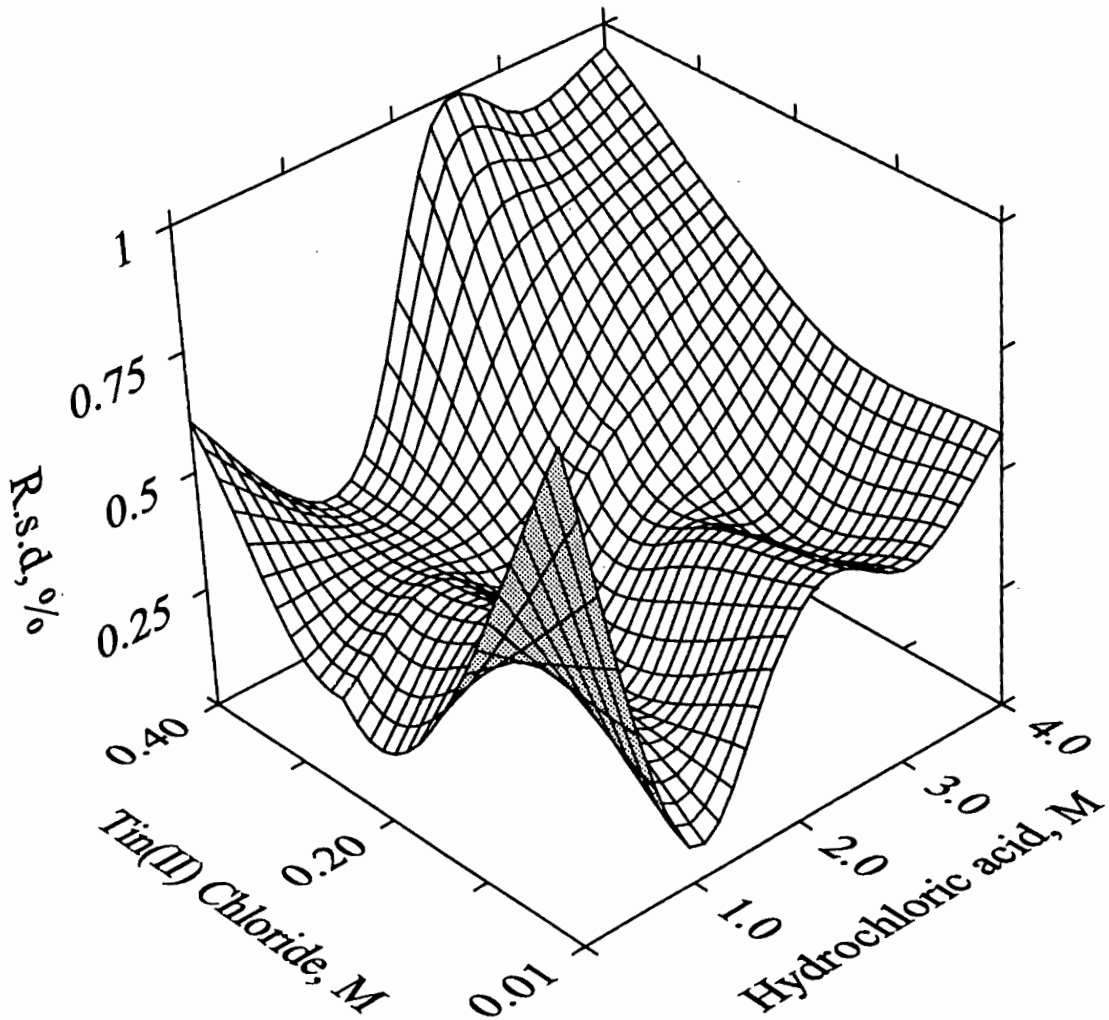
R.s.d, %
1
0.75
0.5
0.25
0.40
0.20
0.01
Tin(II) Chloride, M
1.0
2.0
3.0
4.0
Hydrochloric acid, M

The effect of tin(II) chloride and HCl on the response for palladium (Figure 4.11) shows that an increase in the tin(II) chloride concentration is accompanied by a sharp decrease in absorbance. Similarly, an increase in the HCl concentration decreased the absorbance, *albeit* a small amount. A plateau is found in regions of low tin(II) chloride and higher hydrochloric acid concentrations.

The shape of the response surface is indicative of the species being formed under certain experimental conditions only. At higher hydrochloric acid concentrations there is a decrease in the percentage of the active $SnCl_3^-$ species (Figure 4.9) and this effect may be seen clearly in Figure 4.11 at low tin(II) chloride concentrations. In effect, the shape of the plot of percentage tin(II) distribution against the hydrochloric acid concentration for the $SnCl_3^-$ moiety follows the same trend seen spectrophometrically at 0.1 M tin(II) chloride, for example.

A degree of spectral difference is a requirement in the resolution of mixtures. It was therefore important to obtain adequate sensitivity for palladium at wavelength ranges where the platinum absorption spectrum differed substantially from that of palladium. A compromise in terms of platinum sensitivity and r.s.d. was made in the selection of operating conditions of 1 M hydrochloric acid and 0.05 M tin(II) chloride. Although the platinum sensitivity was lower, the palladium sensitivity was considerable higher as compared to a position on the surface corresponding to 0.3 M tin(II) chloride and 3 M HCl. These considerations clearly illustrate the value of considering all the factors, not only sensitivity in selection of operating conditions.

Figure 4.11 *Absorbance response surface map on peaks for a 20 μg.cm^{-3} Pd(II) sample at 400 nm. The tin(II) chloride concentration was varied in 0.05 M increments and the hydrochloric acid concentration in 0.5 M increments to create the surface.*

0.01
0.2
0.4
Tin(II) Chloride, M
1.0
2.0
3.0
4.0
Hydrochloric acid, M
0.08
0.04
Absorbance, AU

4.2.5 Sample Acid Concentration

The effect of the sample hydrochloric acid concentration is of importance as changes in the nature of the sample, for example, an acid process stream being monitored, may occur. The FIA method should be sufficiently robust to handle such variations.

An increase in the sample hydrochloric acid concentration (between 2 and 4 M) resulted in nearly a two-fold increase in the r.s.d. of the peak height absorbances. The response did not alter significantly. The increased r.s.d. trend may, as before, occur due to the increased solution viscosity, changed mixing processes, and complex chemistry taking place. The merging stream manifold reduced the effect of the sample hydrochloric acid concentration.

The optimum sample acid concentration is that of the reagent and carrier streams HCl concentration, i.e. 1 M HCl. Samples in 4 M HCl could still be accurately analysed.

4.3 Conclusion

In FIA a form of univariate optimisation is usually sufficient to find experimental conditions that give good sensitivity and high sample throughput as the response surfaces are usually in the form of a hill (with shape "∩") or slope (with shape "/"). However, care is required to ensure that sub-optimum maxima are not obtained when using this type of optimisation.

Three-dimensional response surfaces provide a uniqueness not present when viewing data in two-dimensions. The requirement for large volumes of data points to generate these three-dimensional graphics is not an obstacle. A FIA system that is fully automated may readily collect such data over an extended period. The interaction of parameters and comparisons of response surface for different components, facilitates the selection of conditions for multi-component analysis.

Optimisation usually involves consideration of the response of the system. Given a suitably versatile data acquisition system, surfaces of other parameters, such as the r.s.d. of the response, are generated without any additional experiments. It is evident from this chapter that

a critical consideration of several manifold parameters is necessary to yield a working FIA manifold for determination of the PGMs. A further requirement of the optimum conditions was that they could be used in the simultaneous determination of mixtures of platinum and palladium. This was found to be the case.

Finally, where several parameters are to be considered, the possibility of moving from a three-dimensional space into higher, multi-dimensional vector space does not impose a limitation as such mathematical routines can be readily accomplished with sophisticated microcomputer software.

4.4 References

1. Betterridge, D., *et al.*, *Anal. Chem.*, 1983, **55**, 1292.
2. Kowalski, B.R., Ruzicka, J., and Christian, G.D., *Trends in Anal. Chem.*, 1990, **9**(1), 8.
3. Auer, D., and Koch, K.R., *Talanta*, 1993, **40**(12), 1975.
4. Stone, D.C., and Tyson, J.F., *Anal. Chim. Acta*, 1986, **179**, 427.
5. Ham, G., *Anal. Proc.*, 1981, **18**, 69.
6. Young, J.F., Gillard, R.D., and Wilkinson, G., *J. Chem. Soc. Dalton*, 1977, 239.
7. Ruzicka, J., and Hansen, E.H., "*Flow Injection Analysis*", 2nd edn., Wiley Interscience, New York, 1988.
8. Spendley, W., Hext, G.R., and Himsworth, F.R., *Technometrics*, 1962, **4**, 441.
9. Nelder, J.A., and Mead, R., *Comput. J.*, 1965, **78**, 308.
10. Betteridge, D., Howard, A.G., and Wade, A.P., *Talanta*, 1985, **8**B, 723.
11. Morgan, S.L., and Deming, S.N., *Anal. Chem.*, 1974, **46**, 1170.
12. Prownpuntu, A., and Titapiwatanakun, U., *Analyst*, 1991, **116**, 191.
13. Ruzicka, J., and Hansen, E.H., *Anal. Chim. Acta*, 1978, **99**, 37.
14. Lachman, S.J., and Tompkins, F.C., *Trans. Faraday Soc.*, 1949, **40**, 136.
15. Koch, K.R., and Yates, J.E., *Anal. Chim. Acta*, 1983, **147**, 235.
16. Milner, O.I., and Shipman, G.F., *Anal. Chem.*, 1955, **27**(9), 1476.
17. Wyrley-Birch, J.M., *MSc. Thesis*, University of Cape Town, Rep. S. Africa, 1984.

Chapter 5.

Single Component Analysis of the Platinum-Group Metals

The reaction of tin(II) chloride with the platinum-group metals has been widely used in the colorimetric determination of platinum and palladium.[1,2,3] Brightly coloured complexes form very rapidly in hydrochloric acid solution. The nature of the complexes, and hence the colour, are critically dependant on the reaction conditions. These rapid reaction rates are ideal for application in flow-injection analysis (FIA). An intense red-orange colour forms on reaction of platinum with tin(II) chloride, whereas in the case of palladium a series of colour changes occur that ultimately result in an olive-green colour.

The palladium-tin(II) chloride reaction was investigated by means of a stopped-flow approach. Visualisation of the data in three-dimensional surfaces aided correlation of the colour changes with local absorption maxima. This graphical approach assists the elucidation of underlying complex chemistries. Evidence is presented regarding the nature of species causing the final olive-green colour by considering the reaction of palladium with tin(II) chloride and tin(II) bromide.

The reaction of rhodium with tin(II) chloride is slower than the reaction with platinum and palladium. Lengthy incubation times are required that often involve boiling of the solution.[4] This limits the application of tin(II) chloride as an analytical reagent for rhodium by FIA. Similarly, iridium and ruthenium react very slowly at room temperature with tin(II) chloride.[5] Rhodium, iridium, and ruthenium, should therefore be determined with a reagent other than tin(II) chloride. The reaction of tin(II) bromide[6] with rhodium is considerably more rapid and sensitive for rhodium than the corresponding reaction with tin(II) chloride.

Results pertaining to the single component analysis of platinum and palladium with tin(II) chloride, and rhodium with tin(II) bromide, are detailed. A preliminary interference study shows the potential of this work in a process environment.

5.1 The Determination of Platinum

The origin of the red-orange colour on reaction of platinum with tin(II) chloride is known to result from the rapid reduction of any Pt(IV) species to Pt(II),[7] followed by, or concomitant with, complex formation of $PtCl_4^{2-}$ with the $SnCl_3^-$ moiety. This results in a series of $[Pt(SnCl_3)_nCl_{4-n}]^{2-}$ (n = 1 to 4) complexes as well as the relatively stable $[Pt(SnCl_3)_5]^{3-}$ complex anion.[7,8] This reaction is well known and forms the basis of an established manual spectrophotometric method for trace levels of platinum.[9]

Investigation here sought to develop an automated approach based on FIA for trace determination of platinum. This forms the foundation for the simultaneous determination of platinum and palladium, and the simultaneous determination of other PGMs with platinum.

The manifold configuration and experimental conditions used in the following SCA determinations (unless specified otherwise) are a merging stream manifold with a final flow rate of 1.6 $cm^3.min^{-1}$, a reaction coil length of 300 cm, and sample injection volume of 125 μL. All solutions (reagent, carrier, and samples) were made up in 1 M HCl or 1 M HBr.

5.1.1 The Effect of the Platinum Oxidation State

The effect of the oxidation state of the platinum was investigated by preparation of separate solutions containing identical amounts of Pt(IV) and Pt(II) respectively. The concentrations were verified to be the same by flame atomic-absorption spectrometry and ICP-AES. All else being equal, any variation in the FIA response would be due to the different oxidation states of the platinum.

A range of tin(II) chloride concentrations and manifold configurations (flow rate, reaction coil length) were examined using solutions of Pt(II/IV) having concentrations of 10 $\mu g.cm^{-3}$ and 100 $\mu g.cm^{-3}$. Triplicate injections were made in each case. Peak height and peak area comparisons were made. Peak height absorbance results for one configuration are shown in Table 5.1. No significant difference was found, and it is concluded that the platinum valency has no significant effect upon the FIA response. Pt(IV) was subsequently used throughout this work.

Table 5.1

Comparisons between the FIA peak height absorbances of Pt(II) and Pt(IV) sample solutions. The concentration of the reagent was varied, and a flow rate of 1.6 $cm^3.min^{-1}$ and reaction coil length of 300 cm used.

Tin(II) chloride, M	Pt(II) 10 $\mu g.cm^{-3}$	Pt(IV) 10 $\mu g.cm^{-3}$	Pt(II) 100 $\mu g.cm^{-3}$	Pt(IV) 100 $\mu g.cm^{-3}$
0.05	0.071	0.070	0.731	0.729
0.20	0.092	0.091	0.918	0.916
0.40	0.089	0.091	0.899	0.903

5.1.2 Visible Spectra of the Platinum-Tin(II) Chloride Complexes

When tin(II) chloride is added to a platinum chloride solution in hydrochloric acid, an immediate colour change from the inherent light yellow colour of the platinum chloride salt in HCl solution to bright yellow occurs. The intensity and visible colour are dependant on the reaction conditions and the Sn:Pt ratio.[10] The general appearance of the final solution varies between a yellow and a red-orange colour.

The absorption spectrum of the platinum complex with tin(II) chloride, Figure 5.1, shows an absorption maximum at 400 nm with a shoulder near 460 nm. No significant absorbance is measurable at wavelengths greater than 560 nm.

One way to verify adequate sensitivity, and near-completion, of a reaction is to use a stopped-flow approach. Any further increase in response means the the reaction is incomplete. After passage through the shortest possible length of tubing (of the order of 6 cm), the flow of the sample zone is stopped within the flowcell. The response measured is a function of the chemical reaction occurring. This method is useful to investigate reaction kinetics. Figure 5.2 shows clearly that only one species, or group of species, forms. This is evident from the fact that only the magnitude of the response changes over time, *albeit* slight, and not the shape of the absorption spectra.

Figure 5.1 *Electronic (absorption) spectra of the platinum-tin(II) chloride complexes recorded using 0.2 M tin(II) chloride on passage through the flowcell. The spectra correspond to (1) 8.0 μg.cm^{-3} and (2) 4.0 μg.cm^{-3} Pt(IV). Individual data points are shown at 4 nm intervals.*

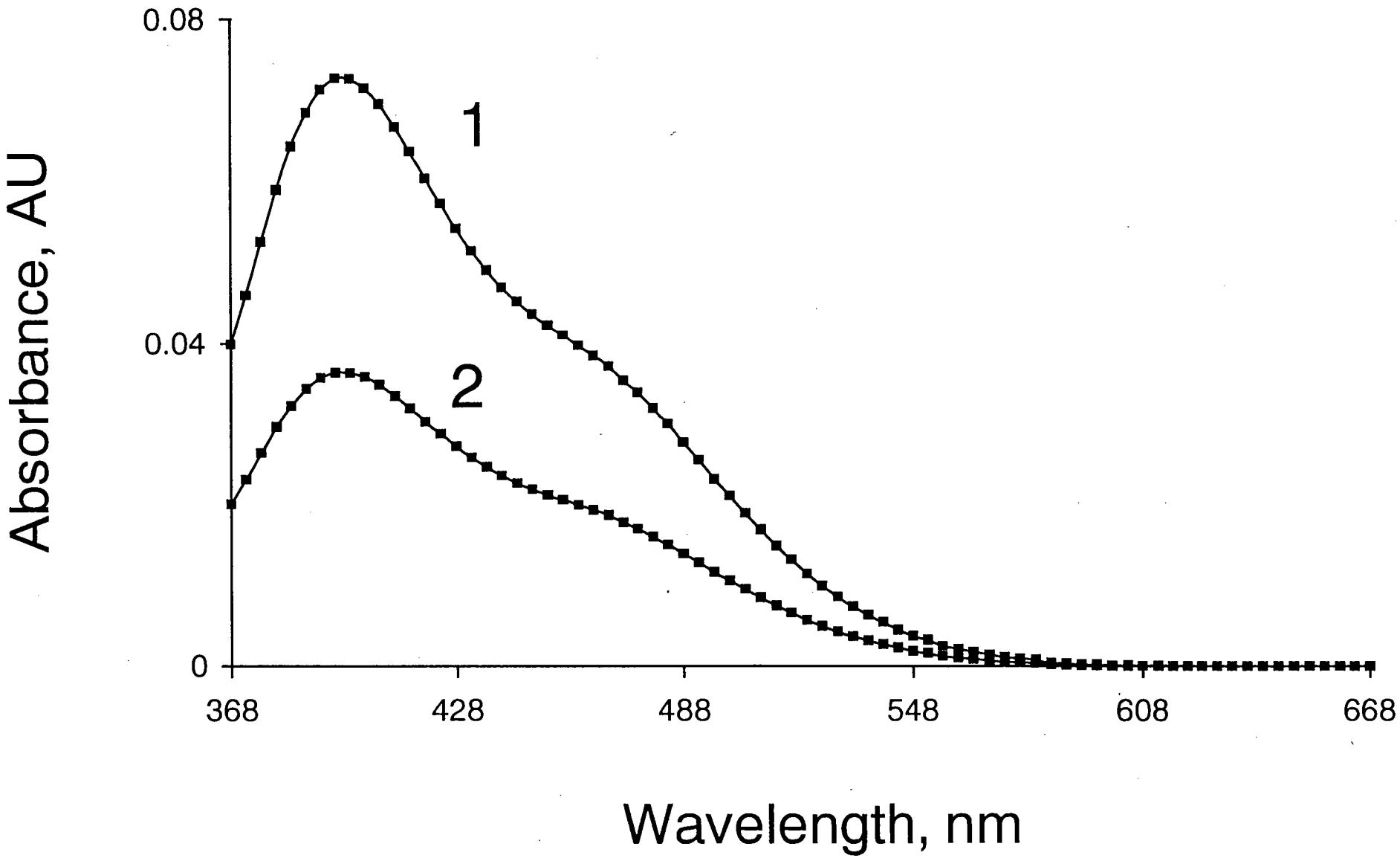
0.08
0.04
0
Absorbance, AU
1
2
368
428
488
548
608
668
Wavelength, nm

Figure 5.2 *Absorption spectra of a 10 μg.cm^{-3} Pt(IV) solution recorded when the flow of the sample is stopped within the flowcell. Spectra were collected over 600 seconds; constant absorbances were obtained from 250 seconds onwards and are not shown for clarity.*

250
180
120
50
20
10
5
Time, seconds
668
600
540
480
420
368
Wavelength, nm
1.2
0.0
Absorbance, AU

5.1.3 Calibration

As the transient FIA signal height is proportional to the concentration of the analyte contained in the injected sample, measurement of the peak height absorbance for each calibration standard yields a calibration graph. Calibration computations of this nature were performed by ReduceTEK.

Since aqueous standards and synthetic samples were used, it was unnecessary to use a standard additions approach. Calibration was performed immediately prior to sample analyses by injection of at least four calibrants, each measured in at least triplicate, spread across the linear range. Replicate injection of an analyte-free "blank" solution showed no significant difference from the continuously flowing carrier solution even after signal amplification. Accordingly, the carrier stream was used as a continuous measure of the blank solution.

Statistical features of the calibration graphs for recorded data at three wavelengths are shown in Table 5.2. Linearity between 1 and 100 $\mu g.cm^{-3}$ Pt(IV) was found. An upper limit of 100 $\mu g.cm^{-3}$ was set for the determination of Pt(IV). Linearity may be extended to a concentration of 700 $\mu g.cm^{-3}$ by reducing the injection volume. This effectively results in "on-line" dilution of the sample allowing large concentrations to be handled without the need for serial dilution.

The reproducibility, expressed as the relative standard deviation for replicate (n = 11) injections of a 10 $\mu g.cm^{-3}$ Pt(IV) sample, and sensitivity were excellent at all tin(II) chloride concentrations used.

Noise over the wavelength range used was found to be negligible even when the reagent and carrier were pumped through the Spectra FOCUS™ detector flowcell. The digital readout of the detector for the continuous blank solution was invariably less than 0.0003 AU.

Attempts to extend the calibration graph below 1.0 $\mu g.cm^{-3}$ Pt(IV) using a tin(II) chloride concentration of 0.2 M proved successful at a wavelength of 400 nm. Although the calibration graph was linear to 0.1 $\mu g.cm^{-3}$ Pt(IV) (r = 0.998), the relative standard deviation of replicate injections (n = 16) for the lower standards were higher. A solution of 0.1 $\mu g.cm^{-3}$

Pt(IV) had an absorbance response of 0.0008 AU and r.s.d. of 9.7%, and a 0.25 $\mu g.cm^{-3}$ Pt(IV) solution had a response of 0.0016 AU and r.s.d. of 4.7%. Although such exceedingly low absorbance values are not practically measured with conventional spectrophotometers and diode-array instruments, they are attainable with the highly stable Spectra FOCUS™ rapid scanning detector.

Table 5.2

Features of the calibration graphs for the determination of platinum at various wavelengths and tin(II) chloride concentrations.

Tin(II) chloride, (M)	λ (nm)	Calibration Equation [a] (x 1000)	Correlation Coefficient (r)	Linear Range ($\mu g.cm^{-3}$) [b]	R.s.d. (%)[c] (n = 11)
0.05	400	y = 7.27x + 1.18	0.9994	1 - 100	0.24
0.20	400	y = 9.11x + 2.95	0.9999	1 - 100	0.36
0.40	400	y = 8.95x + 5.28	0.9998	2 - 100	0.84
0.05	420	y = 6.05x + 1.56	0.9996	1 - 100	0.45
0.05	460	y = 3.98x - 0.98	0.9989	1 - 100	0.27

[a] Calibration : y ≡ AU and x ≡ concentration in $\mu g.cm^{-3}$.

[b] An upper limit of 100 $\mu g.cm^{-3}$ was set.

[c] Relative standard deviation for a 10 $\mu g.cm^{-3}$ Pt(IV) sample.

5.1.4 Analysis of Synthetic Solutions

A series of 15 synthetic Pt(IV) solutions were prepared and analysed after calibration. The sample concentrations were in the range 0.5 to 100 $\mu g.cm^{-3}$. The results obtained for the determination of platinum are shown in Table 5.3 as the correlation between concentrations "taken" and "found" at different wavelengths. The line of identity (perfect correlation) would have a theoretical slope of 1.0 and intercept zero.

The same series of 15 synthetic Pt(IV) solutions were also analysed for platinum by ICP-AES to validate the accuracy. Comparisons were made by means of least-squares regression of the results obtained by FIA and ICP-AES. Regression of FIA *versus* ICP-AES results gave a slope = 1.02 ± 0.03, intercept = 0.18 ± 0.13 $\mu g.cm^{-3}$, and correlation coefficient = 0.998.

Table 5.3

Least-squares statistical fits of "true" versus "found" concentrations for the determination of Pt(IV). The tin(II) chloride concentration was 0.05 M.

λ (nm)	Intercept ± s ($\mu g.cm^{-3}$)	Slope ± s	Correlation Coefficient (r)
400	0.055 ± 0.053	0.997 ± 0.001	1.000
420	0.072 ± 0.066	0.994 ± 0.009	0.998
460	0.063 ± 0.071	0.996 ± 0.006	0.999

Typical replicate injections for platinum standards and samples of varying concentrations reacting with 0.2 M tin(II) chloride, and measured at 400 nm, are shown in Figure 5.3. The figure was constructed from the multiple peak profile data files recorded by FlowTEK™ at a wavelength of 400 nm.

After an extended period of operation (overnight), the FIA system showed minor variation of the calibration slope (less than 4%). A change in the elasticity of the peristaltic pump tubing, and thus the flow rate, accounted for this deviation. Periodic calibration would obviate this being a disadvantage.

Figure 5.3 *Typical replicate injections for platinum standards and samples of varying concentrations using a tin(II) chloride concentration of 0.2 M. Numerals refer to concentration in* $\mu g.cm^{-3}$. *The letters refer to samples of (a) 60, (b) 10, (c) 45, (d) 90, (e) 30, and (f) 80* $\mu g.cm^{-3}$ *Pt(IV).*

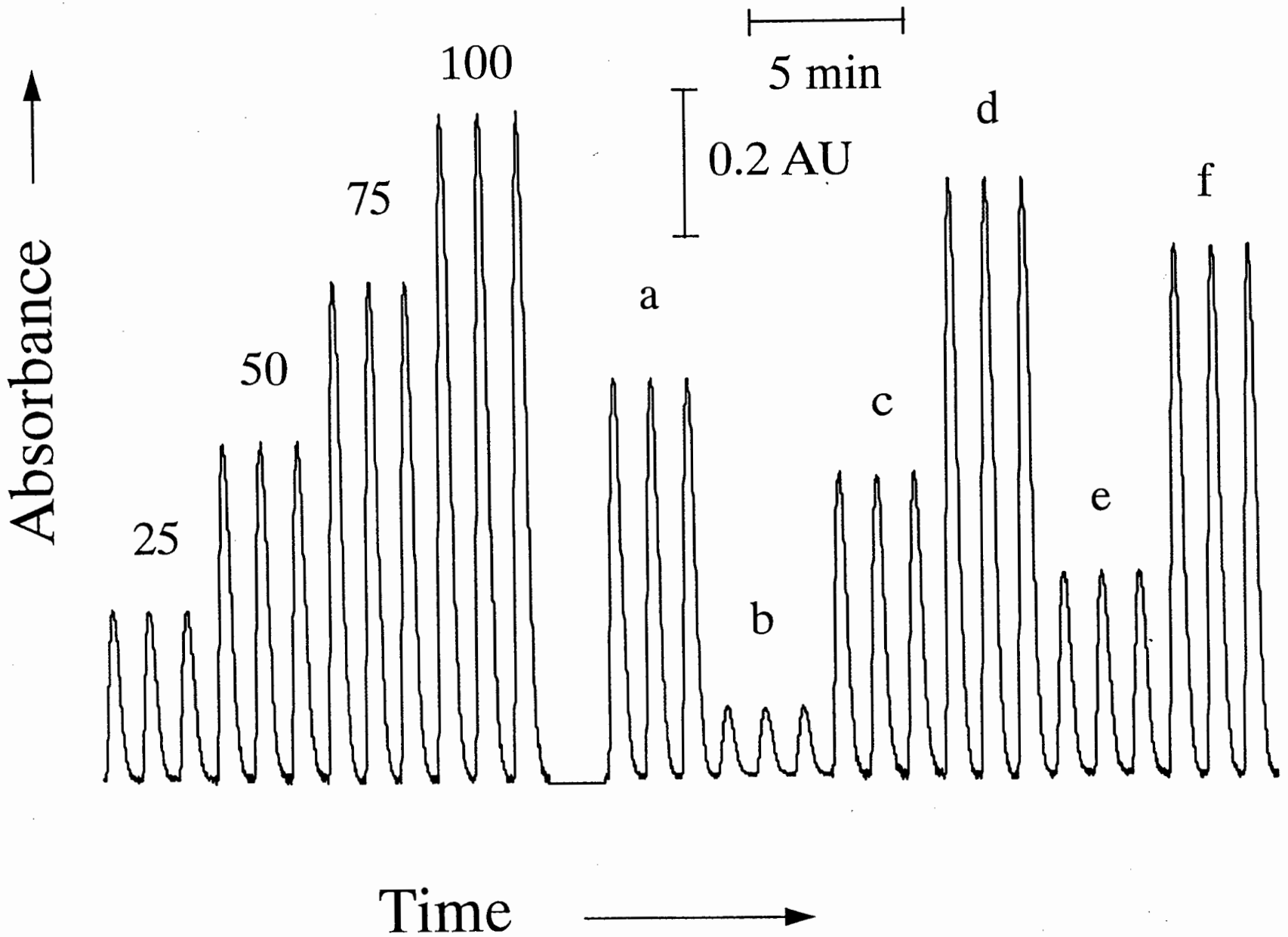
Absorbance
Time
5 min
0.2 AU
25
50
75
100
a
b
c
d
e
f

5.1.5 Analytical Features and Performance

Studies on the detection limit were carried out by injecting a blank solution and measuring at 400 nm. The limit of detection and limit of determination were calculated according to the IUPAC recommendations.[11] IUPAC recommends that the limit of detection, defined in terms of either concentration (C_L) or amount (q_L), be related to the smallest measure of response (x_L) that can be detected with reasonable certainty in a given analytical procedure, where

$$x_L = x_B + k\,S_B$$

and x_B is the mean of the blank measures (at least 30 replicates were used in this work), S_B is the standard deviation of the blank measures, and k is a numerical constant. The detection limit is given by

$$C_L \text{ (or } q_L) = k\,S_B / S$$

where S is the sensitivity of the method. A value of $k = 3$ is strongly recommended for computation of the limit of detection. In turn, the limit of determination is computed with a value of $k = 10$.

The limit of detection was calculated to be 47 $\mu g.dm^{-3}$ Pt(IV), and the limit of determination at 156 $\mu g.dm^{-3}$ Pt(IV) using a tin(II) chloride concentration of 0.05 M. Subsequently, a solution of 50 $\mu g.dm^{-3}$ Pt(IV) was prepared and analysed. The response did not differ significantly from the baseline. The limit of determination was fixed at 156 $\mu g.dm^{-3}$. A solution of 100 $\mu g.dm^{-3}$ Pt(IV) was differentiable from the baseline noise, however the r.s.d. of 16 replicate experiments was as high as 9.7%.

No "carry-over" was found when alternating between high (100 $\mu g.cm^{-3}$) and low (5 $\mu g.cm^{-3}$) concentration standards provided sufficient time was allowed for the baseline signal to be re-established. The sampling rate was 54 $hour^{-1}$. The FIA manifold allowed unattended operation for extended periods under FlowTEK™ control.

5.2 The Determination of Palladium

A series of colour changes take place when solutions of palladium are treated with tin(II) chloride in hydrochloric acid. The prominent colour changes are from a yellow-orange colour (λ = 420 nm), to red (λ = 355, 420 nm), through blue, and finally to an olive green colour (λ = 380, 460, 636 nm).

The aim of this investigation was to develop an automated approach of analysis based on FIA for the trace determination of palladium. This work would also serve as a foundation for the simultaneous determination of platinum and palladium. The previously uncharacterised blue colour was investigated. Evidence is provided that strongly suggests that the green colour may be ascribed to the existence of specific complexes and not to a colloidal material as has been postulated.[12]

Complexes give rise to absorption bands in the absorption spectrum. These bands are manifested in the colour of the solution. The differing spectral characteristics of these colours, apart from indicating the presence of complex species in solution, provide a means to study these complexes. In this way, an association of colour changes with local absorption maxima are confirmed and the absorption maximum associated with the blue colour determined. A qualitative consideration of the effects of tin(II) chloride, H^+, and Cl^- concentrations assist in elucidation of the underlying complex chemistry.

5.2.1 Stopped-Flow Investigation

Stopped-flow injection is based on stopping the flow of the sample zone when it is in the detector flowcell and recording the response as a function of time at a particular wavelength, or wavelengths. Since stopping of the sample zone is highly reproducible, it is possible to accurately compare reactions under differing experimental conditions. The physical dispersion component of the signal is removed and the response becomes a function of the chemical reaction occurring.

A stopped-flow method was essential to capture the absorbance spectra for characterisation of the red, yellow, and blue colours since these colour changes take place very rapidly. A merging stream manifold with the shortest possible length of tubing between the merging tee-piece and the spectrometer flowcell was used. Inertia on stopping the flow of the solution occurred. As a result, knowledge of the exact time required until the sample zone was stationary and positioned in the flowcell is essential. This was found by injecting bromothymol blue dye and monitoring at a wavelength of 620 nm. The sample zone was completely stationary in the flowcell after four seconds and the first spectral scan was initiated one second later. Thereafter, scans were recorded at predetermined time intervals. A 100 $\mu g.cm^{-3}$ Pd(II) sample was used in the stopped-flow study.

The following points should be regarded when viewing absorption spectra of complexes in solution. An increase of absorbance at one wavelength and a corresponding decrease at another wavelength is indicative of a complex, or series of complexes, forming and changing or decomposing (not necessarily in equilibrium). An isosbestic point is the point of intersection of a number of absorption curves on changing one of the parameters of a system in equilibrium. Such a parameter may be concentration, temperature, or time.

Isosbestic points correspond to contour lines that are parallel to the time axis and in the contour plot, have unchanged absorbance. A plateau in the absorption spectrum corresponds to a contour line being parallel to the wavelength axis. The proximity of contour lines to one another determines the absorption gradient of the particular spectral feature (for example, a very sharp absorption peak would have circular contours close to one another).

Once the absorption spectra had been recorded as a function of time, an "animation" of the chemical reaction was viewed over time. This allowed observation of the exact sequence of events that finally gave the characteristic green colour. These results are presented graphically in Figure 5.4 and Figure 5.5 using a three-dimensional graphic and a contour plot to clearly indicate the spectral characteristics.

Figure 5.4 *Absorbance response surface map for a solution of 100 μg.cm^{-3} Pd(II) in 0.1 M tin(II) chloride recorded using a stop-flow approach. Absorption spectra were recorded at one second intervals until 15 seconds, and thereafter at 5 second intervals. See text for details.*

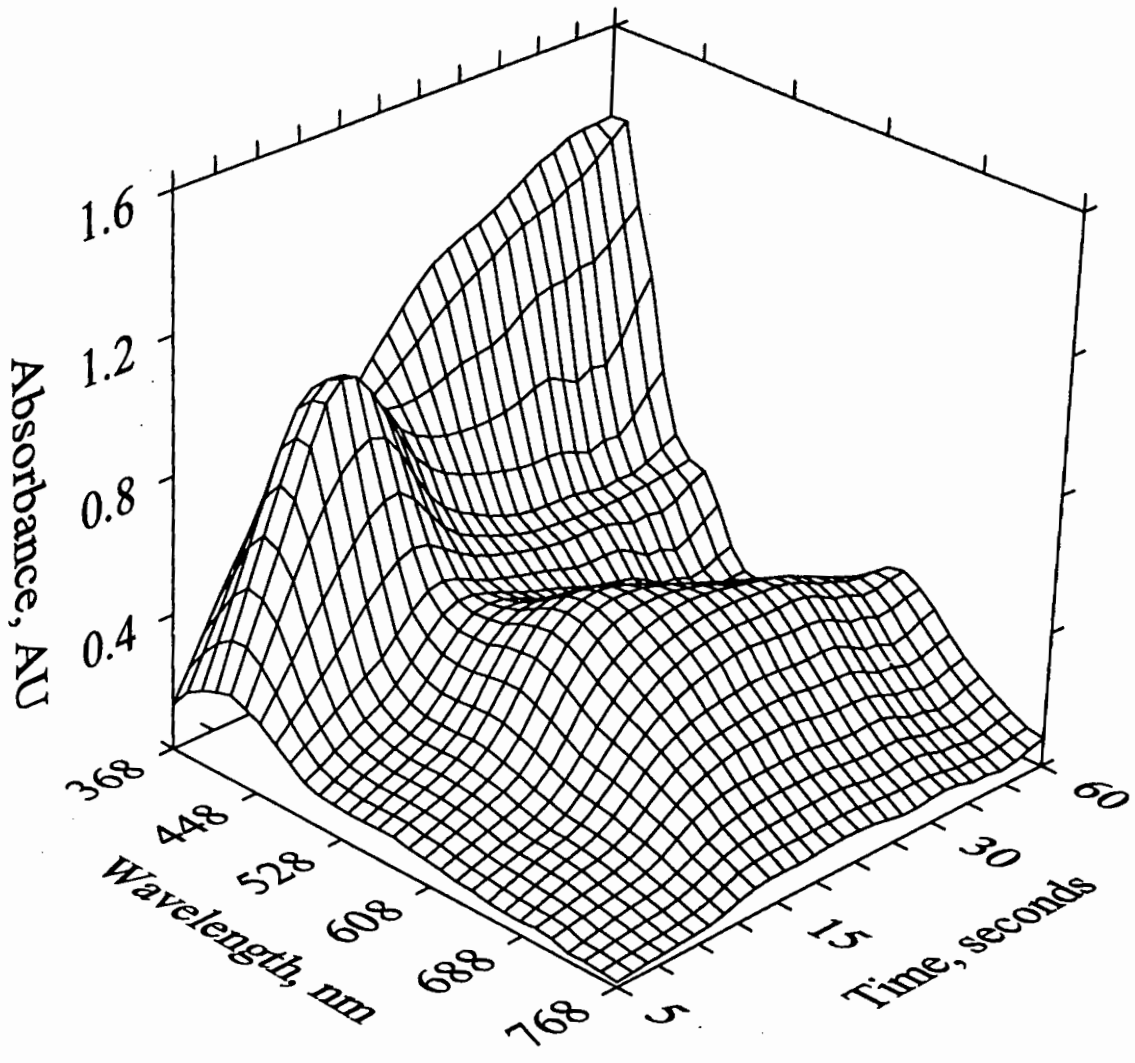
Absorbance, AU
1.6
1.2
0.8
0.4
368
448
528
608
688
768
Wavelength, nm
5
15
30
60
Time, seconds

Figure 5.5 *Contour plot for Figure 5.4 to show the distinct spectral character as a function of time for palladium using a stop-flow approach. See text for details.*

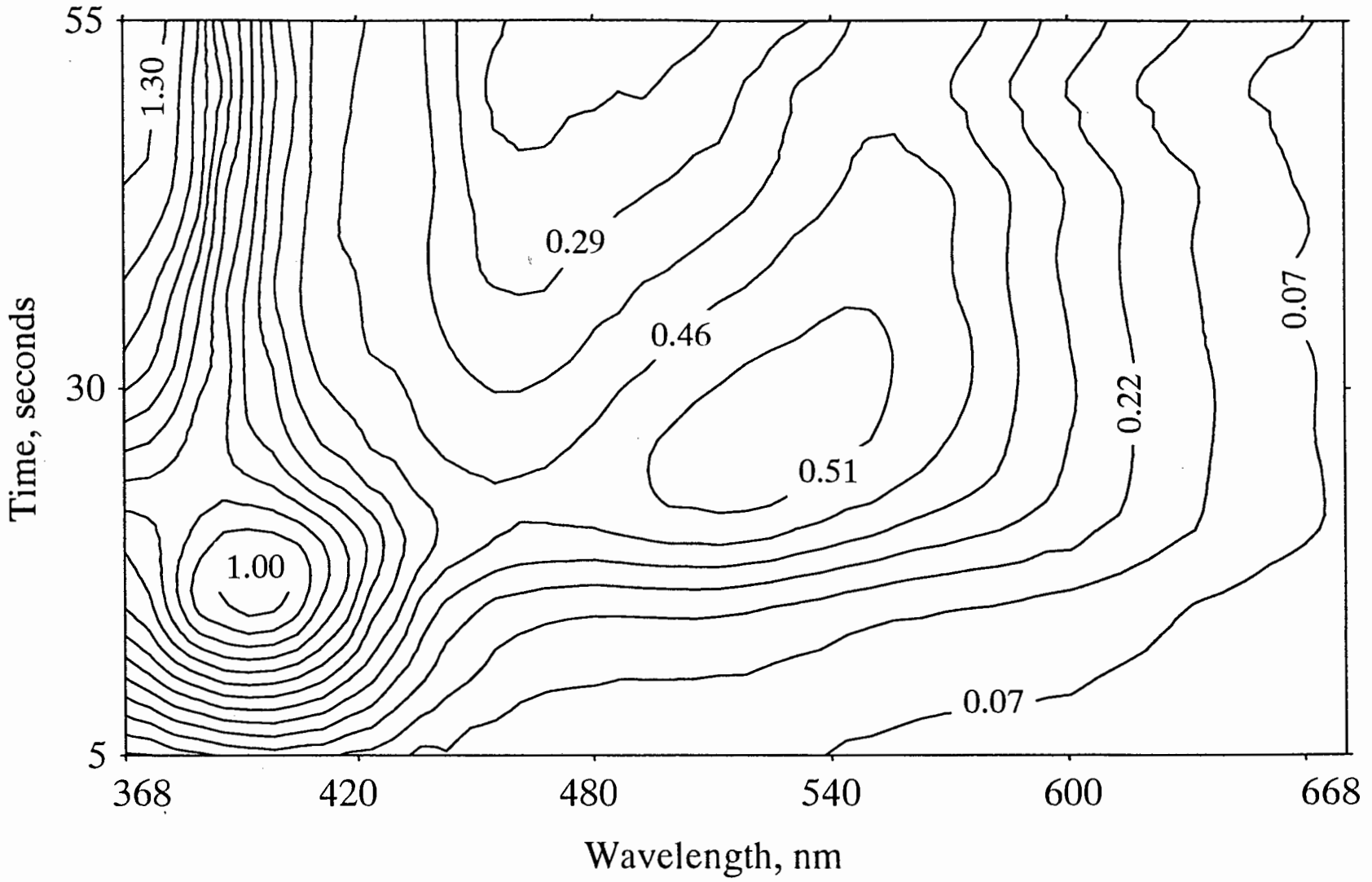
55
30
5
Time, seconds
1.30
0.29
0.46
0.51
0.22
0.07
1.00
0.07
368
420
480
540
600
668
Wavelength, nm

The complexity of the absorption spectra is evident from the three-dimensional surface map, Figure 5.4. A large number of overlapping components (theoretically Gaussian-shaped absorption bands) are observable and interpretation of these is difficult. The association of colours with actual complexes is not possible without further investigation and the use of structural elucidation techniques such as NMR spectroscopy. This is necessary because the visible colour could be a result of combination of the absorption bands of several complexes existing in solution. The possible polymeric nature of these species in solution should also not be discounted. It is possible, nevertheless, to associate the observed colour changes with local absorption maxima and postulate the possible associated complex interactions.

The sequence of events resulting in the spectral changes are discussed with reference to Figures 5.4 and Figure 5.5. The observed colour changes, proposed to be associated with these spectral features, are indicated. Band assignments were aided by consideration of the absorbance maxima of solutions having similar colours to those seen here.

The formation of a yellow colour may be associated with the sharp peak at 420 nm. Yellow is the first colour observed when the light yellow-orange palladium solution reacts with tin(II) chloride in hydrochloric acid. The species which result in the red colour are short-lived and are known to exist in equilibria with those yielding the yellow colour.[14] Distinction between the red and yellow is made difficult by the lack of UV absorption data because a peak at 355 nm is associated with species yielding the red colour.

As the peak at 420 nm attains maximum intensity and begins to decrease, so a plateau near 510 nm forms. This may be seen as the region from approximately 13 seconds to the "saddle point" (the trough between two peaks) at 15 seconds on the contour plot. The plateau at 510 nm is evidently a result of two absorption bands overlapping. The two absorption bands have maxima at 420 nm and 590 nm respectively.

The peak at 590 nm (Figure 5.4) is assigned to species causing the appearance of the blue colour. An isosbestic point at 480 nm may correspond to species associated with the yellow and blue colours existing in a state of dynamic equilibrium. The transitory nature of the species associated with the blue colour is evident from the contour plot (Figure 5.5) where the peak maximum at 590 nm decreases to give rise to the green colour.

The final green colour is associated with the absorbance maximum at 636 nm. This colour forms over the widest range of reaction conditions and the complexes associated with this colour may be considered to be the most stable of the palladium-tin(II) chloride complexes. An isosbestic point at 400 nm indicates a further equilibrium between complexes in solution. The absorption spectra attained after 60 seconds has a shoulder defined at 460 nm and absorption maxima at 380 nm and 636 nm. No further absorbance changes occur.

On standing for several hours the absorption decreases across the whole spectrum as a fine, brown colloidal material[13] settles out of solution. The solution becomes clear. This material contains metallic palladium from the reduction of palladium to the metallic state by the tin(II) species. This was verified by collecting the material, washing, and dissolving it in nitric acid. Subsequent analysis by ICP-AES showed that this residue contained substantial amounts of palladium. This substantiates the existence of a charge-transfer reaction and a palladium oxidation state change from Pd(II) to Pd(0). This, however, does not exclude the possibility that this material is composed of palladium metal and palladium-tin(II) complexes.

Consideration of the effect of the tin(II) chloride concentration on these complex interactions showed that is more pronounced for some species. Stopped-flow experiments were performed at various tin(II) chloride concentrations. These response surface maps are shown in Figure 5.6. At higher concentrations of tin(II) chloride (greater than 0.2 M) the species associated with the yellow colour (λ = 420 nm) are not favoured (Figure 5.6, d) This is seen in the decreased intensity of the peak at 420 nm at these higher tin(II) chloride concentrations. The rate of formation of the species that are associated with the green colour (λ = 636 nm) are also not favoured at these higher concentrations of tin(II) chloride.

Species associated with the blue colour (λ = 590 nm) are favoured in intermediate tin(II) chloride concentrations as seen in Figure 5.6 (b and c) whilst at higher concentrations, a notable decrease in the intensity of the peak at 590 nm is found. At low tin(II) chloride concentrations (0.05 M), virtually no peak at 590 nm can be seen in Figure 5.6 (a). Evidence of the formation of the red colour (λ = 355 nm) is seen in Figure 5.6 (c and d) as the side of the absorption band. Species associated here are formed preferentially to those associated with the yellow colour.

Figure 5.6 *Absorption response surface maps for a solution of 100 μg.cm^{-3} Pd(II) as recorded using a stop-flow approach. The letters refer to the tin(II) chloride concentration used; viz. (a) 0.05 M, (b) 0.1 M, (c) 0.2 M, and (d) 0.4 M tin(II) chloride.*

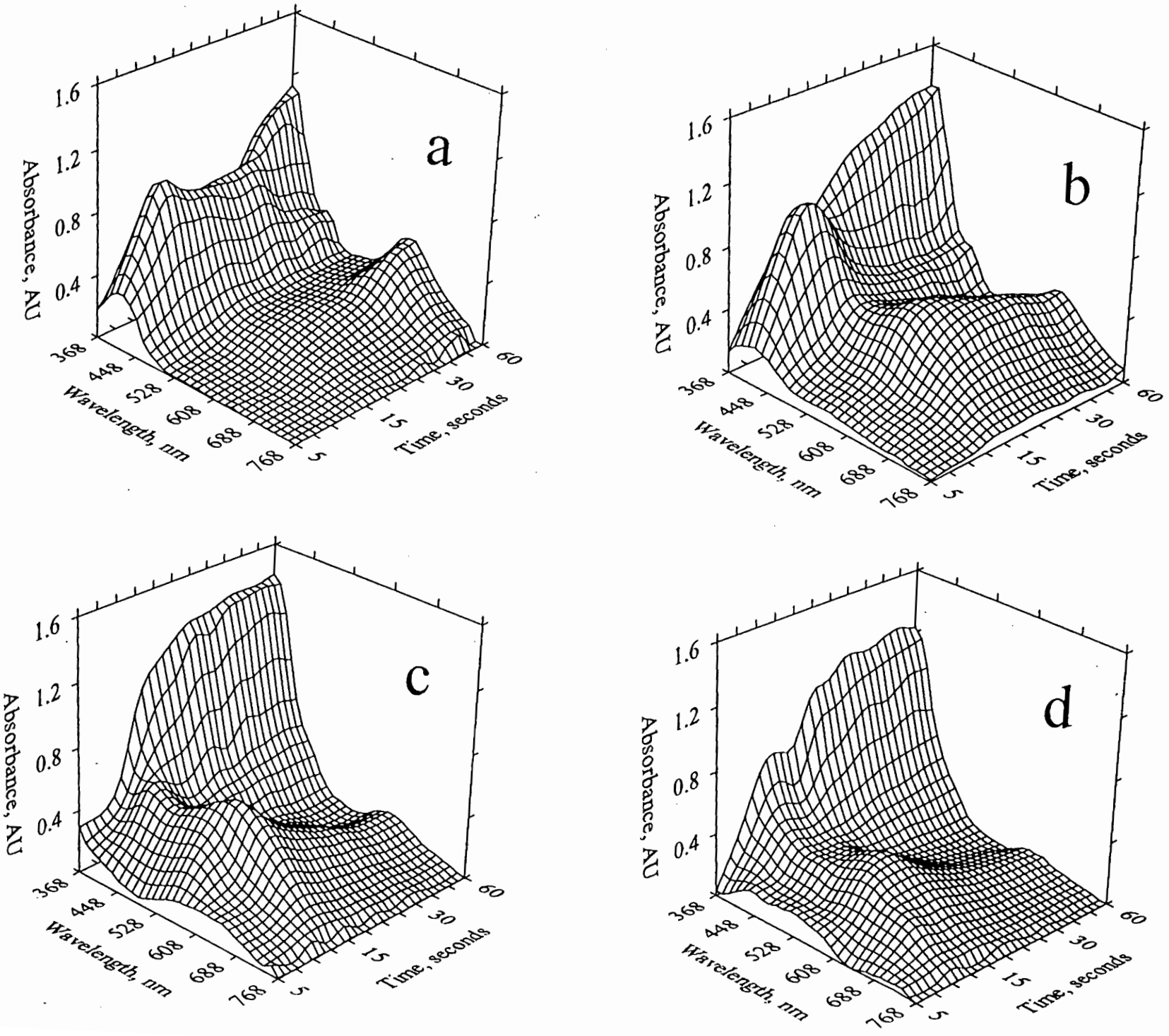
a
b
c
d
Absorbance, AU
1.6
1.2
0.8
0.4
Wavelength, nm
368
448
528
608
688
768
Time, seconds
5
15
30
60

The HCl concentration showed a marked effect on colour development. The rate of formation of the species associated with the blue and green colours are severely inhibited, however, the formation of the yellow colour remains unchanged, when the acid concentration is increased, to a maximum of 4 M HCl. No subsequent decrease of absorbance is found at 420 nm when strongly acidic solutions of 4 M HCl are used. This suggests that the yellow species favour higher acidities and any changes in the complex nature occur very slowly under these conditions. In 1 M HCl, species associated with the yellow colour are rapidly converted to those associated with the green colour. This type of observation is important when considering the possible chemical composition of the species in solution.

A study as to whether the H^+ or the Cl^- ion was the contributing factor to this phenomenon is reported. Increasing the concentration of H^+ ion to 3 M by preparing all solutions using perchloric acid showed no significant effect on the response. The fact that changes in H^+ ion concentration do not affect the colour formation is evidence that the chloro-complexes of the palladium and tin(II) species are involved in the reactions. Tin(II) has a propensity to form labile chloro-complexes. The concentration of these in solution affect the resulting complex formation.

The effect of the Cl^- ion concentration was the most marked. The intensity of the absorption bands decrease as the Cl^- concentration is increased above 1.5 M (the H^+ concentration being kept constant). This may be explained by a consideration of the chloro-species which are likely to be formed in equilibria.

$$SnCl_2 + Cl^- \rightleftharpoons SnCl_3^-$$

$$SnCl_3^- + Cl^- \rightleftharpoons SnCl_4^{2-}$$

At high Cl^- concentration the above equilibria would be shifted to the right favouring formation of the $SnCl_4^{2-}$ species which is not known to form complexes with palladium. This effect was observed at Cl^- concentrations greater then 1.5 M.

This is also a feasible explanation for the finding that higher HCl concentrations reduce the formation of both the blue and green colours. The replacement of the Cl^- ligand from the co-ordination sphere of the tetrachloropalladate(II) species, $PdCl_4^{2-}$, on reaction with the $SnCl_3^-$ moiety, may also be inhibited by high concentrations of the Cl^- ion. This results in a reduction of the colour intensity.

Furthermore, on the basis of these observations, it is proposed that the yellow colour may be attributed to a species having fewer $SnCl_3^-$ than Cl^- ligands surrounding the palladium central ion. This is seen since increased concentration of tin(II) chloride results in a decrease in the intensity of the yellow colour at 420 nm. Higher concentrations of tin(II) chloride would presumably favour species having more $SnCl_3^-$ ligands. As the yellow colour forms first when tin(II) chloride is added, the replacement of at least a single Cl^- ion from the co-ordination sphere would be expected. The replacement of more Cl^- ligands would be expected to be inhibited in higher concentrations of HCl. The finding that the yellow colour is the most stable in high HCl concentrations suggests that the species associated with the yellow colour could well be of the form $[PdCl_3(SnCl_3)]^{2-}$. An NMR study would be necessary to substantiate this postulate.

The red and blue colours are attributed to intermediate complexes as their colour formation depends critically on reaction conditions. The species associated with the green colour could be expected to have more $SnCl_3^-$ than Cl^- ligands. At higher concentration of tin(II) chloride the rate of green colour formation at 636 nm is inhibited, whilst no significant change is found in the case of the peak at 380 nm. The reaction, nevertheless, does occur and exemplifies the stability of species associated with the green colour. The possibility of several species existing simultaneously is evident by considering the number of overlapping absorption bands.

The complexes associated with the green colour are stable for a relatively long period of time before decomposition to a brown colloid. The fact that solutions containing these complexes obey the basic law of light absorption (Table 5.4) at several tin(II) chloride concentrations indicates the existence of a species with a constant composition. The molar absorptivity of species yielding the green colour in 0.5 M tin(II) chloride was calculated to be of the order of 1500 $dm^3.mol^{-1}.cm^{-1}$.

The molar absorptivity is dependant on the reaction time and reaction conditions. Manipulation of these could result in an increase of the molar absorptivity, however, long residence times for samples in FIA are undesirable. The increased time per experiment lowers the number of samples per hour that may be analysed. The sensitivity does compare favourably with the batch method where a molar absorptivity of 2800 $dm^3.mol^{-1}.cm^{-1}$ is found after more than 20 minutes contact time.[14]

Conclusive support that the species associated with the green colour are in fact true species and should not be associated with the brown hydosol is evident when comparisons with the tin(II) bromide system are made. If these species do indeed give rise to a colloidal material then the peak at 636 nm would be expected to remain in the same position if HBr replaced HCl, and tin(II) bromide replaced tin(II) chloride. This is however not the case. The wavelength of the absorption maximum in chloride medium (λ = 636 nm) shifts to a longer wavelength (λ = 710 nm) in the bromide medium. The spectrum is similar except for the shift to longer wavelengths. Since bromine has a lower ionisation potential than that of chlorine, replacement of the chloride atoms in complexes possibly in solution, such as $[PdCl_{4-n}(SnCl_3)_n]^{2-}$ (n = 1 to 4),[14] with bromide would result in a shift to longer wavelengths.

The above discussion of the complex chemistry reveals the power of spectral analysis for qualitative, as well as quantitative, analysis. A platform for future work to study these complex species and interactions has been established.

5.2.2 Visible Spectra of the Palladium-Tin(II) Chloride Complexes

Palladium reacts rapidly with tin(II) chloride to give a series of colour changes, corresponding to complex species forming and equilibrating. The transient species are unstable. The solutions containing species yielding the green colour obey the basic law of light absorption across the whole visible spectrum and, therefore, only this colour was used analytically.

The spectra of the palladium complex with tin(II) chloride in 1 M HCl are shown in Figure 5.7. Absorption maxima at 380 nm and 636 nm are evident. A shoulder exists at 460 nm and a plateau in the range 500 nm to 530 nm.

Figure 5.7 *Absorption spectra of palladium-tin(II) chloride complexes recorded on passage through the flowcell using a tin(II) chloride concentration of 0.05 M. The spectra correspond to (1) 100, (2) 80, (3) 60, (4) 40, (5) 20, (6) 10, and (7) 5 $\mu g.cm^{-3}$ Pd(II).*

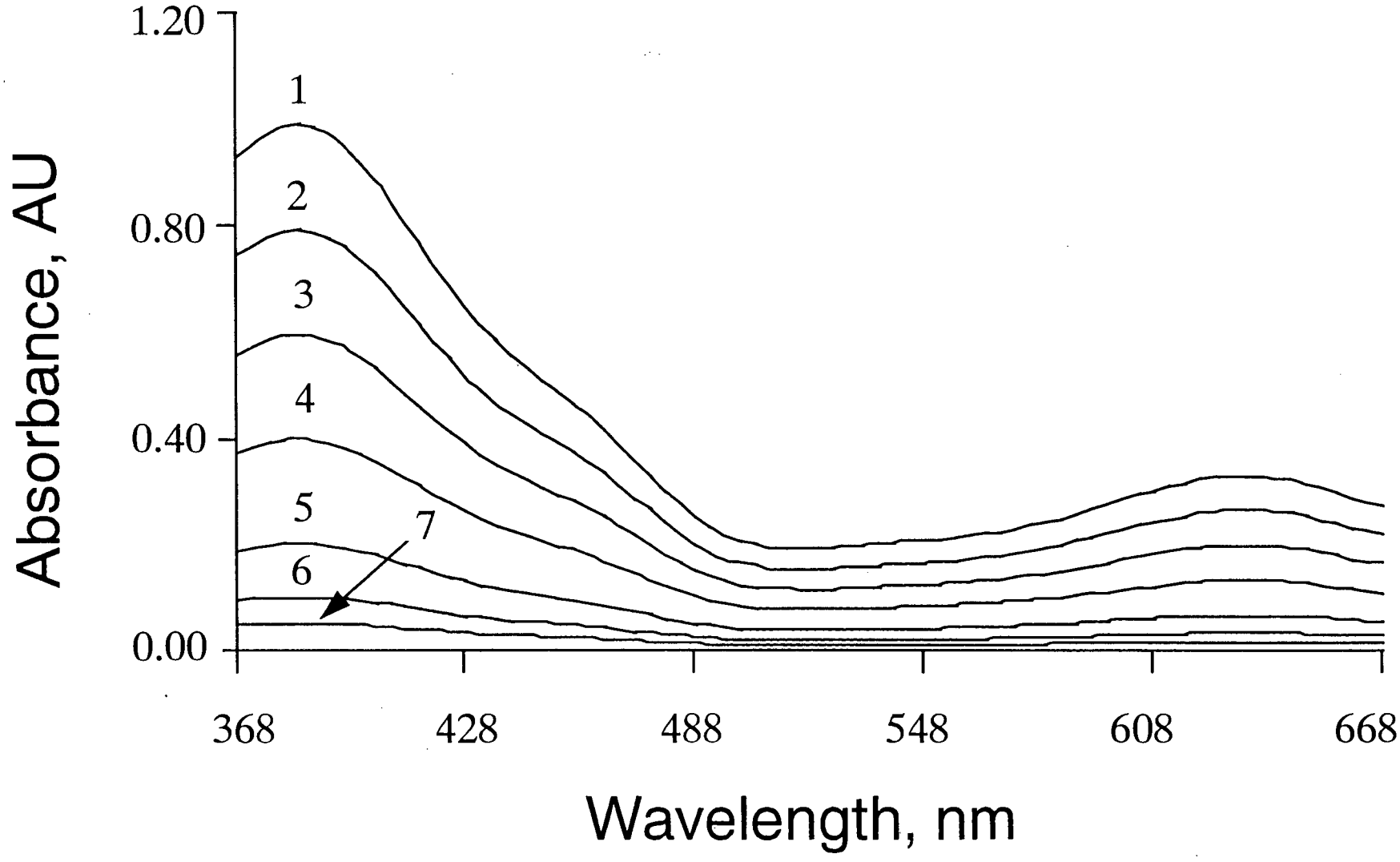
1.20
0.80
0.40
0.00
Absorbance, AU
1
2
3
4
5
6
7
368
428
488
548
608
668
Wavelength, nm

5.2.3 Calibration

Typical features of calibration graphs are shown in Table 5.4 for measurements made at 3 wavelengths. Linearity between 2 and 100 $\mu g.cm^{-3}$ Pd(II) was found. A concentration upper limit of 100 $\mu g.cm^{-3}$ was set in the determination of Pd(II). Palladium may, however, be determined over a wider range of concentrations extending to 800 $\mu g.cm^{-3}$ with adequate reduction in injection volume, or by measurement at a wavelength other than the absorption maximum. Reproducibility for replicate (n = 11) injection of a 10 $\mu g.cm^{-3}$ Pd(II) sample was better than 2%. The sensitivity of this method for palladium is good across the whole absorption spectrum.

Table 5.4

Features of the calibration graphs for the determination of palladium at various wavelengths and tin(II) chloride concentrations.

Tin(II) chloride, (M)	λ (nm)	Calibration Equation [a] (x 1000)	Correlation Coefficient (r)	Linear Range ($\mu g.cm^{-3}$) [b]	R.s.d. (%)[c] (n = 11)
0.05	380	y = 9.85x + 4.22	0.9997	2 - 100	0.62
0.10	380	y = 9.80x - 5.61	0.9990	2 - 100	0.71
0.20	380	y = 9.83x + 3.98	0.9996	2 - 100	0.88
0.05	460	y = 4.46x - 7.18	0.9994	2 - 100	0.47
0.05	636	y = 3.27x - 5.58	0.9986	3 - 100	0.98
0.10	636	y = 1.87x + 3.58	0.9986	4 - 100	1.46
0.20	636	y = 0.62x - 2.23	0.9986	5 - 100	1.72

[a] Calibration : y ≡ AU and x ≡ concentration in $\mu g.cm^{-3}$.

[b] An upper limit of 100 $\mu g.cm^{-3}$ was set.

[c] Relative standard deviation for a 10 $\mu g.cm^{-3}$ Pd(II) sample.

5.2.4 Analysis of Synthetic Solutions

A series of 18 synthetic Pd(II) solutions were prepared and analysed after measurement of Pd(II) calibration solutions. The sample concentrations were in the range 2 to 100 $\mu g.cm^{-3}$. The results obtained for these determinations are shown in Table 5.5 as the correlation between the concentrations "taken" and "found". The line of identity (perfect correlation) would have a theoretical slope of 1.0 and intercept zero.

Table 5.5

Least-squares statistical fits of "true" versus "found" concentrations for the determination of Pd(II). The tin(II) chloride concentration was 0.05 M.

λ (nm)	Intercept ± s ($\mu g.cm^{-3}$)	Slope ± s	Correlation Coefficient (r)
380	0.077 ± 0.044	0.997 ± 0.005	0.998
400	0.015 ± 0.068	0.996 ± 0.004	0.996
460	0.010 ± 0.041	0.996 ± 0.008	0.999
636	0.093 ± 0.053	1.012 ± 0.006	0.997

The same series of 18 synthetic Pd(II) solutions were analysed by ICP-AES to validate the accuracy. Comparisons were made by means of least-squares regression of the results from FIA and ICP-AES. Regression of the FIA *versus* ICP-AES results gave a slope = 1.04 ± 0.02, intercept = 0.11 ± 0.17 $\mu g.cm^{-3}$, and correlation coefficient = 0.997. Good accuracy and correlation with ICP-AES was found.

5.2.5 Analytical Features and Performance

Detection limit studies were carried out by injecting a blank solution and measuring at the wavelengths 380 nm and 636 nm. The limits of detection and determination were calculated according to IUPAC recommendations[11] using a tin(II) chloride concentration of 0.05 M.

The limit of detection at 380 nm was 0.50 $\mu g.cm^{-3}$ Pd(II) and the limit of determination, 1.67 $\mu g.cm^{-3}$ Pd(II). The limit of detection was higher when a wavelength 636 nm was used due to the lower sensitivity. A limit of detection of 1.41 $\mu g.cm^{-3}$ Pd(II) and a limit of determination of 4.70 $\mu g.cm^{-3}$ Pd(II) were found at 636 nm. In both cases, the concentration of solutions corresponding to the limit of determination could be detected and accurately quantified.

An absorption maximum (λ = 636 nm) in the case of palladium is more than 200 nm away from the absorbance maximum of the platinum. It was thus possible to accurately determine palladium in the presence of large excesses of platinum. Similarly, should any other interference exist in a particular region of the absorption spectrum then, by selecting an analytical wavelength removed from such a region, analysis may still be continued.

The sampling rate was 54 $hour^{-1}$ and no "carry-over" was found. No build-up of the brown colloid was found on the manifold tubing at low concentrations of Pd(II). However, at very high concentrations of Pd(II) (> 400 $\mu g.cm^{-3}$) this residue appeared and coated the tube walls. Injection of a 10% nitric acid wash solution was sufficient to remove it. Since the upper concentration limit of Pd(II) was set at 100 $\mu g.cm^{-3}$, this problem was not of immediate concern. Addition of a surfactant, such as Triton-X, would assist in preventing this material from coating the manifold tubing walls.

5.3 The Determination of Rhodium

Preliminary FIA experiments using tin(II) chloride as a reagent for rhodium were performed. As a result of the slow kinetics of this chemical system, extended reaction time and heating of the reacting solution was required to ensure adequate colour development. This was implemented by introducing a stop-flow period when the sample zone was in the reaction coil. Despite this increase of the residence (reaction) time, and heating of the reaction coil within a temperature controlled water bath, the sensitivity was not adequate for a suitable FIA method. Poor reproducibility of these measurements further bedevilled the application of tin(II) chloride in the determination of rhodium.

An alternative reagent, tin(II) bromide,[15] was then tested. Colour formation resulted without the requirement of special reaction conditions such as elevated temperature or extended reaction time. The same FIA manifold used for the determination of platinum and palladium was used directly for rhodium. The sensitivity found when tin(II) bromide was used was adequate for development of a FIA method.

5.3.1 Visible Spectra of the Rhodium-Tin(II) Bromide Complexes

The reaction of tin(II) bromide with rhodium in hydrobromic acid results in a red-orange colour (λ = 468 nm) that develops at room temperature. A second peak forms after several minutes at 408 nm and appears as a yellow colour. The red-orange colour was used analytically to develop a FIA method for the rapid determination of traces of rhodium using tin(II) bromide.

A stop-flow experiment enabled the development of the red-orange colour to be monitored over a period of time (Figure 5.8). Similar stop-flow surface plots were obtained over a wide range of reagent concentrations.

Figure 5.8 *The absorption spectra of a 100 μg.cm^{-3} Rh(III) solution as recorded on stopping the flow of the sample within the flowcell. The rapid kinetics of the reaction of rhodium(III) with tin(II) bromide in an acidic HBr medium is clearly evident.*

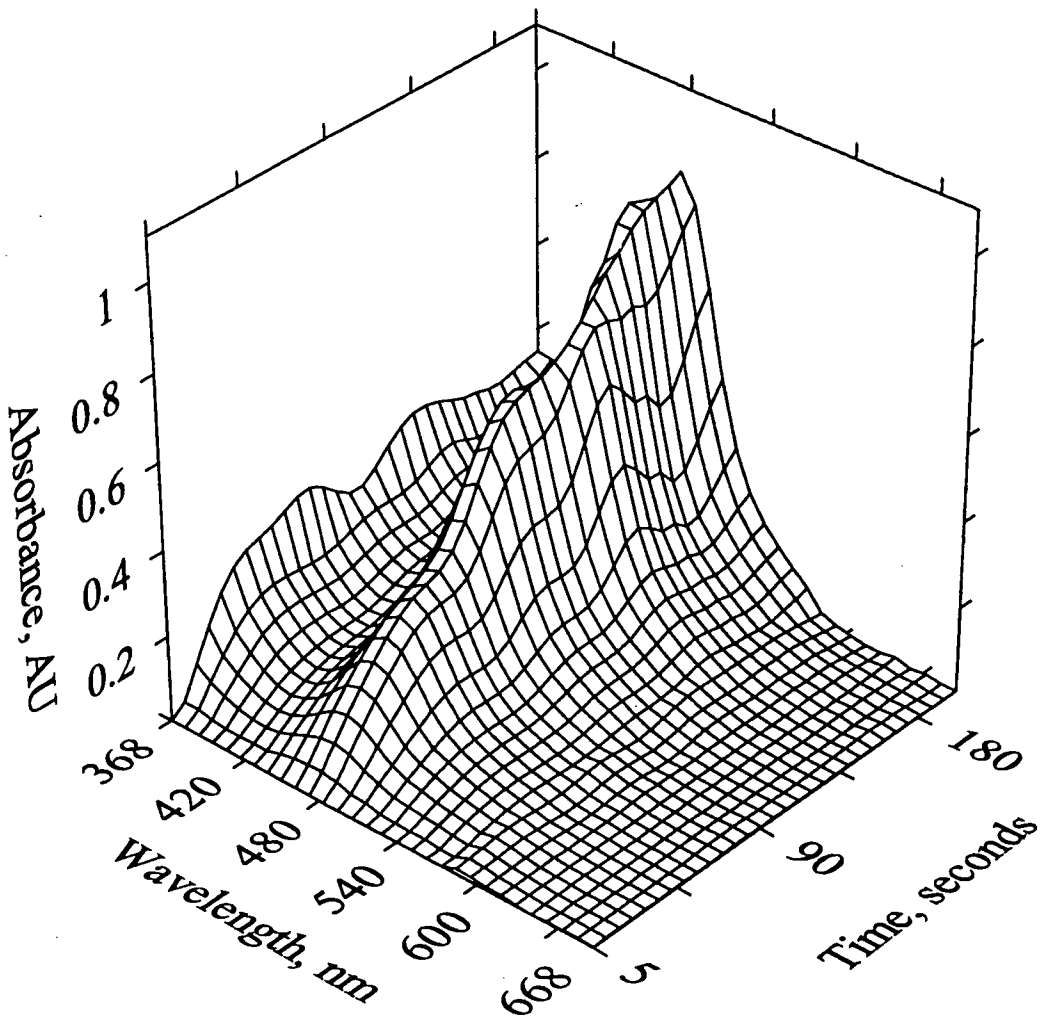
Absorbance, AU
1
0.8
0.6
0.4
0.2
368
420
480
540
600
668
Wavelength, nm
5
90
180
Time, seconds

5.3.2 Calibration

Typical features of the calibration graphs are shown in Table 5.6. Linearity was found to levels of 100 μg.cm^{-3} Rh(III). As before, an upper limit of 100 μg.cm^{-3} was set for the determination of Rh(III). The reproducibility for replicate injection (n = 11) of a solution of 5 μg.cm^{-3} Rh(III) was good. The excellent sensitivity for rhodium at higher tin(II) bromide concentrations is noteworthy. The absorption spectra, recorded on passage through the flowcell, for three Rh(III) standard solutions are shown in Figure 5.9.

Table 5.6

Features of the calibration graphs for the determination of Rh(III) at various wavelengths and tin(II) bromide concentrations.

Tin(II) bromide, (M)	λ (nm)	Calibration Equation [a] (x 1000)	Correlation Coefficient (r)	Linear Range (μg.cm^{-3}) [b]	R.s.d. (%)[c] (n = 11)
0.05	408	y = 3.29x + 0.40	0.9995	0.5 - 100	0.93
0.05	468	y = 5.50x + 1.21	0.9994	0.5 - 100	0.56
0.20	468	y = 13.90x + 3.64	0.9987	1 - 100	1.05
0.40	468	y = 18.42x + 7.42	0.9939	1 - 100	0.79

[a] Calibration : y ≡ AU and x ≡ concentration in μg.cm^{-3}.

[b] An upper limit of 100 μg.cm^{-3} was set.

[c] Relative standard deviation for a 5.0 μg.cm^{-3} Rh(III) sample.

Figure 5.9 *Absorption spectra for (1) 100, (2) 50, and (3) 20 μg.cm^{-3} Rh(III) recorded on reaction with 0.2 M tin(II) bromide in 1 M HBr.*

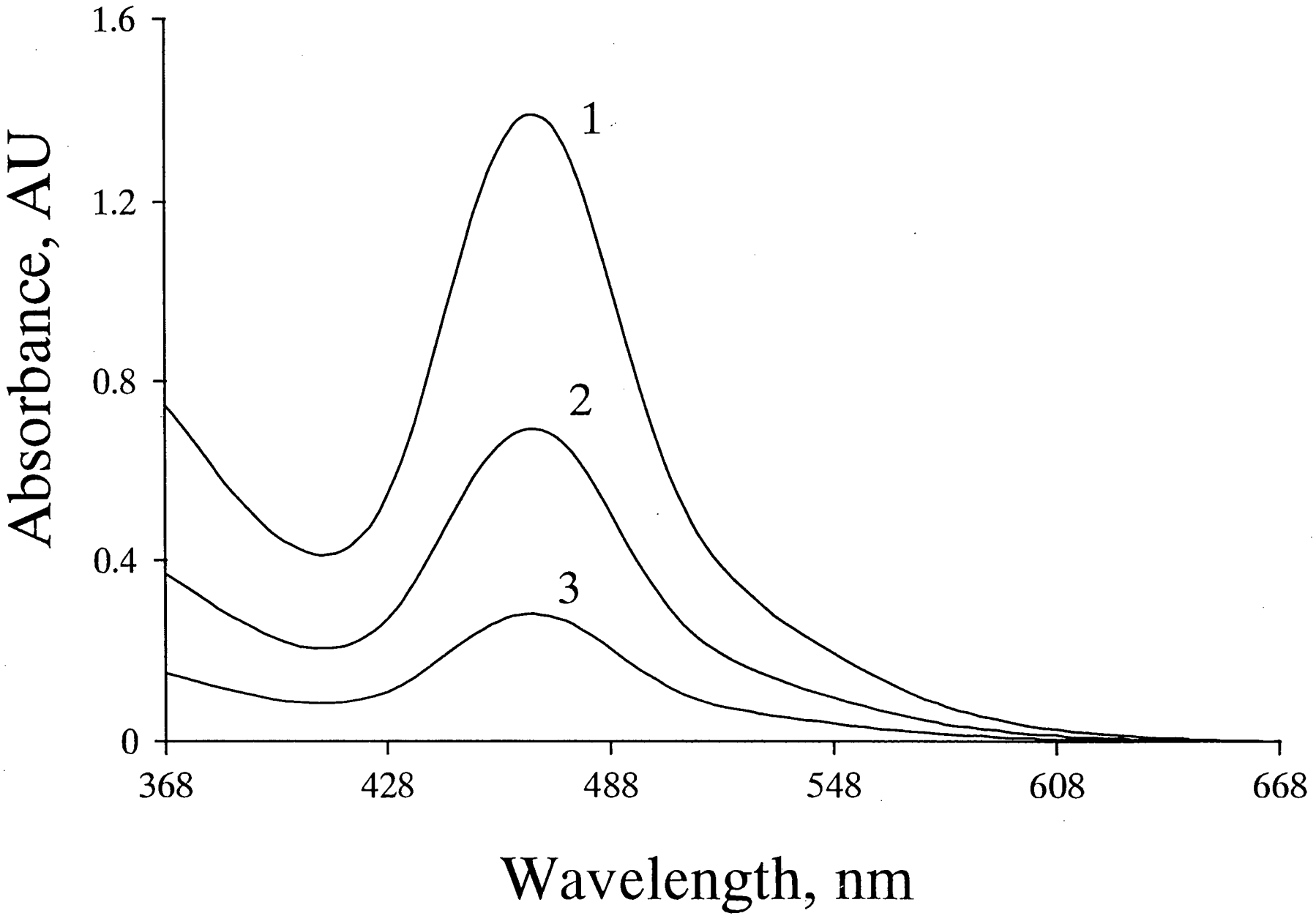
Absorbance, AU
1.6
1.2
0.8
0.4
0
1
2
3
368
428
488
548
608
668
Wavelength, nm

5.3.3 *Analysis of Synthetic Solutions*

A series of 12 synthetic Rh(III) solutions were prepared and analysed after measurement of Rh(III) calibration solutions. The sample concentrations in the range 1 to 100 $\mu g.cm^{-3}$ were analysed. These results are shown in Table 5.7 as the correlation between the concentrations "taken" and "found". The line of identity (perfect correlation) would have a theoretical slope of 1.0 and intercept zero. The correlation between the "true" and "found" concentrations corresponded well at the three wavelengths shown.

Table 5.7

Least-squares statistical fits of "true" versus "found" concentrations for the determination of Rh(III). The tin(II) bromide concentration used was 0.2 M.

λ (nm)	Intercept ± s ($\mu g.cm^{-3}$)	Slope ± s	Correlation Coefficient (r)
468	0.039 ± 0.053	0.998 ± 0.003	0.998
408	-0.015 ± 0.068	1.011 ± 0.004	0.996
500	-0.064 ± 0.081	0.990 ± 0.008	0.991

5.3.4 *Analytical Features and Performance*

The limit of detection,[11] at a wavelength of 468 nm, and using a tin(II) bromide concentration of 0.2 M, was calculated as 0.19 $\mu g.cm^{-3}$ Rh(III), and the limit of determination[11] 0.64 $\mu g.cm^{-3}$ Rh(III). The concentration of solutions corresponding to the limit of determination could be detected and quantified. No "carry-over" between consecutively injected samples of high (80 $\mu g.cm^{-3}$) and low (5 $\mu g.cm^{-3}$) concentrations of rhodium was found. The sampling rate was 54 $hour^{-1}$.

5.4 Preliminary Interference Study

The platinum-group metals occur in small quantities in deposits of copper-nickel sulphide ore. The ore concentrate produced after pre-treatment by fire assay and other mineralogical means consists of about 50% PGMs, the remainder being gold, copper, nickel and base metals such as iron, cobalt, magnesium and aluminium, amongst others.[16] High quantities of iron and lead would be expected in catalytic converters. High levels of tellurium may also be found after precipitation of the PGMs with tellurium.[16]

Since these base metals are likely to be in solutions of real samples, it is important to determine the tolerance of analytical methods for these interferents, and whether approaches circumventing their interference are possible. On this note, a preliminary evaluation of potential interferences was made for the reaction of platinum and palladium with tin(II) chloride.

The potential interferences for the reaction between tin(II) chloride and the PGMs may be roughly grouped into three categories, *viz.*

(i) oxidative interferences, leading to competitive consumption of the reagent, tin(II) chloride,

(ii) absorptive interferences, having high molar absorptivities in the wavelength region of interest, and

(iii) non-selective reaction of tin(II) chloride with substances other than the PGMs.

In general, the established high selectivity of the reaction of tin(II) chloride with the PGMs[17,18] makes interferences of type (iii) unlikely. However, interference from other PGMs and Au(I/III) may be expected.

Since the carrier stream is 1 M in HCl, substantial interferences of the type (i) and (ii) from the first row transition metals are unlikely, with the possible exception of Fe(III) and Cr(VI) (as $Cr_2O_7^{2-}$) which would be present in relatively high concentrations.

Anions such as SO_4^{2-}, NO_3^-, ClO_4^-, and PO_4^{3-} do not interfere at relatively high levels (< 0.1 M), although bromide and iodide ions should be kept to a minimum. Gross quantities of nitric acid may be tolerated as this acid may be expelled by repeated evaporation with hydrochloric acid prior to the residue being taken up in hydrochloric acid.

5.4.1 Base Metal Interferences

The determination of platinum and palladium by the proposed FIA method tolerates many transition metals remarkably well. Interference tolerances at 20 $\mu g.cm^{-3}$ levels for Pt(IV) and Pd(II) were investigated. The interferent concentration that could be handled was such that the response did not differ by more than 2% from that of a pure standard solution. The maximum amount of each interferent tested was 400 $\mu g.cm^{-3}$ for Pt(IV) and 200 $\mu g.cm^{-3}$ for Pd(II), unless otherwise specified. Each experiment was performed in triplicate.

The tolerance levels, shown in Table 5.8, were better than those previously reported[19], presumably due to the merging configuration and the subsequent dilution of the interferents' effect. It is clear that platinum and palladium can be measured in the presence of relatively large amounts of the first row transition elements; particularly for Cr(VI) and Fe(III). The colour inherent in these solutions is seen to decrease in intensity. This is due to reduction to Cr(III) and Fe(II) on addition of tin(II) chloride.

Table 5.8

Interference tolerance at the 20 μg.cm^{-3} Pt(IV) and Pd(II) levels monitoring at the given wavelength with a tin(II) chloride concentration of 0.05 M. Tabulated numerals represent the maximum tolerated concentration of an interferent in μg.cm^{-3}. See text for details.

	Pt(IV)		Pd(II)	
Metal ion added	400 nm	460 nm	400 nm	636 nm
Al^{3+}	400	β	250	400
Co^{2+}	400	β	200	250
Cu^{2+}	400	β	200	200
Cr(VI)	200	β	200	200
Fe^{3+}	900	β	600	600
Mg^{2+}	200	300	200	400
Mn^{2+}	400	β	200	400
Ni^{2+}	400	β	200	200
Pb^{2+}	200	β	200	400
Te(IV)	400	600	200	400

β ≡ Concentrations of the same order as at 400 nm could be tolerated.

The absorbance response of Pt(IV) and Pd(II) is not affected by a decrease in the concentration of the $SnCl_3^-$ concentration as a result of oxidation of tin(II) chloride since reactions occur in an excess of tin(II) chloride. An example is the minimal effect of oxidation incurred by Fe(III) species. The reduction of iron(III) by tin(II) chloride is depicted here showing the formation of Sn(IV) species that do not react with Pt(IV), nor Pd(II).

$$2\,Fe^{3+} + Sn^{2+} \longrightarrow 2\,Fe^{2+} + Sn^{4+}$$

Synthetic mixtures of platinum were prepared with varying amounts of base metals, and in some cases iridium(IV), added as interferents. These solutions were resolved using SCA methods at three wavelengths. R.s.d. values were similar and within the range 1 to 4%. The results, Table 5.9, verify the feasibility of measuring platinum in solutions containing relatively large quantities of interferents.

Table 5.9

The resolution of synthetic mixtures containing interferences and 10 μg.cm^{-3} Pt(IV) at various wavelengths by SCA. Tabulated numerals represent concentrations in μg.cm^{-3}.

Metal ions added, μg.cm^{-3}	368 nm	400 nm	460 nm
400 Fe^{3+}, 100 Pb^{2+}	9.6	9.7	9.6
400 Te(IV), 100 Cr(VI)	9.7	9.7	9.7
100 Fe^{3+}, 300 Ni^{2+}, 50 Mg^{2+}	10.0	10.3	9.6
300 Fe^{3+}, 200 Ni^{2+}, 200 Te(IV)	10.0	10.0	9.6
200 Cr(VI), 200 Al^{3+}, 200 Mn^{2+}	10.4	10.2	10.5
200 Co^{2+}, 200 Cu^{2+}, 100 Ni^{2+}	10.9	10.3	10.6
200 Te(IV), 200 Mg^{2+}, 100 Ir(IV)	9.6	9.7	9.7
150 Ir(IV), 200 Fe^{3+}, 200 Pb^{2+}	10.7	10.3	10.2

5.4.2 Interferences from other Platinum-Group Metals

Gold interfered in the determination of platinum and palladium with tin(II) chloride by forming a colloidal material that suppressed absorbance. The colloidal material deposited on the walls and could only be removed with nitric acid. This characteristic reaction of gold with tin(II) chloride is one of the earliest qualitative colorimetric methods for the detection of small quantities of gold.[20] The nature of the precipitated "purple of Cassius" has been established[21] to be mainly finely dispersed metallic gold, adsorbed onto an insoluble form of hydrous stannous oxide. Gold should be removed prior to analysis by extraction with dibutyl

"Carbitol"[22] or amyl acetate from solutions of hydrochloric acid.[23] The PGMs remain in the aqueous phase.

It was found that the primary interferences in the determination of platinum with tin(II) chloride were other PGMs, such as iridium, ruthenium, and rhodium. Methods to handle such interferences are outlined in Chapter 6.

5.5 Conclusions

Single component FIA methods were successfully developed for the determination of traces of platinum, palladium, and rhodium. Platinum and palladium were determined using tin(II) chloride, and rhodium using tin(II) bromide. Excellent recoveries for these methods were obtained when synthetic samples were analysed. Investigation of the rhodium-tin(II) chloride reaction showed that the kinetics of this reaction were not suited to FIA.

The investigation into the nature and composition of the complexes causing the colour changes on reaction of palladium with tin(II) chloride affords conclusive evidence to the existence of uncharacterised, transient species that give rise to a blue colour. Based on the experimental evidence found in this study, it is stated that true complexes give rise to the olive-green colour when palladium reacts with tin(II) chloride in hydrochloric acid solution.

A consideration of interferences in the developed FIA methods showed the high selectivity of tin(II) chloride for the PGMs. Good tolerance of the FIA methods for base metals is clear, however, the tolerance of other PGMs is poor.

In order to determine platinum, palladium, and rhodium in the presence of each other, and in the presence of other PGMs, it is necessary to either separate the PGMs from one another, or to develop mathematical approaches that may accommodate such interferences. The latter approach was further investigated in this work. To perform such mathematical manipulation, it is imperative to move from the single wavelength mode of measurement into a multi-wavelength mode. The application of these single component methods to multi-component analysis will be outlined in the next chapter.

5.6 References

1. Meyer, A.S., and Ayres, G.H., *J. Am. Chem. Soc.*, 1955, **77**, 2671.
2. Elizarova, G.L., and Matrienko, L.G., *Russ. J. Inorg. Chem.*, 1973, **18**, 254.
3. Ayres, G.H., and Alsop, J.H., *Anal. Chem.*, 1959, **31**, 1135.
4. Maynes, A.D., and McBryde, W.A.E., *Analyst*, 1954, **79**, 230.
5. Young, J.F., Gillard, R.D., and Wilkinson, G., *J. Chem. Soc.*, 1964, 5176.
6. Berman, S.S., and Ironside, R., *Can. J. Chem.*, 1958, **36**, 1151.
7. Moodley, K.G., and Nicol, M.J., *J. Chem. Soc. Dalton*, 1977, 239.
8. Wilson, W.L., Holt, M.S., and Nelson, J.H., *Chem. Rev.*, 1989, **89**, 11.
9. Sandell, E.B., *"Colorimetric Determination of Traces of Metals"*, 3rd edn., Interscience, New York, 1959.
10. Meyer, A.S., and Ayres, G.H., *J. Am. Chem. Soc.*, 1955, **77**, 2671.
11. Analytical Methods Committee, *Analyst*, 1987, **112**, 199.
12. Ayres, G.H., and Meyer, A.S., *Anal. Chem.*, 1951, **23**(2), 299.
13. Harrington, D.E., *Atomic Absorption Newsletter*, 1970, **9**(5), 106.
14. Shlenskaya, V.I., Biryukov, A.A., and Moryakova, L.N., *Russ. J. Inorg. Chem.*, 1969, **4**, 256.
15. Pantini, F., and Piccardi, G., *Anal. Chim. Acta*, 1960, **22**, 231.
16. Jones, E.A., National Institute for Metallurgy, Rep. S. Afr., 1971, No. 1260.
17. Brackenbury, K.F.G., *et al.*, *Polyhedron*, 1987, **6**, 71.
18. Ayres, H.G., and Meyer, A.S., *Anal. Chem.*, 1951, **23**, 299.
19. Auer, D., and Koch, K.R., *Talanta*, 1993, **40**(12), 1975.
20. Von Wagner, R., *"Manual of Chemical Technology"*, J. and A. Churchill, London, 1904, 452.
21. Schneider, E.A., *Z. Anorg. Chem.*, 1894, **5**, 80.
22. Palmer, R., *et al.*, National Institute for Metallurgy, Rep. S. Afr., 1971, No. 976.
23. Lehner, V., and Kao, C.H., *J. Phys. Chem.*, 1926, **30**, 126.

Chapter 6.

Multi-Component Analysis of the Platinum-Group Metals

This chapter will serve two purposes. First, the promising application of multi-component analysis to the determination of the PGMs by FIA will be presented, along with data in its support. And second, suggestions for a reasonable direction of future research in the field of multi-component analysis will be given.

Multi-component analysis (MCA) methods have become increasingly important due to their ability to resolve systems of two or more components. Such simultaneous determination of a mixture of components from their absorption spectra, by means of a least-squares fit, has led to the extension of the boundaries of FIA which were previously limited to single component determinations. A consequence and noteworthy advantage of application of multi-wavelength detectors is that the complete absorption spectrum is available for quantitative analysis. No additional time period is incurred in obtaining such data. Although large volumes of multi-channel data are usually involved in MCA, the advent of powerful computers and numerous mathematical procedures for handling data enables rapid resolution of mixtures.

In the previous chapter, FIA methods were developed for the rapid and single component determination of platinum, palladium, and rhodium using the tin(II) halides in strongly acidic solution. This foundation is added to in this chapter as single component FIA methods are incorporated into methods for multi-component determinations. The MCA mathematical approaches introduced in Chapter 2, and the spectrophotometric data manipulation software program that was outlined in Chapter 3, are used to develop such multi-component analysis methods.

It should be noted that this is by no means a complete study of MCA of the PGMs by FIA. Several stumbling blocks in terms of the complex chemistry and instrumental limitations need to be circumvented in order to make this use of MCA in FIA an accepted and useful

approach. The advantages, as well as problems associated with this endeavour, will be discussed. The initial steps in the development of a suitable mathematical procedure to aid wavelength selection for MCA are also described in this chapter.

6.1 The Determination of Platinum and Palladium in HCl

Having established the optimum conditions and found good analytical performance for the single component determinations of platinum and palladium with tin(II) chloride, the natural succession was to combine these two platinum-group metals and resolve their mixtures by multi-component analysis.

The multi-component analysis of the platinum-palladium-tin(II) chloride chemical system with a high speed scanning spectrophotometer exemplifies the transition from single wavelength methods to multi-wavelength methods in the analysis of complex systems. The resolution of binary mixtures of these elements covering a range of concentrations and concentration ratios using various MCA methods was performed.

The MCA methods used are classical simultaneous linear equation determinations, sequential determination of components, multi-wavelength linear regression analysis (MLRA),[1] and a reference determination where the response of one component is computationally removed. Although the latter method is not multi-component analysis in the true sense, it nevertheless does involve two components (the response of one component is computationally removed) and more than one wavelength. Each of these methods necessitates selection of wavelengths, or a wavelength range, to enable accurate resolution of the mixture into its component concentrations.

6.1.1 Wavelength Selection

During single component determinations the maximum absorption position, or a shoulder position, are taken as the analytical wavelengths. Any errors made in taking these as analytical wavelengths (*viz.* wavelength resettability imprecision) are kept to a minimum. However, one wavelength is not adequate for resolution of a mixture. In MCA the wavelengths selected

should include the wavelengths that give higher absorbances for both components, or at least for one component of a mixture.

The general criteria for the selection of analytical wavelengths (Section 2.2.4) are based on an assumption that the uncertainty of measurement at each wavelength is similar. It is important that the uncertainty of replicate absorbance measurement be low at the analytical wavelength(s) so as to maintain precision and ensure accuracy. Similarly, any deviations from a linear calibration suggests that Beer's law is not adhered to.

A plot of wavelength *versus* the relative standard deviation of replicate measurements at that wavelength for platinum is shown in Figure 6.1. Responses at wavelengths greater than 480 nm had higher r.s.d. values due to lower sensitivity for platinum. This type of plot aids in the selection of wavelength ranges. Wavelengths with a high r.s.d. for replicate measurements were not used. A similar situation is found for palladium with the r.s.d. increasing above 2% in regions of low sensitivity. Similarly, these wavelength regions were not used. The deviations from linearity of calibration curves for platinum and palladium over the analytical wavelength ranges used were negligible. The platinum calibrations had a correlation of 0.998, or better, for the range 368 to 480 nm. Palladium calibrations had correlation of 0.997, or better, for the range 368 to 640 nm.

The best way to find wavelengths that satisfy the requirements of larger spectral absorptivities and large differences between components is to plot the quotient of the absorptivities of the two components as a function of the wavelength. Regions, or points, of unity indicate the same absorptivity for each component at that wavelength(s). Maxima and minima signify regions of best resolution for the component being the numerator and denominator respectively.

Figure 6.2 shows the regions of best resolution for platinum (the numerator in the equation) to be near 484 nm, and for palladium (denominator) to be near 368 and 636 nm. Two intersection points, with values of unity, show wavelengths of constant absorbance for both platinum and palladium. A plateau, approximately 410 to 440 nm, exists where there is similar spectral character in both components. These regions should be avoided as a high degree of spectral difference is required for accurate mixture resolution.

Figure 6.1 *Relative standard deviation (R.s.d.,%) of quadruplicate injections of platinum samples as a function of the wavelength to aid wavelength selection. The letters correspond to concentrations of (a) 10 μg.cm^{-3}, and (b) 50 μg.cm^{-3} Pt(IV). R.s.d. values were higher than 1.6% at wavelengths above 480 nm.*

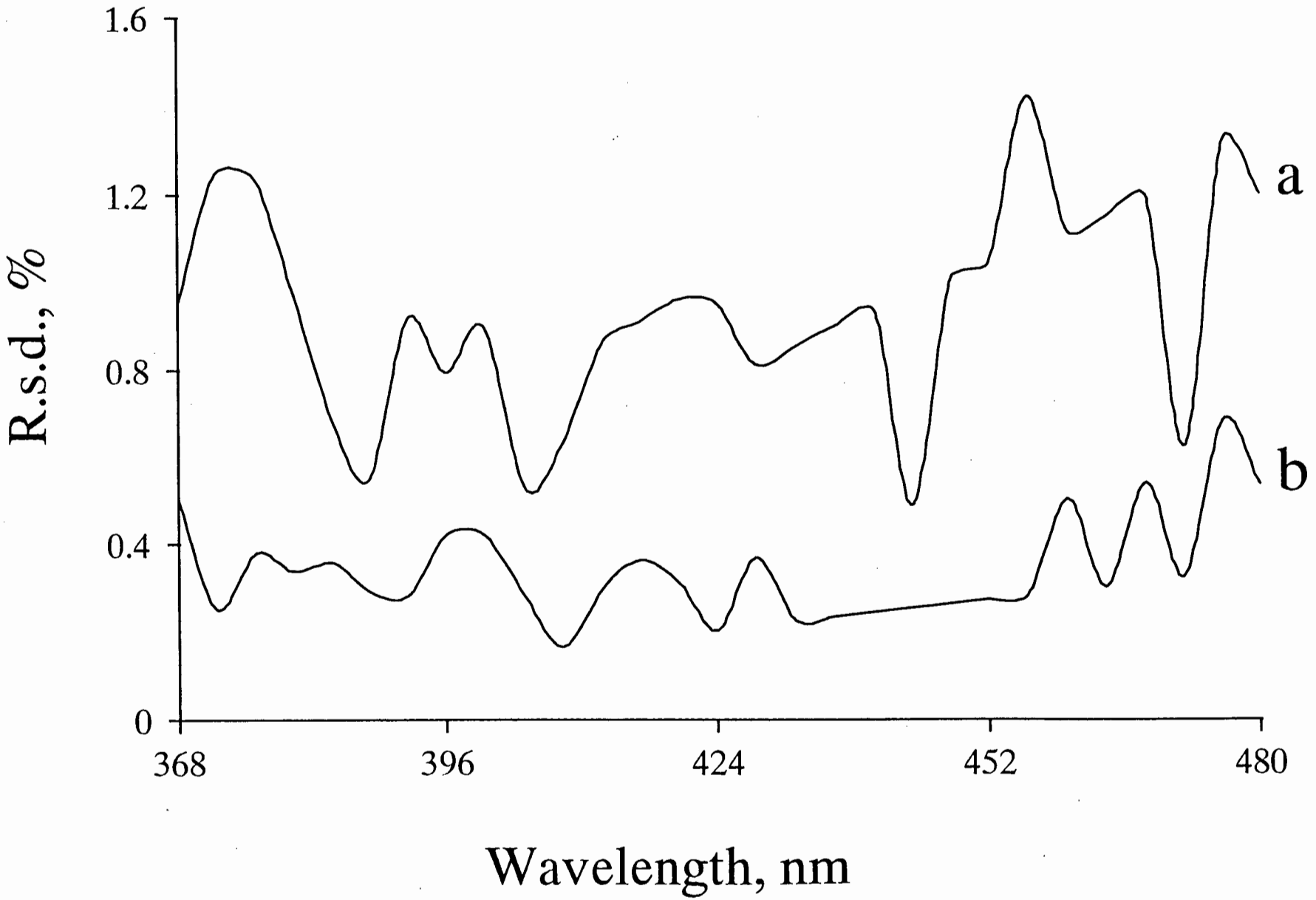
1.6
1.2
0.8
0.4
0
R.s.d., %
a
b
368
396
424
452
480
Wavelength, nm

Figure 6.2 *Plot of the quotient of the absorptivities ($a_{1,j}$ and $a_{2,j}$) as a function of the wavelength, j, to show regions of maximum and minimum curve divergence. The curves correspond to (1) quotient of the absorptivities, (2) 100 $\mu g.cm^{-3}$ Pd(II), and (3) 100 $\mu g.cm^{-3}$ Pt(IV).*

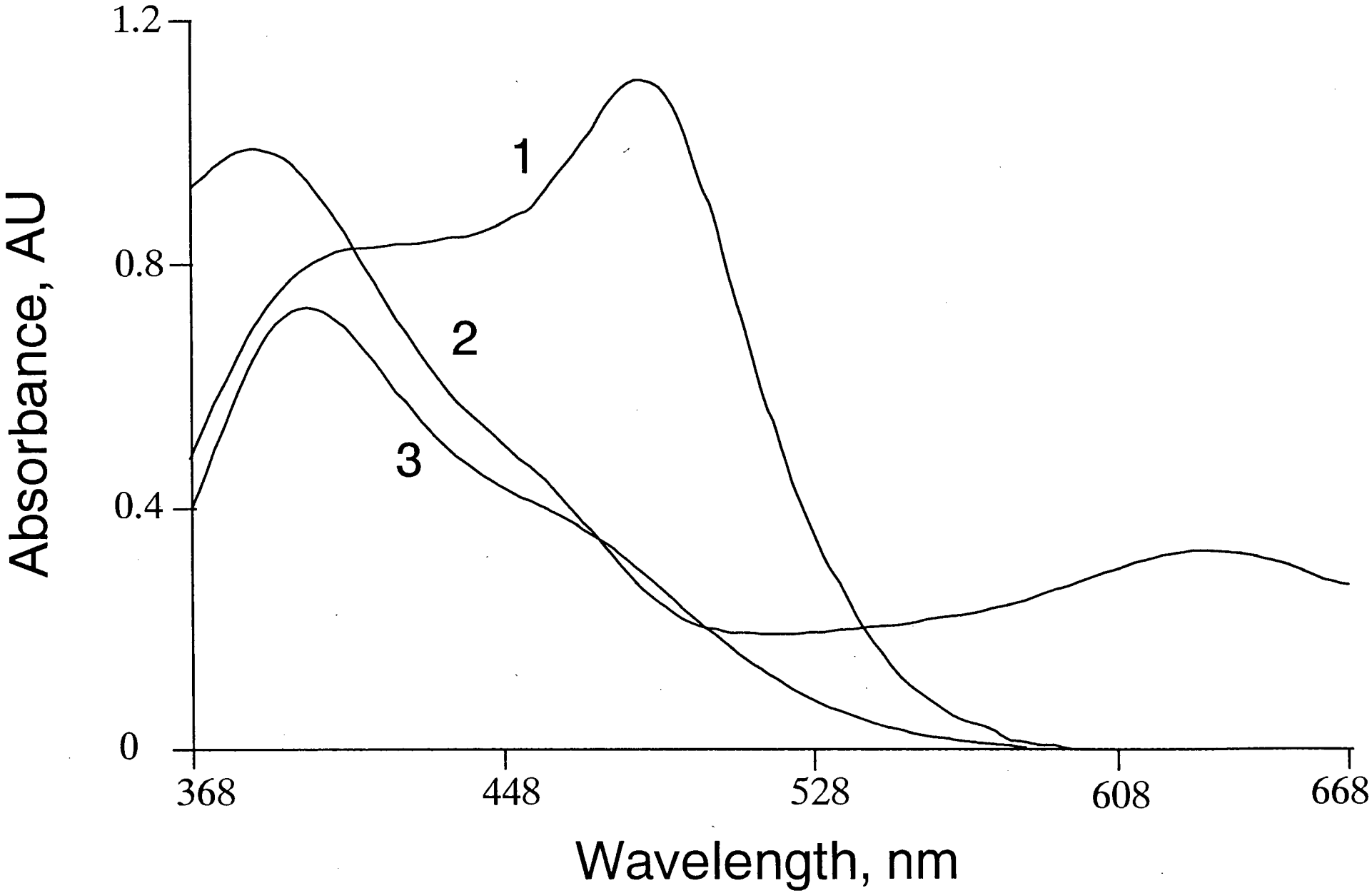
1.2
0.8
0.4
0
Absorbance, AU
1
2
3
368
448
528
608
668
Wavelength, nm

A mathematical approach for wavelength selection for MCA would indeed be of exceptional value. Such an approach must incorporate the criteria indicated in Chapter 2 (Section 2.2.4). These criteria essentially ensure that data adhere to basic spectrophotometric laws. However, these are insufficient for implementation in a mathematical approach which would require algorithms to evaluate wavelength selection.

The fact that some analytical wavelengths are better than others with respect to accuracy and precision needs consideration. A weighting scheme applied to spectral data points would be relevant here. As the best precision is associated with the complete absorption spectrum, and there is a corresponding loss of accuracy at wavelengths of lower sensitivity, the requirement of a compromise between these two competing factors is clearly illustrated.

In the meantime, the consideration of the parameters such as adequate spectral differences, maximum ratios between absorptivities, low r.s.d. at selected wavelengths, and good agreement with Beer's law remain important in present empirical wavelength selection approaches.

6.1.2 Multi-Component Analysis

Synthetic mixtures of platinum and palladium were analysed and resolved by four multi-component methods - classical simultaneous linear equations, sequential analyte determination, multi-wavelength linear regression analysis, and reference determination of one component. The computations were performed on identical sets of data by ReduceTEK.

6.1.2.1 Classical Simultaneous Linear Equations

The method of classical simultaneous linear equations involves solving a system of two linear equations based on the absorbances of the two analytes measured at two wavelengths (usually their respective absorbance maxima).

The equations used for such a simultaneous determination at 368 nm and 400 nm are -

$$A_{368} = a_{Pt,368}\,[Pt]\,l + a_{Pd,368}\,[Pd]\,l$$

$$A_{400} = a_{Pt,400}\,[Pt]\,l + a_{Pd,400}\,[Pd]\,l$$

where [ ] ≡ concentration of Pt or Pd, l is the illuminated flow cell path length, $a_{i,j}$ is the absorptivity of component i at wavelength j, and A_j the absorbance of the mixture at wavelength j.

6.1.2.2 Sequential Analyte Determination

Sequential analyte determination involves the computation of one analyte concentration and with that knowledge, the calculation of the concentration of the second analyte. The absorbance measured at 636 nm is solely as a result of palladium in the sample. Palladium, in the presence of excess platinum, may thus be determined. With the knowledge of the palladium concentration, and the absorptivities (obtained from the calibration), the responses at another wavelength, for instance at 400 nm, may be resolved into its' component absorbances.

The equations used in the resolution of a binary mixture at two wavelengths, 400 nm and 636 nm, are shown -

$$A_{636} = a_{Pd,636}\,[Pd]\,l$$

$$A_{400} = a_{Pt,400}\,[Pt]\,l + a_{Pd,400}\,[Pd]\,l$$

where [ ] ≡ concentration of Pt or Pd, l is the illuminated flow cell path length, and $a_{i,j}$ is the absorptivity of component i at wavelength j, and A_j the absorbance measured at wavelength j.

6.1.2.3 Multi-Wavelength Linear Regression Analysis

Multi-wavelength linear regression analysis involves the use of several wavelengths to "over-determine" a system comprising several linear equations. Least-squares fitting over the range of wavelengths is performed and is represented graphically for the user on-screen in ReduceTEK. The derivation of the equation is outlined in detail in Section 2.2.3. The equation for the resolution of a binary system of components at wavelengths, j, is shown -

$$A_{1,j} / A_{mixture,j} = (1/c_1) - (c_2/c_1)(A_{2,j} / A_{mixture,j})$$

where c_1 and c_2 are the concentrations of component 1 and 2, $A_{i,j}$ is the absorption of component i at λ_j, and $A_{mixture,j}$ the absorption of the mixture at λ_j.

The relevant plot of $A_{1,j} / A_{mixture,j}$ *versus* $A_{2,j} / A_{mixture,j}$ gives a straight line with a slope of $-c_2/c_1$, and y-axis intercept of $1/c_1$. This allows the calculation of concentrations c_1 and c_2. An example of such a plot for a mixture of platinum and palladium is shown earlier in Chapter 2 (Figure 2.12). The absorption spectrum recorded for the mixture compares well with the theoretical absorption spectrum (Figure 2.13) that is computed from the calibration solutions. During preliminary testing, mixtures were analysed over several wavelength ranges and at wavelengths spread over the complete spectrum range. The former gave more accurate results due to the selection of wavelength ranges that satisfy the criteria required for mixture resolution.

6.1.2.4 Reference Determination

Reference determination involves the computational removal of the response of one component by selecting two wavelengths of identical absorptivity for that component. The wavelength of lower sensitivity is subtracted from the higher sensitivity wavelength so as to yield a positive result for the concentration computation of the sought analyte. The criteria for resolution in this manner is that the difference in absorptivity for the other component at the two wavelengths be adequately high for measurement.

The term "reference" is used as this method is a variation of a similar method used in diode-array instrumentation. Here an internal reference wavelength is chosen where no absorption of solution components occur. The response at this wavelength is subtracted from the absorption spectrum. This approach compensates for all effects that cause erroneous absorbance readings, but which are independent of wavelength. An example of this is any lamp instability.

The manipulation of spectrophotometric data using reference determination is illustrated in the computational removal of palladium by difference measurement at the wavelengths 480 nm and 624 nm. It is also possible to remove the platinum component by difference measurement at 388 nm and 412 nm. The equations used in the computational removal of palladium are:

$$A_{480-624} = (a_{Pt,480} - a_{Pt,624})\,[Pt]\,l$$

$$\because\ a_{Pd,480} = a_{Pd,624}$$

where [ ] ≡ concentration of Pt, l is the illuminated flow cell path length, $a_{i,j}$ is the absorptivity of component i at wavelength j, and $A_{480-624}$ is the absorbance difference between 480 nm and 624 nm.

Selection of wavelengths that satisfy the criteria for the reference method is facilitated by an on-screen display in ReduceTEK. The calibration slopes given in text, and the spectral scans at different concentrations depicted graphically, allow facile comparisons and reference wavelength selection.

Another wavelength manipulation approach that was tested was that of wavelength averaging. This approach involves averaging readings of a range of wavelengths spread around a wavelength of interest. It is a useful approach in that a decreased r.s.d. may be found where very "noisy" spectra are measured. No significant improvement of the SCA results were found when using wavelength averaging for low absorbing samples and this was not investigated further.

6.1.3 Calibration

A minimum of four calibration standards of each component, Pt(IV) and Pd(II), were prepared with concentrations in the linear range. These standards were injected in triplicate and spectra for each standard were obtained on averaging, after subtraction of the blank. A normalised spectrum for each standard was obtained by regression of the absorbance *versus* concentration. These normalised spectra were stored to disk and used for the resolution of the mixtures. Spectra for standards and samples were acquired under the same experimental conditions.

The typical calibration features for Pt(IV) and Pd(II) are very similar to those tabulated earlier in Chapter 5. The calibrations were linear and correlation coefficients were better than 0.997 in each case over the complete wavelength range.

6.1.4 Analysis of Synthetic Solutions

A series of 35 synthetic mixtures of platinum and palladium solutions were prepared and analysed using the pertinent standard solutions. Mixtures contained varying amounts of platinum and palladium in the range 5 to 100 $\mu g.cm^{-3}$. No synergistic effects were observed within the ranges used. Hence, the responses of the mixtures were independent of their respective component concentrations. The ratios of the one component to the other varied between 1:10 and 10:1.

The mixtures were analysed using each of the resolution methods. Resolution by simultaneous linear equations was performed at the absorbance maximum of each component. The results obtained for these determinations are shown in Table 6.1 as the correlation between concentrations "taken" and "found". Inductively coupled plasma-atomic emission spectrometry, results found on analysis of the same solutions, showed good correlation with the FIA multi-component determinations.

Table 6.1 *Results of analysis of 35 mixtures of Pt(IV) and Pd(II) shown as the correlation between the concentrations "taken" and those "found". Various mixture resolution methods were used. Comparative results found by ICP-AES are shown.*

Resolution	Pt(IV)			Pd(II)		
	Intercept ± s	Slope ± s	Corr. coeff.	Intercept ± s	Slope ± s	Corr. coeff.
Simultaneous (λ = 380 and 400 nm)	3.19 ± 1.15	1.08 ± 0.02	0.989	-2.54 ± 0.95	0.91 ± 0.03	0.991
Sequential (λ = 368 and 636 nm)	-0.67 ± 0.60	0.99 ± 0.03	0.999	-0.30 ± 0.40	1.00 ± 0.01	0.999
Sequential (λ = 400 and 636 nm)	-0.14 ± 0.43	1.01 ± 0.01	0.998	-0.30 ± 0.40	1.00 ± 0.01	0.999
MLRA (λ range 368-400 nm)	1.54 ± 0.46	1.00 ± 0.01	0.999	-1.40 ± 0.24	0.99 ± 0.01	0.999
MLRA (λ range 368-460 nm)	1.96 ± 0.58	1.04 ± 0.02	0.997	-1.82 ± 0.41	0.96 ± 0.02	0.998
Pd(II) "subtraction" (λ_{480} - λ_{620})	1.23 ± 0.46	1.02 ± 0.02	0.998	-	-	-
ICP-AES	0.38 ± 0.25	1.09 ± 0.01	0.998	-3.39 ± 0.21	1.03 ± 0.01	0.999

The classical method of spectral resolution based on linear equations resulted in substantial errors and deviations from linearity. This was expected because of the degree of spectral overlap. The sequential approach of first computing the palladium concentration and then using this result to compute the platinum concentration gave improved results and superior correlation when compared to the results obtained using simultaneous equations. The sequential approach enables accurate determination of palladium, at 636 nm, in the presence of up to a 10-fold excess of platinum.

The MLRA approach also afforded good correlation over wavelength ranges from 368 nm to 400 nm, and 368 nm to 460 nm. The correlation over the latter range is slightly poorer because of the similar spectral character found in this region (Figure 6.2). The computational removal of palladium and measurement of platinum proved successful and is useful particularly if the palladium concentration is not required.

6.1.5 Analytical Features and Performance

The precision (r.s.d.) achieved in the repeated (n = 11) resolution of a mixture (using MLRA) of 15 $\mu g.cm^{-3}$ Pt(IV) and 20 $\mu g.cm^{-3}$ Pd(II) was 1.8% and 2.3% respectively. Resolution of mixtures at levels lower than 5 $\mu g.cm^{-3}$ of each component was possible. However, precision was poor (> 5%) as a result of the low absorbances and associated increase in the r.s.d. of the measurement.

Accurate resolution of mixtures of platinum and palladium covering a broad range of concentrations was performed by various multi-component methods. The possibility of extending the number of components is only possible when MLRA is used because additional wavelengths are required for component resolution.

Resolution of three component mixtures of platinum, palladium and rhodium were attempted, but the poor sensitivity of rhodium in tin(II) chloride precluded it from being resolved. The platinum and palladium concentrations obtained were consistently higher in the presence of rhodium. This would be expected with the colour forming reaction of rhodium and tin(II) chloride, *albeit* slow, does occur to some extent. The potential for MCA using tin(II) bromide in HBr solutions is outlined later in this chapter. By using tin(II) bromide it is

possible to increase the sensitivity considerably for platinum, palladium, and especially rhodium. This increase of sensitivity, and the widely differing absorption spectra on reaction of these metals with tin(II) bromide, forms the basis for a possible resolution of a three component system by FIA. This will form part of future MCA investigations.

6.1.6 Base Metal Interference Study

The base metal interferences were investigated by monitoring the effect of base metals on resolution of a platinum-palladium mixture with various amounts of interferent being added. These base metals are expected to be present with the PGMs in ore samples and further processing solutions. Resolution of these mixtures was only possible using MLRA with least-squares fitting to the selected spectral range.

Results obtained for the resolution of synthetic mixtures containing 10 $\mu g.cm^{-3}$ Pt(IV) and 24 $\mu g.cm^{-3}$ Pd(II) in the presence of various quantities of base metals, and in cases iridium, are shown in Table 6.2.

Table 6.2

The resolution of synthetic mixtures of 10 $\mu g.cm^{-3}$ Pt(IV) and 24 $\mu g.cm^{-3}$ Pd(II) containing interferences by MLRA over a wavelength range of 368 nm to 420 nm.

Metal ions added, $\mu g.cm^{-3}$	Pt(IV) $\mu g.cm^{-3}$	Pd(II) $\mu g.cm^{-3}$
400 Fe^{3+}, 200 Pb^{2+}	9.0	22.2
200 Te(IV), 200 Al^{3+}, 200 Cr(VI)	11.2	23.0
100 Al^{3+}, 100 Cr(VI), 100 Co^{2+}	10.1	23.5
200 Mn^{2+}, 100 Mg^{2+}, 100 Te(IV)	10.4	23.7
100 Ir(IV), 200 Fe^{3+}, 200 Pb^{2+}	10.8	23.6
200 Fe^{3+}, 200 Cu^{2+}, 100 Ni^{2+}	10.5	24.2

The FIA methods developed for the determination of platinum and palladium, simultaneously, and as single components, tolerate the presence of diverse interferent ions well. This preliminary study of interferences illustrates the selectivity of tin(II) chloride for the PGMs, and demonstrates the successful resolution of PGM mixtures by MLRA containing substantial levels of typical interferents.

6.2 The Determination of Platinum and Ruthenium in HCl

Addition of tin(II) chloride to a test solution of commercial ruthenium (III/IV) chloride results in the change of the original dark red-orange colour to pale blue, and then to pale yellow on further standing. The colour change to blue can be attributed to a reduction from Ru(IV) to Ru(III).[2] The blue colour has been attributed to either Ru(III) or Ru(II)[3,4] complexes with tin(II) chloride, possibly involving chloride bridges.

It seems that the Ru(IV) present in commercial ruthenium trichloride is first reduced to Ru(III) and thereafter, the Ru(III) reduced to Ru(II) with concomitant complex formation with tin(II) chloride to give yellow complexes of the type $[Ru(SnCl_3)_nCl_{6-n}]^{4-}$ (n = 1 to 6) in HCl solution. Complexes of the form $[Ru(SnCl_3)_2Cl_2]^{2-}$ have also been found.[5]

The yellow colour formation is more rapid on heating. However, this is not convenient in FIA applications. Tests with heating the reaction coil to 70 °C in a water bath resulted in poor reproducibility.

6.2.1 Visible Spectra of the Ruthenium-Tin(II) Chloride Complexes

The absorbance spectrum of ruthenium in 0.2 M tin(II) chloride shows an absorbance maximum at 368 nm and plateau for wavelengths greater than 450 nm (Figure 6.3). The intensity of the yellow colour was also a linear function of concentration (10 to 300 $\mu g.cm^{-3}$). Higher tin(II) chloride concentrations promote the kinetics of complex formation. Although sensitivity for ruthenium is lower than that for platinum with the reaction being far from completed, results confirm that the yellow colour may be used analytically.

6.2.2 *Calibration*

The calibration procedure followed was the same as that used for the simultaneous determination of platinum and palladium in Chapter 5 and is not repeated here. Typical features for the ruthenium calibrations are shown in Table 6.3.

Although no single component analysis investigation was performed on ruthenium, there is no reason why this reaction with tin(II) chloride may not be exploited analytically, *albeit* a low sensitivity method for ruthenium.

Table 6.3

Features of the calibration graphs for the multi-component determination of ruthenium.

Tin(II) chloride, (M)	λ (nm)	Calibration Equation [a] (x 1000)	Correlation Coefficient (r)	Linear Range ($\mu g.cm^{-3}$) [b]	R.s.d. (%)[c] (n = 11)
0.2	368	y = 3.76 + 1.31	0.9988	10 - 100	1.14
0.2	400	y = 2.37 - 4.13	0.9998	10 - 100	0.89
0.2	440	y = 0.61 - 2.45	0.9997	10 - 100	1.43

[a] Calibration : y ≡ AU and x ≡ concentration in $\mu g.cm^{-3}$.

[b] An upper limit of 100 $\mu g.cm^{-3}$ was set.

[c] Relative standard deviation for a 50 $\mu g.cm^{-3}$ Ru(III/IV) sample.

Figure 6.3 *Absorption spectra recorded at the FIA peak maximum on passage through the detector flowcell, for (1) 10 μg.cm^{-3} Pt(IV), and (2) 20 μg.cm^{-3} Ru(III/IV), recorded using a tin(II) chloride concentration of 0.2 M.*

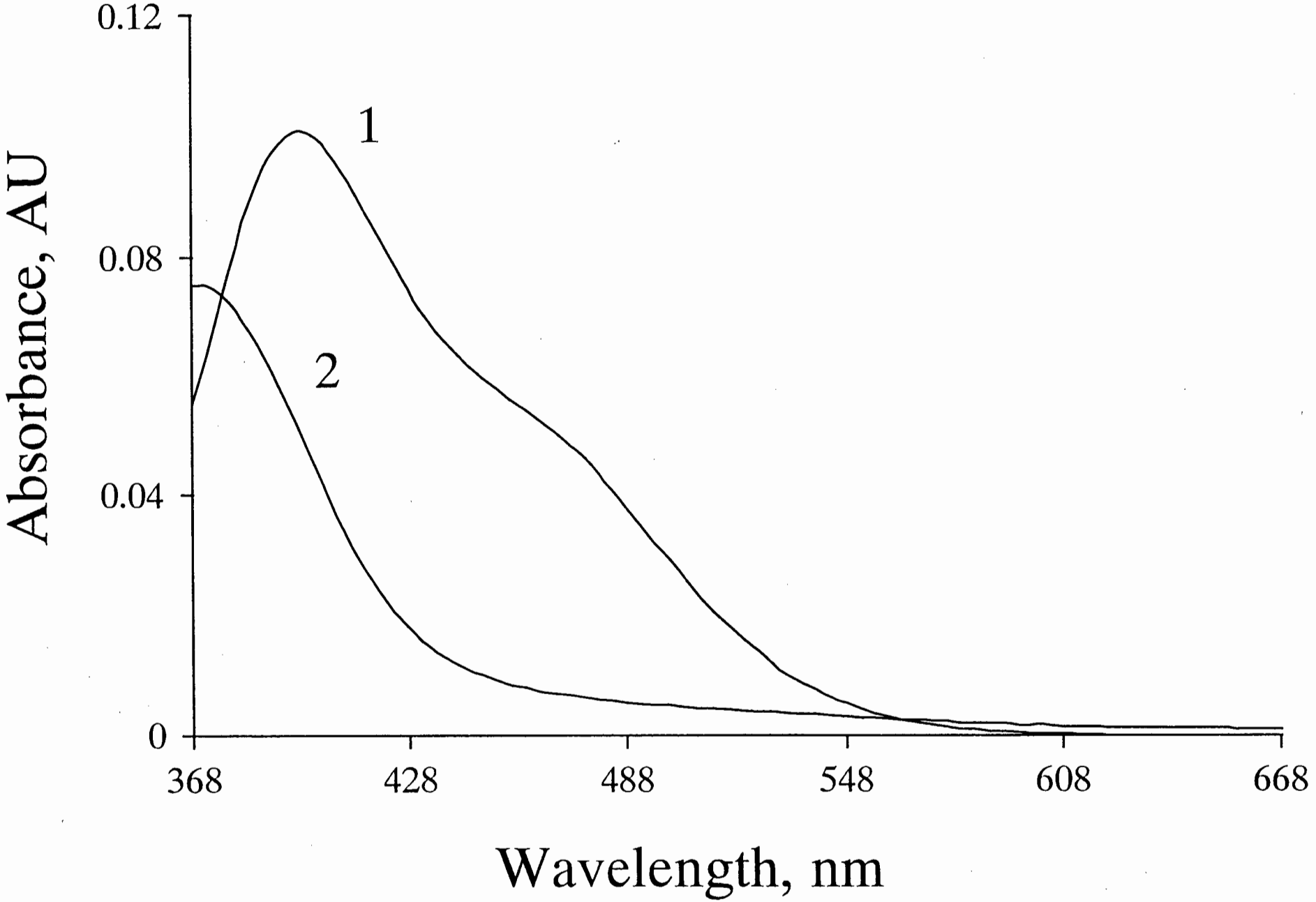
0.12
0.08
0.04
0
Absorbance, AU
1
2
368
428
488
548
608
668
Wavelength, nm

6.2.3 Analysis of Synthetic Solutions

A series of 10 mixtures of Pt(IV) and Ru(III/IV) were prepared with a Pt(IV) range from 5 to 95 $\mu g.cm^{-3}$, and a Ru(III/IV) range from 20 to 100 $\mu g.cm^{-3}$. The concentrations were in the ratios (Ru:Pt) 0.1:12. Due to the extensive spectral overlap, only the MLRA resolution method enabled accurate analysis. A wide wavelength range of 368 nm to 460 nm was necessary.

Linear least-squares results of the "found" *versus* "true" concentrations for platinum were, slope = 0.99 ± 0.01; intercept = -0.42 ± 0.54 $\mu g.cm^{-3}$; and correlation coefficient = 0.999; and for ruthenium, slope = 1.04 ± 0.02; intercept = -1.80 ± 1.29 $\mu g.cm^{-3}$; and correlation coefficient = 0.998. Good correlation was found with ICP-AES results for platinum. Ruthenium concentrations were not measured.

Linear least-squares results for platinum by ICP-AES of the "found" *versus* "true" concentrations gave a slope = 0.99 ± 0.01; intercept = 0.86 ± 0.41 $\mu g.cm^{-3}$; and correlation coefficient = 0.999. Typical results are shown in Table 6.4 for mixtures of platinum and ruthenium analysed by MLRA.

Table 6.4

Results of resolution of mixtures of Pt(IV) and Ru(III/IV) by MLRA.

"True", $\mu g.cm^{-3}$		"Found", $\mu g.cm^{-3}$	
Pt(IV)	Ru(III/IV)	Pt(IV)	Ru(III/IV)
95.0	10.0	92.1	9.0
70.0	30.0	69.7	29.2
20.0	80.0	18.6	78.5
5.0	60.0	5.1	58.9
50.0	50.0	50.1	51.2
5.0	20.0	4.9	19.8

6.2.4 Analytical Features and Performance

A mixture of Pt(IV) and Ru(III/IV), 20 $\mu g.cm^{-3}$ and 80 $\mu g.cm^{-3}$ respectively, was repeatedly (n = 11) analysed and gave a precision (r.s.d.) of 1.9% and 2.6% for platinum and ruthenium respectively. No attempts were made to analyse ruthenium at lower levels on account of the lack of adequate sensitivity with tin(II) chloride. An alternative reagent would be recommended for trace analysis of ruthenium by FIA.

Thus far, the determinations have primarily entailed the MLRA least-square fit of standard spectra to mixture spectra in order to resolve the mixtures. The concentrations of the PGMs determined by this approach correspond well with the theoretical values. The ability to vary the wavelength ranges according to the chemical system being investigated, and being able to fine-tune the resolution presents a formidable step in "interactive" multi-component analysis. The importance of wavelength range selection is crucial to accurate MLRA-based analyses.

6.3 The Determination of Platinum in the Presence of Other Platinum-Group Metals in HCl

The determinations presented in subsequent sections make use of only two carefully selected wavelengths and mathematical manipulation to enable mixture resolution. Again, although these determinations are not in the true sense multi-component, they involve the use of the responses of a multi-component absorbing system and more than one wavelength to determine the concentration of a single component.

This demonstration of the use of two wavelengths may readily be extended to more wavelengths to eliminate, or compensate for, interferences. Where previously separation of the platinum from the iridium or rhodium was required prior to analysis, this approach makes the separation step unnecessary. The intention here is not to replace the crucial separation steps, but to illustrate the potential of this approach when interferences may be difficult to remove.

6.3.1 The Determination of Platinum in the Presence of Iridium

When tin(II) chloride is added to a test solution of iridium(IV) chloride, the orange-brown colour of the solution changes rapidly to pale yellow. It was found that this yellow colour is a linear function of the iridium concentration. Although a coloured product forms on heating,[6] this method cannot be made the basis of an absorptiometric method for iridium using FIA.

Although various iridium complexes involving the $SnCl_3^-$ moiety are known,[7] the reaction between Ir(IV) chloride and tin(II) chloride has not been examined in detail. As is the case with Pt(IV), the reaction with tin(II) chloride is likely to involve a reduction of Ir(IV) to Ir(III), followed by complex formation with $SnCl_3^-$. Complex formation is very slow, or possibly incomplete, at room temperature. Prolonged heating is required at 100°C to produce, for example, $[(CH_3)_4N]_4[Ir_2Cl_2(SnCl_3)_4]$.[7]

The intensity of the yellow colour is proportional to the iridium concentration over the range 20 to 300 $\mu g.cm^{-3}$ Ir(IV) in the wavelength range 368 nm to 550 nm (correlation coefficients were better than 0.997). The response was too low for accurate resolution by multi-component analysis, however, a semi-quantitative indication of the iridium concentration could be obtained.

Computational removal of iridium was possible if the response at 428 nm was subtracted from that at 400 nm (the absorptivity of Ir(IV) is the same at these two wavelengths). The residual platinum response was adequate for accurate resolution using SCA. The absorption spectra for standard solutions of platinum and iridium are shown in Figure 6.4. The poorer sensitivity for iridium is clearly seen.

A series of 18 mixtures with Pt(IV) concentrations between 2 and 20 $\mu g.cm^{-3}$, and Ir(IV) concentrations between 40 and 300 $\mu g.cm^{-3}$ (ratios Ir:Pt of 0.5:34) were analysed. Higher concentrations of platinum are readily determined due to the negligible iridium component of the absorption spectrum in these situations.

Figure 6.4 *Absorption spectra recorded at the FIA peak maximum on passage through the detector flowcell, for (1) 10 μg.cm^{-3} Pt(IV), (2) 150 μg.cm^{-3} Rh(III), and (3) 200 μg.cm^{-3} Ir(IV).*

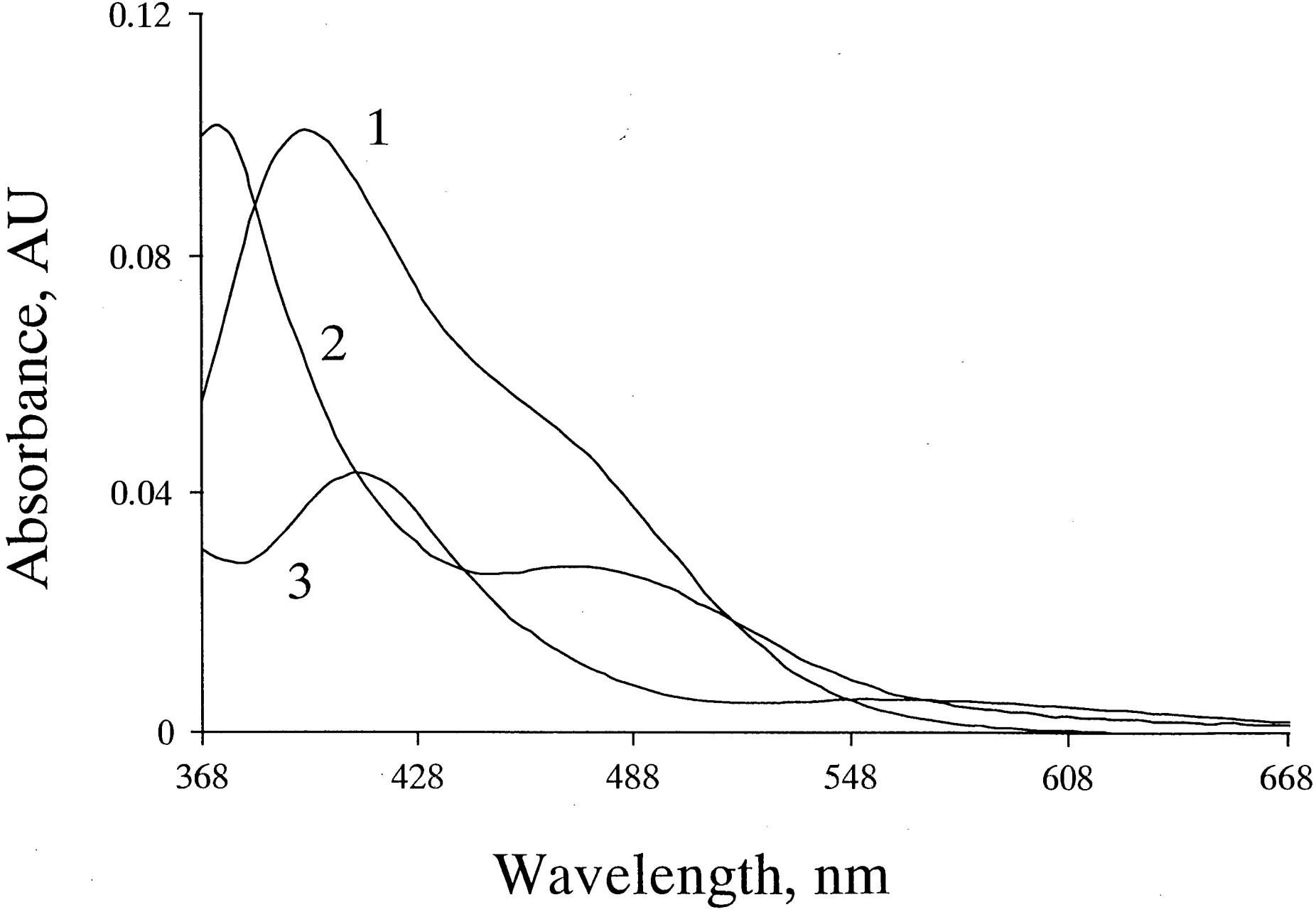
0.12
0.08
0.04
0
Absorbance, AU
1
2
3
368
428
488
548
608
668
Wavelength, nm

Linear least-squares results of the "found" *versus* "true" concentrations for platinum were, slope = 1.03 ± 0.03; intercept = 0.30 ± 0.36 $\mu g.cm^{-3}$; and correlation coefficient = 0.991. The regression of ICP-AES results *versus* FIA results for the same solutions were, slope = 1.05 ± 0.10; intercept = -0.01 ± 0.01 $\mu g.cm^{-3}$; and correlation coefficient = 0.998. A mixture of Pt(IV) and Ir(IV), containing 5 $\mu g.cm^{-3}$ and 100 $\mu g.cm^{-3}$ respectively, was repeatedly (n = 11) analysed and gave precision of 3.1% for Pt(IV).

6.3.2 The Determination of Platinum in the Presence of Rhodium

Addition of tin(II) chloride to a test solution of rhodium(III) chloride resulted in the light red colour changing to light yellow, and then, very slowly, to a deep raspberry red. Rhodium(III) chloride reacts with tin(II) chloride in a manner similar to platinum. A variety of Rh(III) and Rh(I) chloro(trichlorostannato)rhodium(III/I) complex anions, such as $[Rh(SnCl_3)_nCl_{6-n}]^{3-}$ (n = 1 to 5), are formed.[8,9] Heating increases the rate of colour formation significantly. The colour development is critically dependant on the reaction conditions.

Rhodium was treated in the same way as iridium with computational subtraction when determined in mixtures with platinum. A plateau is seen in the region 450 nm to 480 nm. This plateau is the beginning of the slow formation of the purple-red (λ_{max} = 475 nm) complex anion that has been assigned the formula $[Rh(SnCl_3)_5]^{4-}$.[10] By subtracting the response of the mixture of platinum and rhodium at 488 nm from that at 448 nm, the concentration of platinum is determined from the resulting calibration. The absorption spectra for solutions of platinum and rhodium are shown earlier in Figure 6.4.

A series of 15 mixtures of Pt(IV) and Rh(III) were prepared with a Pt(IV) concentration range from 5 to 100 $\mu g.cm^{-3}$, and a Rh(III) concentration range from 2 to 100 $\mu g.cm^{-3}$ (with ratios of Rh:Pt of 0.1:13).

Linear least-squares results of the "found" *versus* "true" concentrations for platinum were, slope = 1.00 ± 0.01; intercept = 0.08 ± 0.25 $\mu g.cm^{-3}$; and correlation coefficient = 0.999. The results found by ICP-AES (for platinum only) were, slope = 1.04 ± 0.01; an intercept = -0.10 ± 0.32 $\mu g.cm^{-3}$; and correlation coefficient = 0.998.

A mixture of Pt(IV) and Rh(III), 10 $\mu g.cm^{-3}$ and 50 $\mu g.cm^{-3}$ respectively, was repeatedly (n = 11) analysed and gave precision (r.s.d.) of 3.0% for platinum.

6.4 The Potential of Multi-Component Analysis in HBr

The potential for the multi-component determination of the PGMs - more specifically platinum and rhodium - in hydrobromic acid solution with tin(II) bromide is significant. Considerable improvement in the sensitivity of this system is evident for both metals, and the kinetics of the rhodium reaction are far superior to that of the tin(II) chloride system. However, the complex and varied chemistries occurring in solution pose a limitation on the development of a simple method.

Attempts were made to perform the simultaneous determination of platinum and rhodium in bromide medium. The reagent was prepared by dissolving the appropriate amount of tin(II) chloride in HBr. All solutions were prepared in 1 M HBr. The absorption spectra of a rhodium solution showed no difference when using tin metal dissolved in HBr to prepare tin(II) bromide.

Attempts at resolution of mixtures proved unsuccessful since the Additivity Principle did not hold. Although comparisons of the experimental and theoretical absorption spectra showed some agreement, there were no definite trends that could indicate the reasons for the discrepancies. Further attempts to find a set of conditions (such as the reagent concentration) over which additivity could be found failed.

As encountered with the tin(II) chloride system, there is extensive overlap of the absorption spectra (Figure 6.5) of platinum and rhodium. The absorption spectra are very similar (a difference of about 30 nm at their respective maxima) and resolution was anticipated to be difficult should any chemical effects alter the spectra even slightly. This seems to have been the situation.

Figure 6.5 *Plot of the slope of the linear calibration curves for (1) Rh(III), and (2) Pt(IV), as a function of wavelength using 0.2 M tin(II) bromide as the reagent.*

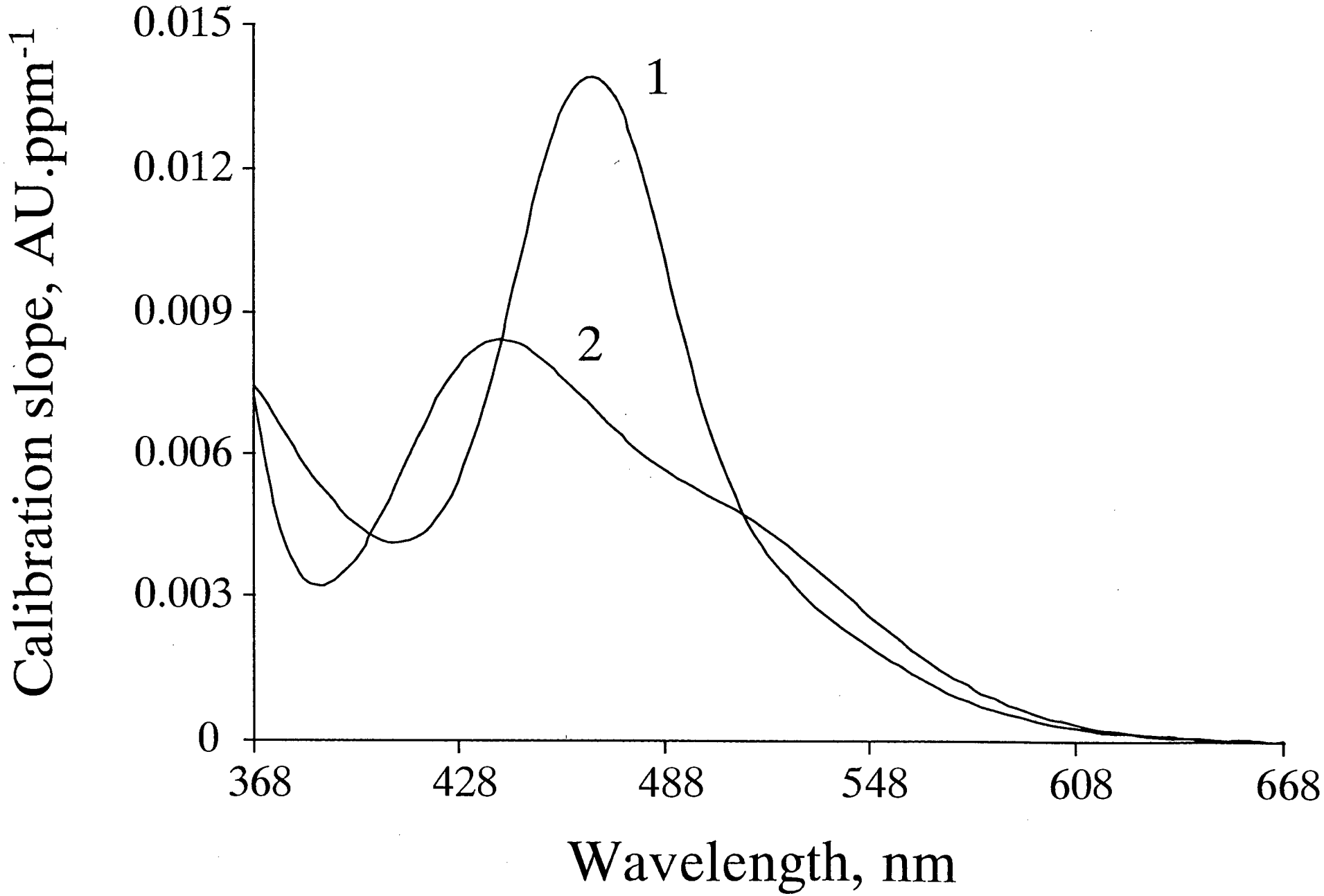
0.015
0.012
0.009
0.006
0.003
0
Calibration slope, AU.ppm-1
1
2
368
428
488
548
608
668
Wavelength, nm

Possible explanations reside in the nature of these chemical effects. The possibility of competition between the rhodium and platinum for the reagent may largely be discounted as large excesses of the reagent are present, and increasing the reagent concentration resulted in little improvement in additivity. Despite an inherent colour of rhodium and platinum complex bromides, it was determined that this colour was negligible relative to the colour formed on reaction with tin(II) bromide.

The possibility of intermetallic clusters should also not be discounted without further investigation. Such complexes would have a direct influence on the additivity of mixtures. The possibility of the chemical system inducing some form of synergisitc effects should also be investigated.

The most likely explanation is that the chloride, introduced when tin(II) chloride is used in the reagent preparation, may result in complexes forming that contain both bromide and chloride. The result would be a solution comprising complexes of the $SnBr_3^-$ and $SnCl_3^-$ moieties, but more likely a mixture of the two, or even some intermediate species. Substitution of ligands in the complexes by Cl^- and Br^- to give mixed species is also possible. The influence on the reproducibility of colour development and absorption spectra by these interactions would be noticeable.

Attempts were also made to perform simultaneous determination of rhodium in the presence of iridium in bromide media. The iridium component of the response was small and thus not ideal for simultaneous determination. Simple mathematical elimination of the iridium component also proved difficult in these investigations. A range of conditions was investigated once again, but an consistently high result was found for rhodium. No significant improvement was found when using different experimental conditions. As mentioned earlier, the complex chemistry occurring is most probably the cause of these difficulties.

6.5 Future Work

The ability to manipulate MCA data that has been introduced in this work should be expanded to encompass other multi-channel resolution methodologies. Multi-component calibration standards could be used to resolve the complex chemical systems encountered here. Although this form of calibration is conceptually more complex than linear regression methods, the future of MCA is founded on its ability to resolve mixtures in complex and real systems. Therefore, it is imperative that the data generated by the added dimension introduced by a multi-wavelength detector should be exploited fully by use of sophisticated software programs.

No attempt was made to include a comprehensive kinetics study of the various PGMs with the stannous halides, although attention is drawn to their widely differing kinetics. This is particularly so in tin(II) chloride solutions. The slow kinetics of the rhodium colour formation may be exploited analytically in mixtures with, platinum for example, by making use of a stopped-flow approach. As the platinum reaction is rapid it reaches completion after a few seconds whereas the rhodium reaction will continue for a longer time period. The increasing absorbance is thus directly attributed to the rhodium-tin(II) chloride reaction. This response may be quantified with standard solutions.

The preliminary work using the tin(II) bromide system shows the potential for a method to simultaneously determine platinum and rhodium by FIA. Further work toward realising this is required. It is expected that such a determination will require more complicated chemometric routines to enable accurate mixture resolution. The possibility of exploiting kinetic differences between the rhodium and platinum in the bromide system should also be investigated.

The fact that only the tin(II) halides were considered here should not detract from the importance or potential of other reagents for the photometric determination of the PGMs by FIA. The tin(II) halides merely provided a launch pad for multi-component work and software development, and are well known and trusted reagents.

6.6 Conclusions

It is clear that the MCA-based methodologies described in this chapter show the advantages of utilising the partial, or full, absorption spectrum instead of a single wavelength. The MCA methods developed give excellent correlation of experimental and theoretical data. To facilitate future MCA, an expansion of the criteria for wavelength selection used in this work into the form of an algorithm is necessary.

The present work has added an original dimension to spectrophotometric determinations based on exploiting and manipulating vast quantities of information-rich data. Where traditional methods for the determination of PGMs in mixtures have been to separate them virtually completely, a partial separation, or in certain cases no separation, may now suffice for accurate analysis.

It is also intended that this preliminary investigation of the PGMs using FIA and MCA will encourage further research to find innovative solutions to the limitations encountered. Solutions to these limitations would make FIA, in conjunction with MCA methods, a very useful adjunct to trace methods of analysis in the PGM industry.

6.7 References

1. Blanco, M., Iturriaga, H., Gene, J., Paspochi, S., and Riba, J., *Talanta*, 1987, **34**(12), 987.
2. Howe, J.L., *J. Am. Chem. Soc.*, 1927, **49**, 2393.
3. Griffith, W.P., *"The Chemistry of the Rarer Platinum Metals (Os, Ruthenium, Ir, and Rh)"*, Interscience Publishers, London, 1967.
4. Starik, I. E., and Barbanel, Y.A., *Russ. J. Inorg. Chem.*, 1961, **6**(1), 109.
5. Balcerzak, M., and Wozniak, W., *Microchem J.*, 1988, **37**, 326.
6. Kember, N.F., and Wells, R.A., *Analyst*, 1955, **80**, 735.
7. Young, J.F., Gillard, R.D., and Wilkinson, G., *J. Chem. Soc.*, 1964, 5176.
8. Moriyama, H., Aoki, T., Shinoda, S., and Saito, Y., *J. Chem. Soc., Dalton Trans.*, 1977, 639.
9. Davies, A.G., Wilkinson, G., and Young, J.F., *J. Am. Chem. Soc.*, 1963, **85**, 1692.
10. Iwasaki, S., Nagai, T., Miki, E., Mizumacji, K., and Ishimori, T., *Bull. Chem. Soc. Jpn.*, 1984, **57**, 386.

Chapter 7.

Summary

"Where, at last, you reach the end of the beginning."

7.1 Process Analytical Science

The new sub-discipline of Analytical Science, called Process Analytical Science (PAS), is gaining in stature throughout the world. This has been a direct consequence of the requirement for on-line and real-time monitoring of process streams. The virtually instantaneous analysis of the sample stream allows immediate corrective action to be implemented where necessary. Little human intervention is required and the financial benefits of such an approach are considerable.

The use of FIA with its inherent economy of solution volumes, its uncomplicated apparatus, and ready automation, is ideal for PAS. A chemical method developed in the laboratory for FIA may be transferred to a robust Process Analyser to allow continuous monitoring of a process stream. Not only are rapid measurement times required in the field, but laboratories are also required to offer rapid turn-around times. These routine tasks can in principle be performed automatically in suitable flow-injection instrumentation.

This investigation has laid the foundation for methodology suitable for implementation in the laboratory and process environment. Such methodology, in the form of an analyser, would naturally complement, not compete against, the existing and well-proven atomic absorption and ICP-AES spectroscopic techniques. FIA has already proved itself as a viable approach to Process Analysis. Future work will be focused on implementing the multi-element techniques developed in this investigation to the automated environs of the process and modern laboratory.

7.2 Automated Data Acquisition and Device Control

Flow-injection analysis, by virtue of its configuration and components, lends itself to ready automation in the laboratory. Devices such as peristaltic pumps, injection valves, selection valves, and detectors may be placed under microcomputer control to perform repetitive and routine tasks. In so doing, the analyst is relieved of the need to perform such mundane sample manipulations. An inexpensive FIA manifold may be operated manually with the detector output being directed to a chart recorder. However, the advantages of an automated approach in terms of productivity, financial savings and improved quality of data outweigh the limited advantages of a manual approach.

Extensive use is made of automated device control in this work. The relative ease by which a FIA manifold may be automated for analysis, whether for repetitive or diverse tasks, is illustrated in the FIA methods developed. The microcomputer controlled data acquisition and device control package, FlowTEK™, provides the means for the integration of hardware (devices) and software (user commands).

In this investigation, the automated system permits the rapid optimisation of the FIA experimental parameters by a grid search approach. Data were collected for experiments over a wide range of conditions. These data were used to generate three-dimensional plots which enabled convenient selection of the optimum experimental conditions. Three-dimensional data were also used to further understand the underlying chemical reactions occurring. The requirement for a convenient data acquisition system to obtain this information is essential.

The least used output in FIA is the transient peak shape. The customary and convenient measurement of peak height is bound to give way to the use of the entire transient profile. The well-defined concentration gradient of the injected sample zone contains a virtually infinite number of elements comprising different concentration ratios of the sample and reagents. Previously the points on the transient profile were inaccessible, however now microcomputer data acquisition renders these available for analytical use. Their adequate and novel exploitation will discharge any reservations regarding the advantages of automation in FIA methodologies.

7.3 The Determination of Platinum-Group Metals by FIA

The viability of the determination of the PGMs by FIA, and the usefulness of FIA for multi-component analysis, has been demonstrated in this study. The combination of this methodology, with the developed software, provides for a new application of FIA in the multi-component determination of the PGMs. This was achieved by making use of the familiar stannous halide chemistry in a new and innovative way. The results attained using FIA in this way could not be achieved using conventional approaches.

Emphasis was placed on the optimisation of the FIA manifold and on-line reaction conditions using a combination of univariate techniques and three-dimensional response surface maps. The latter provides an insight into interactions that would not normally be observed when univariate optimisation is used. A criterion other than the FIA peak height, namely the precision (expressed as the r.s.d.), was introduced as a means to select the most suitable experimental conditions. Regions of high precision (i.e. low r.s.d.) are preferred.

Methods for the trace determination of platinum, palladium, and rhodium by FIA were successfully developed after manifold optimisation. The sample throughput was 54 $hour^{-1}$. Calibration curves were linear to 100 $\mu g.cm^{-3}$, and the lower limits for accurate analysis were of the order of 0.2 $\mu g.cm^{-3}$ for Pt(IV), 1.5 $\mu g.cm^{-3}$ for Pd(II), and 0.7 $\mu g.cm^{-3}$ for Rh(III) when measuring at their respective absorption maxima. The multi-component methods developed in this study enabled resolution of binary mixtures of platinum and palladium, and platinum and ruthenium. Methods were also developed to enable the determination of platinum in the presence of large quantities of iridium and rhodium. The analysis of synthetic samples yielded excellent results. Preliminary interference studies indicated good tolerance of interferences that would be expected to occur in typical PGM samples.

The use of three-dimensional graphics and two-dimensional contour surfaces to enable visualisation of the experimental data proved highly informative and introduced a novel way of deconvoluting the chemistry occurring, especially in the case of palladium. By using a stopped-flow method, a qualitative investigation of the sequence of colour formation in the palladium(II)-tin(II) chloride system was made. The colour changes were correlated with absorption spectrum features that are found spectrophotometrically. The effect of tin(II)

chloride and hydrochloric acid concentrations on the complex formation, and thus the absorption spectrum, were also considered. Several complexes give rise to the sequence of colour changes resulting ultimately in an olive-green coloured solution. Conclusive evidence was presented as to the nature of the complexes giving rise to this coloured solution.

Preliminary work with tin(II) bromide indicated that this reagent should receive more attention as a reagent for multi-component PGM analysis. Evidently more sophisticated calibration and chemometric routines will be required for this system. Implementation of such routines in the software must endeavour to make these easily accessible to non-chemometricians.

Criteria for the difficult task of wavelength selection for mixture analysis were outlined. Notably some spectral difference is required for accurate mixture resolution and the spectral wavelengths should be distributed over the spectral range of higher absorptivities. Steps towards the development a suitable mathematical approach to wavelength selection were presented. Further work, on real and simulated spectra, will be required to assess the merit of any mathematical approach to wavelength selection.

The principles established in this work can also be applied to other multi-component chemical systems using multi-channel photometric data. Application of this approach can be found in chromatography, quantitative solution infra-red spectrometry, and FIA with other multi-channel detectors such as electrode arrays. Furthermore, higher order derivative spectra could be resolved in a similar way. The increased selectivity attainable with derivative spectra results from the fact that bands which overlap in the absorption spectra (zero order spectra) appear as separate bands in the derivative spectra.

The analysis of mixtures of the PGMs without prior separation is however only possible with software that can manipulate the multi-wavelength data. This necessitated the design and development of a software program to perform such tasks.

7.4 Visual Basic™ Software and Data Manipulation

The ReduceTEK software program was developed using the full-featured programming platform, Visual Basic™, in order to exploit the key features of Microsoft® Windows™. The requirement for this software arose due to the lack of software for the multi-channel detector used in this work and others like it.

Tandem operation with the DOS®-based FlowTEK™ software enabled manipulation and quantification of vast quantities of FIA data. A comprehensive file management system ensured the integrity of the spectral data. Totally flexible single and multi-component analysis routines were incorporated, along with easy spectral manipulation. The use of multiple window views enabled a complete "picture" of the data to be generated.

This investigation has demonstrated the advantages of the graphical user-interface for system optimisation, diagnosis, and interpretation of data. It is expected that GUIs will form an integral part of future computer-integrated analytical instrumentation. The advances in the instrumentation *per se* have slowed considerably in recent years and attention has become somewhat focused on making the available instrument more user-friendly *via* the anticipated unprecedented use of software and GUIs. Where previously an interface with an instrument was a dial that was turned, a button pressed, or a meter needle observed - a graphical and visual computer user-interface will be a worthy replacement.

The requirement for a Windows™-based software package for flow-based techniques that incorporates the powerful device control features of FlowTEK™, and using GUI-based data manipulation capabilities introduced in ReduceTEK, would be an invaluable asset to the FIA researcher. It is reasonable to speculate that such a software package will extend the boundaries of flow-based technology and their applications. The development of such a package is underway in the Process Analytical Science Group at MINTEK. This has been largely sparked by a realisation of the limitations of present software packages for multi-element determinations that have been highlighted in this study.

7.5 Multi-Array Photometric Detectors in FIA

The prime incentive behind the use of multi-channel photometric detectors is their ability to provide additional scientific data without incurring any additional time or effort. This additional data enables the application of multi-component analysis which results in analytical information not readily available by using other methodology. There are some guidelines to consider prior to the use, or purchase, of such multi-array photometric detectors for flow-based methods. These are often neglected and endanger the successful application of MCA to a particular absorbing system.

- The detector should be mechanically simple and robust with high precision optics,
- have a well-designed flowcell that will not trap bubbles, or become fouled with reaction products,
- conform to high standards of stability and low electronic noise levels,
- allow a high scan rate - with a minimum requirement of 2 seconds per absorption spectra, although a greater frequency would be more desirable,
- include versatile MCA software (commercial or developed) with ready access to data,
- and allow remote control facilities (autozero, start scan, etc.) from a microcomputer.

FIA enjoyed an exponential growth for the first 10 to 15 years of its existence. In recent years, as the technology has matured, that growth has tended to plateau out. This investigation has focused on a new development on FIA, *viz.* multi-component analysis. All indications are that as researchers investigate this new area, FIA will again enjoy a period of rapid growth. Developments in this area will allow FIA to migrate from its present status as a single element technique to the point where it is recognised as a viable multi-element technique. This investigation confirms the viability of this new area of growth for FIA.

Prior to the advent of multi-array detectors the manipulation of the sample zone in elegant ways was required to extract information that could be used in simultaneous determinations. The use of the multi-array detectors has allowed a return to simple manifolds with the detector providing the required discrimination for simultaneous determinations. A combination of these two approaches will allow even greater accomplishments.

The result of a highly innovative physical and chemical manipulation of the sample zone in conjunction with the detection capabilities of multi-array detectors would be unrivalled. It is anticipated that tremendous breakthroughs, not predictable from extrapolation of current trends, will be seen as FIA moves toward more exciting ways to gather chemical information.

7.6 Closing Comments

This thesis has focused on ways in which to determine the platinum-group metals by flow-injection analysis - as a single component, or simultaneously, with the stannous halides, in strongly acidic solutions. The pictorial presentation of multi-dimensional data has been shown to facilitate a more complete understanding of the underlying chemistry. These same multi-dimensional plots aid in the design and optimisation of FIA manifolds. It has been shown that the application of a multi-array detector to multi-component analysis depends heavily on suitable software for mathematical manipulations of the vast quantities of data and the careful selection of analytical wavelengths. Despite the dependence on sophisticated data acquisition and manipulation techniques, the primary importance of a well-founded understanding of the underlying chemistry has again been clearly demonstrated.

An important finding of this study is that analytical scientists, with their required skills of statistics, computer science, physics, chemometrics, and electronics will continue to depend on a fundamental understanding of chemistry.

Chapter 8.

Experimental

This chapter provides details on the experimental apparatus, reagents and their suppliers, as well as experimental techniques used during the course of this work. The instrumentation and the instrument settings used are tabulated. The FIA apparatus used in the construction of the manifold is outlined in detail.

8.1 Chemicals, Reagents and Glassware

All chemicals and reagents used for experimental work were analytically pure and obtained from various suppliers. K_2PdCl_4, K_2PtCl_4, K_2IrCl_6, and $RuCl_3 \cdot 3H_2O$ were obtained on loan from Johnson Matthey Chemicals Limited. $RhCl_3 \cdot nH_20$ and $La(NO_3)_3 \cdot 6H_2O$ was supplied by E.Merck, Darmstadt. Pt(IV) was obtained in the form of an atomic absorption standard with a concentration of 1000 $\mu g.cm^{-3}$ from BDH Chemicals. All additions in the interference studies were made from their respective atomic absorption standards (BDH Chemicals). Potassium iodate, KIO_3 was dried at 110°C for two hours and stored in a desiccator. Chloroform (Analar grade) was used in the potassium iodate titrations. Sodium tetraborate decahydrate (E. Merck), bromothymol blue, and 96% ethanol (Analar grade) were used in the dispersion experiments.

Tin(II) chloride, $SnCl_2 \cdot 2H_2O$ (Analar grade), was obtained from NT Laboratory Supplies and used without further purification. Tin(II) chloride solutions were prepared by dissolving the desired amount of the salt in the required volume of concentrated HCl. The initially cloudy solution was allowed to stand for 15-20 minutes in a warm water bath until it was completely clear. It was then cooled and diluted to volume. Metallic tin pieces (~ 3 to 5 g) were added to all stannous halide solutions as a preservative against oxidation by atmospheric oxygen. Acid concentrations were kept above 0.5 M to prevent hydrolysis of the tin(II) chloride. A similar approach was used in the preparation of tin(II) bromide solutions. Here tin(II) chloride was used in hydrobromic acid. No significant difference was found whether dissolving tin metal in

HBr to prepare tin(II) bromide, or using tin(II) chloride in HBr. Spectrophotometric and titrimetric comparisons were made. All stannous halide solutions were used the day after preparation.

All solutions were prepared using fresh glass distilled water (GDW). The GDW was stored in a large 25 dm^3 glass container. Analytical grade concentrated hydrochloric acid (10 M) and concentrated hydrobromic acid (8.8 M) were used directly. Acid concentrations were checked by standardisation against sodium tetraborate, although extreme accuracy of acid concentration was not essential. The concentrations of the noble metal stock solutions were standardised, where possible, against commercially available atomic absorption standards by flame-atomic absorption spectrometry or inductively coupled plasma-atomic emission spectrometry. Satisfactory agreement was obtained in both instances.

Glassware and polyethylene storage bottles were soaked in a strong Contrad solution and then in a minimum of 10% nitric acid. Vessels were thoroughly rinsed several times with GDW and allowed to dry on a drying rack. A mixture of A and B grade glassware (volumetric apparatus) was used throughout. A Gilson adjustable pipette (the maximum dispensed volume being less than 1.2 cm^3), previously calibrated by weighing the dispensed volumes, was used. Larger volume solution manipulations were performed with grade A glass pipettes (5-50 cm^3).

All weighing was done on a Mettler four decimal place balance and rough weighing on an electronic top-loading balance. Flame-atomic absorption was performed on a Varian Techtron 1000 AAS instrument. Inductively coupled plasma-atomic emission spectrometry was performed on a Jobin-Yvon JY 70C combined simultaneous and sequential instrument.

Ultra-violet and visible spectrophotometry was initially performed on a Varian Superscan-3 UV/Visible spectrophotometer and an LKB Novaspec I (single wavelength) spectrophotometer. All quantitative spectrophotometry was performed using a Spectra FOCUS™ forward optical scanning system with a 6 mm path length inert flow cell.

Two microcomputers were utilised - a 286 12 MHz processor was used as a file management system and provided the initial automation, and a 386 DX 33 MHz processor (with 8 Mb RAM and an Intel® math co-processor), running the OS/2 2.0 multitasking

operating system, enabled simultaneous data capture and processing. An Epson LX-400 printer was used for printing purposes. A Microsoft™ mouse was used as a pointing device.

8.2 Atomic Absorption of Platinum

Platinum stock solutions were prepared by dissolving solid K_2PtCl_4, and making up to volume in the appropriate HCl concentration. A $La(NO_3)_3$ stock solution of 20,000 $\mu g.cm^{-3}$ was made and diluted ten times on addition to the standards to give a final lanthanum, La(III), concentration of 0.2% (w/v). Lanthanum is used as a "releasing" agent.[1] A blank solution was prepared without the addition of platinum. The solutions were in 1 M hydrochloric acid.

The Varian Techtron Model 1000 AAS was used in all measurements. No background correction was used. A strongly-oxidising fuel-lean air-acetylene flame gave good sensitivities for platinum with the spectrometer settings shown in Table 8.1.

Table 8.1 *Flame-atomic absorption spectrometer operating parameters.*

Lamp current (mA)	10
Wavelength (nm)	265.9
Slit Width (nm)	0.2
Flame characteristics	Oxidising, fuel-lean air-acetylene flame

The system was optimised by aspirating a standard and adjusting the gas flow and burner positioning parameters to give maximum sensitivity and stability. All analyses were done in triplicate. The calibration curves for Pt(II) at wavelength 259.9 nm were linear to 100 $\mu g.cm^{-3}$ (the maximum tested) with a characteristic concentration[2] of 2.9 $\mu g.cm^{-3}$ for 1% absorption (1% absorption ≡ 0.0044 A.U.).

The calibration slopes of the Pt(II) and Pt(IV) solutions were the same, within experimental error. The prepared concentrations of Pt(II) (by weighing) where verified by this means. Periodic verifications of the platinum concentration in standards and mixture solutions were performed.

8.3 Inductively Coupled Plasma-Atomic Emission Spectroscopy

Inductively coupled plasma-atomic emission spectrometry was performed on a Jobin-Yvon JY 70C combined simultaneous and sequential instrument. The sequential and simultaneous operational modes were both used in this work. No significant differences were found.

Standards and samples used for FIA were used directly. All the solutions were in 1 M hydrochloric acid. Calibrations were repeated at regular intervals and the instrumental long term precision was better than 0.5% over the duration of the measurements. All standards and samples were measured in at least triplicate.

Typical operating parameters and ICP instrument details are listed in Table 8.2. Calibrations, using a minimum of three standard solutions, were repeated when the correlation was poor ($r < 0.97$), or in the case of high deviations of individual data points. As synthetic solutions were used throughout, these minimum requirements are appropriate. Some typical experimental calibration least-square results are shown in Table 8.3.

Table 8.2 *ICP-AES spectrometer operating parameters.*

Tangential-flow torch:	
Central-gas flow rate (auxiliary) ($dm^3.min^{-1}$)	0
Intermediate-gas flow rate (sheath) ($dm^3.min^{-1}$)	0.8
Outer-gas flow rate (cooling) ($dm^3.min^{-1}$)	15.0
Nebulizer (Meinhard concentric) gas flow rate ($dm^3.min^{-1}$)	0.4
Incident rf power (W)	1400
Reflected rf power (W)	< 5
Gilson Minipuls 3 peristaltic pump:	
Sample solution flow rate ($cm^3.min^{-1}$)	1.5
Computer and software:	
486 DX 33 MHz IBM computer with VGA monitor	
JY Version 4.0 Quantitative and control software package	

Table 8.3 *Linear least-squares equations for calibration curves of platinum, palladium and rhodium by ICP-AES.*

Element	Wavelength (nm)	Slope [α]	Y-intercept [β]	Correlation Coefficient [δ]
Pt	265.945	11.9	14.2	1.000
Pd	340.458	93.6	103.9	0.999
Rh	343.489	83.7	102.8	1.000

[α] Instrument response intensity per $\mu g.cm^{-3}$.

[β] Values here correspond to the blank intensities.

[δ] Each calibration line consists of at least 4 to 6 standards analysed in triplicate.

8.4 Potassium Iodate Oxidations

The titrimetric determination of tin(II) in hydrochloric acid by oxidation with potassium iodate is a well-documented and widely used method.[2,3] Potassium iodate solution reacts quantitatively with tin(II) in the presence of concentrated hydrochloric acid, according to the overall equation:

$$2\,SnCl_2 + KIO_3 + 6\,HCl \rightarrow 2\,SnCl_4 + KCl + ICl + 3\,H_2O$$

$$1\ KIO_3 \equiv 2\ Sn(II)$$

The titrimetric procedure involves the use of an immiscible organic solvent, chloroform, with which the end point of the titration is determined. The end-point is marked by the disappearance of the last trace of violet colour from the chloroform. This colour is a result of the iodine formed during the reaction as a by-product. Iodine monochloride is not extracted and imparts a pale yellow colour to the aqueous phase.

In the titration procedure for standardising a tin(II) solution, an aliquot of the solution (1-3 cm^3) was transferred to a conical flask. Rapid addition of 10 cm^3 of concentrated HCl, 5 cm^3 of chloroform, and 10 cm^3 of GDW was made. The KIO_3 solution, 0.025 M, was added by burette with vigorous shaking of the conical flask.

Initially both the aqueous and organic phases were colourless. On addition of approximately 65% of the required volume of iodate the aqueous phase became reddish-brown and the organic layer acquired a violet colour due to iodine. Addition of smaller increments of the iodate caused the organic layer to go faintly violet. The titration was continued drop-wise until the end-point was reached. Titrations were repeated until agreement to within 0.05 cm^3 was attained.

The titrations were not performed under oxygen-free nitrogen as it was determined that oxidation of Sn(II) to Sn(IV) by oxygen in the air was minimal over the duration of the titration. The requirement of extremely accurate Sn(II) concentrations were not essential as

calibration standards are always analysed prior to samples. However, a minimum requirement of at least 90% Sn(II) in a solution having been used for a few days was practised.

Freshly prepared solutions of tin(II) chloride/bromide had concentrations of Sn(II) in the range 93% to 97%. Solutions were not used for more than a few days. Nevertheless, two solutions were used for over a week and then were left to stand for a further week. They had Sn(II) concentrations of 89% and 91%.

8.5 FIA Apparatus and Sample Injection Technique

8.5.1 Peristaltic Pumps

Peristaltic pumps used in this study were the Spectec Perimax 12 (Spetec GmbH, Erding, Germany) and the Gilson Minipuls II (Gilson Medical Electronics, Inc., Wisconsin, U.S.A.). Pump flow tubing of 1.42 mm I.D.(yellow tags) and 1.85 mm I.D.(green tags) were used and calibrated gravimetrically. Pump tubing was replaced periodically, depending on the wear of the tubes. The peristaltic pumps had a minimum of 10 rollers - contact of the pump tubing with at least 5 at any time sufficed to keep pulsation low.

8.5.2 Injection Valves

The valves were of the rotary type from Rheodyne (Rheodyne, California, U.S.A.), a Model 5020 fixed-loop injection valve and a Model 5011 six-position selection valve, were used. Both have uniform flow passages of 0.8 mm I.D. and "wettable" surfaces are made of the fluoropolymers - Teflon™ (stator) and Kel-F™ (rotor). Both the injection and selection valves were pneumatically operated, either manually *via* an over-ride switch, or under microcomputer control using TTL input. Pneumatic actuators (operating at 70 psi minimum) and solenoid control valve kits (240-VAC) were supplied by Rheodyne. Nitrogen was used to drive the actuators.

8.5.3 Connectors and Tubing

All FIA manifold tubing, of 0.5 mm I.D., was made of poly(tetrafluoroethylene) (PTFE). Tubing of 0.8 mm I.D. was used only in parts of the manifold not affecting the peak signal, *viz.* the tubes used for drawing up samples and reagents. The injection valve was dismantled to replace the 0.8 mm I.D. flow passages with 0.5 mm I.D. tubing. Tubing connections were made either with commercially available Omnifit PTFE or PEEK™ threaded connectors and 90° mixing tees, or by push-fit connections. Reactor coils were made by uniformly coiling tubing of varying length around a 15 mm I.D. perspex cylinder. All long lengths of tubing were fixed in position to prevent movement and influence on the flow characteristics.

8.5.4 Sample Injection Technique

The use of time-based injections was preferred to changing sample loops to give different injection volumes. The injection valve was under computer control with timing accuracy better than one millisecond. The precision (r.s.d.) for replicate injections (n = 10) was better than 0.7%. The injection valve was fitted with either a 200 µl or 300 µl sample loop. By varying the delay time between switching the valve to the "inject" position and returning to the "load" position, different injection volumes were obtained.

The volume injected was calculated by repeated injection of standardised 5.0 M sodium hydroxide into a clean vessel and titration with hydrochloric acid. Volume computations using the volume flow rate and delay time, assuming negligible residual volume, compared favourably. An alternative approach of injecting mercury and then weighing was not desirable.

The actual volume of the injected sample, V in µl, is related to the valve residual volume, V_d in µl, the tubing radius, r in mm, and the sample loop length, L in mm, as in Equation 8.1. Using three sample loops of different volumes, the residual volume was found to be 7 µl. This is negligible for all practical purposes.

$$V = V_d + \pi r^2 L$$

Equation 8.1 *Equation used to calculate the sample injection volume.*

The conventional mode of sample injection is where the contents of the sample loop are all flushed into the carrier stream. This means that both the front and rear interfaces of the sample zone undergo dispersion, the rear to a greater extent than the front as a result of the longer path through the sample loop. However, if the valve is switched back to the "load" position *before* the rear interface of the sample zone passes into the manifold, then the rear interface will be as dispersed as the front interface. As a result, the time it takes for the FIA peak signal to return to the baseline is shorter, and a high sample throughput may be maintained. This method of sample injection was used throughout this work.

8.6 References

1. Pitts, A.E., Van Loon, J.C., and Beamish, F.E., *Anal. Chim. Acta*, 1970, **50**, 181.
2. Ebdon, L., "*An Introduction to Atomic Absorption Spectroscopy*", Heydon & Son Ltd., London, 1982, 57.
3. Vogel, A.I., "*A Textbook of Quantitative Inorganic Analysis*", 3rd edn., Longman, London, 1961.
4. Wilson, C.L., and Wilson, D.W., "*Comprehensive Analytical Chemistry*", Vol. Ic, Elsevier, Amsterdam, 1962.

Appendix 1 : Publications and Presentations

Presentations

D. Auer and K.R. Koch, SACI Young Chemists Meeting, Cape Town, South Africa, June 1992.

D. Auer and K.R. Koch, 3rd IUPAC Symposium on Analytical Chemistry in the Exploration, Mining, and Processing of Materials, Sandton, South Africa, August 1992.

D. Auer and K.R. Koch, Winter Conference on Flow-Injection Analysis, Florida, United States of America, January 1993.

D. Auer and K.R. Koch, Postgraduate Students Seminar, Council for Mineral Technology, Randburg, South Africa, November 1993.

D. Auer and K.R. Koch, Analytika 1994, Stellenbosch, South Africa, December 1994.

Publications

D.Auer and K.R. Koch, *Talanta*, 1993, **40** (12), 1975.

D.Auer and K.R. Koch, submitted to *Computers and Chemistry*, 1995

D.Auer and K.R. Koch, submitted to *Analytica Chimica Acta*, 1995

D.Auer and K.R. Koch, submitted to *Talanta*, 1995

D.Auer and K.R. Koch, in press, *Analytica*, 1995

Poster Presentation

D. Auer and K.R. Koch, *"Flow-Injection Analysis of the Platinum-Group Metals. Is Multi-Element Analysis Possible ?"*, 32nd Convention of the South African Chemical Institute, Halfway House, South Africa, February 1994.